Connecting the Tips – a Study on Sprout Fusion in Angiogenesis

Giovanni Mariggi

University College London

and

Cancer Research UK London Research Institute

PhD Supervisor: Dr. Holger Gerhardt

A thesis submitted for the degree of

Doctor of Philosophy

University College London

January 2012

Declaration

I, Giovanni Mariggi, confirm that the work presented in this thesis is my own. Where information has been derived from other sources, I confirm that this has been indicated in the thesis.

Abstract

Angiogenesis is characterized by the sprouting of new vessels from pre-existing ones, with sprouts headed by a specialized endothelial cell (EC) known as the tip cell. The trailing ECs are referred to as stalk cells and help form the vessel proper and lumenize. Newly formed sprouts must come into contact with adjacent tip cells via filopodia to fuse and lumenize to form an additional functional vessel loop able to support blood flow. Here I describe the process of anastomosis in detailed spatial and temporal resolution. Interestingly tip cells do no necessarily form a new connection at their first contact but tend to have a "negotiation" phase whilst tip cells are in contact. This time delay is between 1 hour and 2.5 hours suggesting a possible genetic regulation of anastomosis. Interestingly cessation of filopodia activity is observed upon lumenization of the sprouts and not on the establishment of cell junctions.

A gene important in fusion cells in *Drosophila* tracheal morphogenesis (the equivalent of EC tip cells) was investigated for its role in angiogenesis and anastomosis. Knockdown of *heca*, the homologue of the drosophila *headcase* gene, leads to precocious and ectopic connections between the Dorsal Lateral Anastomotic Vessels (DLAVs) over the neural tube in zebrafish embryos. *Heca's* function does not appear dependent on the TGF/BMP pathway as in the trachea. Gain of function experiments at the whole organism and cell-autonomous level show that *Heca* overexpression leads to complete lumenization of some of the migrating intersegmental vessels by 26hpf.

This suggests that *heca*'s possible involvement in instructing ECs to form a lumen or to sense the level of oxygenation/requirement to decrease activity may explain the opposing phenotypes observed. Taken together with observations about lumen formation with initiation of flow and the termination of filopodia activity, the data here presented could mean that lumenization is involved dampening EC activation.

Acknowledgement

I would like to begin to thank all the people at Cancer Research UK that do their very best in running the Charity, and have allowed me such a privileged experience here at the London Research Institute. With this, I must not forget all the thousands of supporters and volunteers that are the backbone of the Charity's success.

I owe an awful lot to Holger Gerhardt for placing his confidence in me almost 5 years ago and welcomed me into the VBL. I received immense support from you for all these years, while also allowing me the freedom to learn, develop and mature my scientific methodology and thinking. You have been a great mentor and I hope our paths will cross many times in the future so that I can repay you. And it seems you didn't appreciate too much your first male student, as the following 3 are now girls!

My time here has been so enjoyable also because of the family that I had the pleasure of joining, the VBL. I might have had to break the ice with a group hug but form then on it went splendidly. Thanks to past members: Li-Kun, Denise, Lars and Marta. To the current members: Benni, Irene, Raquel, Eleonora, Katie, Russ, Claudio and Martin you guys were wonderful to work around (most of the time) and congratulations for having survived my abuse for so long, I doubt there are better labs out there. Dominique and Jane, you've had the pleasure of seeing me grow (and regress mentally), you've been great support and fun throughout. Not to forget the sister lab, LDL. Good to have another perspective on almost anything.

Thanks to all my classmates especially Sophie, Caroline and Anna. Having someone complaining to you and to complain to is very therapeutic, you girls are awesome. A big thank you to all the people in the Institute that I've been able to interact with scientifically and socially, it has all helped to heighten the experience.

The work presented here would not have been possible without the help received from Peter Jordan in Light Microscopy; Phil Taylor, Darren Martin and Chris Seargent in the fish facility; Sue, Claire and all those who have helped along the way at the mouse unit in Clare Hall and Lucy and Hannah in the EM unit, great science with great smiles, the

perfect collaborators. Sally, Emma, Nicola and the rest of the admin and assistants team always ready to lend a hand wherever possible, and of course all the support staff. Thanks also to the many external collaborators: Richard Lang' group, Andy Bushby's group and Tim Chico' group have all helped out in the work in some way or another.

Last but not least thanks to my parents and my sister for always allowing me to do as I please and trying to understand all about my work.

Of course it must not be forgotten why so many of us strive to understand more about cancer and ways to cure it, therefore I dedicate this work to all those patients who suffer and show great bravery dealing with cancer. Hopefully all our little pieces of the puzzle will help them all one day.

Table of Contents

Table of figures

List of tables

Abbreviations

Ang1-2	Angiopoetin 1-2
bFGF	basic Fibrobalst Growth Factor
bHLH	Basic Helix-Loop_Helix
BM	Basement membrane
CNS	Central Nervous System
COUP-TFII	Chicken ovalbumin upstream promoter-transcription factor II
CSL	CBF/Suppressor of Hairless/Lag2
DA	Dorsal Aorta
DLAV	Dorsal Lateral Anastomotic Vessel
Dll1	Delta-like 1
Dll3	Delta-like 3
Dll4	Delta-like 4
DSL	Delta, Serrate, Lag2
EC	Endothelial cell
ECM	Extracellular matrix
EGF	Epidermal growth factor
eGFP	Enhanced Green fluorescent protein
Flt1/VEGFR1	FMS-like tyrosine kinase 1/ VEGF receptor 1
Flt4/VEGFR3	FMS-like tyrosine kinase 4 /VEGF receptor 3
Hes	Hairy/Enhancer of Split
Hey	Hes-related protein
hpf	hours post fertilization
HSPG	Heparan sulfate proteoglycan
ISA	Intersegmetnal Artery
ISH	*In situ* hybridization
ISV	Intersegmetnal Vein
Jag1/2	Jagged 1/2

JAM	Junctional adhesion molecule
Kdr/flk1/VEGFR2	Kinase insert domain protein receptor/fetal liver kinase 1/VEGF receptor 2
Lfng	Lunatic Fringe
Mfng/Rfng	Manic fringe/ Radical fringe
MO	Morpholino
NG2	Chondroitin sulfate proteoglycan 4
NICD	Notch intracellular domain
Nrp1/2	Neuropilin 1/2
P	Postnatal day
PAV	Parachordal vessel
PCV	Posterior cardinal vein
PDGFB	Platelet-derived growth factor B
PDGFRβ	Platelet-derived growth factor receptor β
PECAM	Platelet endothelial cell adhesion molecule
PI3K	Phosphoinositide(3,4,5)-phosphate kinase
qPCR	Quantitative Polymerase Chain Reaction
S1P	Sphingoshine-1-Phosphate
SEM	Scanning Electron Microscopy
TAM	Tumour Associate Macrophage
TEM	Transmission Electron Microscopy
Tie2	Endothelial-specific Tyrosine Kinase
VE-cadherin	Vascular Endothelial cadherin
VEGF	Vascular Endothelial Growth Factor
vSMC	vascular Smooth Muscle Cell
ZO-1	Zona Occludens-1

Chapter 1. Introduction

The evolution of organisms from single cells to multicellular beings raised a new problem with regards to the supply of oxygen and nutrients and the removal of metabolic waste products. The development of a vascular system helped overcome the limitations of diffusion and allowed multicellular organisms to increase in size and complexity, by keeping up with increased metabolic demands.

The vascular system is composed of two separate but connected tubular networks, the blood vasculature and the lymphatic vasculature. The blood vessels act as conduits for the transport of nutrients from the stomach and intestine, and oxygen from the lungs to all tissues while removing metabolic waste and delivering it to the kidneys and lungs. The driving force for blood flow is supplied by the pumping of the heart. The vasculature transports red blood cells to carry gases, platelets required for clotting and wound healing and white blood cells allowing them to carry out immunosurveillance and respond to injury and inflammatory insults. Long-range hormone signalling takes advantage of the extent of the vasculature's reach to deliver signals at distant sites or at the whole organism level.

The lymphatic vasculature is responsible for maintaining the tissue fluid balance by removing excess extracellular liquid and macromolecules and delivering them back to the blood circulation through the lympho-venous connection in the subclavian vein. The movement of lymph is a more passive process that occurs without a pump but it is believed that muscle contraction and the presence of unidirectional valves aid the flow away from the extremities towards the trunk to prevent backflow. The lymphatics are composed of blind-ended capillaries where absorption occurs, which drain into collecting vessels that carry the lymph to the thoracic duct prior to re-entering the blood stream. Defects in the lymphatic vasculature due to genetic mutations or physical damage to the vessels (as through surgery) result in poor tissue fluid homeostasis leading to lymphoedema, a swelling of tissues which tends to concentrate in the limbs and especially the legs.

The blood vasculature comprises arteries and arterioles that carry oxygenated blood from the heart to capillaries within tissue where exchange of substances occurs, and venules and veins that return deoxygenated blood back to the heart. The different types of vessels have specific characteristics at the macroscopic and cellular level that are crucial to their function. Arteries possess thick muscular walls to withstand the high pressure with which blood is pumped from the heart, as well as maintaining this pressure during transport. Capillaries are thin walled, small diameter vessels to maximise the surface area of contact with the tissues and allow efficient diffusion or transport of nutrients, oxygen and metabolic waste. Veins have unidirectional valves to prevent backflow of blood due to the lower pressure present in such vessels. Blood vessels are composed of a layer of endothelial cells (ECs) that surround the lumen and are important in modulating vessel permeability (especially in the capillary network). Accessory cells such as pericytes and smooth muscles cells (SMCs) are associated with the EC to help them carry out their function, and extracellular matrix (ECM) is deposited to form the basement membrane (BM), which also provides physical support.

1.1 Vascular Development

Because of its critical role in the survival and growth of tissues, the blood vasculature is the first organ system to develop during embryogenesis. Accordingly most mutations that severely affect vessel growth lead to embryonic lethality by mid-gestation (Carmeliet et al., 1996, Ferrara et al., 1996, Shalaby et al., 1995). Vascular development occurs in two distinct stages: vasculogenesis, which leads to the formation of a primary capillary plexus, and angiogenesis which expands the initial plexus and remodels it giving rise to a mature, hierarchical and functional network. Vasculogenesis (Fig 1.1) begins with the differentiation of precursor cells in the lateral plate mesoderm into a bipotent cell type known as haemangioblasts.

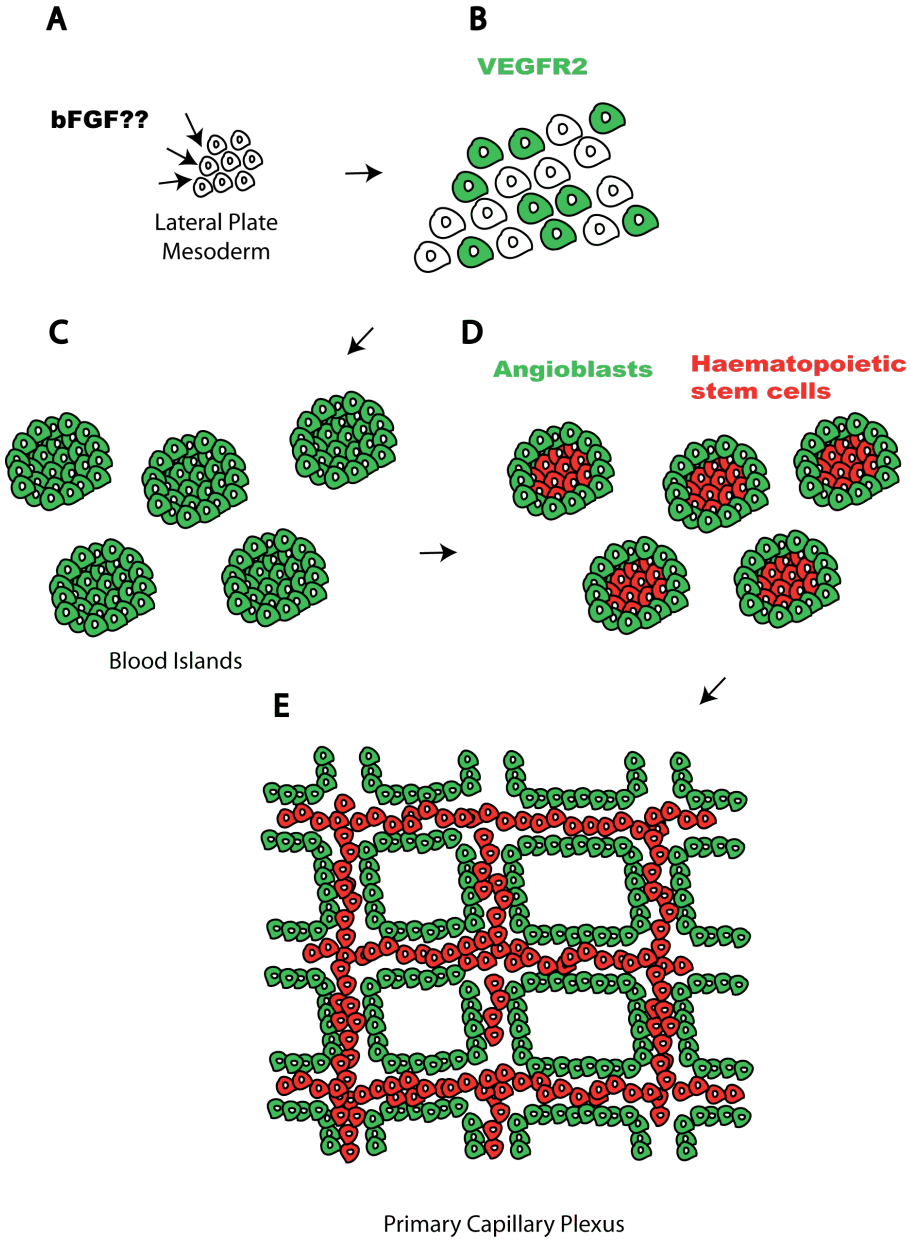

Figure 1.1 Vasculogenesis and the formation of the primary capillary plexus.
A. Lateral plate mesodermal precursor cells are induced to express VEGFR2 (**B**, green), possibly through the action of bFGF. **C.** The resultant haemangioblasts aggregate into structures known as blood islands through VEGF-directed migration. **D.** Haemangioblasts begin to differentiate into haematopoietic stem cells (red) or angioblasts (green) that will later differentiate into endothelial cells. **E.** Angioblasts proliferate, migrate and coalesce to form a rudimentary vascular network known as the primary capillary plexus.

The exact factors involved in this initial differentiation step are still unknown but it is believed FGF family members are involved (Fig 1.1A)(Risau, 1997). Haemangioblasts express *flk1* (also known as VEGF Receptor 2 described in 1.3.1) (Fig 1.1B), the most important receptor for Vascular Endothelial Growth Factor A (VEGFA, described in 1.3.1). In response to VEGFA haemangioblasts aggregate into structures known as blood islands and differentiate to either the haematopoietic lineage or into EC precursors known as angioblasts (Fig 1.1C-D)(Risau, 1997). More recent work has revealed the possibility of a haemogenic endothelium intermediate where cells only acquire the haematopoietic fate following initial angioblast differentiation (Lancrin et al., 2009). The resulting blood islands are composed of an inner core of haematopoietic cells surrounded by endothelial-like angioblasts (Fig 1.1D), which subsequently connect to a rudimentary network termed the primary capillary plexus (Fig 1.1E). The main axial vessels, the dorsal aorta and the cardinal vein, form through this vasculogenic process and are not dependent on angiogenesis. However, once the primary plexus has been established it must expand to keep up with the growth of the embryo and this occurs through angiogenesis.

1.2 Angiogenesis

Angiogenesis is the process by which new vessels are formed from pre-existing ones. Two modes of angiogenesis are currently known, sprouting angiogenesis and intussusceptive angiogenesis. The latter occurs through the enlargement of the parent vessels through EC proliferation, leading to a large calibre vessel. This vessel can then split via the formation of extracellular, intraluminal pillars that expand resulting in the bifurcation of the parent vessel until two separate, smaller calibre vessels are formed (Burri and Djonov, 2002).

Sprouting angiogenesis (from here on also referred to as angiogenesis, Fig 1.2) occurs when ECs from a pre-existing vessel branch out and form a blind-ended structure that grows towards the target tissue that requires increased blood supply. This newly formed sprout must then connect to another growing sprout or to an existing

vessel through anastomosis. Anastomosis is the process by which two separate tubular structures connect (from hereon also referred to as fusion, not to be confused with cellular fusion). The main concepts surrounding the mechanism of sprouting angiogenesis leading to a mature hierarchical vasculature will be introduced in this chapter.

1.3 Models for the Study of Sprouting Angiogenesis

1.3.1 The mouse post-natal retina

Peri-natal mouse retinas are void of blood vessels and their vascularisation begins shortly after birth. ECs enter the retina from the optic nerve and grow through the superficial layers of the retina, between the inner limiting membrane and the retinal ganglion cells (Fig 1. 3A), expanding radially and reaching the periphery within 7-8 days following birth (Fig 1.3B). The growth of this primary plexus is tightly regulated by the establishment of a VEGFA gradient (Gerhardt, 2003). The retina is pre-patterned by a network of astrocytes, microglial cells required for the support of the vasculature in the CNS. Astrocytic expression of VEGFA is a hypoxia driven process (Stone et al., 1995). The greater the distance from the optic nerve, the greater the hypoxia and therefore the higher VEGFA expression. As the ECs migrate towards the periphery and establish functional vessels, the hypoxia is relieved and VEGFA expression is downregulated, maintaining a steep gradient away from the centre of the retina (Gerhardt, 2003). The vascular pattern of the growing plexus tightly aligns with the adjacent astrocytic plexus, which act as a track to direct outgrowth (Gerhardt, 2003). Mural cells and pericytes are recruited to stabilize the vessels and as the primary plexus expands, the older parts begin to mature and acquire arterial-venous identity, while the capillary beds are pruned by vessel regression to remove excessive vasculature. The orchestration of these morphogenetic processes forms a functional, patterned and hierarchical vascular tree (Fruttiger, 2007).

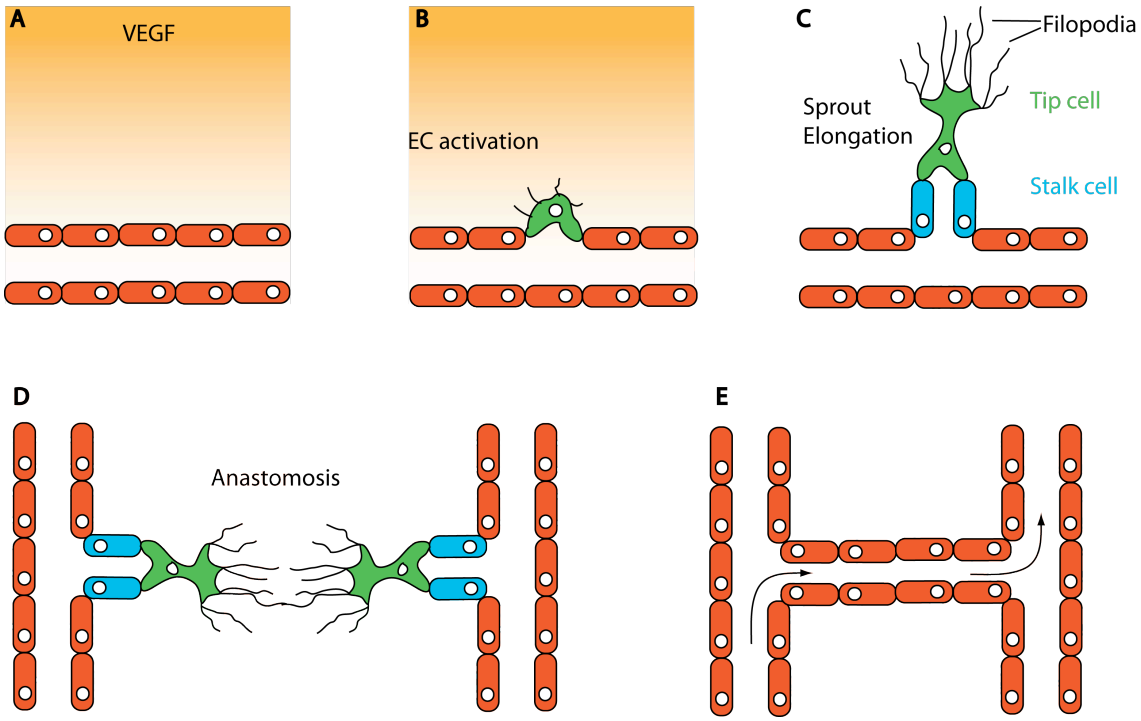

Figure 1.2 Sprouting Angiogenesis and Anastomosis.
A. ECs in a quiescent vessel are activated upon exposure to angiogenic factors such as VEGF. **B.** This leads to migratory behaviour, detachment of pericytes and breakdown of the basement membrane through secretion of matrix metalloproteases. **C.** One EC is selected to lead sprout migration, the tip cell (green). Trailing ECs are referred to as stalk cells (blue) and are involved in sprout elongation through proliferation and lumen formation. **D.** Newly formed sprouts must connect with one another through anastomosis to give rise to a functional vessel loop (**E**).

Figure 1.3 Mouse post-natal retinal angiogenesis.
A. Schematic representing a cross-section of the layers in the mouse retina, highlighting the positions of the 3 vascular plexus. RGC: retinal ganglion cell, IPL: inner plexiform layer, INL: inner nuclear layer, OPL: outer plexiform layer, ONL: outer nuclear layer, RPE: retinal pigment epithelium. Adapted from (Fruttiger, 2007). **B.** Retinal vasculature highlighted with isolectin B4. The vasculature enters the retina through the optic nerve head (white asterisk, left panel) and grows radially towards the periphery. The vascular front can be observed at P1 and P5 (white arrows, left and middle panel). Differentiation of vessels commences around P5 and can be clearly observed at P8(a – artery, v-vein right panel) and sprouts migrate into the deeper layers (white arrows, right panel). Adapted from (Gerhardt, 2003).

As the superficial plexus matures two further plexus are formed deeper in the retina. In this instance VEGFA is expressed by the Müller cells in the inner nuclear layer, attracting sprouts to firstly migrate to the outer plexiform layer boundary to form the outer deeper plexus and later just above the inner nuclear layer to form the inner deeper plexus (Fig 1.3A).

Even though the use of this model currently only allows imaging on fixed tissue one can gain information on morphogenetically distinct processes thanks to its stereotyped development and spatio-temporal relationship. Active angiogenesis occurs at the leading edge of the growing plexus, vessel morphogenesis and recruitment of pericytes occurs behind the growing front, differentiation, regression and pruning occurs further back in the plexus. Therefore one snapshot of the retina includes all processes involved in angiogenesis, allowing the interrogation of genetic or pharmacological manipulations on all phases simultaneously.

1.3.2 The Zebrafish Intersegmental Artery Sprouting

The tropical fresh water fish *Danio reiro*, commonly known as the zebrafish, has become an important tool in biomedical research over the last 40 years. Zebrafish possess many characteristics that have been instrumental in their rise in popularity as a model system for developmental biology. They are easy and cheap to maintain, mating is easily controlled and females produce large amounts of eggs. The embryos develop externally from their mothers and are optically clear allowing the visualization of developmental processes, which occur quickly. These attributes enable live imaging of growing embryos giving unprecedented detail on tissue morphogenesis dynamics. The ability of dynamic live visualization, which has been difficult to perform in other organisms, opened up a whole new avenue in vascular biology. The use of angiography with fluorescent microbeads in the mid 90s initiated the use of zebrafish in the study of vasculogenesis and angiogenesis (Weinstein et al., 1995).

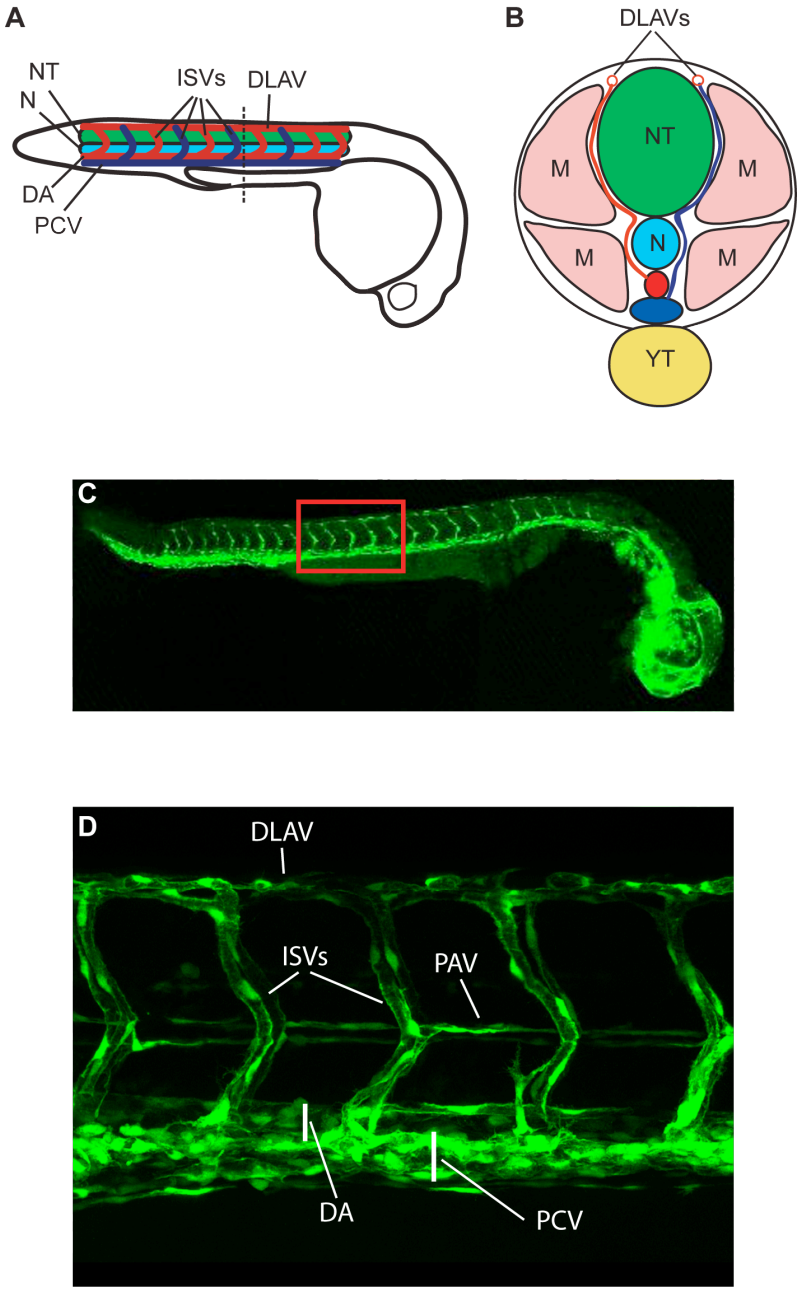

Figure 1.4 Zebrafish Vascular Development.
A. Schematic representation of the zebrafish trunk vasculature at 36hpf. N –Notochord, light blue; NT- Neural Tube, green; DA – Dorsal Aorta, red; PCV – Posterior Cardinal Vein, Blue; DLAV – Dorsal Lateral Anastomotic Vessel; ISVs – Intersegmental Vessels, red and blue. Adapted from (Armer et al., 2009). **B.** Cross section through trunk from A (dashed line), M – Myotomes, YT – Yolk Tube. **C.** Confocal micrograph of a 48hpf *fli1:eGFP* zebrafish embryo (Lawson, 2002). **D.** High magnification electron micrograph from C (red box). DA, PCV, ISVs and DLAVs are fully formed by this stage. PAV – Parachordal Vessel, is almost formed.

Another important development for zebrafish in research has been the use of Morpholino oligonucleotides to induce sequence-specific gene knockdown, promoting the investigation of gene function during vascular development (Nasevicius and Ekker, 2000). Morpholinos are oligonucleotides with a modified backbone where morpholine rings replace ribose residues and are linked through uncharged phosphorodiamidate groups instead of the charged phosphates for improved stability. Morpholinos exert their function by either binding over the mRNA ATG and blocking translation or by binding at exon/intron boundaries and preventing correct splicing of the nascent RNA (Summerton and Weller, 1997). It must be noted that thanks to their minute size, zebrafish embryos are able to continue developing without blood flow or functional blood vessels up to at least 48hpf as sufficient oxygen is obtained through passive diffusion. This enables the investigation into genes that are embryonic lethal in mouse models and therefore unsuitable for understanding their roles in vasculogenesis and early angiogenesis. With the development of further technologies and discovery of tissue specific promoters, transgenesis in zebrafish became reality and with it the possibilities for use of confocal live imaging expanded. The first and still most widely used transgenic line is the *Tg(fli1:eGFP)y1* line (from here on *fli:*eGFP) generated by Lawson and Weinstein (Lawson, 2002). The line expresses eGFP under control of the *fli1* promoter, which drives expression almost exclusively in ECs. Many more lines have since been generated using different promoters (such as *flk1*) and expressing fluorescent proteins with different subcellular localizations or as part of a fusion protein.

The zebrafish vasculature is less complex than that of higher vertebrates. Most studies have focused on the trunk vasculature as both vasculogenesis and angiogenesis occur in a stereotyped fashion (Fig 1.4) (Isogai, 2001, Isogai, 2003). The zebrafish trunk vasculature is initially composed of the axial vessels: the Dorsal Aorta (DA) and the Posterior Cardinal Vein (PCV). They form through the coalescing of angioblasts that differentiate in the lateral mesoderm and migrate to form the Inner cell Mass (ICM), later giving rise to ECs and haematopoietic cells (Herbert et al., 2009). The aggregation of angioblasts forms a precursor DA by 19.5hpf from which EC progenitors sprout and segregate to form the PCV, allowing the differentiation of the precursor vessel into the DA . By 23hpf both vessels are formed, become lumenized and circulation commences

around 25hpf (Herbert et al., 2009). The other vessels in the trunk are the intersegmental vessels that connect the DA to the Dorsal Lateral Anastomotic Vessels (DLAVs). The intersegmental vessels emerge from DA at ~22hpf through primary angiogenic sprouting and at this stage are referred to as InterSegmental Arteries (ISAs) as they have yet to assume venous identity. They emerge from the DA ipsilaterally at the level of the myotome boundaries giving rise to parallel vessels on both sides of the embryo. ISAs migrate dorsally between the notochord and the somites in the ventral portion of the embryo and between the neural tube and the somites in the dorsal portion as they make their way to dorsal aspect of the embryo (Fig 1.4B). Around 28hpf the ISAs reach the top of the neural tube and bifurcate, growing rostrally and caudally to make connections with adjacent ISAs to form the DLAVs through anastomosis (Isogai, 2001). By 1.5dpf all ISAs complete migration and fuse to form the DLAVs, resulting in a new lumenized and functional vascular loop originating from the DA (Fig 1.4C-D). At this stage a secondary round of sprouting originating exclusively from the PCV begins. Secondary sprouts can fuse with the ISAs, connecting the PCV to the primary angiogenic network (Isogai, 2003). This connection is rapidly lumenized and upon the initiation of blood flow, the portion of the ISA connecting it to the DA regresses, leaving the intersegmental vessels connected solely to the PCV and inducing venous differentiation. Alternatively the sprout can migrate dorsally between the somites and the notochord to the level of the myoseptum and become integral part of the parachordal vessel (PAV). The PAV was believed to be a functional vessel but more recent analysis has demonstrated that these are ECs pre-destined to become part of the lymphatic system, which develops later (Hogan et al., 2009). The PAV-derived lymphatic ECs require ISAs to direct their migration during lymphangiogenesis (Bussmann et al., 2010). The decision whether to connect to an ISA or to form the PAV is believed to be stochastic but leads to an almost equal and well-spaced pattern of ISAs and ISVs through the trunk. The PCV expands in the tail region through sprouting to form the posterior caudal plexus. By 48hpf the trunk vasculature has developed with DA, PCV, ISAs, ISVs and the DLAVs carrying blood flow (Fig 1.4D). At this stage the parallel bilateral DLAVs begin to zipper up in a caudal to rostral direction, forming a plexus over the neural tube by 7dpf (Isogai, 2001).

The study of the zebrafish trunk vasculature development has confirmed many discoveries made in mouse and *in vitro,* combining the benefits of an *in vivo* setting with the possibility of live imaging. The genetic tractability and ease of genetic manipulation through Morpholino knockdown and mRNA injection or transient expression of DNA constructs have helped this model to become a standard in the field of vascular biology. Recently the importance of understanding single cell behaviour within a population of endothelial cells has been uncovered, and clonal expression and tracking by transient expression of DNA constructs in zebrafish has allowed this type of investigation (Jakobsson et al., 2010).

1.3.3 Embryoid Body Sprouting Assay

Embryonic Stem Cells (ESCs) derived from blastocysts can be cultured and induced to differentiate into most if not all cell lineages present in the adult organism (Thomson, 1998). Using immortalised EC lines in culture systems can be laden with many potential drawbacks, especially on the relevance of the biological discoveries made. Therefore many have employed an *in vitro* system utilizing ESCs and inducing their differentiation into ECs in a 3D sprouting assay (reviewed in (Jakobsson et al., 2007b)). ESC are cultured in the absence of feeder cells and Leukaemia inhibitory factor (LIF) as hanging droplets in a petri dish, and incubated for 4 days (Fig 1.5A). This induces the aggregation of ESCs and the formation of ESC spheroids, also known as embryoid bodies (EBs). At this stage VEGF and VEGFR2 signalling are not required for the initial differentiation of ESC into ECs, but are necessary for cell migration and vessel formation (Schuh et al., 1999). The EBs can be plated on a 2D surface to assess their potential for EC network formation or they can be seeded in 3D collagen gels to induce sprouting. Once placed in collagen the growth medium is supplemented with VEGF-A to induce EC sprouting and migration, which can be observed eight days after initiation of spheroid formation (Fig 1.5B). Sprouts are headed by tip cells displaying filopodia extensions polarized in the direction of growth, as described in *in vivo* models (Fig 1.5B/C) (Gerhardt, 2003, Lawson, 2002, Jakobsson et al., 2007b),

Figure 1.5 ES cell embryoid body sprouting assay.
A. ES cells are grown in hanging drop suspensions to induce spheroid formation. **B.** Following a four day incubation the spheroid are plated in collagen gels and grown with VEGF-supplemented medium to induce EC differentiation. **C.** The ES cell spheroid sprout, migrate and form tubular structures reminiscent of blood vessels as they have tip cells, are lumenized and are covered by pericytes. Adapted from (Jakobsson et al., 2007b)

The vessels formed are composed of cells expressing many EC-specific markers such as CD31 and VE-cadherin (Vittet et al., 1996) (Fig 1.5C). Due to the presence of ESCs in the EB core, other vascular associated cells can also differentiate and take part in vessel formation. Mural cells are found in close contact with and surrounding the vessels (Fig 1.5B), expressing cell-specific markers NG2 and smooth muscle actin (SMA). Recent work has highlighted the importance of understanding EC-EC interaction and how slight genetic variations (such heterozygous loss of a gene) can influence cellular behaviour (Jakobsson et al., 2010); the EB sprouting system offers an opportunity to investigate such relationships and competitive behaviours through the use of chimeric spheroids. This system can be easily imaged live to further investigate the dynamics of angiogenic processes at the single cell level.

The EB sprouting assay circumvents the problem of early embryonic lethality in mice lacking genes critical for vascular development, as loss of the same genes does not affect cell viability in this assay (Ng et al., 2004). One of the limitations of this model is the lack of flow and therefore the role of haemodynamic forces.

1.4 Mechanism of Sprouting Angiogenesis

The requirement for angiogenesis and thus the increase in blood supply to a tissue is linked to an increase in metabolic needs. Angiogenesis is induced through the expression of the most important morphogen required for vessel growth, Vascular Endothelial Growth Factor-A (VEGFA). VEGFA activates VEGFR2 to induce sprouting through the activation of ECs, leading to a change in behaviour from the basal quiescent state. Upon stimulation, ECs break out from the pre-existing vessel, lose pericyte coverage and degrade the ECM to allow outgrowth. Angiogenic sprouts are headed and directed by an EC characterized by polarized migratory morphology towards the VEGFA gradient, long filopodia extensions to sense the environment for guidance cues and lack of proliferation (at least in the mouse retina), which is hence referred to as tip cell (Gerhardt, 2003). The ECs that trail behind tip cells, supporting sprout growth by proliferation, keeping up with migration and establishing the vascular lumen are known as stalk cells. It is clear that these two phenotypically different ECs

respond to VEGF in different ways: tip cells polarize and migrate with regards to a gradient whereas stalk cells proliferate proportionally to total VEGF present and take part in vascular morphogenesis (Gerhardt, 2003) .

Tip cell selection at initiation of sprouting is dependent on the lateral inhibition pathway involving Delta-like 4 ligand (Dll4) and Notch receptors, evidence for which has been provided in both zebrafish and mouse (Leslie et al., 2007, Siekmann and Lawson, 2007, Hellström et al., 2007, Suchting et al., 2007, Lobov et al., 2007). It is now clear that tip/stalk cell fates are not permanent but are in flux, with stalk cells overtaking the original tip to assume its role and cells within the sprout shuffling (Jakobsson et al., 2010). Alongside morphological differences, tip and stalk cells also display differential gene expression. Some genes that are expressed at higher levels in tip cells (or at least in the sprouting front) include *dll4, pdgfb, lama4a, unc5b, flk1 and flt4* (Fig 1.6A) (Gerhardt, 2003, Claxton and Fruttiger, 2004, Lu et al., 2004, Siekmann and Lawson, 2007, Tammela et al., 2008, Del Toro et al., 2010, Strasser et al., 2010, Estrach et al., 2011a, Stenzel et al., 2011). Conversely other genes are present at higher levels in stalk cells such as *robo4* and *flt1* (Huang et al., 2009). Tip and stalk cells also deposit different BM components, for example laminin α4 is deposited by tip cells (Stenzel, 2011) while stalk cells deposit fibronectin (Stenzel et al., 2011). However, no tip cell specific markers have yet been characterized.

1.5 VEGF Signalling in Angiogenesis

When cells sense a decrease in oxygen tension, the enzyme prolyl hydroxylase (PDH) becomes unable to hydroxylate Hypoxia Inducible Factor 1α (HIF1α), which is then not degraded and instead accumulates in the cell, forming heterodimers with HIF1β. HIFα and β are basic Helix-Loop-Helix (bHLH) transcription factors and HIFα/β heterodimers initiate the transcription of genes with a Hypoxia Responsive Element (HRE) in their promoter. Hypoxia responsive genes change the cellular behaviour leading to altered metabolism, erythropoiesis and the induction of angiogenesis. One such gene is VEGFA.

Figure 1.6 Tip / stalk cells and the role of Dll4/Notch signalling in tip cell selection. **A.** Morphological, behavioural and molecular differences between tip and stalk ECs. Tip cells (green) are highly migratory, possess filopodia and tend to express *dll4, flk1, flt4* etc at higher levels compared to stalk cells. Stalk cells (light blue) proliferate and are involved in lumen formation, expressing higher *robo4, jag1 and flt1*. Adapted from (Phng and Gerhardt, 2009) **B.** Schematic representation of junction between two ECs prior to tip cell selection. VEGFA and VEGFC can act through VEGFR2 and VEGFR3

(Kdr and flkt4 respectively) to induce upregulation of *dll4* expression. This will increase Notch signalling in the neighbouring cell, resulting in a downregulation of VEGFR2, VEGFR3 and Nrp1 and upregulating VEGFR1, acting as a VEGFA sink and further decreasing VEGFR2-driven signalling, resulting in low *dll4* expression. **C.** Following lateral inhibition through Dll4/Notch signalling a tip cell is selected (green) with high DLL4 and VEGFR2, whilst the stalk cell (light blue) will have high VEGFR1 and low Dll4 and VEGFR2. Adapted from (Phng and Gerhardt, 2009).

VEGFA is a member of the vertebrate VEGF family that also comprises PLGF, VEGFB, VEGFC and VEGFD (Fig 1.7A). VEGFC and D have a major role in lymphangiogenesis, although VEGFC has also been shown to induce angiogenesis (Benest et al., 2008), for example in zebrafish VEGFC is required for correct ISA migration (Covassin et al., 2006). Two variants of VEGF have also been found in viruses (VEGFE) and snake venom (VEGFF). VEGF is a secreted homodimeric glycoprotein of around 40kDa consisting of head-to-tail monomers connected by two disulphide bridges (Olsson et al., 2006). VEGFA is crucial for the proliferation of ECs and haematopoietic cells, and later differentiation, vasculogenesis and angiogenesis. The effects of VEGFA are dose-sensitive as loss of one functional allele results in embryonic lethality at around embryonic day 11 (E11) due to abnormal and delayed vessel development. . This haploinsufficiency is exacerbated by loss of both alleles but does not prevent initial EC differentiation (Carmeliet et al., 1996, Ferrara et al., 1996). Zebrafish VEGFA morphants exhibit similar vascular defects, where the initial specification and patterning of the axial vessels is not altered but vessel enlargement and intersegmental vessel development are defective (Nasevicius and Ekker, 2000). VEGFA is also critical in neonatal development as loss of VEGF function, either by gene deletion or by VEGF sequestration, leads to lethality up to the fourth week post-partum (Gerber et al., 1999).

VEGF-A can be spliced into various isoforms that differ in their ability to bind heparan sulphate proteoglycans (HSPGs, heparin), important for the establishment of a gradient, and the VEGF co-receptors neuropilin 1 and 2 (*nrp1* and *2*). There are 12 reported human isoforms, 7 pro-angiogenic $VEGFA_{xxx}$ (denoting the number of residues): 121, 145, 148, 165, 183, 189 and 206; and 5 anti-angiogenic isoforms: 121b, 145b, 165b, 183b and 189b. Anti-angiogenic b isoforms are believed tp exert much reduced angiogenic activity resulting from the C-terminal exon with a variant lacking an

Nrp1-binding site, thus induces suboptimal phosphorylation of VEGFR2 (Harper and Bates, 2008). Murine isoforms have one less residue compared to human and are therefore denoted VEGF120 etc. In mouse VEGF120 and 164 are the most highly expressed even though cells express a combination of isoforms. The heparin/HSPG binding capaity of the longer VEGF isoforms (164, 188) is important for setting up the gradient required for correct vascular patterning (Ruhrberg, 2002, Gerhardt, 2003). The difference in HPSG binding leads to different retention of the VEGF isoforms by cells (on their surface) and by the ECM, resulting in differential diffusion. The shortest isoform (120) is thought to be freely diffusible and thus acts at long range, affecting the steepness of the gradient (Ruhrberg, 2002). In HUVECs VEGF165 binding to heparin increases VEGFR2 phosphorylation, an effect dependent on VEGF's exon 7 (Ashikari-Hada, 2005). Growth factor binding to HSPGs stabilizes growth factor interaction with its cognate receptor (Ibrahimi et al., 2004) (Fig 1.7B) and recent work confirmed that such interactions potentiate signaling and biological activity, whilst altering signaling properties (Chu et al., 2011, Chen et al., 2010). EBs deficient for N-deacetylase/N-sulfotransferase 1 and 2 (NDST1/2), an enzyme important for the biosynthesis of HSPGs, and VEGFR2$^{-/-}$ are unable to sprout in response to VEGF164. This sprouting defect can be overcome by co-culturing cells so that the *VEGFR2*$^{-/-}$ ESCs supply HSPGs in trans, potentiating VEGFR2 signalling in the *NDST1/2*$^{-/-}$ cells to allow normal sprouting (Jakobsson et al., 2006).

Embryonic vascular development occurs normally in mice expressing exclusively VEGF164 (Stalmans, 2002), suggesting this isoform has intermediate retention, sufficient to set up a steep enough gradient to properly pattern the vasculature. On the other hand sole expression of VEGF188 in the mouse retina induces a denser capillary plexus but hinders arterial specification (Stalmans, 2002), possibly as a result of proteolytic cleavage and thus minimal diffusion, preventing gradient formation. If the VEGF gradient is completely abolished by either expressing only the freely diffusible isoform VEGF120 or by injecting VEGF120 in post-natal eyes, tip cell display decreased migration and filopodia extension, the plexus has a shorter migratory distance and ECs overproliferate forming larger calibre vessels (Ruhrberg, 2002, Gerhardt, 2003).

Figure 1.7 Vascular Endothelial Growth Factor family and Receptors.
A. The 5 members of the mammalian VEGF family are homodimeric secreted proteins and consist of VEGFA, B, C, D and PLGF. Certain viruses and snakes respectively produce VEGFE and F. VEGFs bind to the VEGFRs that are single pass transmembrane tyrosine kinase receptors. There are 3 receptors: VEGFR1, 2 and 3. The receptors homodimerize upon activation and transphosphorylate the intracellular tail resulting in downstream signalling through PI3K, p38MAPK and Erk1/2 leading to survival, proliferation and migration. There is some promiscuity in the receptors specificities but generally speaking VEGFA binds to VEGFR2, VEGFB and PLGF bind to VEGFR1 (of which there is also a soluble isoform), and VEGC and D mainly bind to VEGFR3. VEGFC also binds VEGFR2 with a role in developmental angiogenesis, whilst a soluble isoform of VEGFR2 binds VEGFC in the context of lymphangiogenesis to prevent overgrowth. **B.** VEGFR signalling is modulated by the binding of coreceptors such heparan sulphate proteoglycans that help stabilize the ligand/receptor interaction and complex half-life, or neuropilins that are necessary for targeting the endocytosed complex to the right endosomal compartment activating specific signalling pathways. **C.** Shear stress cause by blood flow is sensed by a mechanosensory complex believed to be composed of VEGFR2, VE-cadherin and Platelet Endothelial Cell Adhesion Molecule-1 (PECAM-1). The signal is relayed downstream and activates integrins (Tzima et al., 2005). All adapted from (Olsson et al., 2006)

VEGF family members bind to their cognate receptor tyrosine kinases Vascular Endothelial Growth Factor Receptors (VEGFR) 1, 2 and 3, respectively encoded by *flt1, flk1*and *flt4* (Fig 1.7A). VEGFRs belong to the type III receptor tyrosine kinase family, single-pass transmembrane proteins containing seven extracellular immunoglobulin domains and a split intracellular tyrosine kinase domain. Zebrafish express *flt1* and *flt4* as well as two other VEGFR genes It was initially thought that *kdra* and *kdrb* arose through gene duplication but sequence analysis revealed that *kdrb* is the closest homologue to *flk1* and that *kdra* is part of a fourth group of VEGFRs lost in placental mammals, and has therefore been named *kdr-like* (*kdrl*) (Bussmann et al., 2008). VEGF ligands have different affinities for the 3 receptors, with VEGFR1 binding VEGFA+B and PLGF, VEGFR2 with VEGFA, C and D (following processing) and VEGFR3 with VEGFC+D (Fig 1.7A) (Olsson et al., 2006). These receptors are mainly expressed in ECs but VEGFR2 also plays a role in neuronal maturation (Khaibullina et al., 2004) and VEGFR1 is involved in macrophage migration (Sawano, 2001). VEGFR3 drives lymphatic development but also has a role in developmental angiogenesis (Tammela et al., 2008). VEGFRs homodimerize upon ligand binding, bringing together the kinase domains and inducing catalytic activity. The receptor auto-phosphorylates the adjacent monomer on the intracellular tail, activating downstream signalling pathways such as PI3K, p38MAPK and ERK1/2 to induce migration, proliferation and survival. VEGFRs can heterodimerise in a context and cell-specific manner, such as VEGFR2/3 complexes (Dixelius, 2003, Nilsson et al., 2010) but the signalling events downstream of such heterodimers are yet to be elucidated.

VEGFR2 and VEGFR3 effectively induce receptor phosphorylation and downstream signalling whereas VEGFR1 has weak signalling activity in ECs. VEGFR1 has a much higher binding affinity for VEGFA, with K_d of 2-10pM whereas the affinity of VEGFR2 is at least one order of magnitude lower (Shibuya, 2006). This has led to the hypothesis that *flt1* acts as a VEGFA sink and sequesters it, thus preventing binding to VEGFR2 and activation of downstream signalling. VEGFR1 negatively regulates tip cell formation by antagonizing the effects on VEGFA in zebrafish (Krueger et al., 2011). Expression of a soluble isoform of VEGFR1 results in decreased angiogenesis (Zygmunt et al., 2011), which is necessary to keep certain clear tissues avascular i.e. the cornea (Ambati et al., 2006). Loss of VEGFR1 increases EC proliferation and network

formation resulting in embryonic lethality by E9 (Fong et al., 1995), suggesting this may be due to increased VEGFR2-driven signalling. Loss of both VEGFR2 alleles induces embryonic lethality at E8.5, with defects in vascular network formation as in VEGF knockouts, but also defects in EC specification and early migration (Shalaby et al., 1995). Recently, a soluble isoform of VEGFR2 has been described and is important for modulation of lymphangiogenesis by blocking VEGFC function (Albuquerque et al., 2009). Apart from its role in lymphangiogenesis VEGFR3 is involved in vasculogenesis, with associated embryonic lethality at E9.5 in knockout mice (Dumont, 1998), as well positively influencing angiogenic post-natal sprouting (Tammela et al., 2008), findings that have been observed in zebrafish (Ober et al., 2004).

The longer isoforms of VEGFA can bind neuropilins, single pass transmembrane receptors best known for their expression in the nervous system and ability to bind semaphorins (Larrivee et al., 2009). *Nrp1* and *2* are expressed during early vascular development with *nrp2* becoming restricted to the lymphatic endothelium. *Nrp1* co-immunoprecipitates with VEGFR2 whilst *nrp2* associates with VEGFR2 and 3. *Nrp1* deficiency leads to embryonic lethality caused by early heart and vascular defects, along with neuronal guidance defects (Kawasaki et al., 1999). These defects are dependent on aberrant sprouting and arterial differentiation but not EC proliferation. Accordingly, *nrp1* becomes preferentially expressed in arterial ECs later in development (Stalmans, 2002). Similarly, in zebrafish loss of *nrp1* expression abrogates VEGF-dependent ISA sprouting (Lee et al., 2002). *Nrp2* loss affects the lymphatic vasculature but not the blood vasculature (Yuan et al., 2002). Overexpression of *nrp1* induces ectopic vascular sprouting that ultimately leads to embryonic lethality, similar to loss of VEGFR1. The co-binding of Nrp1 to VEGF is not important in the activation of VEGFR2 and its phosphorylation (Fig 1.7B) (Larrivee et al., 2009), but recent work suggests a role in the sorting of the endocytosed receptors to different endosomal compartments in a synectin-dependent mechanism, leading to altered downstream signalling (Ballmer-Hofer et al., 2011). The guidance of EC tip cell migration is dependent on the presence of functional Nrp1 (Gerhardt et al., 2004). Evidence also points to the requirement of Nrp1 for p38MAPK phosphorylation downstream of VEGFR2, important for EC sprouting, branching and interaction with pericytes (Kawamura et al., 2008). A recent hypothesis on the VEGFA specificity of

Nrp1 hint that Nrp1 binds both VEGFA164 and VEGF120, but the latter cannot induce Nrp1-VEGFR2 complex formation and thus fails to activate downstream signalling (Pan et al., 2007). Overall the above data suggest *nrp1* is an important player in sprouting angiogenesis through its interaction and affect on VEGFR2 downstream signalling. Blood flow can also influence VEGFR2 signalling through interactions with VE-cadherin and PECAM-1 (Tzima et al., 2005) and this mechanosensory complex can activate integrin-mediated shear stress responses (Fig 1.7C).

1.6 Delta/Notch Signalling in Tip Cell selection and Angiogenesis

1.6.1 The Notch Pathway

Upon VEGFA stimulation ECs begin to sprout from a pre-existing vessel. The mechanism of tip cell selection has been attributed to effects of Delta/Notch signalling pathway. The Notch pathway is a well-conserved cell-to-cell lateral signalling pathway that relies on contact between adjacent cells and has been implicated in inhibition/induction of cell fates in many tissues (reviewed in (Lewis, 1998)). In mouse the pathway consists of four Notch receptors and five canonical Delta, Serrate, LAG-2 (DSL) ligands: Delta-like1 (Dll1), Dll3, Dll4, Jagged-1 (Jag1) and Jag2.

Notch receptors are type I single pass transmembrane proteins, comprising an extracellular domain responsible for ligand interaction (with many EGF-like repeats), a transmembrane domain involved in receptor activation and an intracellular domain that relays downstream signalling. DSL ligands are type I transmembrane proteins with many EGF repeats in the extracellular domain. Jag1 and Jag2 have almost twice as many EGF repeats and contain a cysteine rich region in the juxtamembrane extracellular portion. Notch signalling requires the signal-sending cell to express one of the DSL ligands and the signal-receiving cell to express one of the receptors. DSL ligands interact with the extracellular domain of Notch receptors, activating a proteolytic cleavage cascade. This begins with the ADAM family metalloprotease TACE, cleaving the Notch receptor extracellular domain (S2 cleavage). This domain remains bound to

the DSL ligand and is believed to be endocytosed by the signal sending cell; whether this results in active signalling is the subject of on-going investigations. The final proteolytic cleavage involves γ-secretase that separates the Notch intracellular domain (NICD) from the transmembrane domain (S3 cleavage). NICD can then translocate to the nucleus and bind CBF1, Su(H), LAG1 (CSL) transcription factor. In the absence of NICD CSL represses the transcription of Notch target genes by recruiting a repressor complex involving the histone deacetylase HDAC-1 (Kao et al., 1998). NICD translocation to the nucleus disrupts this repressor complex, allowing transcriptional activators such as *mastermind-like 1* and the histone acetyltransferase p300 to induce expression of Notch target genes such as the *Hairy/Enhancer of Split* (*Hes*) and *Hes-related protein* (*Hey/HRT/HERP*) families. The expression of Notch target genes is cell-type dependent. Some of the induced genes such as *hes* and *hey* act as repressors of other genes as well as of their own transcription, leading to tight feedback regulation of their expression (Phng and Gerhardt, 2009).

Notch receptor maturation requires cleavage by a furin-like protease whilst in the Golgi (S1 cleavage) (Logeat et al., 1998) and the mature heterodimer must be glycosylated to allow correct signaling, evidenced by loss of O-fucosylation leading to inactive receptors. The fucose is then further modified via the addition of N-acetylglucosamine by *fringe* (*fng)* family glycosyltransfereases present in both mouse and zebrafish (Johnston et al., 1997, Prince et al., 2001). *Fng* family members can increase or inhibit DSL-specific Notch signaling, adding another layer of regulation to the Notch pathway (Stanley, 2007).

1.6.2 Notch Signaling in Angiogenesis

The vasculature expresses a specific subset of Notch receptors and DSL Ligands. Notch 1 and 4 are expressed in ECs and Notch 3 in vSMC, while Dll1 and 4, and Jag1 and 2 are expressed in ECs (Villa et al., 2001, Claxton and Fruttiger, 2004). Loss of most of these components either leads to embryonic lethality by midgestation or severe vascular defects, sometimes involving postnatal lethality.

Notch pathway components are mainly found expressed in arterial ECs (Lawson et al., 2001, Claxton and Fruttiger, 2004, Leslie et al., 2007, Siekmann and Lawson, 2007). This finding raised the question of whether Notch pathway components are induced in arteries or whether they are required for arterial differentiation. In zebrafish *mindbomb* (*mib*) mutants, which lack functional Notch signaling, downregulation of arterial marker ephrinB2 is observed in the DA, as well as notch3 and deltaC (Lawson et al., 2001). *Mib* mutants display ectopic expression of the venous marker *flt4* in the DA, suggesting that arterio-venous differentiation is dependent on Notch signalling (Lawson et al., 2001). The *gridlock* mutation (*hes* family) is also implicated in arterio-venous identity as mutants have arterio-venous shunts (Weinstein et al., 1995). Similar results have been described in mice lacking *rbpj* (CSL) (Krebs, 2004) and *hey 1* plus *2* (Fischer, 2004). Heterozygous loss of *dll4* in mice is sufficient to induce arterio-venous malformation and leads to embryonic lethality (Krebs, 2004, Gale et al., 2004, Duarte, 2004). The link between venous fate and Notch signalling is established by COUP-TFII (chicken ovalbumin upstream promoter-transcription factor II), which is required cell-autonomously for venous differentiation and maintenance of the venous fate. Endothelial-specific loss of COUP-TFII results in expression of the arterial marker *ephB2* in veins, along with arterial notch components *notch1*, *Jag1* and *hey* (You et al., 2005) and concurrent downregulation of markers of venous identity (You et al., 2005).

During sprout initiation the Notch pathway plays an important role in tip cell selection. Blocking Notch signaling with pharmacological inhibitors such as γ-secretase inhibitors (GSI), Dll4-Fc, Dll4 blocking antibodies or *dll4* Morpholino results in vessel hypersprouting and ectopic branching with an increased number of tip cells each projecting greater number of filopodia (Leslie et al., 2007, Hellström et al., 2007, Siekmann and Lawson, 2007, Suchting et al., 2007, Lobov et al., 2007). *Dll4* is expressed more strongly at the sprouting vascular front, with a pattern often described as salt and pepper to illustrate the non-homogeneous nature (Leslie et al., 2007, Lobov et al., 2007). It is clear that functional *dll4* is required for correct vascular patterning and the above findings have led to the current model of tip cell selection (Fig 1.6B-C): VEGFA stimulates ECs to increase *dll4* expression and stochastically, one cell acquires slightly higher levels (Fig 1.6B). The cell expressing higher levels of Dll4 signals to the adjacent ECs through Notch1 receptor. As loss of Notch signalling results in higher

levels of VEGFR2 (Suchting et al., 2007), it is likely that Notch activation results in downregulation of VEGFR2 through expression of *hey1* (Holderfield et al., 2006) and upregulation of VEGFR1, making the signal-receiving cell less receptive to VEGF (Fig 1.6C). This difference in VEGF responsiveness gives rise to the different behaviour of tip and stalk cells: high VEGF signalling due to higher expression of VEGFR2 allows tip cells to migrate, lower VEGFR2 and higher VEGFR1 leads to decreased VEGF signalling in stalk cells and which respond by proliferating.

A recent investigation has uncovered that EC dependence on VEGFR levels of EC behaviour is only important in the presence of active Notch signalling. In EB sprouting assays, cells possessing only half the amount of VEGFR1 or 2 (*flt1*$^{+/-}$ and *flk1*$^{+/-}$) were grown as chimeras with wildtype cells. A lower level of VEGFR2 allows normal differentiation and sprouting but cells are less likely to be found at the tip position. Conversely, having half the amount of VEGFR1, thought to act as a VEGF sink, increases the competitive potential of cells to reach the tip position. Blocking Notch signaling with GSI abolishes the difference in tip cell prevalence between heterozygous cells and wildtype cells, suggesting that Notch acts upstream of VEGFRs during sprouting angiogenesis. The creation of chimeric mice containing heterozygous *VEGFR*s cells recapitulated the competitive advantage of VEGFR1$^{+/-}$ and the lower presence at the tip of VEGFR2 $^{+/-}$cells (Jakobsson et al., 2010). ECs can shuffle and change position within growing sprouts in the EB assay. The levels of VEGFRs do not alter the directionality and speed of migration but the persistence at the tip position was lower for VEGFR2$^{+/-}$ and substantially higher for VEGFR1$^{+/-}$ compared to wildtype cells (Jakobsson et al., 2010).

Jag1 has been recently implicated in this regulatory mechanism by competing with Dll4 for Notch receptor, decreasing signaling and therefore having proangiogenic effects by preventing Dll4-induced VEGFR2 downregulation (Benedito et al., 2009). Loss of *lunatic fringe* phenocopies Jag1 gain of function (increased sprouting) as it normally enhances Dll4 signaling while dampening Jag1 signaling. It is important to note that Notch pathway components can sometimes segregate asymmetrically to induce different cell fates in daughter cells (Le Borgne and Schweisguth, 2003) but this has so far not been observed for Notch components in ECs. Notch signaling can be

affected at the level of NICD stability through sites competing for acetylation and ubiquitination that control its degradation, as has been shown to be the case for SIRT1, a member of the sirtuin family of NAD^+-dependent deacetylases. SIRT1-induced deacetylation allows ubiquitination and subsequent degradation of NICD, reducing its signaling effect (Guarani et al., 2011). Some ECM components can alter Notch signaling. Laminin α4 can influence tip/stalk cell selection by enhancing *dll4* expression in ECs (Estrach et al., 2011b).

1.6.3 CSL-independent Notch activity

Notch signaling is able to induce CSL-independent events such as the activation of β1 integrin. Notch1 activation increases β1 integrin affinity for fibronectin, collagen I and IV, and is independent of transcriptional activation but reliant on the release of NICD from the membrane fraction (Hodkinson et al., 2007). The small GTPase R-Ras is responsible for the increase in integrin binding and Notch activity counteracts H-Ras and MAPK-dependent decrease of integrin binding (Hodkinson et al., 2007). This effect is not dependent on changes in integrin expression. Notch signaling has also been implicated in increased expression of ECM such as fibronectin, laminin and collagen I and IV. As stalk cells experience higher Notch signaling, the upregulation of basement membrane components fits with their role in vessel morphogenesis, along with the decreased expression of metalloproteases important in ECM break down (Trindade et al., 2008).

Notch signaling is able to affect the vasculature by directing differentiation of cells other than ECs. It is known that smooth muscle cells surrounding arteries and veins are functionally and molecularly different. Arterial vSMCs express smoothelin, a marker for contractile function (van der Loop et al., 1996), along with SM22α (Moessler et al., 1996). Notch is implicated in arterio-venous differentiation of ECs as described above, but it is also involved in the determination of arterial/venous vSMCs. Loss of Notch3 in mice results in deficiency in arterial vSMCs identity without affecting ECs' expression of *ephB2* and thus their arterial identity (Domenga, 2004).

Aberrant Notch3 signalling is linked to defective expression of Platelet Derived Growth Factor Receptor-β (PDGFR-β), an important receptor in the differentiation and recruitment of vSMCs, an effect that is CSL-dependent (Jin et al., 2008). CADASIL syndrome (cerebral autosomal dominant arteriopathy with subcortical infarcts and leukoencephalopathy) is a hereditary disorder characterized by stroke, dementia and vSMC dysfunction. Notch3 mutations are responsible for the syndrome and lead to a similar PDGFR-β downregulation as in mice and loss of arterial vSMCs in CADASIL patients (Jin et al., 2008).

1.7 Repulsive cues in angiogenesis

The growing vessels not only experience attractive cues, but are also affected by repulsive signals, which prevent the vascularization of tissues where blood vessels are not required and could even be detrimental. There are a number of signaling pathways identified as repulsive cues in angiogenesis such as Semaphorins/Plexins, Ephrins/Eph receptors, Netrins/Unc5B and Slit/Robo. All these pathways were firstly characterized in neuronal guidance, stressing the similarities of the guidance and patterning mechanisms between the two branched systems.

1.7.1 Semaphorins/Plexins

Semaphorins (Semas) are secreted or membrane-associated glycoproteins implicated in heart morphogenesis, skeletal muscles development, immune system signaling, cancer and vascular development (Kruger et al., 2005). Over 20 Semas have been described to date and are classified based on their similarity. They all contain a SEMA domain, a conserved 400-residue stretch containing a seven blade β-propeller fold similar to the one found in integrins.

Semas can bind to the extracellular domains of neuropilins and plexins (Fig 1.8). Plexins are transmembrane receptors that contain the SEMA domain required for interaction with Semas. Additionally Plexins contain cysteine rich extracellular domains homologous with the Met scatter factor receptor. The Sema3 family (Seam3A-G) and PlexinA1-4 and D1 have been implicated in vascular development. Nrp1 and 2 provide the ligand recognizing subunit while Plexins signal downstream of Sema3s, and the three together form the functional ligand-receptor complex (Takahashi et al., 1999). The common effect of Sema signaling in neurons is the repulsion of growth cones and thus excluding particular nerves from certain areas of tissue (Kruger et al., 2005). Compelling work in zebrafish using Morpholinos targeted against the *plexinD1* gene confirmed that in ECs, Sema/Plexin signaling is involved in the repulsion of angiogenic sprouts and the prevention of mispatterning of the vasculature (Torresvazquez, 2004). Similar mispatterned vasculature develops in *out of bounds* (*obd*) mutants, where the ISA sprout from regions of the DA that are not at the somite boundaries. The *obd* mutation has been pinpointed to *plexinD1 (plxnD1)* (Torresvazquez, 2004). PlexinD1 deficiency is reiterated by loss of its ligand *sema3a2* expression, normally expressed in somites dorsal to the DA, although the phenotype is not as severe, possibly due to redundancy between Sema3s (Torresvazquez, 2004). Transplantation experiments indicate that *plxnD1* is required EC-autonomously for the correct guidance of ISA migration (Torresvazquez, 2004, Zygmunt et al., 2011). Loss of Sema/PlexinD1 signaling not only leads to mispatterning of ISAs, it also increases the number of angiogenic ECs in the DA of zebrafish embryos. Loss of one allele of *plxnD1* (as in heterozygous *obd*/+ embryos) is sufficient to increase the angiogenic potential of ECs, with such cells being found at the tip of ISAs in ~70% of cases in chimeric embryos (Zygmunt et al., 2011). This increase in angiogenic potential is a consequence of Sema/PlexinD1-dependent post-transcriptional splicing of *flt1* mRNA. It increases the amount of *flt1* that is translated as the soluble isoform, supported by the finding that sflt1 expression is absent in *obd* embryos (Zygmunt et al., 2011). Mispatterning is not related to membrane bound *flt1* (*mflt1*) changes, and overexpression of *mflt1* causes extremely mild inhibition of sprouting, whereas ectopic expression of *sflt1* has drastic effects (Zygmunt et al., 2011). The effect of *sflt1* on ISA sprouting and patterning is cell-autonomous, only preventing ectopic sprouting in expressing cells. Surprising as

this is, it means that soluble decoy receptors are not able to diffuse far from the secreting cell. This data therefore indicates that Sema/PlexinD1 effect on sprouting is through modulation of VEGFR output. Interestingly in *obd* mutants Notch signaling is not affected but when disrupted, these pathways can have additive effects on angiogenesis (Zygmunt et al., 2011).

Loss of *plxnD1* in mice results in congenital heart disease and vascular patterning defects, especially in the coronary arteries and the intersomitic vessels, which are unable to follow the somite boundaries as in *obd* zebrafish (Gitler et al., 2004). *Sema3E* deletion phenocopies *plxnD1* deficiency and the signaling involved does not require Nrps as had been earlier suspected (Gu, 2005). Again these effects were shown to be EC-autonomous by use of the Tie2-Cre driver line to induce endothelial-specific gene deletion. Post-natal angiogenesis in the retina also suffers from developmental problems upon *plxnD1* deletion (Zhang et al., 2009). In this model *plxnD1* expression is dependent on VEGF signaling and is strongest at the sprouting front (Kim et al., 2011, Fukushima et al., 2011). The retinal ganglion cells supply Sema3E and Sema3E/PlexinD1 signaling inhibits *dll4* expression in the vasculature (Kim et al., 2011). Surprisingly unlike in the zebrafish, Sema3E/PlexinD1 are required to balance Notch signaling, thus tip/stalk cell selection and network formation (Kim et al., 2011).

1.7.2 Eph Receptors/Ephrins

Another receptor/ligand pair that was firstly discovered for their repulsive role in neuronal guidance is the Eph receptor family and the Ephrin ligands. Eph receptors are single pass transmembrane receptor tyrosine kinases containing a globular domain important for ligand interaction. So far there have been 16 receptors described in mouse, 10 EphA and 6 EphB, classified based on their affinity for ephrinA or ephrinB ligands (Kuijper et al., 2007). In zebrafish the situation is a lot more complex due to gene duplication. Ephrin ligands are grouped based on their mode of membrane attachment: ephrinAs are anchored via glycosylphosphatidylinisotol while ephrinBs are transmembrane proteins (Kuijper et al., 2007).

Figure 1.8 The involvement of repulsive cues in angiogenesis.
Various ligand receptor pairs described in the development of neuronal system and the guidance of growth cones, mainly through repulsion. Semaphorins bind Plexins and Neuropilins and Sema3s have repulsive properties in vascular development by binding PlexinD1. Netrin1 and Unc5b are present in the vasculature but whether they are pro or anti-angiogenic is still the topic of debate due to conflicting results. It is likely to be context and vascular bed specific along with the fact that Unc5b is a dependence receptor and will therefore signal with or without bound ligand. With regards to Slit2 and Robo receptor binding, it appears that Slit2 is not able to bind Robo4 but can bind Robo1. Some evidence suggests Robo1-Robo4 heterodimers are required for signal transduction. Slit-Robo signalling is required for vessel stability to avoid excessive vessel permeability. Domain acronyms - PSI - plexin-semaphorin-integrin; IPT: Ig-like fold/plexin; SP1/2: Ser/Thr protein kinase catalytic domain; CUB: complement binding domain; MAM: meprin/A5 protein/phosphatase-μ-related; Ig: immunoglobulin domain; Tyk: tyrosine kinase domain; TSP1: thrombospondin-1-like; ZU5: zona occludens-1-like; DB: DCC binding; DD: death domain; FNIII: fibronectin type 3-like; P1/2/3: conserved regions in cytoplasmic domain of DCC; CC: Robo4 conserved motifs; Lam: laminin domain; LRR: leucine-rich repeat. Adapted from (Larrivee et al., 2009).

The peculiarity of Eph receptor/ephrin signaling is the presence of two types of signaling: the classical forward signaling where the ligand activates the receptor, which in turn relays the signal to intracellular pathways, but also reverse signaling where the ligand signals back into the signal-sending cell. The main members expressed in ECs are EphB4 (*ephB4)* in venous ECs and ephrinB2 (*efnB2*) in arterial ECs. As described above their expression is regulated by Notch signaling as well as by blood flow (Héroult et al., 2006). Because of their arterio-venous specific expression pattern, it was believed that EphB4 and ephrinB2 were important for vascular specification. Indeed loss of EphB4 and ephrinB2 leads to defects in vascular remodeling causing embryonic lethality by midgestation. However, these embryos do not display defects in the overall differentiation of arteries and veins, only in their maturation. It has also been hypothesized that EphrinB2/EphB4 are important for arterio-venous segregation, due to their repulsive behaviour. However, this is not observed in knockout embryos. Along with this, knockout mice for the TGF-ß co-receptor *endoglin,* which lack proper arterio-venious segregation, still express ephrinB2 (Sorensen et al., 2003).

In vitro work has shown that activating either forward or reverse signaling can lead to a pro-angiogenic response to EphrinB2, even though some conflicting reports describing opposite effects have been published (Adams and Alitalo, 2007). Two investigations have highlighted a contribution from ephrinB2 to enhancing VEGF-induced sprouting. EphrinB2 is required for the internalization of VEGFR2 and VEGFR3 (Sawamiphak et al., 2010, Wang et al., 2010b), and EC-specific loss of *efnb2* results in decreased endocytosis of the VEGFRs. This internalization is critical to activate downstream signaling (Rac1, Akt and Erk in the case of VEGFR3) (Wang et al., 2010b), and VEGF-induced filopodia extension through ephrinB2 PDZ signaling-dependent mechanisms (Sawamiphak et al., 2010). This could also explain why sprouting vasculature tends to express arterial markers such as ephrinB2, possibly giving ECs an angiogenic advantage. The PDZ domain of ephrinB2 is similarly vital for correct lymphatic development (Makinen, 2005). The migration and recruitment of pericytes to microvascular capillaries requires the cell-autonomous presence of ephrinB2, suggesting it might also have a cell-to-cell-independent function (Foo et al., 2006).

1.7.3 Netrins/Unc5B and Slits/Robos

Netrins are secreted laminin-like proteins that were discovered for their ability to attract or repel neuronal growth cones depending on the receptor they engage (Fig 1.8) (Colamarino and Tessier-Lavigne, 1995). Netrin-1 can have a pro- or anti-angiogenic effect and much debate around the supporting data has occurred. The receptor to which netrin-1 binds in believed to be Unc5B, a member of the dependence receptor family, composed of DCCs and the Unc5 families. Unc5B can signal upon ligand binding but will also signal (albeit differently) in the absence of netrin-1, often leading to apoptosis (Mehlen, 2005). Unc5B is selectively expressed in ECs and the first report of an Unc5B knockout mouse describes increased filopodia, suggesting the receptor possess anti-angiogenic properties, reliant on Netrin-1/Unc5B signaling (Lu et al., 2004). Unc5B is described as expressed exclusively in arteries in quiescent vasculature but is rapidly upregulated upon the initiation of angiogenesis (Larrivee et al., 2007). Tumour xenograft studies highlight the importance of netrin-1/Unc5B in the repulsion of ECs as observed in the full knockout mouse. Unc5B-dependent signaling is responsible for Netrin-1 induced repulsion and is believed to dampen sprouting angiogenesis (Larrivee et al., 2007). The opposing school of thought reported that Netrin-1 is an EC and vSMC chemoattractant and mitogen *in vitro* (Park et al., 2004). This effect synergizes with VEGF in *in vivo* angiogenesis assays (Park et al., 2004). The same group later reported that in their EC-specific Unc5B knockout the only vascular abnormalities were in the placental vasculature, where the plexus is structurally and functionally deficient, especially the arterioles (Navankasattusas et al., 2008), thus ascribing a pro-angiogenic role to the receptor, in line with their earlier data. It therefore remains unclear the exact role of Netrin/Unc5B signaling in the vasculature, possibly due to the dependence nature of the receptor and what appears to be vessel-bed specific effects. Another report attempts to reconcile the different interpretations by suggesting Unc5b in zebrafish induces caspase-mediated apoptosis in the absence of Netrin-1. Sprouting defects in Netrin-1 morphants can be rescued by caspase inhibition, Unc5b silencing as well as its downstream target DAPK (Castets et al., 2009). Overall it is clear that Netrin-1/Unc5B signaling is required for angiogenesis and hopefully further investigations will clear the divergences of current data.

Slits/Roundabout (Robo) are another ligand receptor pair that was identified in axonal growth. The name given to the receptor, roundabout, stems from the Drosophila knockout phenotype where *robo* mutants possess neurons that instead of crossing the midline once, turn around and cross back over (Seeger et al., 1993) and similar neuronal defects occur in mouse knockouts (Kidd et al., 1998). In the Robo family of receptors, Robo4 is endothelial-specific and plays a role in vascular development (Huminiecki, 2002, Park, 2003). Robo4 contains only two of the usual five extracellular immunoglobulin domains, and only two out of three fibronectin type III domains compared to other members of the Robo family (Fig 1.8) (Huminiecki, 2002). In mouse Robo4 is expressed during embryonic vascular development, firstly in the trunk vessels and then intersomitic vessels and capillaries (Park, 2003). Interestingly, Robo4 expression is highly upregulated in TGF-ß receptor Alk-1 deficient embryos that show general vascular patterning defects as well as lack of arterio-venous segregation (Park, 2003). This expression pattern persists in the adult, where it is also present in vessel-associated vSMCs. Slit2-Robo4 signaling is able to prevent EC migration *in vitro* (Park, 2003). In contrast to this, it seems that expression of soluble Robo4 Fc-fusion acts to inhibit angiogenesis suggesting that its physiological role and that of Slits is to promote angiogenesis, in contrast with Park *et al*. In zebrafish, *robo4* and *slit-like2* are expressed in the vasculature (Bedell et al., 2005, Chen et al.). Endothelial *robo4* expression in zebrafish is reliant on *sox7* and *sox18* transcription factors, without affecting endothelial differentiation (Samant et al., 2011). Morpholino knockdown of *robo4* results in misguidance of ISA sprouting (Bedell et al., 2005). R*obo4* overexpression almost completely prevents angiogenic sprouting from the DA. This suggests that *robo4* directed signaling has a repulsive effect or at least is required for proper guidance. In agreement with this, loss of Robo4 in mouse post-natal retina aggravates pathological angiogenesis whereas ectopic Slit2 is able to dampen it, hinting that Slit2-Robo4 signaling is important in vascular stability by affecting VEGF-induced increase in vascular permeability and EC migration (Jones et al., 2008). Slit2-Robo4 signaling can attenuate the effects of sepsis-induced cytokine storm and resultant vascular hyperpermeability. This is through a decrease in cytokine-induced VE-cadherin endocytosis by stabilizing VE-cadherin/p120-catenin complex, stabilizing EC-junctions and decreasing vascular leakage (London et al., 2010). The two opposing mechanisms

have been linked with differing downstream pathways: the pro-angiogenic effect of Robo4 is dependent on Cdc42 and Rac1 Rho GTPases and *in vitro* experiments indicate that Robo4 expression changes EC morphology and phenotype in a similar fashion to Rho GTPases (Kaur, 2006). EC motility and filopodia formation depend not only on Robo4 but also on heterodimeric complexes containing Robo1 and Robo4, the former being required for signal transduction. Robo4 activates actin remodeling pathways by interacting with Wiskott-Aldrich syndrome protein (WASP) (Sheldon et al., 2008). The repulsive effects of Slit2-Robo4 depend on the recruitment of paxillin and the Arf-GAP GIT1, inhibiting Arf6 activation and therefore Rac1. This prevents VEGF165-dependent effects such as increased vascular permeability and migration (Jones et al., 2009).

More recent work has provided further evidence for a lack of binding between Robo4 and Slit2 but indicates that Robo4 might actually be binding to Unc5B, the dependence receptor described above. This interaction is able to block VEGFR2-Src association and signaling, along with VE-cadherin phosphorylation (Koch et al., 2011). Robo4-Unc5B complex formation is important in postnatal angiogenesis but not during development (Koch et al., 2011), reiterating what is observed in *robo4*$^{-/-}$ mice, where an effect is seen on vascular permeability and stability but not on patterning (Jones et al., 2008).

1.8 Macrophages in Angiogenesis

Macrophages are myeloid derived cells that are produced in tissues upon differentiation of monocytes. Their primary role is the phagocytosis of necrotic cell debris and pathogens, playing a role in both innate and adaptive immunity.

Macrophages have become an important component in understanding the effects of the tumour microenvironment on tumour progression. Many inflammatory cells are found in the tumoral stroma and most of these are tumour-associated macrophages (TAMs). Depletion of Tie2-expressing macrophages results in inhibition of tumour angiogenesis in subcutaneous xenograft models (De Palma et al., 2005). Similar effects

are observed in mice deficient for *csf-1,* a cytokine required for macrophage development, crossed with MMTV-PyMT oncogene-induced breast cancer mouse model. Tumours display decreased vascularization and progression (Lin et al., 2006). The use of liposome-encapsulated clodronate, which leads to macrophage apoptosis upon phagocytosis, delays angiogenesis and tumour growth (Zeisberger et al., 2006). It is thus clear that macrophages play a role in stimulating angiogenesis during tumour growth. Many signaling pathways have been implicated in the stimulation of tumour vascularizton by macrophages: VEGFA, PLGF, angiopoietins, SDF-1, MCP-1 and semaphorins have all been reported to play a role (Squadrito and Palma, 2011). Recent work suggests that the Tie2/Ang2 axis mediates cell-to-cell interaction between TAMs and ECs to induce tumour angiogenesis. Blockade of Ang2 prevents Tie2 upregulation by TAMs and thus decreased EC interaction and angiogenesis. TAM-specific deletion of Tie2 is sufficient to reduce tumour angiogenesis, stressing the importance of this signaling axis between TAMs and ECs to promote vessel growth (Mazzieri et al., 2011).

With regards to macrophage function in developmental angiogenesis, the picture is not as clear but recent reports have begun to shed light on possible mechanisms. Polverini *et al* first suggested their role in angiogenesis by demonstrating that activated macrophages induced vascular proliferation in the corneal stroma, concluding they are a major source of proangiogenic factors (Polverini et al., 1977). Neuronal tissue specific macrophages, termed microglia, are present in the retina prior to the emergence of the vasculature form the optic nerve head. They pre-pattern the retinal superficial layers, with even spacing from the center to the periphery (Gerhardt, 2003). The first direct evidence of the importance of macrophages in developmental angiogenesis is their effect on hyaloid vessel regression. Hyaloid vessels supply the lens during its development, and must regress to allow proper vision. PU.1 is an ETS-domain transcription factor important for gene expression leading to myeloid cell differentiation, especially macrophages and B cells. In *PU.1*$^{-/-}$ mice, loss of macrophages prevented proper hyaloid regression through lack of EC apoptosis. Macrophage-induced apoptosis is dependent upon secretion of Wnt7b ligand (Lobov et al., 2005). Macrophages are not required but appear to fine tune post-natal retinal vascularization as well as pathological neoangiogenesis, without affecting mature vasculature in the adult. Similar observations were made in osteopetrotic mice (*op/op*)

that lack functional M-CSF resulting in the failure of macrophage differentiation (Kubota et al., 2009). Developmental defects are also manifested in lymphatics but again the adult lymph vessels are not affected. In these mutants tumour angiogenesis and lymphangiogenesis are reduced, with a decrease in tumour metastasis (Kubota et al., 2009).

Fantin *et al* demonstrate that microglia are found in the hindbrain prior to vascularization and interact with VEGFA-induced tip cells to aid their anastomosis with adjacent tip cells. Loss of macrophages in *PU.1*$^{-/-}$ or *op/op* mice show decreased branching in the hindbrain vasculature. This was shown not to be dependent on monocyte-derived macrophages and VEGFA was not required in microglia (Fantin et al., 2010). Interestingly the microglial cells that aid tip cell anastomosis display similar molecular characteristics as angiogenic TAMs, with expression of *tie-2* and *nrp1*, but are not necessary for the initiation of angiogenesis (Fantin et al., 2010). In post-natal retinal vascularization, microglia play a similar function and seem to act as bridges to aid tip cell anastomosis (Gerhardt, 2003, Rymo et al., 2011). Microglial loss results in decreased branching of the plexus along with reduced filopodia on tip cells, and a more radial trajectory of the growing sprouts (Rymo et al., 2011). *In vitro* experiments show that such an effect is dependent on two-way communication between microglia and ECs, reliant on the release of pro-angiogenic factors by the microglia, the identity of which still remains to be determined (Rymo et al., 2011). Microglia are also required to limit the extent of vascularization in the development of the deeper retinal plexus. Autocrine non-canonical Wnt signaling induces sFlt1 expression and secretion in microglia, limiting the angiogenic potential of the adjacent migrating sprouts (Stefater et al., 2011). Some evidence suggests that Notch1 is activated in microglia by Dll4 present on tip cells and Notch1 in myeloid cells is necessary for the correct recruitment of microglia to sites of anastomosis. Myeloid loss of Notch1 results in a vascular plexus that resembles macrophage ablation described above, with decreased branching and anastomosis (Outtz et al., 2011).

Overall it is becoming clearer that macrophages play a non-essential role in angiogenesis, fine-tuning the vasculature in some vascular beds during development. The interactions between ECs and macrophages still remain to be investigated as well

as the factors secreted by macrophages that are important in their modulation of angiogenesis.

1.9 Tubulogenesis and Lumen Formation

The process of angiogenesis must result in the formation of a functional vessel loop. Following EC activation, tip cell selection and sprouting, sprout migration and anastomosis, the newly formed vessel must lumenize. Vessel morphogenesis must occur without affecting the integrity of the tubular structure, whilst allowing the blood to flow through the newly formed lumen.

In vitro experiments with human endothelial cells in 3D matrix gels highlighted that lumen formation in such a model occurred through the development of intracellular pynocytic vesicles, which fused into a larger vacuole that subsequently fused with the plasma membrane giving rise to an intracellular lumen (Davis and Bayless, 2003). The evidence for the pynocytic nature of the intracellular vacuoles is the presence of extracellular membrane proteins and fluorescent tracer found within such vacuoles (Davis and Bayless, 2003). Integrins are important in the formation of such vacuoles in 3D matrix gels, with integrin $\alpha 2\beta 1$ necessary in collagen gels whilst RGD-dependent vacuole formation and lumenization in fibrin gels depend on $\alpha v\beta 3$ and $\alpha 5\beta 1$ (Davis and Camarillo, 1996, Bayless et al., 2010, Davis and Bayless, 2003). The formation of integrin-dependent vacuoles relies on the function of the Rho GTPases Cdc42 and Rac1, found localized to the intracellular structures. Expression of dominant-negative variants decreases vacuole and lumen formation (Davis and Bayless, 2003).

Figure 1.9 Models for vascular lumen formation.
A. The pynocitic vesicle fusion model. ECs form intracellular vesicle through pinocytosis, later fusing to a large vacuole. This vacuole fuses with the cell membrane, resulting in an intracellular lumen; adapted from (Kamei et al., 2006). **B.** Mechanism of lumen formation in the mouse dorsal aorta. Sialomucins are transported to the apical membrane in a VE-cadherin dependent process. Recruitment of Moesin and subsequent phosphorylation of MLCII , combined with the negative repulsive charge on sialomucins, leads to lumen opening and cell shape changes; adapted from (Strilic et al., 2009).

Cdc42 and Rac1 regulate lumen formation through the p21-activated kinases Pak2 and Pak4, which alter endothelial cell stability and cytoskeletal architecture respectively (Koh et al., 2008), signaling downstream to induce cell polarization though the polarity proteins Par3 and Par6 (Koh et al., 2008). A much-debated paper reported the involvement of pinocytic vacuole fusion in vivo where the authors describe the presence of Cdc42-positive vacuoles within ECs (Fig 1.9A) (Kamei et al., 2006). Time-lapse live imaging of eGFP-Cdc42 transgenic zebrafish embryos suggests intracellular pinocytic vesicle formation and intercellular vacuolar fusion leading to vessel lumenization, findings that were replicated through *in vitro* 3D tube formation assays (Kamei et al., 2006).

The importance of EC membrane polarization is supported by the activation of Par-family proteins (Koh et al., 2008). ECs do not have luminal-abluminal polarization when sprouting and must therefore specify these domains to allow the correct lumenization of the vessel. In formation of the aortic lumen, the targeting of CD34 sialomucins to the luminal membrane is important to induce lumen opening (Strilic et al., 2009). In this model, vessel lumen formation appears to be an extracellular event (Strilic et al., 2009). Sialomucins are found intracellularly prior to lumen formation and later relocalize to EC junctions that will form the luminal domain, relying on VE-cadherin for their relocalization. VE-cadherin may aid the exocytosis of CD34/podocalyxin vesicles by interacting with the phosphoinositide phosphatase PTEN. The requirement of VE-cadherin for the stability of vessels and lumen formation is also important in zebrafish (Montero-Balaguer et al., 2009, Wang et al., 2010a). Podocalyxin, a member of the sialomucin family, is required for lumen formation and the negative charge on sialomucins is required for EC repulsion leading to the initial opening of EC junctions (Strilic et al., 2009, Strilić et al., 2010). CD34 is connected to the actin cytoskeleton through interaction with the Ezrin-Radixin-Moesin proteins and this was shown to be through binding of Moesin, linking the sialomucins to F-actin. Moesin1 is required for ISV lumenization through its effect on luminal membrane formation and regulation of adherens junctions (Wang et al., 2010a). Experiments using PKC and ROCK inhibitors highlighted the requirement for PKC for Moesin1 phosphorylation, allowing it to connect CD34 to the cytoskeleton. ROCK is required for non-muscle MyosinII phosphorylation and activation needed to generate force to induce

cell shape changes to aid lumen opening, a VEGF-dependent process (Strilic et al., 2009). Overall such studies indicate that VE-cadherin-dependent relocalization of sialomucins is required for apical membrane specification and initial opening of the junctions, followed by recruitment of Moesin that is phosphorylated in a PKC-dependent manner. This links the apical membrane to the actin cytoskeleton, followed by recruitment of non-muscle MyosinII, ROCK induces MyosinII phosphorylation and the contractile force changes cell shape leading to lumen formation (Fig 1.9B). Recent 3D collagen assays have implicated RhoJ as another member of the Rho GTPase family in EC lumen formation. RhoJ exhibits endothelial-specific expression and requires the endothelial transcription factor ERG (Yuan et al., 2011). Loss of either protein results in increased activation of RhoA and downregulation of Cdc42 and Rac1 activity and their effectors, decreasing lumen formation (Yuan et al., 2011). The control of Rho GTPase activity is dependent on the Ras interacting protein 1 (Rasip1) and its binding partner Rho GTPase Arhgap29. *Rasip1*$^{-/-}$ embryos exhibit severe lack of lumen and mislocalization of Par3, suggesting defective apical membrane specification, and aberrant adhesion to the ECM (Xu et al., 2011). Loss of ECM adhesion is due to alterations in the cytoskeleton affecting integrin-ECM binding, effects that can be attributed to the increase of RhoA/ROCK/myosinII activity and the concomitant decrease of Cdc42 and Rac1 (Xu et al., 2011).

An alternative mechanism of lumen formation is observed in the zebrafish, which goes hand-in-hand with the unusual mechanism of PCV formation. ECs that sprout from the precursor DA to form the PCV engulf the developing erythrocytes via PI3K-directed migration (Wiley et al., 2011). It is not yet clear whether the differences observed between zebrafish and mouse are simply due to the identity of the vessels being studied but the most likely explanation is probably that a hybrid of the two models best describes lumen formation, where the apical membrane must be specified for initial lumen formation, and this is later expanded by vesicular fusion.

As described above, interfering with EC-ECM interaction through integrin activity can affect vessel morphogenesis and lumen formation. *In vitro* tubulogenesis is severely affected by the reduction of fibroblast-secreted ECM components (Berthod et al., 2006). Components of the basement membrane include laminins, heterotrimeric

basement membrane glycoproteins composed of an α, β and γ subunits, with various members present in each family. Loss of most subunits leads to early embryonic lethality. In the embryoid bodies sprouting assay *lamc1* deficiency (encoding laminin γ1) results in normal EC differentiation and vessel formation but increases the vessel diameter, an effect independent of flow but dependent on EC proliferation (Jakobsson et al., 2007a). Correct cell movement is required during tubulogenesis and lumenization, and is partially governed by EGF-like domain 7 protein (*Egfl7*). *Egfl7* is expressed in the developing vasculature of mouse and zebrafish. Deficiency in *egfl7* results in aberrant EC rearrangement and lumen formation (Parker et al., 2004), as a consequence of preventing EC junction release and the presence of ectopic junctions at the luminal surface (De Mazière et al., 2008). Embryonic vascular development is delayed in *egfl7* knockout mice, leading to embryonic lethality (Schmidt et al., 2007). Similar rearrangement defects are observed as in the zebrafish, with cells aggregating (Schmidt et al., 2007). The basement membrane shows mislocalization of components such as collagen IV. Egfl7 is found in the ECM suggesting that the migration problems are due to lack of spatial cues to direct polarization and tubule formation (Schmidt et al., 2007). This role in collective EC migration and tubulogenesis was reiterated in EB sprouting assays of *egfl7* knockout ES cells (Durrans and Stuhlmann, 2010). Moreover in neuronal stem cells EGFL7 can interact with all four Notch receptors resulting in inhibition of Jagged driven signaling (Schmidt et al., 2009). The miRNA miR-126 is found within intron 7 of *egfl7*. This miRNA is endothelial specific and believed to be the actual cause of the knockout phenotype. The phenotypes of *egfl7* and miR-126 knockouts are similar but not identical, and *egfl7* is also believed to be a miR-126 target. Overall it is clear that each take part in tubulogenesis during vasculogenesis and angiogenesis (Nikolic et al., 2010). Sphingosine-1-phosphate has been implicated in inducing metalloprotease-dependent migration and lumen formation (Bayless and Davis, 2003) and its role in this process is an active area of interest for a number of groups.

1.10 Endothelial Cell Junctions

An important function of the vasculature is the transport and exchange of gases and solutes with the tissue. This in turn implies that ECs must act as a selective barrier preventing the extravasation of red and white blood cells, platelets and other plasma components unless required. The barrier function of the endothelium must also be adapted to the particular tissue/organ in which it resides. In the central nervous system the vascular permeability must be tightly controlled due to the delicate homeostasis of neuronal tissue and therefore ECs have to prevent vascular leakage that could be fatal. On the other hand in the kidney where blood is filtered for metabolic waste, ECs possess small pores (10 nm range) to allow a lot of small molecules to pass through the cell, a phenomenon known as fenestration. Endothelial cell junctions control the permeability of vascular beds and there are two main types of junctions: adherens and tight junctions.

Adherens junctions are formed by homophilic interactions of cadherins *in trans*. Cadherins are Ca^{2+}-dependent adhesion molecules consisting of a transmembrane glycoprotein. In ECs the main cadherins expressed are VE-cadherin and N-cadherin (Bazzoni and Dejana, 2004). N-cadherin has been shown to be important for the correct recruitment of pericytes, and functional blocking results in disturbed vascular morphogenesis (Gerhardt et al., 2000). N-cadherin does not localize to adherens junctions in the presence of VE-cadherin (Navarro et al., 1998). VE-cadherin (*cdh5*) is a type II classical-cadherin composed of 5 extracellular cadherin domains, a transmembrane region and a highly conserved intracellular tail (Fig 1.10A). It is one of the earliest endothelial markers and is expressed as a cell commits to the endothelial lineage (Breier et al., 1996, Larson et al., 2004). The cytoplasmic tail interacts with the armadillo proteins p120-catenin and either β-catenin or plakoglobin, through which it can indirectly interact with α-catenin, α-actinin, vinculin and ZO-1 linking adherens junctions with the cytoskeleton (Bazzoni and Dejana, 2004). VE-cadherin expression is regulated by ETS family transcription factors such as Erg and Ets-1 (Dejana et al., 2007). Snail family proteins such as Snail, Slug and Twist can directly interact with the VE-cadherin promoter, repressing its expression (Lopez et al., 2009), suggesting that some degree of endothelial-to-mesenchymal transition may be involved in the decrease

of junctional stability or initiation of sprouting. VE-cadherin deficiency in mice does not prevent the formation of the primary plexus but induces vascular remodeling defects resulting in embryonic lethality by E9.5 (Carmeliet et al., 1999). Morpholino knockdown of *cdh5* in zebrafish again does not affect axial vessel formation but prevents formation of new stable junctions during angiogenesis, preventing the formation of lumen (Montero-Balaguer et al., 2009).

The stability of adherens junctions is regulated through a couple of mechanisms, one of which is VE-cadherin phosphorylation. Certain tyrosine residues in the intracellular portion of VE-cadherin are phosphorylated by the activation of receptor tyrosine kinases such as VEGFR2. VEGFA induces Src-dependent phosphorylation of Tyr668 and is required for VEGFA-induced EC migration (Wallez et al., 2007), as well as increased permeability (Eliceiri et al., 1999). Deletion of the cytoplasmic tail can have effects on VEGFA-driven survival signals through VEGFR2 and Akt due to decreased VE-cadherin/VEGFR2/β-catenin/PI3K interaction (Carmeliet et al., 1999). Through interactions with ICAM-1, leukocytes can also induce VE-cadherin phosphorylation at Tyr 658 and Tyr731, binding sites for P120-catening and β-catenin respectively. These phosphorylation events are driven by the activation of Src and Pyk2 kinases, which increase leukocyte transendothelial migration (Allingham et al., 2007). VE-cadherin phosphorylation is negatively regulated by the presence of the EC-specific phosphatase Vascular Endothelial receptor-type PTP (VE-PTP) and loss of VE-PTP induces similar early embryonic defects to VE-cadherin deficiency, stressing the importance of regulated VE-cadherin phosphorylation and dephosphorylation (Dominguez et al., 2007). VEGFA and leukocytes are able to dissociate VE-PTP from VE-cadherin, allowing phosphorylation to increase vascular permeability (Nottebaum et al., 2008). The above-mentioned effects of VE-cadherin phosphorylation on permeability are also observed through phosphorylation of the other adherens junction components (Dejana et al., 2009). A second method of VE-cadherin regulation is through controlling its availability at the cell surface. Association of p120-catenin is believed to prevent VE-cadherin endocytosis, stabilizing EC junctions (Xiao et al., 2005). VEGF can induce the activation of PAK, through Src, Vav2 and Rac1, to phosphorylate VE-cadherin on Ser665 and allowing β-arrestin2 recruitment. This in

turn induces detachment from the cytoskeleton and clathrin-mediated endocytosis of VE-cadherin, thus increasing vessel permeability (Gavard and Gutkind, 2006). Angiopoietin-1 is able to block this by sequestering Src via mDia, resulting in the stabilization of junctions (Gavard et al., 2008). Cells stop proliferating at confluence through contact inhibition; VE-cadherin is required for preventing VEGF-induced proliferation (Lampugnani, 2003). Blocking adherens junction stability with VE-cadherin function blocking antibodies is able to reduce tumour growth and angiogenesis (Corada, 2001, Corada, 2002) and can induce the disassembly of newly formed vessels during development (Crosby et al., 2005).

As VE-cadherin binds β-catenin, adherens junctions can affect Wnt signaling through modulating the availability of cytoplasmic β-catenin. Wnt is involved in vessel stability (Phng et al., 2009) and Wnt/β-catenin is crucial for the establishment of the blood brain barrier (BBB) (Liebner et al., 2008). Endothelial specific deletion of β-catenin results in developmental defects and vessel instability (Cattelino, 2003).

Another type of junctional complexes found between ECs are tight junctions. Tight junctions are composed of three transmembrane proteins, the junctional adhesion molecules (JAMs), occludins and claudins. The architecture of endothelial tight junctions varies depending on the vascular bed, with most found in CNS vasculature due to the requirement for strong barrier function in the blood brain barrier. Occludins are four pass transmembrane proteins of ~65kDa with both the N- and C-temrinus found in the cytoplasmic side of the membrane. They are components of tight junctions but knockout experiments have demonstrated that they are not necessary for the formation of such junctions, even though occludins are expressed at high levels in the BBB (Bazzoni and Dejana, 2004).

Claudins have similar structure to occludins but share no sequence similarity and are much smaller (~22kDa) (Bazzoni and Dejana, 2004). ECs express a specific claudin, claudin-5 (Morita et al., 1999), whose loss results in defective BBB function for molecules below 800Da meaning there exists some functional redundancy with other claudins (Nitta et al., 2003).

Figure 1.10 Endothelial Cell junctional complexes.
A. Diagram of an adherens junction. VE-cadherin interacts through homophilic interaction *in trans* between two ECs. The juxtamembrane portion of the cytoplasmic tail can bind p120 or p0071 catenins. The C-terminal portion interacts with either β-catenin or plakoglobin, which in turn bind to α-catenin. α-catenin links VE-cadherin to the cytoskeleton through an unknown mechanism. VE-cadherin is represented as helical trimmers as this is currently the model used to describe the homophilic interactions; adapted from (Wallez and Huber, 2008). **B.** Tight junction architecture. Claudins and occludins are clustered together through intracellular binding to zona occludins proteins (ZO-1/2/3) and MAGI plus MUPP1, linking the junction to the cytoskeleton. JAMs indirectly bind the cytoskeleton through cingulin. The formation of

such strands gives rise to tight junction belts in epithelial structures; adapted from (Niessen, 2007).

Most of what is known about tight junctions has been studied in epithelial systems due to lack of easily accessible models in the vasculature. There is some interdependence between adherens and tight junctions as adherens junction formation is required for the establishment of tight junctions in ECs and VE-cadherin is required for the upregulation of claudin-5 (Taddei et al., 2008).

1.11 A Model of Tubulogenesis – Drosophila Tracheal Morphogenesis

A well-studied model of tubulogenesis and anastomosis is the Drosophila trachea. Here I will describe its development, cellular and genetic events leading to its correct morphogenesis and the similarities with what has been described in sprouting angiogenesis. Some slight differences in response to the various genes mentioned below are observed between different portions of the developing trachea but for the sake of this introduction I will describe a generalization of their effects and concepts.

1.11.1 Initiation of sprouting

The Drosophila trachea exhibits similar phases of development as the vasculature: differentiation of progenitor cells, initiation of sprouting and associated tip cell selection, sprout elongation to target tissue and anastomosis to form a functional network. The trachea forms from 10 ipsilateral clusters of ectodermal cells, resulting in 20 hemisegments composed of ~80 cells each that migrate and connect to give the tracheal network (Fig 1.11A). The specification of such cells is dependent on the expression of the basic helix-loop-helix-PAS transcription factors (bHLH-PAS)

trachealess (*trh*) and *Ventral veinless (Vvl)*, directing the ectodermal cells towards the tracheal fate and to the formation of the tracheal placode (Wilk et al., 1996, Anderson et al., 1995). Subsequently these 20 hemisegments invaginate and form tracheal buds (Fig 1.11B) through an EGF- and FGF-dependent mechanism (Cabernard and Affolter, 2005). Tracheal cells form primary branches and migrate towards sources of *branchless* (*bnl*) (Fig 1.11B'), an FGF family ligand (Sutherland et al., 1996). The migration is dependent on the expression of *breathless* (*btl*) in the tracheal cells, the sole Drosophila homologue of FGF-R (Klambt et al., 1992, Glazer and Shilo, 1991). FGF signalling leads to the phosphorylation of MAPK, which becomes restricted to the cell at the tip of the sprout (Fig 1.12A) (Ikeya and Hayashi, 1999). *Bnl* and *btl* are expressed throughout tracheal morphogenesis and are important in both the initial sprouting and subsequent elongation and migration of the growing trachea. FGF signalling alters cellular morphology, inducing filopodia extensions at the tip of the growing sprout, polarized in the direction of growth (Fig. 1.11B"') (Ribeiro et al., 2002, Sato and Kornberg, 2002). These primary branches can either connect to form the transverse connective or go on to form secondary branches which will then either become terminal branches or fuse with the neighbouring metameres (Samakovlis et al., 1996a). The pattern of primary and secondary branching is highly stereotyped suggesting the cues guiding the patterning are genetically encoded (Samakovlis et al., 1996a). On the other hand terminal branches that supply the tissue show large variability between embryos hinting at environment-regulated patterning (Samakovlis et al., 1996a). The environmental effects are dependent on the Drosophila version of the human HIF pathway, where *similar* (*sima*) is the closest HIF-1α homologue and the β subunit is represented by *tango* (Bacon et al., 1998), both bHLH-PAS transcription factors. *Sima* is degraded in an oxygen-dependent manner much like HIF and this is dependent on the prolyl hydroxylase *fatiga* (Bruick, 2001). *Sima* induces the expression of *btl,* the FGF receptor, in tracheal cells whereas in non-tracheal cells it induces the expression of FGF ligand *bnl*, therefore increasing responsiveness of tracheal cells whilst upregulating the morphogenetic cue required for growth (Centanin et al., 2008). In the early stages of tracheal development sprout growth is less dependent on hypoxia-driven gene expression, but this becomes more important in later stages, especially during terminal branching and the refinement of the network later in the life cycle (Mortimer and Moberg, 2009).

Figure 1.11 Drosophila tracheal morphogenesis.
A. The Drosophila trachea is composed of 10 ipsilateral metameres (one highlighted in yellow) resulting in 20 fused segments. Lumen is visualized by antibody staining for luminal marker. **B.** Primary branching of tracheal tubules is stimulated by Bnl leading to the initial sprouting of a bud of cell (B) followed by the formation of tip cells with filopodia projection (B') that migrate and intercalate to elongate the growing tubule with two tip cells present (B''). The two tip cells then differentiate into a fusion cell and a terminal cell (white asterisks), reliant on expression of *esg* and *pruned* respectively. The fusion cell goes on to anastomose and lumenized with a neighbouring tubule whilst the terminal cell will extend cytoplasmic projections to cover the target tissue, forming intracellular lumen to allow gas exchange (B'''). **C.** Fusion cells migrate towards one another (one marked with white arrowhead) whilst terminal cell branching is occurring (white asterisks, C-C'). Fusion cells make contact (C'-C''), move their cell bodies and lumenized the fusion point (yellow line, C'''-C'''). Adapted and modified from (Uv, 2003) A and B, and (Samakovlis et al., 1996a) C.

The tracheal system develops without any DNA synthesis, cell division or apoptosis, relying on the initial 80 or so cells contributed by each hemisegment (Samakovlis et al., 1996a). With no increase in cell numbers, the network must form by extensive cell migration, cell shape changes, rearrangements and intercalation. Tracheal tubules start off as paired cells with two cells per cross-section and undergo adherens junction rearrangement and cell intercalation, resulting in the formation of unicellular tubes that surround the lumen and possess autocellular junctions (Ribeiro et al., 2004).

This process is controlled by the presence of Dpp and Wnt at sites distal to the primary trunk tubules, allowing the thinning out and elongation of the sprouts as they grow towards target tissues. Dpp and Wnt prevent the expression of *spalt*, a transcription factor that inhibits cell intercalation and therefore leads to large multicellular tubules unless downregulated (Ribeiro et al., 2002).

1.11.2 Sprout elongation and tip cell selection

Expression of localized *Bnl* is dependent on the presence of the member of the TGF superfamily *decapentaplegic* (*Dpp*) (Vincent et al., 1997). Loss of Dpp signalling through the loss of functional receptors (*tk* and *punt*) results in lack of migration of tracheal cells, an observation mirrored by ectopic expression of Dpp that suggests Dpp is extremely dose sensitive, as both over- and underactivation affect migration. Defective migration is also caused by altering Dpp signalling specifically in tracheal cells, therefore *bnl* expression is not sufficient to induce migration. This FGF signal must be somehow integrated with the Dpp signal within tracheal cells to direct the growth (Fig 1.12A) (Vincent et al., 1997).

Similarly to sprouting angiogenesis, the Delta/Notch lateral inhibition pathway is important in the sprouting and tip cell selection in tracheal development. Btl-driven expression of *Delta* (*Dl*) is present in 2-3 cells upon initial sprouting (Ikeya and Hayashi, 1999), confirming its dependence on FGF. These cells also express pantip markers such as *pointed,* which later become restricted to two tip cells (Samakovlis et al., 1996b, Llimargas, 1999). *Dl* is later restricted to a single tip cell, which will assume

the fusion cell fate. Loss of *Notch* function increases the number of tip cells, with the concomitant increase in cells expressing the fusion marker *esg* (Ikeya and Hayashi, 1999, Steneberg et al., 1999). This coincides with a loss of restriction of MAPK signalling at the tip of growing sprouts, as well as the defective fusion of many sprouts, whereas terminal branching is decreased (Fig 1.12B) (Llimargas, 1999). The Notch target *hairy* is also able to affect tip cell differentiation by modulating *bnl* expression in muscles close to where terminal branching occurs. Loss of *hairy* results in higher *bnl* expression and higher number of terminal cells (Zhan et al., 2010).

1.11.3 Terminal Differentiation

Once the growing sprouts have migrated to their final destination they acquire the terminal branching fate whilst a small number must connect with adjacent subunits by anastomosis to give a complete network. Terminal branching occurs by the extension of cytoplasmic protrusions emanating from the terminal cell adjacent to the fusion cell at the tip of the sprout. Terminal cell branching results in a dense covering of the tissue, with thin processes containing intracellular lumen (Samakovlis et al., 1996a). Terminal cell fate is determined by the expression of terminal markers such as *pruned,* which encodes dSRF and regulates the cytoplasmic branching much like the mammalian SRF does (Fig 1.12B). Loss of *pruned* results in lack of terminal branching, whilst overexpression results in excessive and unregulated branching (Guillemin et al., 1996). *Pruned* expression is regulated by presence of *bnl* (Sutherland et al., 1996), whilst expression of terminal markers is repressed in fusion cells by *esg*. Importantly, other signalling pathways important in angiogenesis also have a role in the guidance of tracheal growth such as the Roundabout (Robo) and Slit family members involved in branch-specific pathfinding (Englund et al., 2002).

1.11.4 Sprout fusion/anastomosis

Tracheal sprouts are headed by a tip cell that begins to express a set of genes important for the fusion of the tracheal network upon reaching target regions (Samakovlis et al., 1996b). The first gene expressed is *escargot* (*esg*), which determines the cell to acquire the fusion cell identity. *Esg* is a zinc finger transcription factor part of the Snail family of transcriptional regulators. Esg expression is induced by Dpp, which is expressed in locations where fusion must occur (Fig 1.12B) (Steneberg et al., 1999). Accordingly, loss of Dpp signalling leads to a decreased number of fusion cells whereas gain of function manipulations increase *esg* expression and result in an increase in fusion cells. Interestingly modifying Dpp effects also affects terminal branch differentiation (Steneberg et al., 1999), hinting at signal integration with the Notch pathway to limit fusion cells.

Expression of *esg* kicks off the fusion cell genetic programme (Steneberg et al., 1999), initiating the expression of the other fusion markers: *dysfusion* (*dys*)*, headcase* (*hdc*)*, members only* (*mbo*)*, shotgun* (*shg*)*, bloated tubules (blot), CG13196* and *CG15252.* These genes are expressed in an order related to the cellular functions they play during the fusion process. *Dys* is a bHLH-PAS transcription factor expressed in all fusion cells. Tracheal tubules in embryos carrying *dys* mutations migrate normally but fusion does not occur in most branches (Jiang, 2006). Filopodia from the two fusion cells come into contact but do not make firm adhesions, as a result of the failure to accumulate DE-cadherin (which is encoded by *shg*). Misexpression of *dys* results in reduced branching and migration, along with various ectopic fusion sites that lack detectable lumen through the fusion points (Jiang, 2006). To induce transcriptional activation *dys* must dimerize with *tango*, and together they bind various NCGTG binding sites (Jiang and Crews, 2007) and go on to activate the expression of *mbo. CG13196, CG15252* and lead to the upregulation of *shg* from basal levels (Jiang, 2006). *Dys* also indirectly affects levels of *trh* resulting in the downregulation of *btl* in fusion cells, thus preventing *bnl*-driven branching (Fig 1.12B)

CG15252 is an unknown protein, but it does share sequence homology with the bacterial FtsI protein that is a transpeptidase involved in cell wall peptidoglycan

synthesis and cell division (Errington et al., 2003), therefore its function in tracheal fusion remains unclear. The function of *blot* is also unclear, as it is a neurotransmitter symporter but has been linked to the formation of actin filaments in the apical cortex (Johnson et al., 1999).

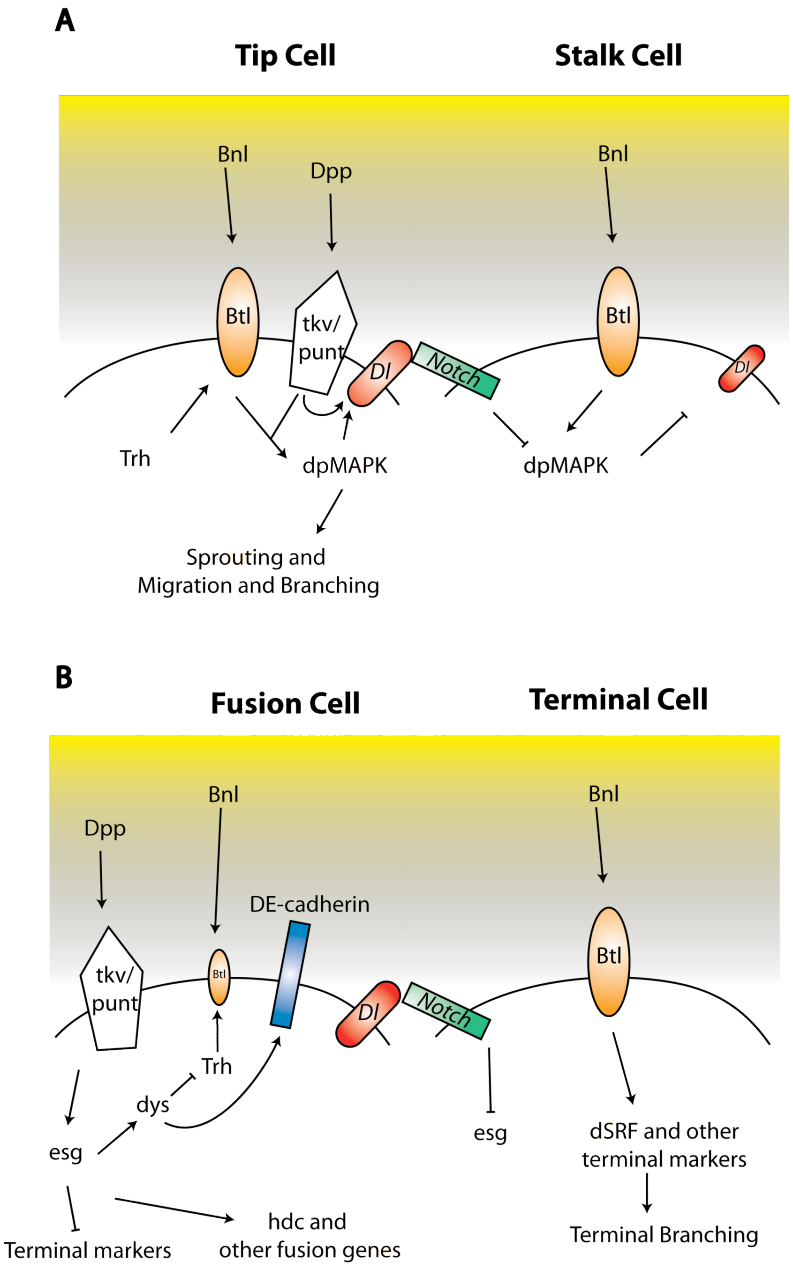

Figure 1.12 Pathways involved in control of tracheal sprouting and fusion/terminal cell fate determination.
A. Schematic representing the major signalling pathways that integrate to control tip cell selection and sprouting. Bnl and Dpp act on their cognate receptors Btl and

Tkv/Punt. Btl expression is induced by Trh, a bHLH-PAS transcription factor. Btl-driven signalling leads to MAPK phosphorylation and this somehow integrates with the Dpp-driven signal, leading to sprouting, migration and branching (Tip cell fate). Dpp signalling also induced the expression of Dl which activates Notch signalling in neighbouring cells, preventing the activation of MAPK, leading to a decrease in Dl as well as a decrease in migration and branching (stalk cell fate). **B.** Upon secondary branching and reaching target tissue, tip cells must assume either a fusion cell fate to connect with neighbouring metameres or the terminal cell fate, which will supply tissues. Here Dpp induces expression of the fusion gene Esg, which leads to the expression of Dys. Dys in turn upregulates DE-cadherin that is required for fusion cells adhesion during anastomosis. Dys also indirectly decreases Trh levels, lowering Btl thus preventing extra branching in fusion cells. Esg also represses terminal cell markers, upregulates Hdc that non-autonomously prevents stalk cell branching, and other fusion genes. The neighbouring terminal cell receives Dl signalling through the Notch receptor which prevents the expression of Esg. This maintains high Btl levels that drive dSRF expression leading to terminal branching.

Mbo attenuates nuclear export of proteins (Roth, 2003) even though it is not clear what its target in fusion cells maybe. It could be important in the nuclear accumulation of *dys* to allow binding to *tango* and therefore affect gene expression. CG13196 is a zona pellucida protein (Jaźwińska and Affolter, 2004) and is likely to be involved in the formation of cell adhesion together with *shg*. Downregulation of CG13196 only slightly affects fusion but misexpression increases ectopic fusion events (Jiang, 2006).

Shg encodes the drosophila homologue of mammalian E-cadherin, DE-cadherin. It accumulates as a dot at the sites of initial contact between two fusion cells. This later expands to a ring as the fusion cell bodies move closer and the ring enlarges to allow the formation of lumen through the fusion point (Tanaka-Matakatsu et al., 1996). These molecular events are very similar to what has been described during zebrafish ISA anastomosis with regards to VE-cadherin accumulation and ring formation (Blum et al., 2008). Mutants with lower levels of DE-cadherin or mislocalization of the protein away from the junctions have defective fusion where either the spot does not expand or the ring fails to enlarge only allowing a very thin lumen to form (Tanaka-Matakatsu et al., 1996). *Shg* expression is *esg*-dependent as *esg* controls *dys* expression, and therefore *esg* mutants show defective DE-cadherin expression and accumulation. These mutants also display increased motility suggesting that affecting cell-cell contacts by downregulating DE-cadherin affects cell motility (Tanaka-Matakatsu et al., 1996).

Interestingly ectopic expression of DE-cadherin in such *esg* mutants was able to partially rescue to fusion defects observed, stressing the importance of making firm adhesions during anastomosis. *Formin3* is a member of the formin family, proteins that are involved in many actin-based processes, and is important in directing the accumulation of DE-cadherin at fusion sites as well as in the formation of actin structures required for the lumenization of the newly connected tubule (Tanaka, 2004). The importance of adhesion molecules such as VE-cadherin during anastomosis has been demonstrated in zebrafish ISA sprouting and anastomosis (Abraham et al., 2009).

1.11.5 Headcase

Hdc is a peculiar protein as it contains no conserved structural/functional domains and is in a protein family that is solely composed of its orthologues. It is cysteine rich, has a pI of 9.6 and accumulates in the cytoplasm of Drosophila cells and therefore it is thought to be involved in protein-protein or protein-RNA interaction (Weaver and White, 1995). *Hdc* was originally discovered in imaginal discs where it is expressed just prior to re-entry of cells into the mitotic cycle, but expressions ceases before the end of proliferation (Weaver and White, 1995). Loss of *hdc* expression neither prevents imaginal disc formation nor changes in their size but causes pupal lethality and affects the development of adult tissues to varying degrees. The tissues affected are the internal structures of the head, hence the gene name *headcase* (Weaver and White, 1995).

Hdc was later described as one of the fusion genes induced by *esg* and used as a marker for tracheal fusion cells. Its expression precedes cell-cell contact (Samakovlis et al., 1996b). Embryos mutant for *hdc* are still able to specify tip cells but extra branching occurs. Misexpression of *hdc* has the opposite effect and reduces terminal branching. These effects are non-autonomous suggesting that *hdc* is preventing its neighbour in the stalk from expressing pantip markers and terminal branching genes (Steneberg et al., 1998). Interestingly the *hdc* gene contains 2 ORFs but only the full length ORF can rescue mutant embryos, though it is not clear whether the smaller fragment has a function working together with the larger one (Steneberg et al., 1998). As there is no

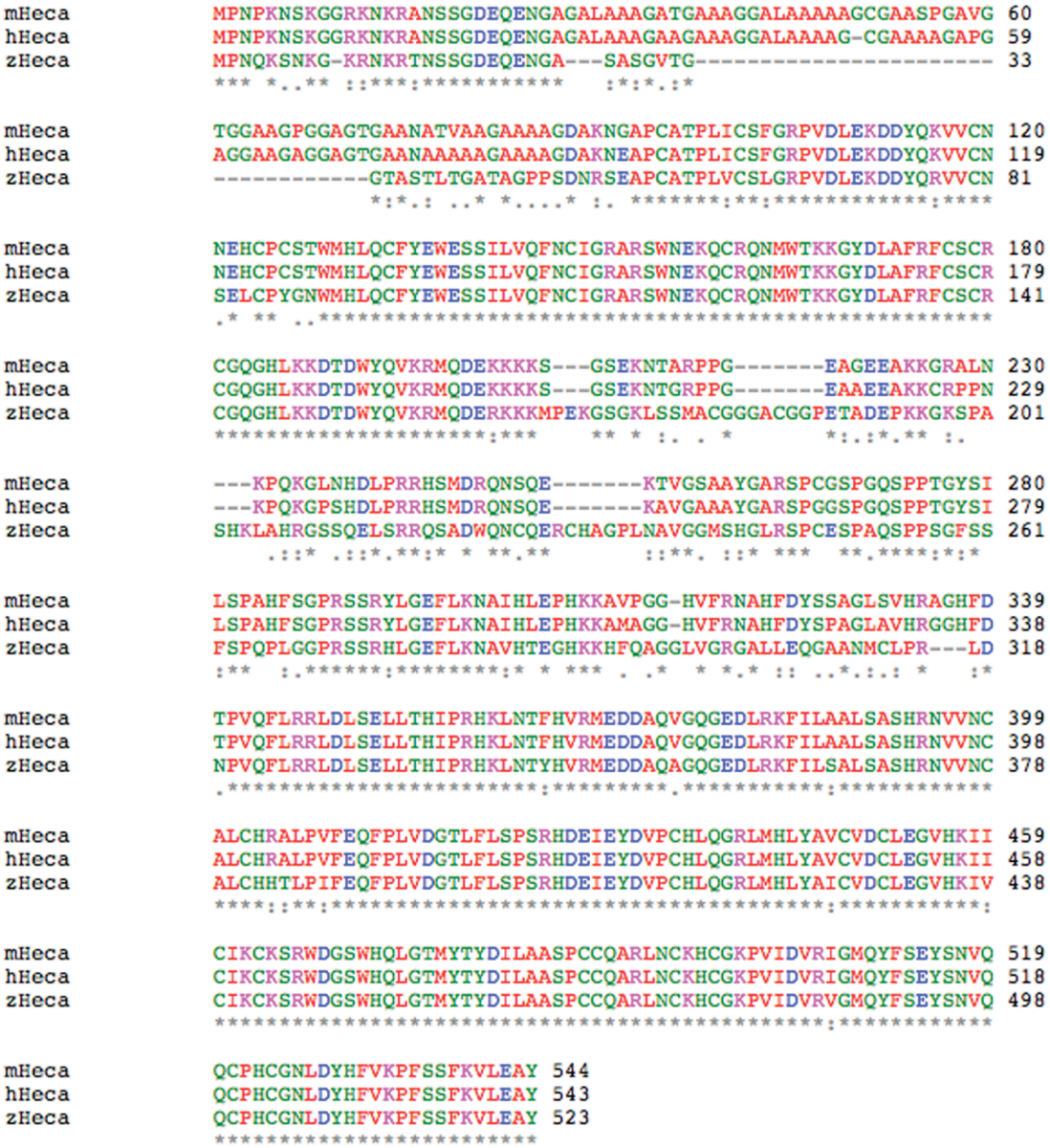

Figure 1.13 Fig 1.13 Protein sequence alignment of *heca.*
Amino acid sequence alignment of human, mouse and zebrafish of *heca* showing high degree of identity, especially at the C-terminus.

cell division during tracheal morphogenesis, *hdc* does not play a role in prefiguring cells for division in this context.

The mouse homologue of *hdc* is *heca*. It is well conserved between vertebrates showing 96% and 70% target identity with humans and zebrafish. The C-terminus is especially conserved showing ~90% identity in the last 100 residues (Fig1.13). The only other investigations regarding the function of *heca* have studied its role in tumours. Heca is expressed at lower levels in the blood or faeces in healthy patients compared to colorectal cancer patients.

The level of expression in cancer patients correlates with the stage of their disease and can be considered an early-stage marker (Chien et al., 2006). Another study reports that a chromosomal region that contains *heca* (6q23-q24) is commonly deleted in pancreatic cancers and ~80% of pancreatic and renal cell carcinoma lines tested show lower *heca* mRNA levels compared to healthy tissue (Makino, 2006)}. In oral squamous cell carcinoma (OSCC) *heca* is less abundant than healthy tissue, especially in basal cells (Dowejko et al., 2009). Overexpression of *heca* in OSCC cell line PCI 13 increases doubling time by 45% and holds cells in G2/M phase, decreasing the number of proliferating cells down to 30% compared to control (Dowejko et al., 2009). No other work investigating the *heca*'s role in tubulogenesis in vertebrate networks (lung, kidney, angiogenesis) has been undertaken.

It is clear that many parallels can be drawn between sprouting angiogenesis and tracheal morphogenesis, for example:

- The requirement for the presence of a morphogen to attract sprout growth and the expression of its cognate receptor in migrating cells
- The role of Dl/notch in the selection of tip/fusion cells
- Regulation of patterning at the genetic and environmental level
- The integration of many pathways leading to a well patterned network (Dpp/TGF. Slit, Robos, Wnts)
- The necessity of anastomosis to form a functional system

1.12 Summary

Vascular development is a complex and tightly regulated process that ultimately enables the supply of oxygen and nutrients to an organism's tissues. Endothelial cells that make up the vasculature can be activated to grow through stimulation by VEGF and other pro-angiogenic factors. Many pathways are involved in the initial sprouting and guidance of vessel growth to result in a well-patterned, hierarchical and functional network. Similar tubular systems such as the Drosophila trachea show similarities in development at the molecular and cellular level, and can therefore be utilised to guide investigations into angiogenesis.

1.13 Aims of PhD

Angiogenesis is a very dynamic process involving multiple steps to lead to the formation of new functional vessels. Only in recent years have we begun to investigate this process in live organisms. This study set out to improve our understanding on the dynamics of sprouting angiogenesis with particular attention to anastomosis. *Headcase,* a gene expressed in Drosophila tracheal fusion cells, was investigated for its potential regulation of sprout fusion. Finally, as macrophages appear to play a role in angiogenesis, zebrafish embryos were used to visualize the interactions between ECs and macrophages.

Chapter 2. Materials and Methods

2.1 Zebrafish Experiments

Zebrafish were maintained at standard conditions (28°C, 14/10 hours light/dark cycle). Fish were fed daily, twice prior to mating.

2.1.1 Transgenic lines

A number of transgenic lines were used in the following studies:

Tg(fli:eGFP)^{y1} generated by Nathan Lawson ((Lawson, 2002) by cloning eGFP downstream of the *fli* promoter region.

Tg(fms:nfsB.mCherry) generated by Caroline Gray (Gray et al., 2011) which is comprised of :

- *Tg(fms:GAL4.VP16)i186* - the *fms* promoter driving the expression of Gal4.VP16

And

- *Tg(UAS-E1b:nfsB.mCherry)i149* - mCherry fusion protein with nitroreductase driven by UAS-E1b promoter

Tg (flk1:mG) which I generated by cloning the mG construct (gift of Richard Behringer) downstream of the zebrafish *flk1* promoter (gift of Markus Affolter)

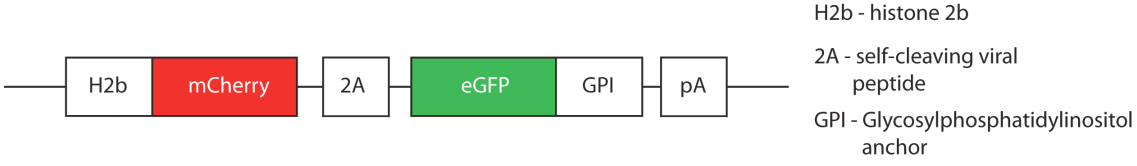

Figure 2.1 flk1:mG construct map

The mCherry-labelled H2b allows the visualization of nuclei whilst the GPI-anchored eGFP labels the inner leaflet of the cell membrane. The self-cleaving 2A peptide is a short stretch of amino acids that allows the bicistronic expression of the two transcripts and has been shown to work in both mice and zebrafish (Szymczak et al., 2004). This is a preferred method of expressing two transgenes from a single promoter as compared to using internal ribosome entry sequences (IRES), which give mixed results in zebrafish (Mizuguchi, 2000)

2.1.2 Morpholino Microinjection

Microinjections were performed using a 200nm borosilicate glass capillary tube to inject 2nl of solution into the yolk/cell of 1-4 cell stage embryos. The following Morpholino oligonucleotides (GeneTools) were used.

The *pu.1* Morpholino sequence has been previously published and shown to induce a significant knockdown in gene expression. (Su et al., 2007) The *heca* and *l*-plastin Morpholinos were designed to block translation (MO1) and splicing of the first and second intron (MO2). *p53* Morpholino was co-injected as Morpholino oligonucleotides can induce p53-dependent but unspecific toxic effects (Robu et al., 2007). The standard control oligonucleotide used was the one offered by GeneTools and should not have any off target effects.

Morpholino	**Sequence**
Control	5'-CCTCTTACCTCAGTTACAATTTATA-3'
Zf p53	5'-GCGCCATTGCTTTGCAAGAATTG-3'
Heca MO1	5'-TCCATCTTTTAAACACAGACGCCAT-3'
Heca MO2	5'-TGACGGTCGGTTCTTACCGCTTCTG-3'
Pu.1 (Su et al., 2007)	5'-GATATACTGATACTCCATTGGTGGT-3'
L-plastin MO1	5'-GATCTGTGCTGCTGCCATCTTCAAC-3'
L-plastin MO2	5'-CATGTCTCTGTACTGACCGACTTTA-3'

Table 2-1 Morpholino oligonucleotide sequences

2.1.3 Microangiography

Embryos were anaesthetised in 1X tricane and immobilised in a dish with low melt agarose. Qdot 655 (3 in10 dilution, Invitrogen) was injected using a glass capillary tube in the pericardial region.

2.1.4 Cell Proliferation Assay

EdU is a synthetic analogue of thymidine and is incorporated into DNA during its replication in S phase. Embryos were incubated in a diluted stock of EdU in fish water for the desired period of time. They were then fixed in 4%PFA for 2 hours at room temperature and subsequently washed with PBT. The Click-iT Imaging kit (Invitrogen) was used to detect EdU by adding azide-conjugated Alexa-Fluor (molecular Probes) that reacts with a chemical moiety on the EdU. Embryos were incubated in the detection solution for 2-4 hours.

2.1.5 Wholemount *in situ* hybridization

2.1.5.1 Probe generation

Zebrafish embryos were collected at 24 and 48hpf and lysed using a glass homogenizer (wheaton) with RTL buffer (RNeasy Mini it, Qiagen) an cleared using a QiaShredder column (Qiagen) and total RNA was isolated using the RNeasy Mini kit protocol. The isolated RNA was used to synthesise first strand cDNA using oligodT (20) primers and SuperScript III (Invitrogen) according to manufacturer's protocol.

Primers were designed to clone the full length *heca* cDNA (Table 2-2) for probe synthesis and later use. The cDNA was generated using *Taq* DNA Pol HotMasterMix (Eppendorf) and cloned into pCR2.1 TOPO® using the TOPO-TA cloning kit (Invitrogen). The plasmid was transformed into One Shot TOP10® (Invitrogen) competent cells and cultured on LB agar antibiotic selection plates at 37°C. Clones were selected and grown in LB broth containing antibiotic and the plasmid was isolated

using Mini/MaxiPrep kit (Qiagen). The plasmid was sequenced using the ABI BigDye Terminator v3.1 kit using the Applied Biosystems 3730 DNA analyser. Plasmids encoding the template for *in situ* probe synthesis were linearized so as to generate probes. The digests were checked on a 1% agarose gel and reactions where either cleaned using column purified (Qiagen) or gel purified. The following *in vitro* transcription reaction was set up:

1ug linearized DNA

1x Transcription buffer

1X DIG-labelled RNA labelling Mix (Roche)

1U RNasin (Promega)

1U T7 RNA polymerase (supplier)

The reaction mixture was made up to 20µl in nuclease free water. The reaction was incubated at 37°C for 2 hours and probe quality was assayed on a 1% agarose gel to check yield and correct size of band. Plasmid DNA was digested by adding 1ul of RNAse-free DNase I (Ambion) and incubating for 30 minutes at 37°C. The probes were precipitated by the addition of 2.5µl of 4M lithium chloride and 75µl of ethanol and incubated at -80°C for 30mins or at -20°C overnight. RNA was pelleted by centrifugation at 10,000*g* at 4°C and washed in 70% ethanol.

For Primer	Rev Primer
5'- CTCGGCTTGACAACCCCGT-3'	5'- TCAATAAGCTTCAAGAACTTTGAA-3'
5'-AACGCACGAATAGTAGCGGGGGCGAGC -3'	5'-TCCTGACAGTTCTGCCAATCTGCTG-3'
5'-GTCAGGCTTCTCCTCCTTCTCC-3'	5'-GGTTTCCCACAATGCTTGCAGTTC-3'
5'-GCAACAAGGGGAAGAGAAATAAACGCACG-3'	5'-AGGAACTCGCCCAGATGTC-3'
5'-TGAGGAGGCTGGATCTTTCAGAGCTGC-3'	5'-CCAGATTGCCGCAGTGAGGACACT-3'

Table 2-2 Primer pairs used to generate fragments for *in situ* probe generation

2.1.5.2 Solutions for ISH

- PBSTw: 1xPBS; 0.1%Tween20
- HB4: 50% formamide; 1.3X SSC; EDTA 5mM; yeast RNA 50ug/ml; 100ug/ml heparin; 0.2%Tween 20; CHAPS 0.5%
- 2x SSCTw: 2x SSC 0.1% Tween20
- Staining buffer (SB): 100mM NaCl; 50mM MgCl2; 10mM Tris pH 9.5
- 0.1% Tween 20
- Staining solution (SS): SB + 3.5ul of NBT and BCIP per ml

Solutions used up to and including the hybridization step were RNase-free

2.1.5.3 Fixation and rehydration

Embryos were dechorionated at desired stage and fixed overnight in 4% PFA. They were subsequently briefly washed twice with PBSTw followed by 3 washes for 5 minutes with PBSTw. 100% methanol was used to fix the embryos at -20°C for 30mins-1hr. Embryos were rehydrated by incubating with 75%MeOH/PBSTw for 5mins at RT, followed by 50% and 25% MeOH/PBSTw, finishing the process with 2 washes of 5mins in PBSTw.

2.1.5.4 Digestion and Hybridization

Embryos were digested with proteinase K for 2 mins. The proteinase K was removed and embryos were fixed with 4% PFA for 20mins at RT and washed twice in PBSTw for 1min followed by 3 washes for 5mins at RT. Embryos were incubated in hybridization mix at 65°C for 2 hours. Riboprobes were diluted 1:10 in HB4 (100ul final/embryo) and heated to 80°C for 10mins following cooling on ice. The hybridization solution was removed from the embryos and replaced with the diluted probes and incubated overnight at 70°C.

2.1.5.5 Colorimetric reaction

Embryos were washed twice for 30 mins in 2x SCCtW/50% formamide at 65°C, once in 2x SSCTw for 15mins at 65°C and twice in 0.2x SSCTw for 30mins at 65°C. Embryos were blocked in 5% sheep serum PBSTw for 2hrs at RT and incubated for 2hrs in 100µl of sheep anti-DIG Fab fragments at 1:2000 in PBSTw at RT and subsequently washed 6 times at RT with PBSTw for 5,10,15, 20,25 and 30 mins. The two subsequent washes were for 5mins with SB to equilibrate the embryos for the colour reaction. Staining solution was added and embryos were incubated at RT in the dark or at 4°C overnight. The reaction was stopped with the addition of EDTA.

2.1.6 Wholemount Immunolfuorescence antibody staining

Embryos were dechorionated at the desired developmental stage and fixed in 4% PFA for 2 hours at RT or O/N at 4°C. Embyos were then washed in PBS + 0.1% Tween20 (PBT) to remove PFA. Embryos were stained as described below and were post-fixed for 15mins in 4% PFA following antibody staining.

Antibody	Species	Reactivity	Supplier	Cat.No.	Dilution
BMP4	Rabbit	Mouse	Abcam	Ab39973	1:200
PECAM-1/CD31	Rat	Mouse	BD	553370	1:200
Heca (C-19)	Goat	Human	Santa Cruz	sc-103543	1;200
IsolectinB4-488	Griffonia	Mouse	Molecular Probes	I21411	1:500
P-Smad 1/5/8	Rabbit		Cell Signaling	9516	1:200
NG2	Rabbit	Mouse	Chemicon	AB5320	1:100
Snail	Rabbit	Mouse	Abcam	Ab17732	1:200
ZO-1	Mouse	Humn	Zymed	268404	1:200

Table 2-3 Antibodies used for immunofluorescence

Acetylated tubulin

This staining protocol was kindly provided by Claudia Linker from the Lewis lab at the London Research Institute. Embryos were washed five times in PBS + 0.5% Triton X-100 following fixation. Blocking was performed in PBS + 10% Goat serum, 2%BSA, 0.5% Triton X-100 and 10mM sodium azide for 1 hour at RT. Incubation with mouse monoclonal anti- acetylated tubulin (1:300) was performed O/N at 4°C. Embryos were then washed 4x30mins at RT with PBS + 0.5% Triton X-100. Goat anti-mouse Alexa-568 (Molecular Probes) was used as the secondary antibody, O/N at 4°C. Six washes of 30mins with PBS + 0.5% Triton X-100.

Heca, Snail and P-Smad1/5/8

Embryos dechorionated and fixed in 4% PFA for 2hours RT and then blocked for 1 hour in PBS + 5% normal goat serum + 1% BSA + 0.5% Tween20. Embryos were incubated in primary antibody (1:200) O/N at 4°C in blocking solution. The following steps were performed as above using the correct secondary antibody.

ZO-1

Embryos were permebilized in PBST + 0.5% TritonX-100 at RT for 30mins. They were then blockedfor 2hours at RTin PBST + 0.1% TritonX-100 + 10% normal goat serum + 1%BSA and the antibody was added at in blocking solution and incubated O/N at 4°C. Six washes with PBST were performed, each of at least 30mins at RT, and one O/N at 4°C. Secondary antibody staining as normal.

Peptides used to immunise rabbits	
aa 442-457: CKSRWDGSWHQLGTMY	aa 487-502: GMQYFSEYSNVQQCPH

Table 2-4 Peptides used for immunization to generate anti-Heca antibodies

2.1.7 Confocal microscopy

For live imaging, embryos were anaesthetised at the desired developmental stage using 1X tricane, dechorionated and immobilised in a cover slip Matek dish using 0.2% agarose. Embryos were imaged on a Perkin Elmer spinning disk confocal set up on a Nikon T2000 microsocpe using a 63X NA1.2 water immersion lens and kept at 28.5°C in an environmental chamber. Confocal stacks were taken every 1-2 minutes.

Fixed tissue samples were mounted on slides using Mowiol mounting medium and later imaged on a Zeiss 710 or 780 point scanning confocal microscope.

2.1.8 Reverse-Transcription PCR

2.1.8.1 RNA isolation

Embryos (~200) were dechorionated at the desired developmental stage and homogenized using a dounce homogenizer with the addition of 350 µl of Buffer RLT (RNeasy Mini kit, Qiagen) and the lysate was cleared of debris using a Qiashredder column (Qiagen). Total RNA was isolated using the RNeasy Mini kit according to manufacturer's protocol, using on-column DNAse I (Qiagen) digestion to remove genomic DNA. The concentration of RNA purified was measured using a NanoDrop ND-1000 spectrophotometer.

2.1.8.2 Reverse transcription

First strand cDNA was synthetized by reverse transcription of isolated RNA using the SuperScriptIII (Invitrogen) kit, with oligo $dT_{(20)}$ primers according to manufacturer's protocol. cDNA was incubated with RNase H for 20 minutes at 37°C to remove the

remaining RNA. The cDNA was then used along with the appropriate primers to carry out a PCR reaction and the products were separated on a 1% agarose gel.

Forward Primer	Reverse Primer
5'-GTAACCCCAGACGCAGAGGCTCC-3'	5'-AAGCACCACCTCCGCAGGCC-3'

Table 2-5 Primers to test *heca knockdown by RT-PCR*

2.1.9 Quantitative Relative PCR

cDNA generated was used to carry out the qPCR reaction. The Taqman Gene Expression Assay system was employed (Applied Biosysitems) following the manufacturer's protocol.

Gene	Taqman probe ID
bact	Dr03432610_m1 or 435241E for mouse
heca	Dr03148787_m1
kdr1	Dr03432904_m1
lcp1	Dr03099284_m1
Snail	Mm00441531-m1

Table 2-6 Taqman qPCR probes used for gene expression assays

2.1.10 3-Dimensional Electron Microscopy

2.1.10.1 Zebrafish Immunostaining

Please see above for acetylated-tubulin immunostaining

2.1.10.2 Transmission Electron microscopy

Zebrafish were fixed at the desired stage with 2% PFA/ 1.5% glutaraldehyde in 0.1 M sodium cacodylate (pH 7.4) for 1 hour and post-fixed in 1% osmium tetroxide/ 1.5% potassium ferrocyanide for 1 hour, followed by staining with 1% tannic acid in 0.05 M

sodium cacodylate (pH 7.4) for 45 minutes at RT. An ethanol series was used to dehydrated the samples, which were then placed in acetone and embedded in Durcupan resin according to the manufacturer's instructions (TAAB Laboratories Equipment Ltd). Embedded embryos were cut into Ultrathin sections of 80 nm, post-stained with lead citrate and imaged in a Tecnai Spirit Biotwin 120 keV TEM (FEI Company). Images were captured using Ultrascan and Orius CCDs (Gatan Inc.) with TIA (Tecnai Imaging and Analysis, FEI Company) and Digital Micrograph software (Gatan Inc.) respectively.

2.1.10.3 Focused Ion Beam/Scanning Electron Microscopy (FIB/SEM)

Embryos were embedded as for TEM above. A razor blade was used to trim the blockface was trimmed to expose either a transverse or a lateral section through the trunk and polished in a UCT ultramicrotome (Leica Microsystems UK) with a 90° diamond trimming knife (Diatome) to ensure all faces were smooth and perpendicular. Excess resin was removed from the top and back surfaces of the sample to minimise the volume of non-conductive material; the sample was mounted onto a 12.5 mm aluminium stub (Agar Scientific) using silver paint (Agar Scientific) and carbon-coated (Blazers CED030) to reduce charging. The sample was placed in the stage of a Quanta 3D FEG FIB/SEM (FEI Company), and adjusted to a distance of 10 mm (where electron and ion beams intersect) and tilted to 52°. The block was imaged at an accelerating voltage of 5 keV and a current of 1.28 nA. The sample was positioned and orientated within the block by using secondary electron imaging mode (SEI, Everhardt Thornely Detector), whereas atomic number contrast of osmium within the tissue was imaged using a solid-state backscattered electron (BSE) detector. Up to 80,000 mm2 of the blockface were coarse-milled at an ion beam current of 65 nA (accelerating voltage 30 keV) removing superfluous resin to expose the embryonic tissue. A 1 mm layer of platinum was deposited using the chamber gas injection system on the block face above the AOI to to prevent edge erosion whilst milling and trenches were milled on either side of the AOI to prevent sputtering of milled material onto the AOI surface. Polishing was performed stepwise at 30, 15, 7, 5 and 3 nA until the surface was smooth. Milling conditions for the Slice and View run (S&V|, FEI Company) were 130610 mm at 50 nm

slice thickness at a current of 5 nA, giving a mill time of 73 s/slice. BSE imaging conditions were set at 5 keV accelerating voltage and 1.28 nA beam current with a dwell time of 30 ms, with an acquisition time of 108 s/image. The image width was 114.5 mm at 2048X1768 pixels giving a final lateral resolution of 56 nm^2/pixel. 693 images were collected over 35 hours.

2.1.10.4 Correlative Live-Confocal FIB/SEM

Embryos at 28 hpf were anaesthetized and immobilized as described above for confocal imaging. Embryos were maintained at constant 28.0°C in an environmental chamber throughout the imaging process. Time-lapse microscopy was carried out on a Zeiss Axiovert 200 M fitted with an LSM 5 Pascal system. Upon identifying a site of anastomosis that was deemed interesting, embryos were fixed in 2% PFA in PBS and the AOI containing the anastomosing blood vessels was imaged with 10X and 40X objectives for correlative measurements. Zebrafish were processed as for FIB/SEM as described above, and placed in specially designed moulds to aid the milling process (TAAB Laboratories Equipment Ltd). The confocal images of the fixed embryo were used to obtain measurements which aided the relocation of the AOI and the sample was manually trimmed and polished to a blockface 700 mm wide by 300 mm deep (including part of the yolk sac as an orientation marker) to expose a lateral cross section of the AOI . The sample was mounted on an SEM stub and imaged in the FIB/SEM as described above. The blockface was coarse milled up to the myotomes followed by orientation of the sample. Milling conditions for the S&V|run were 400X5 mm at 72 nm slice thickness at a current of 7 nA giving a mill time of 69 s/slice. BSE imaging conditions were set at 5 keV accelerating voltage and 1.3 nA beam current with a dwell time of 30 ms, giving an acquisition time of 108 s/ image. The image width was 148.6 mm at 2048X1768 pixels giving a final resolution of 72 nm^3/voxel. 1778 images were collected over 87 hours.

2.1.10.5 Serial Block Face/Scanning Electron Microscopy (SBF/ SEM)

Zebrafish embryos at 72hpf were fixed, immunostained and imaged as described above.

The sample was trimmed to expose a transverse section through the trunk and inserted into the 3View microtome (Gatan Inc.) in the chamber of a Quanta 200 VP-FEG (FEI Company). A 50 nm slice was cut from the face with a diamond knife and the surface was scanned by SEM. This process was sequentially repeated to collect 1000 slices over 15 h. Imaging was performed at an accelerating voltage of 4 keV in low vacuum mode (0.3 Torr) at 2048X2048 pixels with a pixel resolution of 24 nm^2.

2.1.10.6 3D Reconstruction and Segmentation of Data

The FIB/SEM datasets were processed in Adobe Photoshop for optimal brightness and contrast. Alignment, segmentation and reconstruction into a 3D volume were performed using Amira (Visage Imaging Inc.). SBF/SEM datasets were aligned and reconstructed into a 3D volume using Digital Micrograph (Gatan Inc.) and Imaris (Bitplane Scientific Solutions). Features were segmented using Amira and movies were made in Amira and Imaris.

2.2 Embryoid Body Assays

2.2.1 ESC Spheroid formation, Differentiation and Sprouting in Collagen

2.2.1.1 Culturing of Feeder cells

Irradiated feeder cells were seeded at 2.0-2.5x10^6 cells/well (6 well plate) in ES medium the day prior to culturing ES cells.

2.2.1.2 Culturing of ES cells

A vial of wildtype R2 ES cells was thawed by placing in a 37°C water bath, followed by addition of 3ml of ES medium in a 6 well plate previously seeded with feeder cells. The medium was changed after a day to remove all remaining DMSO. Cells can be split every second day after 1:10 split

Product	ES medium (ml)	Supplier	Catalog #
ES Medium			
DMEM Glutamax	406.5	Gibco BRL	61965-059
Foetal Bovine Serum	75	Gibco BRL	10270-106
HEPES (1M)	12.5	Gibco BRL	15630-049
Sodium pyruvate (100mM)	6	Gibco BRL	11360-039
Monothioglycerol (98%)	6.2μl	Sigma	M-6145
ESGRO LIF (10^7U/ml)	50μl	Chemicon	ESBG1107
Collagen type-I (3.0mg/ml)		Nutacon	5409
GlutaMAX		Gibco	

**EB medium does not contain LIF*

Table 2-7 Recipe for ES medium (and EB)

2.2.1.3 ES cell Differentiation (Embryoid bodies)

ES cells were split the same day as medium change. The medium was removed and the cells washed with PBS. 700μl of trypsin were added to each well followed by incubation for 5mins at 37°C. Cells were resuspended in 3ml of ES medium and 1/10 of the cell suspension was placed in each well (without feeder cells) followed by ES medium up to 3 ml. Plates were incubated at 37°C with 5%CO_2.

The following day cells were trypsinized again and resuspended in 7 ml of EB medium (NO LIF). Cells were counted and diluted to around 60,000 cells/ml. 10 ml of sterile water were placed in 10cm Petri dishes. 20μl droplets of cells suspension were placed inside the dishes' lid and the lids were carefully placed of the dishes containing water and incubate as before (D0).

2.2.1.4 Embryoinic body sprouting assay in collagen-I gel

The following were mixed in a 50ml falcon tube, collagen being the last thing added with VEGF final concentration 30ng/ml:

Reagent	Volume 1st layer (μl)	Volume 2nd layer (μl)
NaOH (0.1M)	1125	1210
10X E4 medium	1125	1210
HEPES	225	242
PBS	175.8	189
Glutamax	112.5	121
1X F12	6237	7351
Collagen	9000	9677
Total volume	**18000**	**20000**

Table 2-8 Collagen gel recipe for EB sprouting assay for 15 wells

600μl of suspension were added to each well (12 well plate) and allowed to polymerize in 37°C incubator for 4 hours. 4 days following ES body set up (D3) the ES bodies were flushed into a dish and ~15 were placed in each well with collagen. Another 600μl of collagen suspension were added on top of ES bodies and it was made sure that the collagen adhered to the well walls. This was allowed to polymerize for 4 hours in incubator followed by addition of pre-warmed EB medium (1ml/well). At D7 and D9 the medium was replaced.

2.2.2 Immunostaining

The medium was removed from the wells and the EBs were fixed with 750μl of 4% PFA at RT. The wells were then washed with PBS and the top layer of the gel was removed. If EBs are present on the lower portion of the gel then this was also taken.

Collagen gels were cut down to size and blocked as for immunostaining in the zebrafish.

2.3 bEND5 assays

bEND5 cells were cultured in DMEM medium + 10% FCS + penicillin/ streptomyocin at 37°C and 5% CO_2 .

2.3.1 Quantitative PCR

Cells were washed with PBS and then lysed with RLT buffer from the RNAeasy kit (Qiagen). The same protocol as for zebrafish RNA extraction, cDNA synthesis and qPCR was followed (probes in Table 2-6).

2.4 Mouse experiments

2.4.1 Whole mount immunostaining

Eyes from P5 wildtype pups were fixed in 4% PFA for 2hours at RT, washed in PBS to remove the fixative, followed by dissection of retinas from the eye. For more detail on dissection please refer to (Pitulescu et al., 2010). The immunostaining protocols were the same as for the zebrafish apart from IsolectinB4 and NG2 where the retinas were incubated in PBlec (PBS (pH6.8) + 1% Tween20 + 1mM $CaCl_2$ + 1mM $MgCl_2$ + 0.1mM $MnCl_2$), as well as incubating the sample plus staining reagent in PBlec.

Chapter 3. Qualitative and Quantitative Observation of Zebrafish Angiogenesis

The zebrafish vascular system firstly develops through the formation of the axial vessels in the trunk and tail of the embryo via vasculogenesis. The DA and the PCV form through the coalescing of differentiated angioblasts. Once the axial vessels are formed, primary angiogenic sprouting commences from the DA towards the dorsal aspect of the embryo and occurs ipsilaterally. To our knowledge no detailed studies investigating the migration of the ISAs, the associated filopodia activity and the anastomosis of such sprouts to form the DLAVs at high temporal and spatial resolution have been undertaken. In this part of the study I describe a series of qualitative and quantitative observations in transgenic zebrafish embryos using live confocal microscopy and 3D EM techniques aimed at improving our understanding on the dynamics of tip cell anastomosis and EC interaction with the environment.

3.1.1 Filopodia along the ISA suggests all ECs have some level of activation

Primary angiogenic sprouting in zebrafish embryos begins at ~23hpf, with ISAs sprouting from the DA and migrating along somite boundaries, between the notochord, the neural tube and the somites (Fig 1.4). The ISAs travel to the dorsal aspect of the embryo, bifurcate and anastomose with their neighbours to form the DLAVs (Fig 1.4) (Lawson, 2002). The use of the *fli1:eGFP* transgenic line allows for live imaging of such a process thanks to the endothelial specific expression of a eGFP that can be imaged using confocal microscopy (Lawson, 2002).

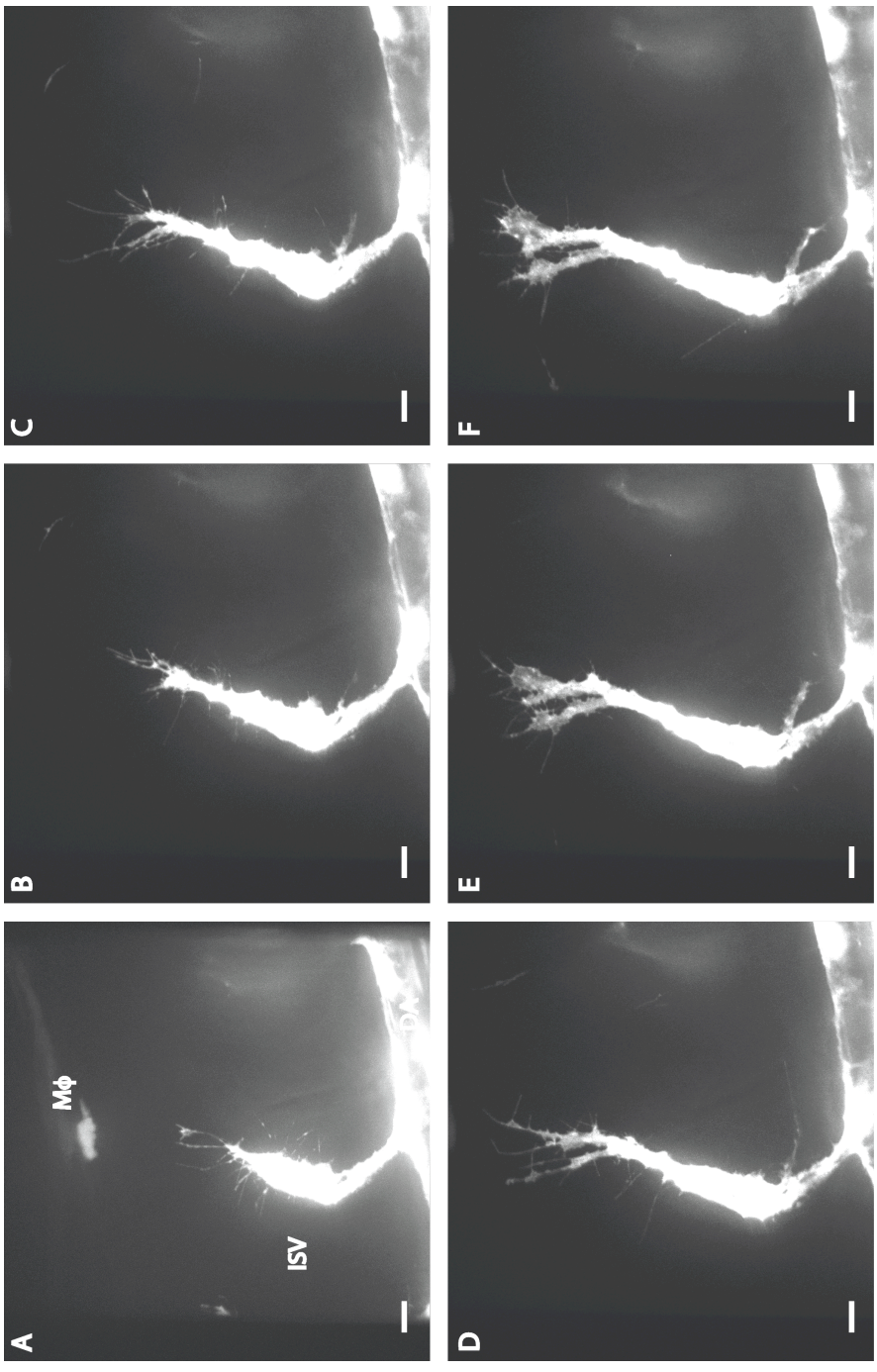

Figure 3.1 ISA sprouting from DA.
Stills from Movie1 showing ISA sprouting in Tg(fli1:eGFP)y1 embryo starting at 28hpf and growing towards the dorsal aspect of the embryo. Left is rostral, right is caudal, top is dorsal and bottom is ventral. Mϕ indicates a migrating macrophage. A. At 28hpf the ISA displays strong filopodia activity from its tip but also from the trunk of the sprout. B-D. The sprout grows towards the dorsal side of the embryo and squeezes between the neural tube and the somites. E-F. The ISA T-branches rostrally and caudally to make contact with adjacent ISAs , later leading to the formation of the DLAV. Scale bar represents 10μm.

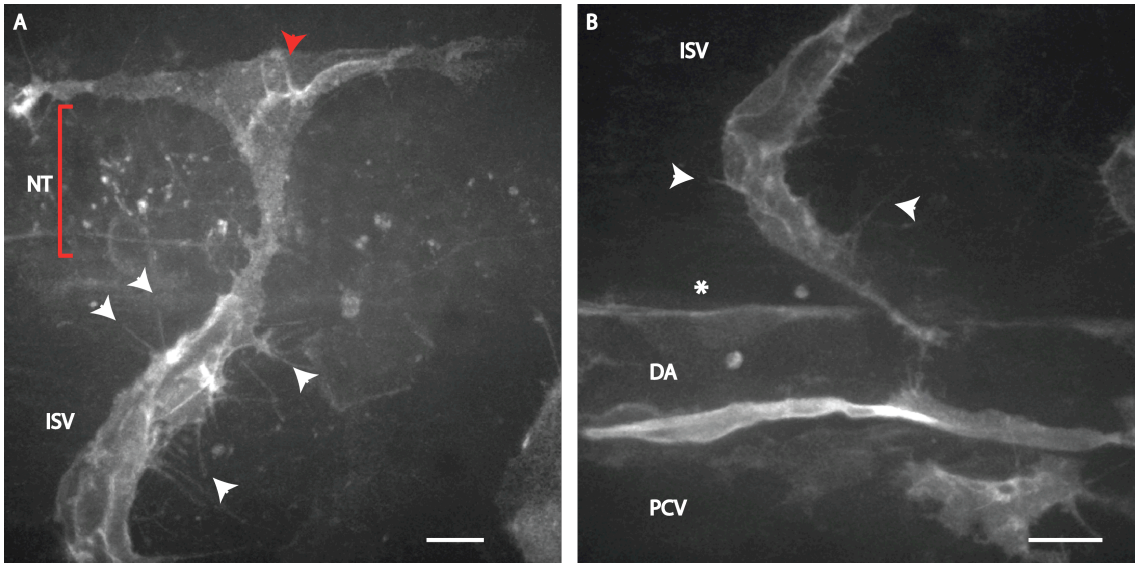

Fig 3.2 Filopodia Projections present on stalk cells.
Zebrafish embryo at ~30hpf that has been injected with *flk1*:mG. Transient expression of *flk1*:mG highlights EC membranes thus improving visualization of filopodia and the architecture of cell junctions. A. Top portion of the ISA showing filopodia projections along most of the sprout. White arrowheads highlight some of such structures. Red arrowhead indicates filopodia projecting over the current tip cell. Red bracket marks position of neural tube (NT). B. Lower portion of the ISA showing filopodia extensions even form the EC directly connected to the DA (white arrowhead). * denotes an area where no filopodia are observed, indicating that not all ECs will have basal filopodia activity as might be deduced when observing a sprouting ISA. DA – dorsal aorta; PCV – posterior cardinal vein. Scale bars represent 10μm.

Fig 3.3 Close up of ECs squeezing upon reaching neural tube
A. ISA sprouting in *Tg(fli1:eGFP)*^{y1} (from Fig 3.1). Red box indicates magnified area in B. **B-B‴'.** Magnified stills from Movie1 showing the change in cellular morphology of the ECs in the sprout upon reaching the neural tube (red dashed line in B), where space available for migration is restricted, thus the cells flatten and spread. White arrowheads indicate the formation of a lamellopodia-like structure. Scale bars represent 10μm.

Extensive use of this transgenic line in recent times has helped us understand the role of various signalling molecules in angiogenesis. Performing live imaging with a conventional point scanning confocal often leads to compromise on frame rate and dynamic range, requiring some image saturation to visualize fine structures within the embryo. Spinning disk confocals enable image collection at a high frame rate whilst maintaining a good signal to noise ratio and dynamic range, important when studying a dynamic process such as angiogenesis and anastomosis. I therefore set out to build on previous descriptions of the sprouting process and implement novel observations.

At 26hpf ISAs can be observed migrating with strong filopodia activity at the tip of the sprout (Fig 3.1), consistent with the current model of tip cell selection and sprouting that is governed by the Dll4/Notch – VEGFRs signalling axis (Siekmann and Lawson, 2007, Leslie et al., 2007, Hellström et al., 2007, Suchting et al., 2007). It is expected that the EC with the highest level of VEGFR2 leads the migration (tip cell), extending long filopodia to sample the environment for morphogenetic cues (Gerhardt, 2003). A puzzling observation is the presence of filopodia along much of the perimeter of the ECs in the sprout (Fig 3.2A). The stalk filopodia are made more noticeable by the transient expression of the *flk1:mG* construct. This is achieved by microinjecting plasmid DNA containing the *flk1:*mG construct and results in the expression of membrane targeted eGFP and thus EC membrane labelling (Fig 3.2.). Very weak expression in the neural tube can be attributed to *flk1* expression in the central nervous system (Fig 3.2A) (Hashimoto, 2003). Filopodia are present along most of the sprout's perimeter (Fig 3.2A-B, white arrowheads) but it must be noted that not all endothelial cells forming the vasculature posses such basal filopodia (Fig 3.2B, marked by *) suggesting that only ISA ECs show this basal activation. An attempt to differentiate the two types of filopodia can be made by describing their physical appearance and behaviour: the tip filopodia are longer, with greater curvature, longer persistence and appear to be actively searching; the stalk/basal filopodia are shorter, straight and project randomly. The searching behaviour of tip cell filopodia during angiogenesis has been attributed to the presence of VEGFR2 on their surface (Gerhardt, 2003), possibly acting as an amplifier of the effect of the VEGF gradient by exposing the cell to higher VEGF level that is present further away from the cell body. This will lead to an increase in response to VEGF in tip cells, upregulating Dll4 and establishing a more robust

mechanism of tip/stalk cell differentiation (Bentley et al., 2008). Membrane labelling of ECs using *flk1:mG* confirms that the sprout is comprised of several endothelial cells, with filopodia protrusions emerging from more than just the leading cells. The intricate cell junction arrangement between the ECs making up the ISA is also highlighted, reiterating recently reported localization of junctional molecules VE-Cad and ZO-1 (Blum et al., 2008). This cellular arrangement is unexpected when taking into consideration the latest model of ISA formation when this study was initiated, where it was believed that an ISA would most likely be composed of only three cells, one at the base, one making up the ISA and one in the DLAV (Childs et al., 2002).

The presence of these filopodia is at odds with the current simplified model of tip cell selection, where only the tip cell possesses filopodia. This does not directly negate the involvement of Dll4/Notch lateral inhibition as recent evidence has begun to build upon the initial model, albeit complicating the picture somewhat. Expression of inhibitors of Notch activation such as Jagged1 are able to modulate tip cells selection *in vivo,* and there are possibly more players in this pathway that will help modulate and fine tune tip cell selection (Benedito et al., 2009) and allow partial activation of trailing stalk cells. The general ISA ECs activation might simply be a result of the continuous competition in which the cells take part, battling for to increasing their Dll4 level and thus for the tip cell position (Jakobsson et al., 2010). These observations also fit with the description of a third phenotype of ECs that was recently described, the phalanx cell (Mazzone et al., 2009), which could ultimately divide ECs in quiescent (Phalanx) partially activated (stalk) and fully activated ECs (tip).

3.1.2 Changes in EC morphology during ISA migration

The ISA migrates towards the dorsal aspect of the embryo and bifurcates rostrally and caudally to make contact and fuse with the adjacent ISA (Fig 3.3). The environment surrounding the ECs changes as they progress towards the top of the neural tube where the DLAV forms. The sprouts start off close the DA, then passes between the NC and somites and finally between the NT and the somites (Fig 1.4B) During this journey the ISA is exposed to different signals that aid its migration, such as

VEGF, Hh, semaphorins, BMPs, Thsd7 to name a few. Furthermore the ECs experience spatial restrictions that force them to adapt their morphology accordingly. The space between the NT and the somites is extremely restricted (Fig 3.16, discussed later in chapter) and the ECs must squeeze into the space (Fig 3.3). This occurs via the formation of lamellopodia-like structures around existing filopodia projecting over the NT. The lamellopodia expand along the filopodia and join with adjacent lamellopodia to give a flattened sheet (white arrowhead Fig 3.3B”-B””). The resulting thin EC cellular process gives an imaging advantage thanks to the lower amount of eGFP present and decreasing the likelihood of saturation (Fig 3.3 and Fig 3.4A). This allows for even greater resolution of signal to the extent that the contrast allows the discerning of eGFP negative structures within the eGFP-filled cytoplasm of ECs. Vesicular and filamentous material can be spotted moving to and from the cell body and the region of high filopodia activity (Fig 3.4). Interestingly Rab13-driven trafficking of protein complexes containing RhoA and its specific GEF Syx from junctions to Grb2-VEGFR2 at the leading edge of migrating ECs has been shown to be important in directional VEFG-driven endothelial cell mobility (Wu et al., 2011).

3.1.3 Tip cell proliferation does not affect sprout elongation

In the mouse retina model of sprouting angiogenesis the differential response of tip and stalk cell ECs to VEGF leads to tip cells extending filopodia and migrating while stalk cells proliferate and are involved in the formation of a vascular lumen (Gerhardt, 2003). Recent work using an endothelial specific nuclear-localized eGFP has shown that the most advanced nucleus in an ISA sprout is able to divide (Blum 2008), suggesting tip cells in zebrafish embryo ISAs are able to proliferate. ECs are able to move along sprouts and shuffle towards the tip position (Jakobsson et al., 2010) therefore a cell’s phenotype cannot be so simply deduced by the position of its nucleus. Clonal analysis clearly indicates that single ECs within an ISA can extend from the DA all the way to the DLAV (Blum et al., 2008).

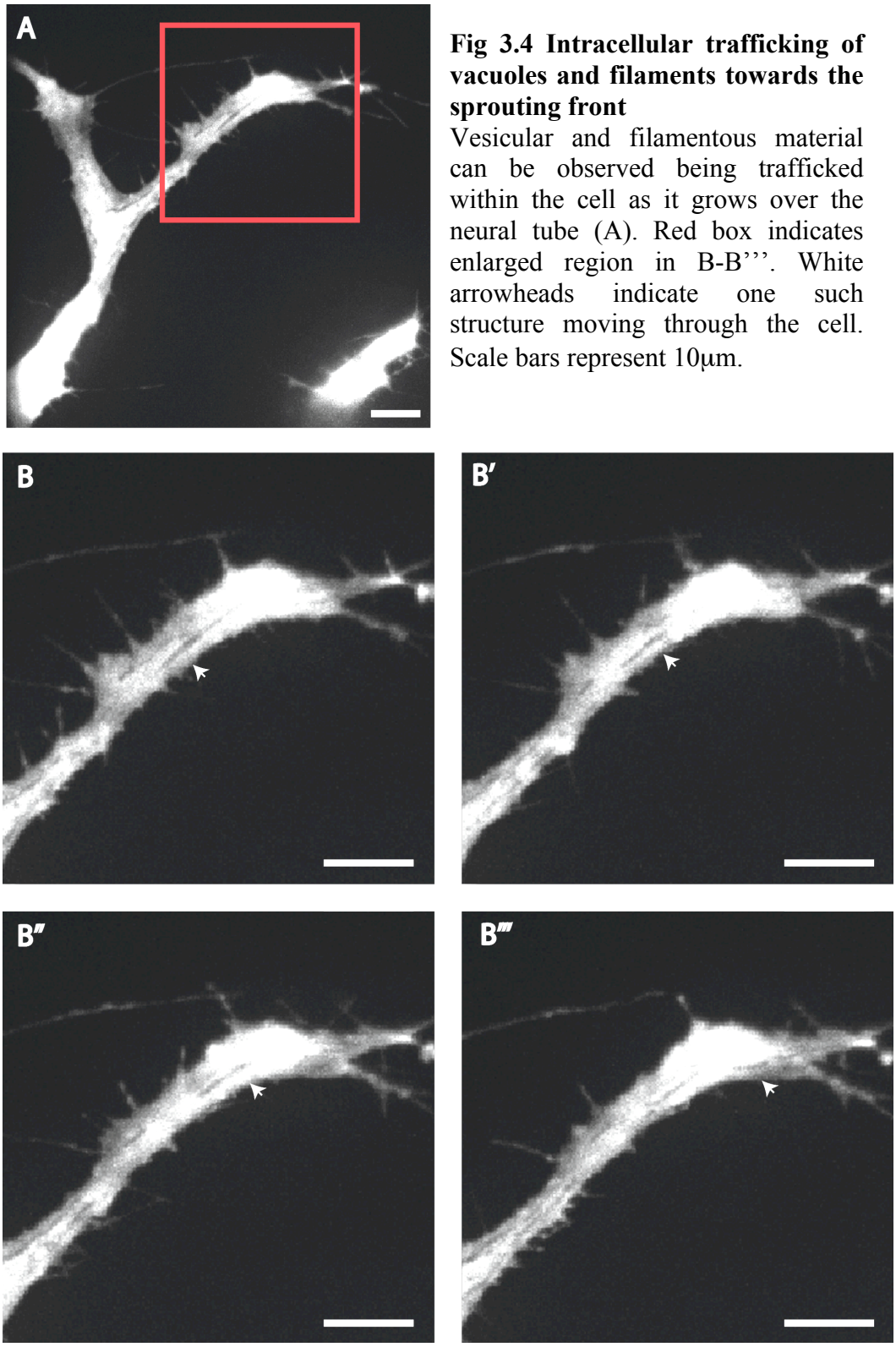

Fig 3.4 Intracellular trafficking of vacuoles and filaments towards the sprouting front
Vesicular and filamentous material can be observed being trafficked within the cell as it grows over the neural tube (A). Red box indicates enlarged region in B-B'''. White arrowheads indicate one such structure moving through the cell. Scale bars represent 10μm.

The position of the whole cell and its morphology must be considered when deterining the tip cell potential for cell division. The EC prepares for division by retracting its lamellopodia and someof its filopodia (Fig 3.5A-C). As the cell divides and undergoes cytokinesis, it acquires a blebbing appearance, which could be due to its attempt to extend filopodia whilst also attempting to round up for the division (Fig 3.5D-F). Soon after cytokinesis the EC reacquires its highly polarized and migratory behaviour, extending filopodia and lamellopodia (Fig 3.5G-H). Division does not have an effect on the overall tip cell selection/migration nor does it induce the formation of second tip cell as would be predicted from a computational model of sprouting angiogenesis involving the Notch/Dll4 – VEGFRs signalling axis (Bentley et al., 2009). The prediction entails that the presence of an additional cell would disrupt the Notch/Dll4 balance between adjacent ECs (tip and subsequent stalk) and thus allow the stalk cell to sprout due to the decreased exposure to Dll4 from the tip cell. Taking into account that there have been no reports of asymmetric Dll4 segregation during cell division in ECs, the newly formed daughter cell should begin battling with the original tip cell as their Dll4 levels are expected to be similar.

Other studies using clonal expression of RFP have shown that ECs in ISAs do not take part in as much tip cell competition/shuffling when compared with the sprouting EB system or in the zebrafish head vasculature (Gerhardt, personal communication (Jakobsson et al., 2010)), even though recent work reports cell overtaking in ISAs when observing nuclei (Zygmunt et al., 2011). Cell division also occurs during tip cell anastomosis, before patent connections are made and a lumen is established. The cellular behaviour is very similar to what is described above for migrating tip cells. The retraction of filopodia and rounding up is more obvious and the cell is able to completely round up, apart form the established connections with the neighbouring ISAs (Fig 3.6A-D).

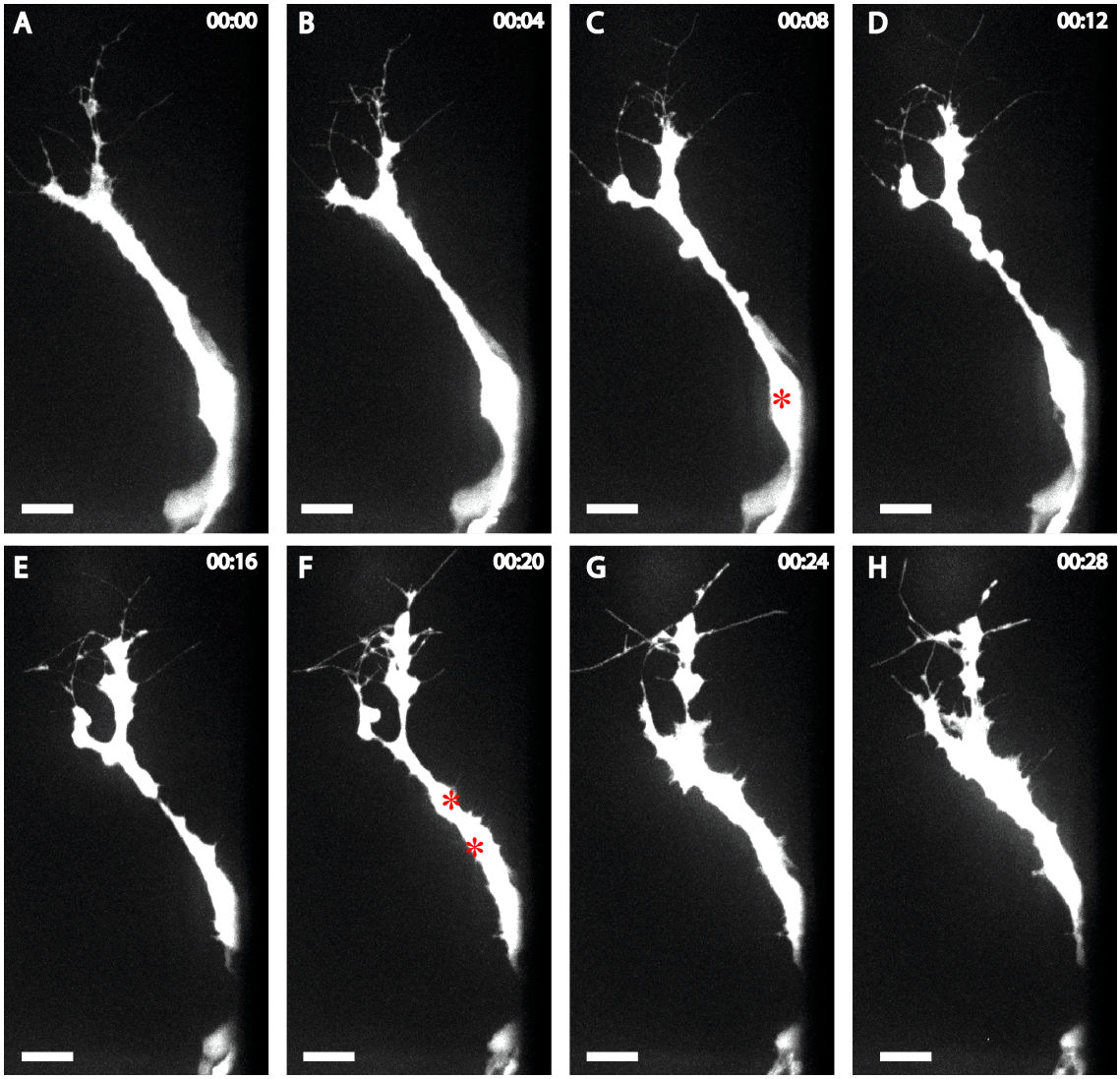

Fig 3.5 Tip cells proliferate in zebrafish ISAs.
Images showing an ISA tip cell retracting its filopodia (A-C), rounding up (C-D), undergoing division (E-G) and re-extending its filopodia (G-H). 4 minutes have elapsed between each image. Red asterisks indicate cell prior to division and the resulting two daughter cells following division. Scale bars represent 10μm.

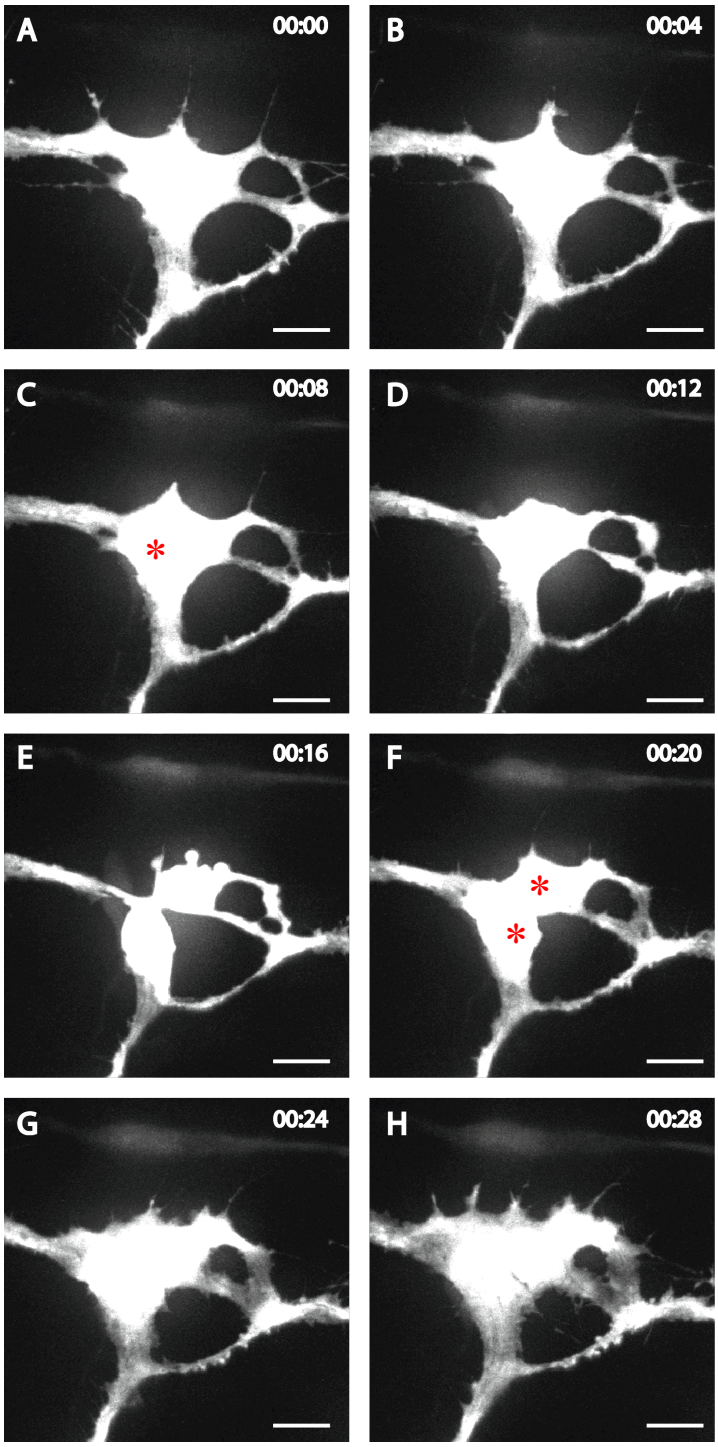

Fig 3.6 Anastomosing cells can undergo division without affecting connectivity of cells.
A tip cell in the process of fusing with adjacent ISAs undergoes cell proliferation, very much like the tip cell in Fig 3.7. The cell retracts its filopodia (A-D), rounds up and undergoes division (D-F) and assumes its previous morphology with filopodia projections (G-H). 4 minutes have elapsed between each image. Red asterisks indicate cell prior to division and the resulting two daughter cells following division. Scale bars represent 10μm.

3.1.4 Qualitative and quantitative observations of tip cell anastomosis

Once the ISAs reach the top of the neural tube they T-branch in rostral and caudal directions to make contact with the neighbouring ISAs and fuse together to form the DLAVs. Previous reports on anastomosis have been based on fixed mouse retinas where the analysis relies on snapshots of the event and inference of timeline and mechanism are extremely difficult. Such observations did not demonstrate the importance of filopodia in the initial stages of anastomosis (Gerhardt, 2003).

Live imaging of *fli1:eGFP* embryos allows us to appreciate dynamics of anastomosis (Fig 3.1, Movie1). Tip cells leading ISA sprouting and migration begin to branch rostrally and caudally and accordingly filopodia project to make contact with the adjacent ISAs (Fig 3.7). The exact interaction and timescale of anastomosis have not been previously investigated. The two tip cells make various contacts via their filopodia prior to remaining connected and forming a patent junction (Fig 3.7). From these images it is unclear whether there is active attraction between the cells/filopodia but one wonders whether such contacts could be made so regularly based solely on stochastic encounters. Most of these contacts do not result in anastomosis and their duration is extremely variable. Some tip cells undergo fusion within a relatively short time from the first contact while others require longer, with what appears to be a "negotiation" period. Such variables were quantified to establish whether any patterns of behaviour are noticeable. Fig 3.8 depicts the variables measured: duration of filopodia contact (A), number of contacts between two tip cells (B), length of filopodia at time of contact (C) and delay between contacts and anastomosis (D). Table3-1 gives an overview of the variables collected.

Tip cells are able to fuse upon first contact but in general tend to make multiple connections with a median of 12 contacts per ISA pair. Most of such contacts are short lived if one considers a range of 1-68 minutes where the median and 75% is 6 minutes (Table 3-1, Fig 3.9A). Filopodia pairs are able to remain connected for extended periods before releasing and single cases of 28, 38 and 68 minutes contacts have been observed (excluded from Fig 3.9A, right panel)

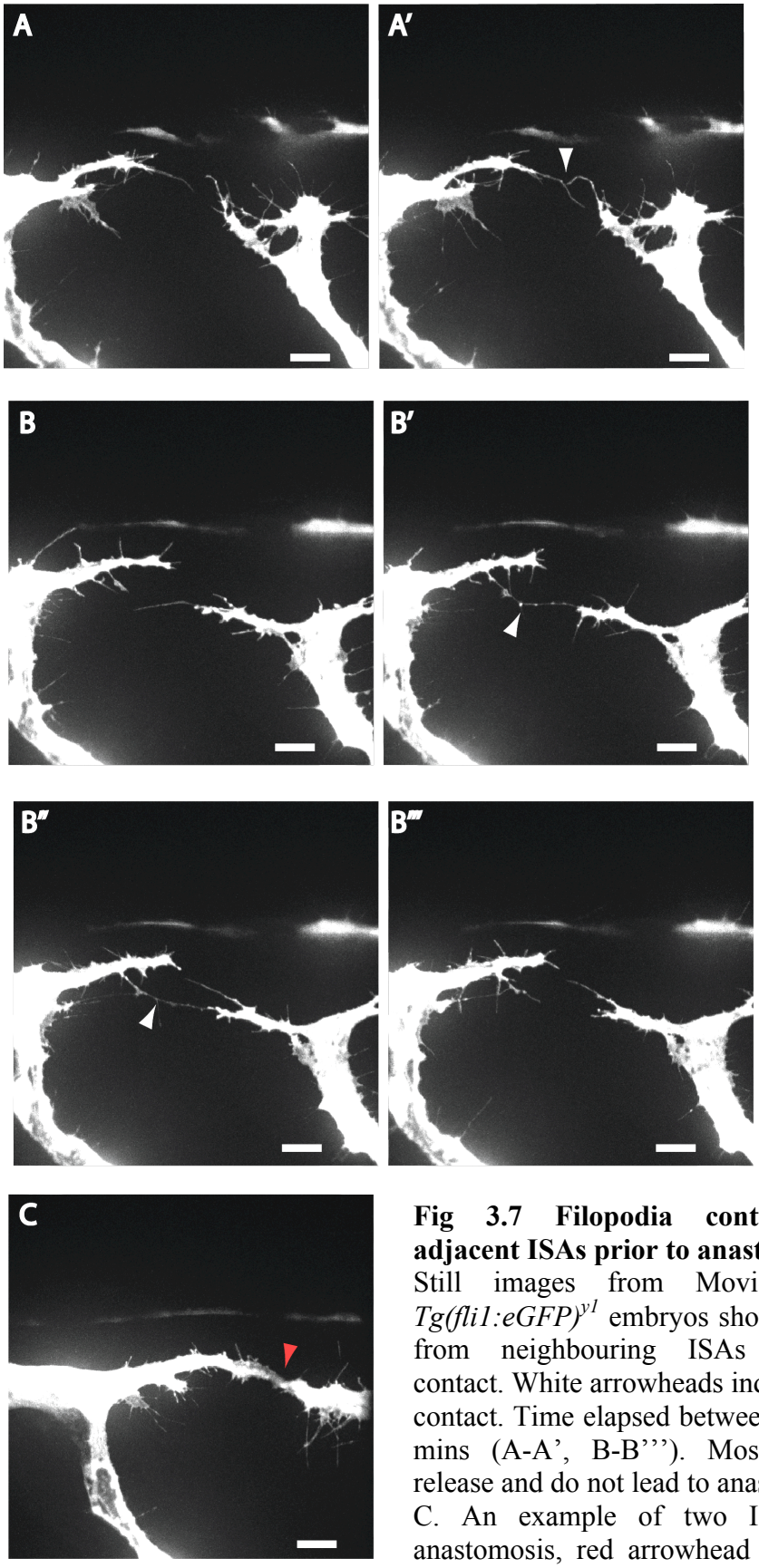

Fig 3.7 Filopodia contacts between adjacent ISAs prior to anastomosis.
Still images from Movie2 of 30hpf *Tg(fli1:eGFP)*^{y1} embryos showing filopodia from neighbouring ISAs coming into contact. White arrowheads indicate a point of contact. Time elapsed between each still is 2 mins (A-A', B-B'''). Most contacts are release and do not lead to anastomosis (B'''). C. An example of two ISAs following anastomosis, red arrowhead indicates point of fusion. Scale bars represent 10μm.

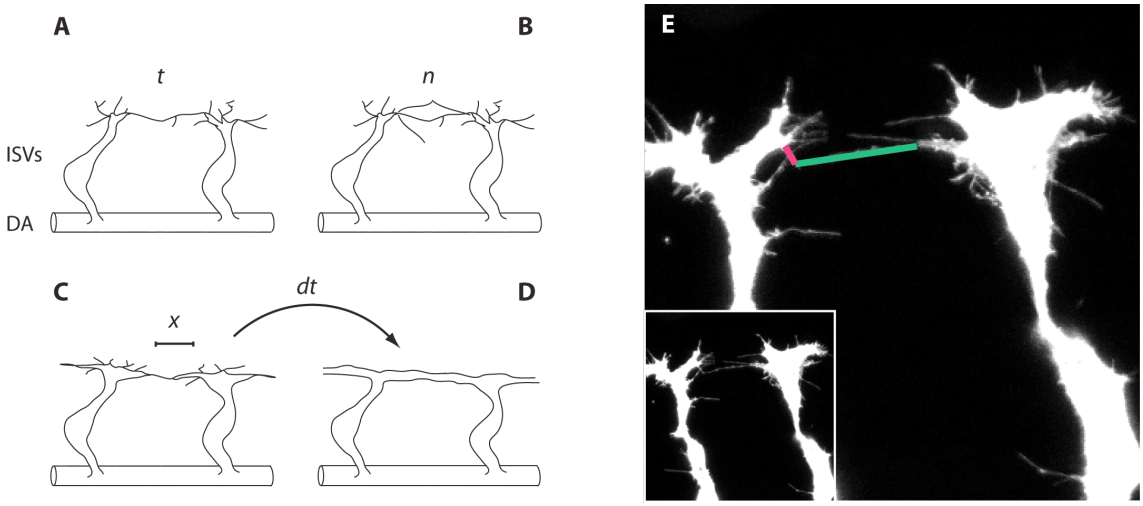

Fig 3.8 Anastomosis parameters for quantification.
A-D depict the various parameters that were quantified from various movies of ISA anastomosis: duration of contacts before release (A), number of total contacts prior to anastomosis (B), filopodia length at contact (C) and time elapsed between contact and fusion occurring (D). E. An example of stills showing how filopodia lengths were measured.

		Range	Mean	Median	25%-75%
# of contacts		1-37	15.46	12	7.5-23
Duration of contacts (mins)		1-68	5.76	6	2-6
Length of filopodia (μm)	**Fusing**	1.7-20.7	8.3	5.6	3.2-13.3
	Releasing	1.2-38.2	9.6	8.4	4.7-13.3
Time elapsed to fusion (mins)	**From 1st contact**	108-262	163	161	130-179
	From last contact	63-144	108	113	80-132

Table 3-1 Summary of quantitative parameters of anastomosis

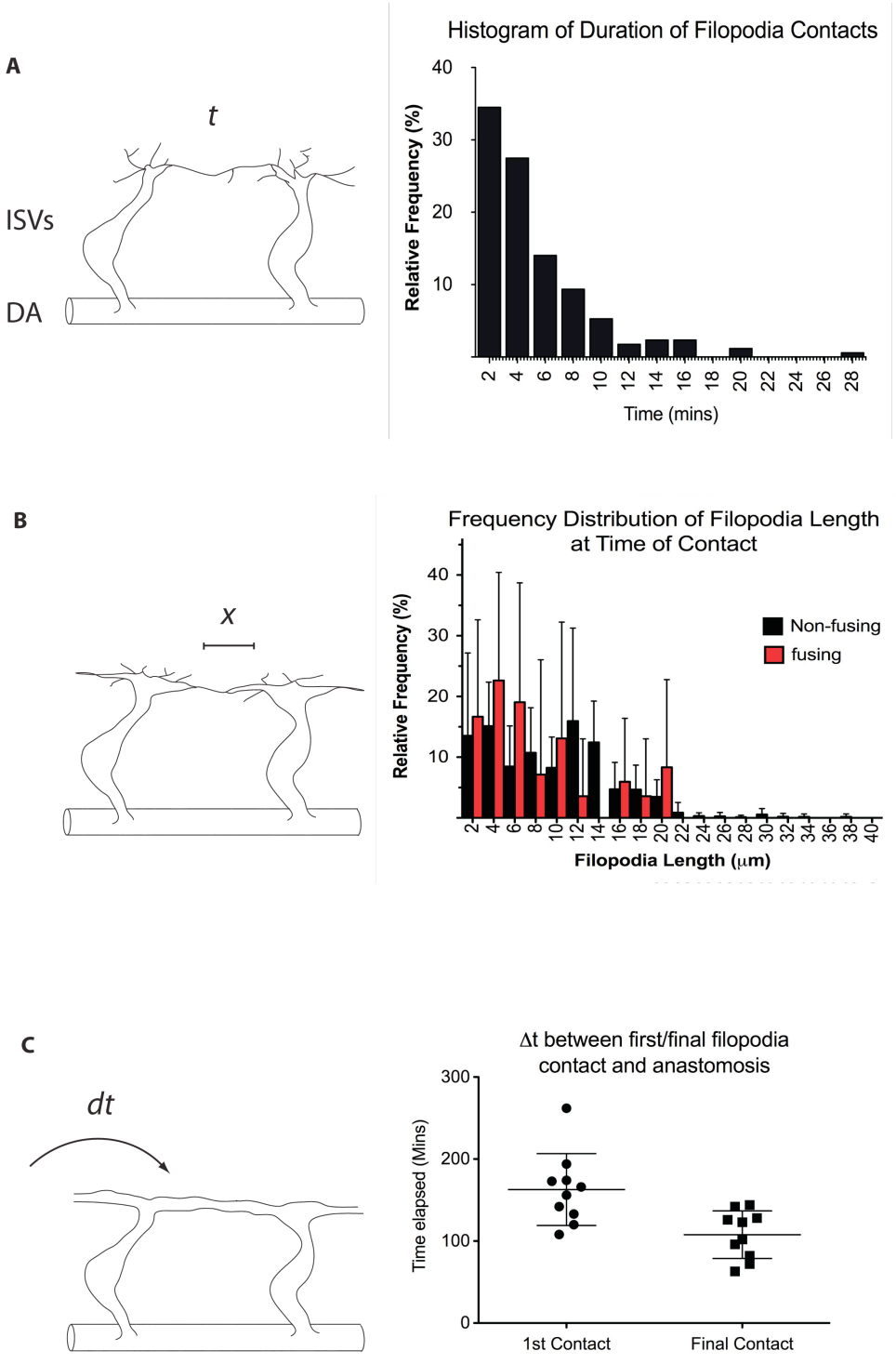

Fig 3.9 Quantitative parameters of anastomosis.
A. Graph showing frequency distribution of duration of filopodia contacts. Most are short lived (2-6 minutes). Two data points are excluded from the graph (38 and 68 minutes). B. Graph of fusing/non-fusing filopodia length. Error bars indicate SD. C. Graph displaying time delay between first contact and fusion as well as final contact and fusion. Error bars indicate SD.

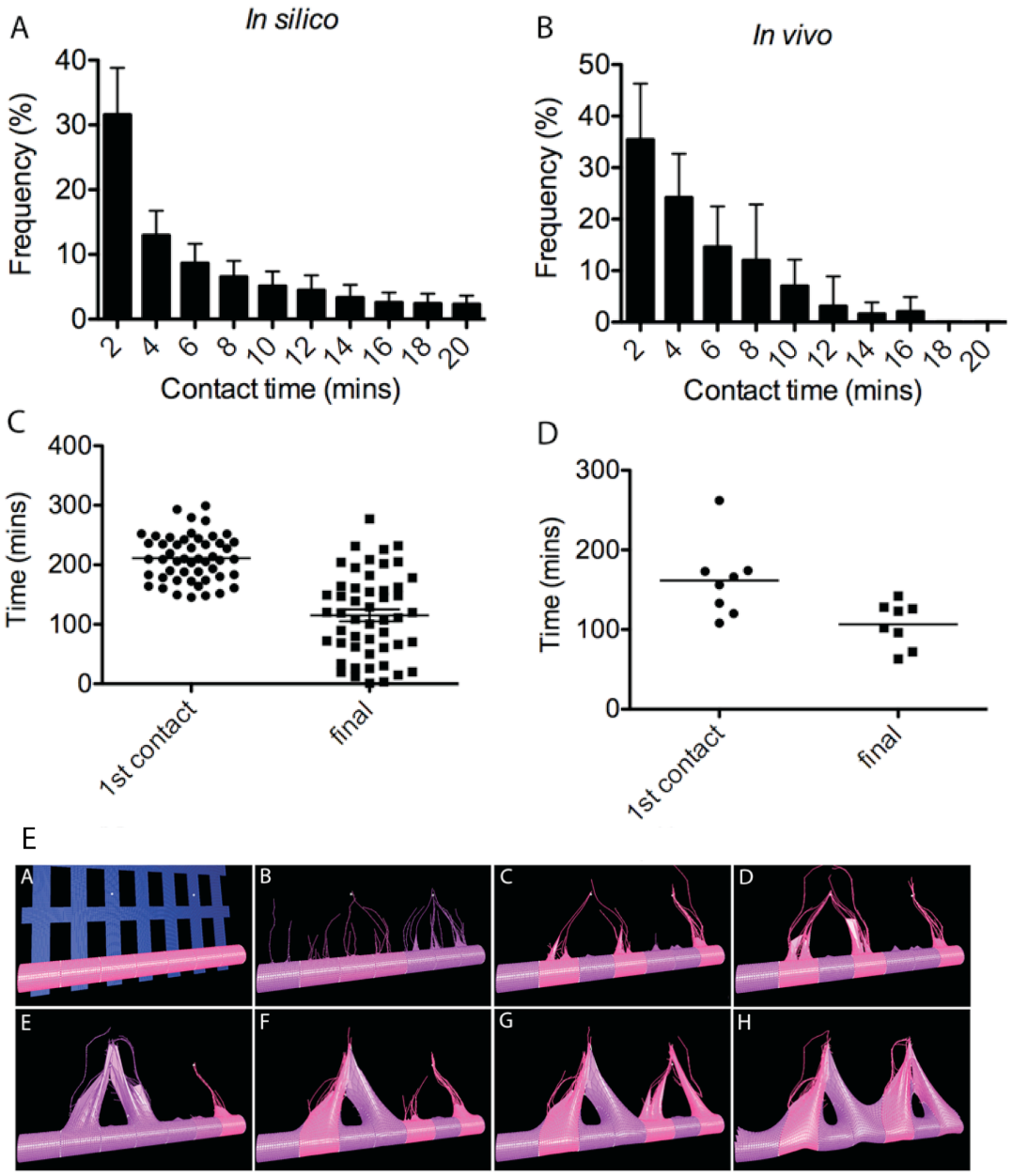

Fig 3.10 Comparison of quantitative parameters from *in vivo* and *in silico* experiments

Quantitative analysis of filopodia contact duration (A-B) and contact to fusion delay (C-D) from *in silico* simulations (A, C) and *in vivo* observations in zebrafish embryos(B,D). Error bars plotted as +/-S.E.M. **E.** Visual output of angiogenic tip cell selection model. All adapted from (Bentley et al., 2009).

Quantification of both fusing and non-fusing filopodia length resulted in some interesting observations. Filopodia that come into contact can be just over 1μm long and up to almost 40μm in length (Table 3-1, Fig 3.9B). Filopodia can also directly contact their neighbour's cell body. ISAs are actively migrating when they come into contact with their neighbours and therefore the time at which they come into contact plays a part in dictating the length of filopodia: the tendency is for the later the contact, the shorter filopodia as the cell bodies have moved closer. Filopodia that lead to anastomosis have a shorter maximal and average length but the latter is not statistically significant, most likely because of the dramatic variation in the data (Table 3-1, Fig 3.9B). The smaller average length at contact of fusing filopodia could be explained by: 1) a purely mechanical limitation to filopodia length, and if this is exceeded there is not sufficient force to hold the filopodia together and preventing their retraction; 2) a spatio-temporal aspect is involved such as the ECs need to find themselves in the correct environment to be prepared for fusion. As time passes and the cell bodies move closer, undoubtedly the filopodia will be shorter before they encounter the neighbouring cell.

The final parameters quantified were the delays between contact and fusion. The first value (first to fusion) refers to the time elapsed between the first time two tip cells come into contact via their filopodia and the moment when these two EC have formed a patent connection following anastomosis. The other value corresponds to the delay between the final filopodia contact between tip cells (as mentioned many might have occurred prior but released) and the fusion event. Of course the first to fusion parameter will always be larger compared to the corresponding final to fusion value unless fusion occurs at the first contact, in which case they will be the same value. The rationale behind these readings was to determine whether anastomosis was a rapid process (minutes) or occurred over a longer timeline (hours). The former scenario would hint towards a mechanism where tip cells are already primed for fusion when they come into contact and only require the relocalization of adhesion molecules to form a patent connection. The latter scenario would suggest that a genetic programme might be regulating anastomosis and thus the time for outside-in signalling, subsequent gene transcription and translation to occur is required. Interestingly the values for the final to

fusion delay range from just over one hour to almost two and a half hours. This hinted at a possible role of gene transcription in regulating anastomosis. This will be explored further in Ch.4.

These observation and quantifications were used to inform the generation of an updated agent-based computational model of angiogenesis (Bentley et al., 2008). The model emulates the Notch/Dll4 – VEGFRs signalling axis to select tip cells upon EC stimulation with VEGF. The quantitative filopodia dynamics data was used to integrate the effect of contacts and anastomosis in the model and determine how this affects the dynamics of tip cell selection. The model was validated by comparing parameters extracted from *in silico* simulations to the same parameters obtained from *in vivo* imaging. The data matched well (χ^2 test - $p>0.05$), suggesting that Notch/Dll4 lateral inhibition plays a role in anastomosis and vice versa (Fig 3.10). This was also confirmation that the set up of the new version of the model (Bentley et al., 2009) is accurately simulating the angiogenic process and predictions made are likely to have a biological significance.

3.1.5 Lumen formation

The process of angiogenesis must lead to the formation of a patent, lumenized and functional vascular loop to satisfy the increased metabolic demands of the target tissue. The process of vessel lumenization is another event in angiogenesis that has recently become of interest as previous models of its mechanism leave many doubts and unanswered questions. At the time this study was initiated, there was a much-debated model of lumen formation that involves pinocytosis and the fusion of intracellular vacuoles into larger ones until a continuous intracellular lumen is formed (Kamei et al., 2006). The pinocytosis and vacuolar fusion were shown to be integrin and Cdc42/Rac1 dependent (Davis and Bayless, 2003). A more recent study attempted to build on these observations and provides evidence for VE-cadherin localization to determine the site of primary lumen formation, with subsequent vacuole fusion to expand it (Wang et al., 2010a). In mice a role for VE-cadherin in lumen formation has been attributed to establishing EC polarity and the localization of CD34 sialomucins (Podocalyxin)

(Strilic et al., 2009). It appears that the negative charge of such proteoglycans at the apical, i.e. pre-lumenal membrane, is responsible for the opening of the lumen (Strilić et al., 2010).

Again the use of zebrafish embryos in the study of lumenization provides incredible details on the dynamics of the process. Observations of lumenization of ISAs in zebrafish embryos here presented suggest there could be multiple mechanisms of lumen formation. Often the junction between two ECs becomes more evident (Fig 3.11) and this correlates with the site of lumen opening. The ECs loosen their junction and this allows for transient opening but collapses immediately. The same junction later opens up once the lumen has pushed through the whole ISA (Fig 3.11). This suggests that the lumen forms via the polarization of the ECs and the selection of a particular junction to release, indicating that the lumen is extracellular and formed through the rearrangement of junctions. The lumen is established but is not visible until the whole vessel opens up. Such a model would be consistent with observations regarding the polarization and junction repulsion (Strilić et al., 2010). In other instances the lumen appears to be intracellular and pushes through the EC until it reaches other open lumen, readjusting the junctions to fuse forming a continuous tube (Fig 3.12, Movie3). Once the lumen is formed, there is still a requirement for ECs to proliferate to keep up with the expansion of the vasculature to supply the growing embryo. This poses a problem in small vessels such as ISVs as usually a maximum of 2 cells are present per cross-section and therefore the division of one cell may result in the loss of vessel integrity. This problem is overcome by the collapsing of the lumen prior to cell rounding (Fig 3.13 A-H), and following cell division the lumen is re-established (Fig 3.13 I-J).

The decrease in filopodia activity upon anastomosis and DLAV formation has been attributed to the Notch/Dll4 lateral inhibition (Leslie et al., 2007) as the two tip cells begin to inhibit one another thus decreasing their tip cell characteristics. Most filopodia activity does not decrease until the lumen is fully established, and the termination of filopodia protrusions is very abrupt (Movie4), suggesting that lumen and possibly blood flow actually play a big part in the dampening of EC activation, similar to recent reports on the effect of haemodynamic forces in zebrafish angiogenesis (Nicoli et al., 2010, Bussmann et al., 2011).

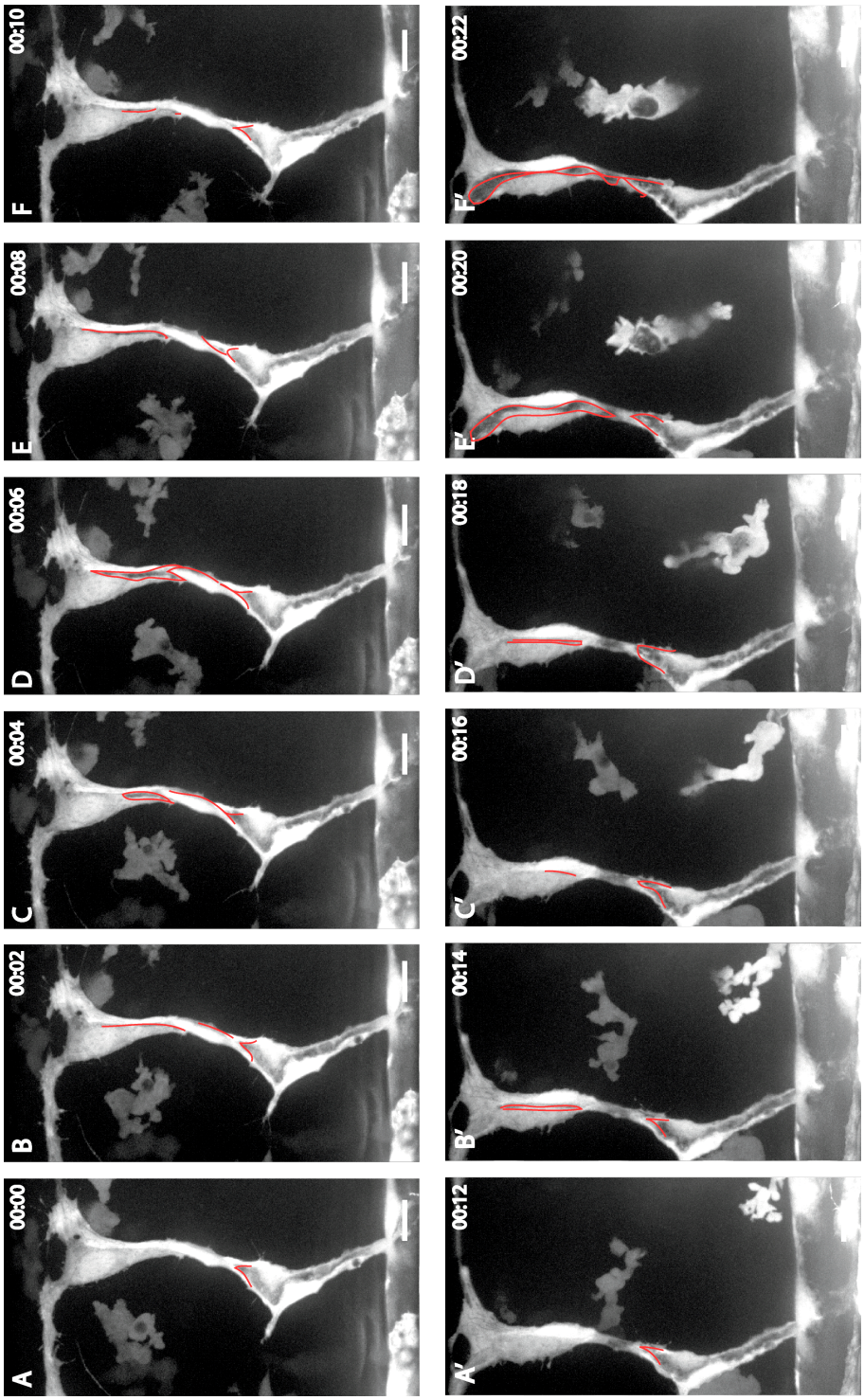

Fig 3.11 Lumen formation by EC junction opening
Images showing lumen opening in an ISA by the separation of EC cell junctions. The lumen opens briefly before collapsing (red line, A'-F'). Later the lumen opens throughout the ISA by the joining of the lumen formed from the DA in the lower part of the ISA and the one open by junction opening near the top of the ISA. 2 minutes elapse between each image. Scale bars represent 10μm.

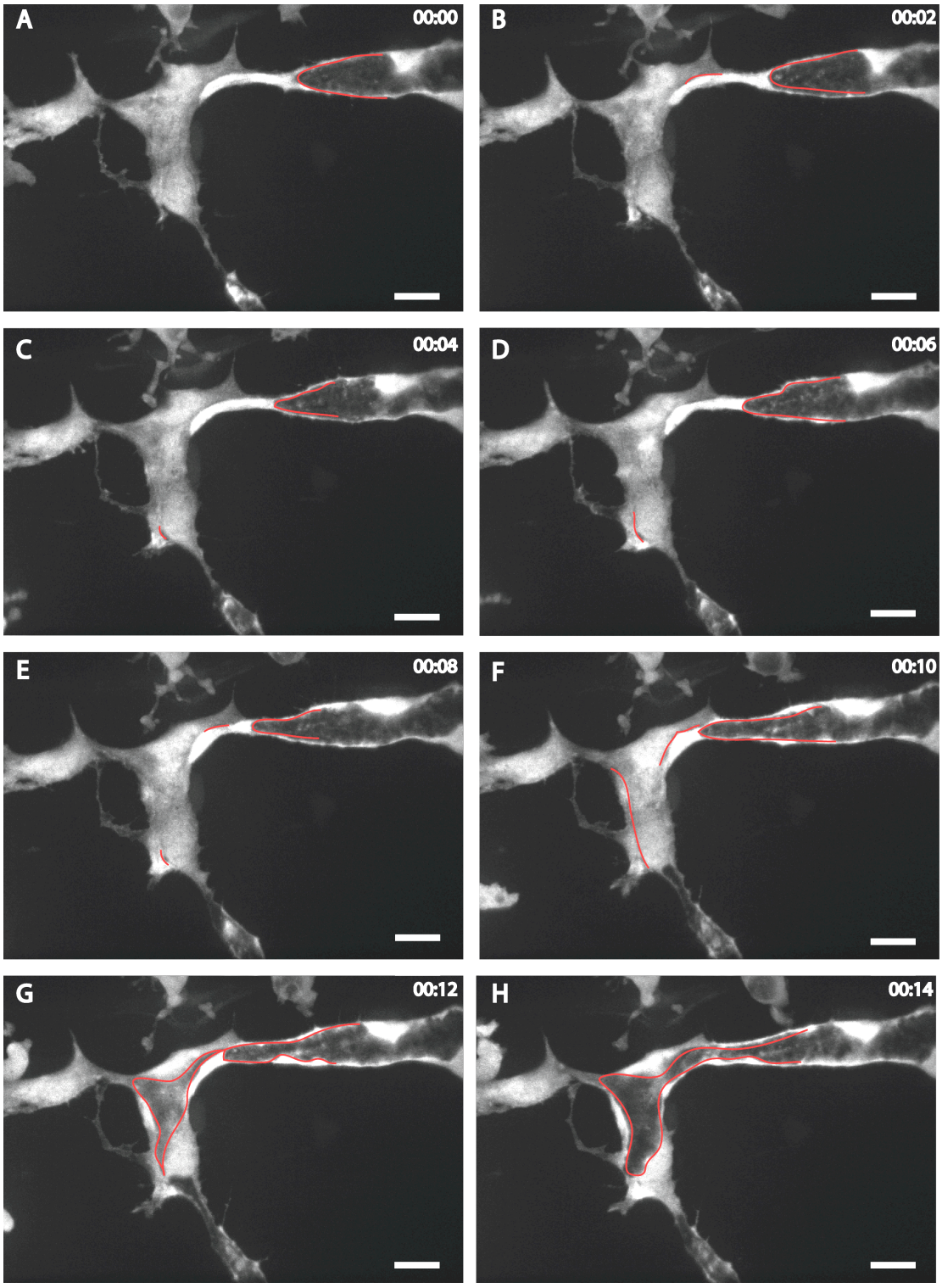

Fig 3.12 Lumen formation by a mechanism that might involve intracellular lumen formation.
Continuous lumen forms by the fusion of what appears to be intracellular lumen (right portion of images, red line) with lumen that forms through cell junction opening as in Fig 3.9 (red line segments, central cell in images). 2 minutes elapse between each image. Scale bars represent 10μm

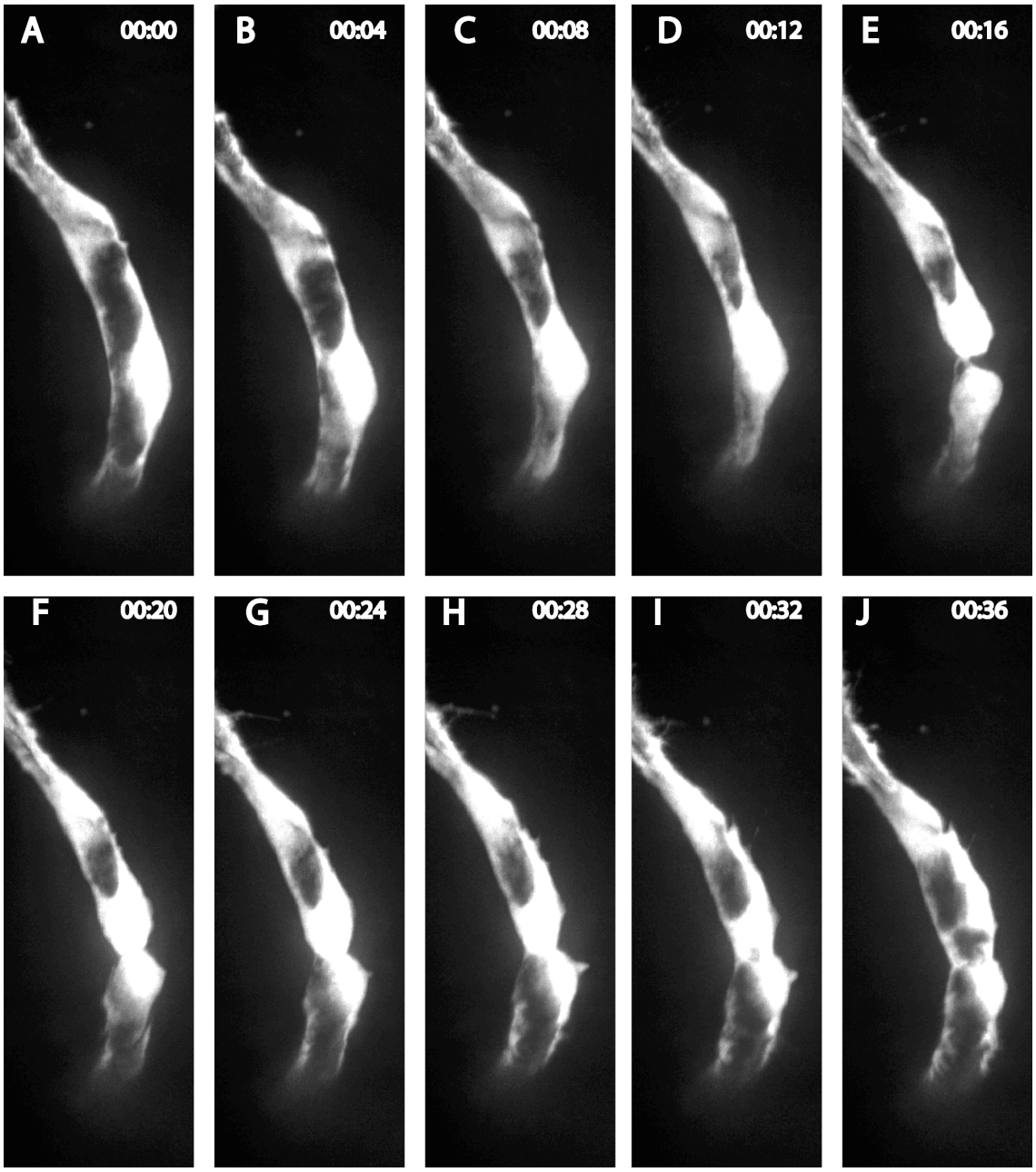

Fig 3.13 Cell proliferation in lumenized vessel.
Snapshots of live imaging of cell division in a lumenized ISA in *fli1:eGFP* 30hpf embryos. The ISA collapses its lumen (A-C) prior to division. Following cell division (D-H) the lumen reopens by(I-J). Time is indicated in minutes.

3.2 3-Dimensional Electron Microscopy

The use of transgenic animals has revolutionized biology by allowing the study of gene function in the whole organism, at the tissue level and at cellular resolution. Thanks to its optical clarity and external embryonic development, the zebrafish is especially amenable for the use of fluorescent protein markers to track lineage specific cells and thus investigate their behaviour during developmental morphogenesis. The drawback with using cell type-specific fluorescent proteins is the lack of information about unlabelled cells and the environment around the cells of interest. One technique that is able to circumvent such a problem is electron microscopy (EM). In EM the sample is stained with contrast agents allowing the visualization of all material within the sample, which is bombarded with electron beams. Electrons have a much narrower wavelength compared to visible/near-visible light used in light and fluorescence microscopy and allowing considerably higher resolution. EM can either be used to obtain topographic images of the sample surface using Scanning Electron Microscopy (SEM) or backscattered images of ultrathin sample section through Transmission Electron Microscopy (TEM). The drawbacks of each are evident: SEM limits the information gathered to the surface of the specimen; TEM requires thin sectioning (nms) of the sample. Even serial sectioning through a samples that is a few μm thick and aligning the subsequent images is extremely laborious and difficult to even the most experienced electron microscopists.

Here I describe an adaptation of electron microscopy imaging techniques that have been extensively used in the semiconductor industry but have had limited use in very small biological samples. The first of such techniques is known as Focus Ion Beam SEM (FIB/SEM). In FIB/SEM a Ga^{2+} beam mills away the top layer of the sample followed by SEM image acquisition of the exposed surface (Fig 3.14C); this process is iterated to ensure a sectioned and well-aligned dataset is collected. The second technique is known as Serial Block Face SEM (SBF/SEM). In this case the sample chamber has a modified ultramicrotome that is able to section the sample *in situ* within the microscope, and the surface can be imaged by SEM following each cut. FIB/SEM and SBF/SEM were adapted to obtain detail on anastomosis at an almost whole

organism level. These techniques can help obtain an incredible amount of data on the ultrastructure and the interaction between the ECs and the surrounding environment during tip cell anastomosis but as will be shown also contain a wealth of information about all imaged tissues.

This part of the study was done in close collaboration with Lucy Collinson and Hanna Armer of the LRI EM unit along with external collaborators for access to the equipment: Ken Png and Andy Bushby (The Nanovision Centre, Queen Mary, University of London, UK) Christel Genoud (Friedrich Miescher Institute, Basel, Switzerland) and Alexander G Monteith (Gatan, Abingdon, UK). All the work described in this part of the thesis is related to the publication Armer E.J.H., Mariggi G. *et al*, PLoS One 2009, and therefore I will not continue referencing this work. I am grateful to our collaborators that performed all the preliminary work on resin selection for this study (in which I had no part) and for allowing us the use of their equipment.

3.2.1 FIB/SEM setup

Standard TEM embedding protocols using osmium and tannic acid were shown to produce suitable atomic number contrast for good backscattered electron imaging in FIB/SEM. The sample was embedded in resin within a purposely-designed mould to facilitate the orientation and trimming and reduce the deposition of milled material during the serial milling/imaging (Fig 3.14A). This also aids the relocation of the trunk and area of interest (AOI). The sample was trimmed until the embryo could be seen using transmitted light (Fig 3.14B). Trenches where milled either side of the AOI to minimise the accumulation of sputtered material from the sectioning onto the surface to be imaged (Fig 3.14B), as well as depositing platinum onto the top surface of the block to protect the edges during data collection (Fig 3.14, TF). The face was milled at thicker sections, using high ion current, until the myotomes were exposed and subsequently the milling was altered to obtain thin (50nm) slices.

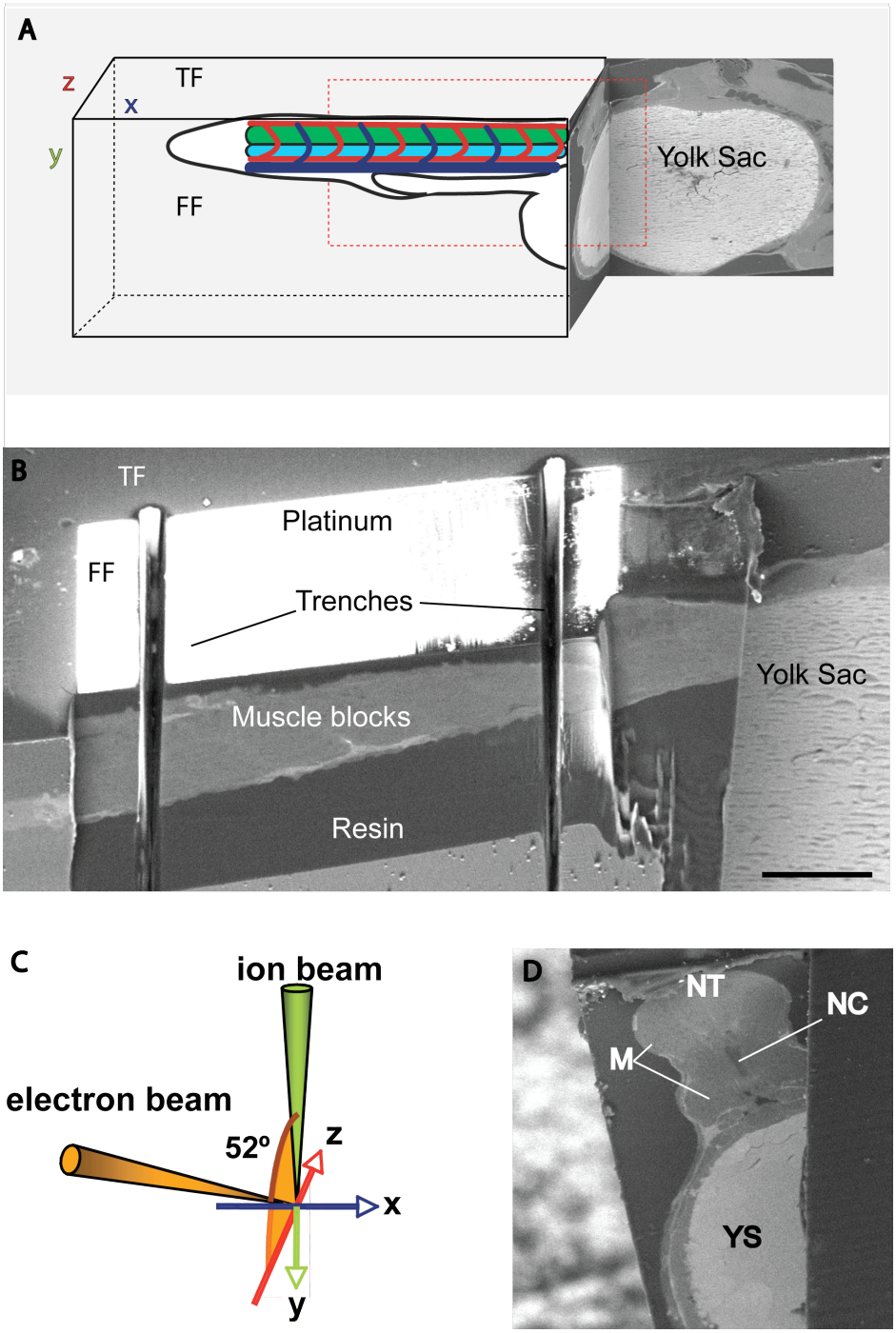

Fig 3.14 FIB/SEM setup.

A. Diagram showing orientation of the zebrafish after resin embedding and trimming with a diamond knife. The AOI in the zebrafish tail is placed in an overhang of resin to optimise milling and minimise curtaining artefacts. The head and yolk sac are used as markers for locating the AOI, and are exposed during trimming, seen here in backscatter electron images from the FIB/SEM. Top face (TF), front face (FF). Arrows represent x (blue), y (green) and z (red) axes. B. Platinum was deposited onto the top face of the block to stabilise the edge during milling. The sample was coarse milled with the gallium ion beam to expose muscle blocks at the predicted area of interest prior

to the milling run. Trenches (arrows) were then milled on either side of the AOI to reduce artefacts due to redisposition of sputtered material on the blockface. Scale bar represents 100 μm. C. Orientation of the electron and ion beams with respect to the front face of the block. D. Transverse view of trimmed trunk and yolk sac (YS) showing myotomes (M), neural tube (NT) and notochord (NC). Adapted (Armer et al., 2009).

As a proof of concept a 32hpf zebrafish embryo was stained and mounted for FIB/SEM, and underwent sequential milling and imaging to test whether this technique was amenable to such a large whole organism sample. 693 serial images were collected in ~35h hours, resulting in a dataset with a volume of ~$3.3x10^5$ μm^3 at $56x56x50nm^3$ resolution. Images were loaded into Amira software (Visage Imaging Inc.) for visualization and 3D segmentation. Thanks to the high 3D resolution of the images, the dataset could be viewed in any orthoslice without loss of quality, aiding the relocation and segmentation process of the sample (Fig 3.16D). Large structures within the trunk of the embryo such as the notochord and the neural tube were easily segmented (Fig 3.16E, blue and cyan) but it was immediately clear that identification of ECs would not be as straight forward due to the presence of many unexpected cells within the AOI. Once the ECs involved in the fusion were located and segmented, they were comparable in morphology with the confocal image prior to fixation (compare Fig 3.16B and C). The two segmented ECs (Fig 3.16, orange and yellow, Movie6) overlap at the point of contact, a mechanism that had been proposed in the formation of proper cell-cell junctions during anastomosis (Blum et al., 2008). This event is hard to pinpoint in the raw images, as the EC processes cannot be viewed in a single plane or orthoslice therefore the CurvedSlice Amira algorithm was used. A sprouting ISA can be observed in serial sections, emerging from the DA and migrating along the somite boundary (Fig 3.15A, red shading). Looking more closely at such an image, the unicellular EC –lined DA and PCV are clearly distinguishable; the ECs display the characteristic elongated nuclei and nucleated erythrocytes are present within the lumen of the axial vessels (Fig 3.15B). Even considering the size of the sample viewed in such images it is possible to discern intracellular structures such as mitochondria in ECs, z-discs within the muscle cells and dense granules in an unidentified cell (Fig 3.15B). Even so, localizing a fusion event remains difficult to pinpoint without markers as it occurs in a small volume of the trunk.

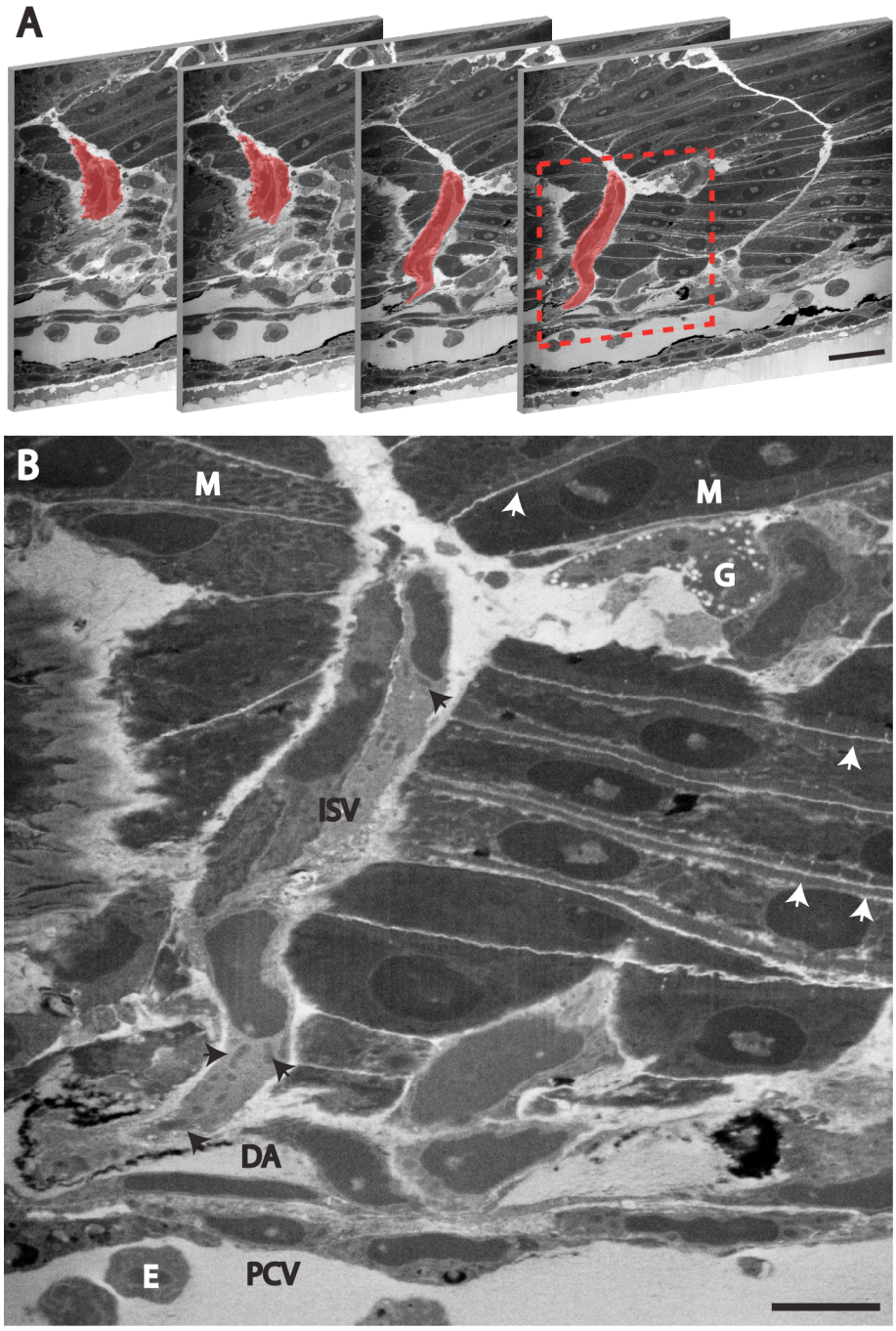

Fig 3.15 Localisation of ISA by FIB/SEM

A. FIB/SEM sections of a 32 hpf zebrafish embryo trunk with the ISA highlighted in red. Slices are non-consecutive sections 661, 669, 687 and 691 where one slice is 50 nm thick. **B.** The posterior cardinal vein (PCV) and dorsal aorta (DA) can be observed as lumenized vessels containing nucleated erythrocytes (E). The ISA sprouts from the DA and migrates in the space between the muscle block (M) and midline structures. Subcellular structure can be resolved including mitochondria (arrows) and dense granules (G). Scale bars represent 30 μm, (A) 10 μm(B). Adapted from (Armer et al., 2009).

3.2.2 Identification and 3D Reconstruction of ISA Anastomosis through Correlative Confocal – FIB/SEM Imaging

The collection of a large dataset as described in the previous section holds a wealth of information but also reiterates how complex tissue and organism architecture is. This complexity increases the difficulty of locating the AOI without the use of markers. It was therefore decided to undertake a correlative imaging study to relocate and images the anastomotic process using FIB/SEM. A 28hpf *fli1:eGFP* embryo was anaesthetised and embedded in agarose for live imaging. The embryo was imaged until ISAs undergoing fusion were identified and measurements to be used for AOI relocation were taken (Fig 3.16A-B). The embryo was subsequently fixed, prepared for FIB/SEM and mounted as in Fig3.13A. A dataset of 1778 images was collected in ~ 87 hours, with a volume of $2.42x10^6 \mu m^3$ at a 1:1:1 voxel resolution of $72nm^3$.

Markers are placed through the 3D dataset to pinpoint parts of the AOI and project a curved slice as a 2D image (Fig 3.17A). The segmented ECs can be superimposed onto the curved slice to identify the ECs within the image (Fig 3.17B); it must be noted that some distortion may occur in displaying the 3D plane as a 2D image and therefore the scale bar is unidirectional. The ECs overlap and touch as suggested by the segmentation (Fig 3.17C). Another observation that is complementary with Fig3.3 and Movie5 is the morphology of ECs in this environment, less than 500 nm in thickness in places, adding evidence for the change in morphology that I have alluded to earlier in this chapter. In line with our aim to investigate the relationship and interaction between the ECS and the environment, a granular cell was observed wrapped around the point of contact between the two ECS (Fig 3.16F and Movie3). Previous work from our group and others (Gerhardt, 2003, Fantin et al., 2010, Rymo et al., 2011) had suggested that macrophages could be playing a role in assisting angiogenesis, and anastomosis in particular. Live imaging of *fli1:eGFP* embryos also sheds light on the role of macrophage-like cells in the process of anastomosis (Movie3). The role of such cells will be discussed in Ch.5.

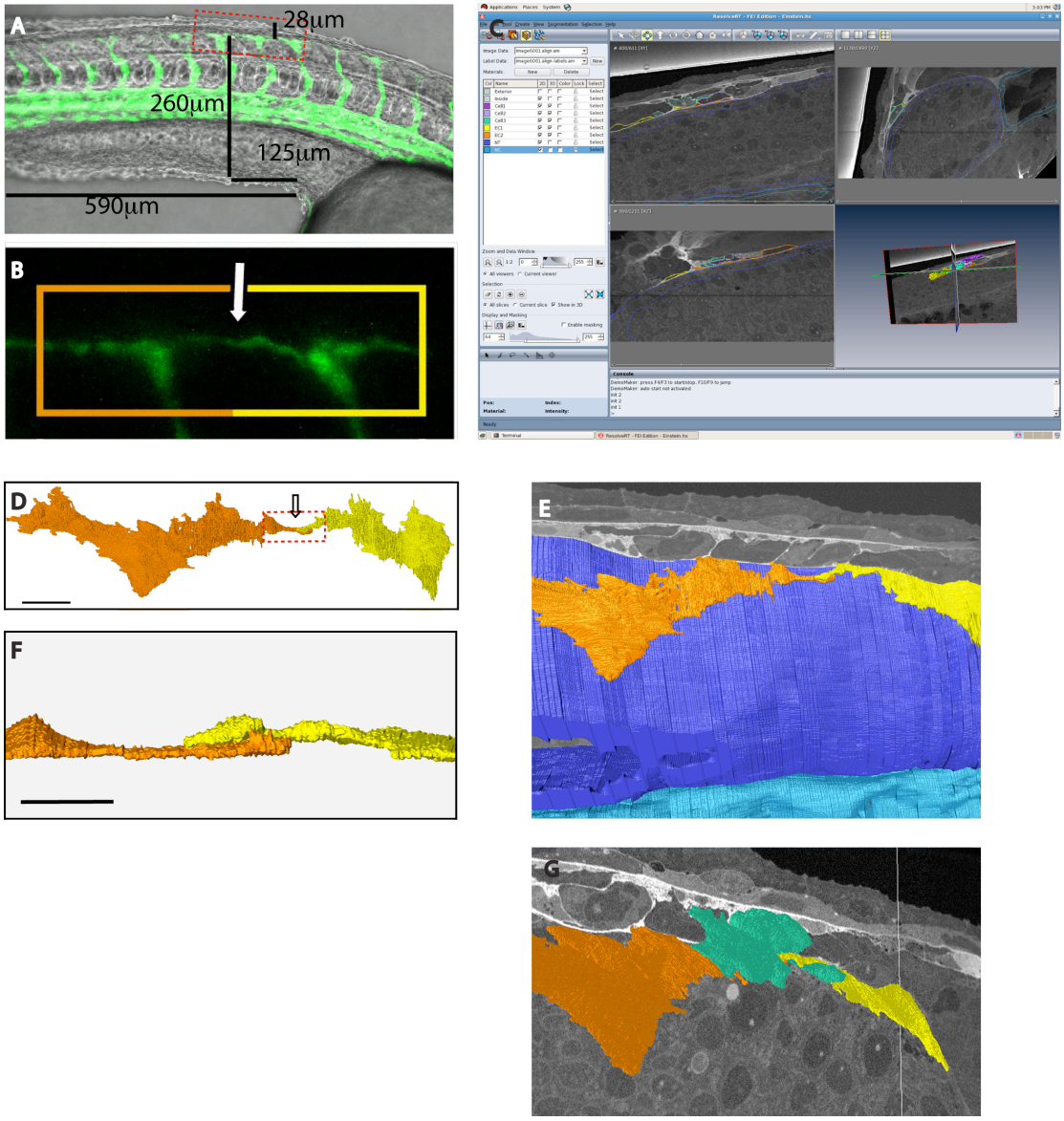

Fig 3.16 Anastomosis of the DLAV by correlative fluorescence confocal and FIB/SEM.

A. Still from live confocal imaging of a 28hpf *Tg(fli1: EGFP)*^{y1} transgenic zebrafish at the point of anastomosis of filopodia from adjacent ISAs, overlaid on a phase image of the zebrafish. Measurements of the AOI are made in relation to gross physical markers like the yolk sac and yolk tube. **B**. High magnification image of boxed area in (A) showing the point of anastomosis (arrow) and indicating vessels reconstructed in D ,E, F and G (orange and yellow box). **C.**Screenshot of Amira software (Visage Imaging Inc.) used to visualize and segment data acquired. It enables the data to be visualized in all orthoslices. **D, E, F and G.** Features within the FIB/SEM dataset were segmented using Amira. Endothelial cells from adjacent ISAs (orange and yellow) form a thin layer between the neural tube (blue) and the somites. At the point of anastomosis filopodia from each cell overlap and contact (arrow). A cell is seen wrapping around the point of connection (G, green cell). Scale bars represent 10 µm in D and 3 µm in F. Adapted from (Armer et al., 2009).

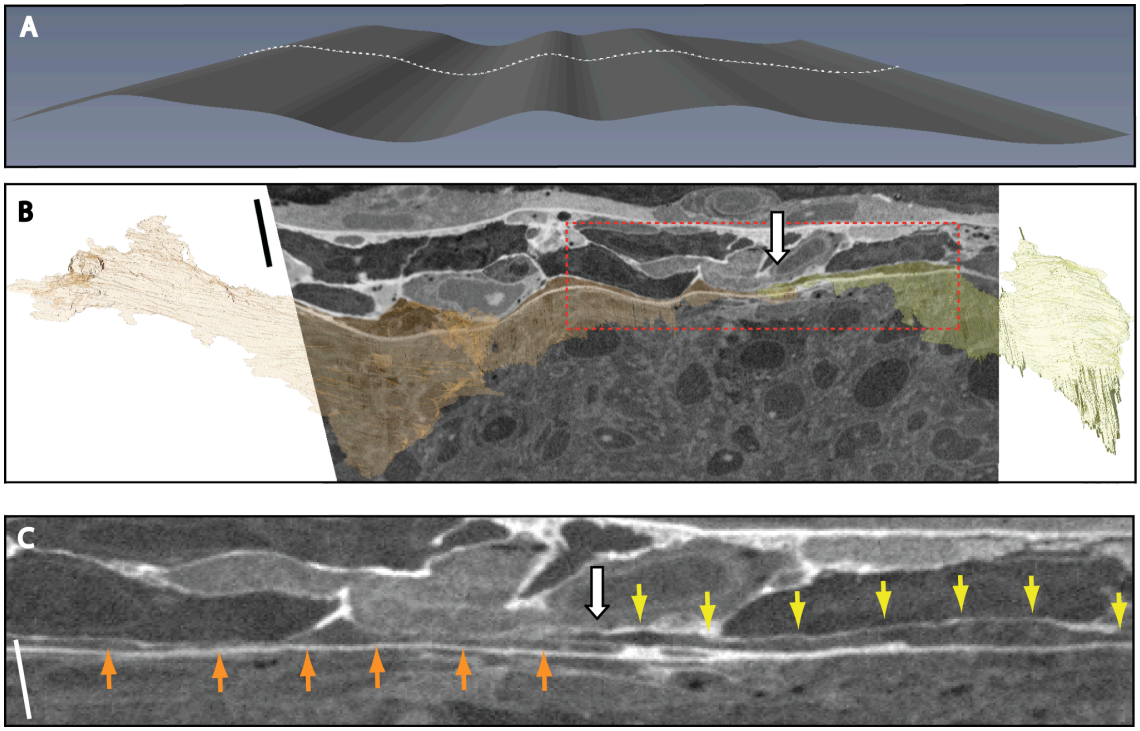

Fig 3.17 CurveSlice to improve visualization of EC connection.
It is only possible to visualise the ECs in the raw data by creating a curving plane through the volume using software (A, CurvedSlice, Amira). **B.** Overview of the CurvedSlice data with the 3D reconstruction overlaid to highlight the filopodia of the ECs which narrow to 500 nm in places. When viewed in two dimensions the CurvedSlice distorts the data but captures the entire filopodia in one section demonstrating continuity. **C.** High magnification of the AOI (box in B) from the CurvedSlice. Scale bars 5 μm in B, unidirectional and 2.5 μm in C, unidirectional. Adapted from (Armer et al., 2009).

3.2.3 Ultrastructure of the Formed DLAV using SBF/SEM

By 48hpf the DLAVs have formed through the fusion of the ISVs. These vessels mature and become lumenized, allowing the flow of blood. To asses the use of SBF/SEM in understanding the ultrastructure of the formed vessels, a 72hpf *fli:eGFP* embryo was imaged, fixed and prepared for imaging (Fig 3.18A). SBF/SEM has the advantage of slicing at a faster rate, collecting 1000 images at 50nm/section in ~15 hours for a total sample volume of $1.2x10^5 \mu m^3$. The detector fitted on this equipment was able to give a lateral resolution of $24nm^2$. The detector gives a different contrast in the SEM images as compared to the one in FIB/SEM (Fig 3.18B and Fig 3.15B) but one can equally well identify sub-cellular structures such as z-discs (Movie7) and the pigmented vacuoles in xanthophores present below the scales (Fig 3.18B and D). One must admire the level of detail obtained when considering that half of the whole embryo trunk is being imaged, whilst still maintaining the resolution to identify such fine structures. These images were not taken at the highest possible magnification but used to image a large field of view to include as much information on the ultrastructure of the zebrafish trunk and associated vasculature. The formed DLAV has a visible lumen and blood cells are present within the vessel (Fig 3.18B and F). As the DLAV is not a straight structure, the CurveSlice algorithm was used to create a curved slice as describe above (Fig 3.18C-D). Some portions of the DLAV have fully opened lumen while others present a more restricted/collapsed lumen (Fig 3.18D). There are electron dense structures present at the ECs boundaries, which could be attributed to tight junctions (Fig 3.18E and F, black arrows) even though at this magnification such a claim is someway overstated. The ISVs running between the neural tube and the muscle blocks (NT and M) do not display a clear open lumen. It is likely that the maintenance of an open lumen relies on the presence of blood pressure as blood flow has been shown to not be required for initial lumen formation but important for its maintenance (Wang et al., 2010a).

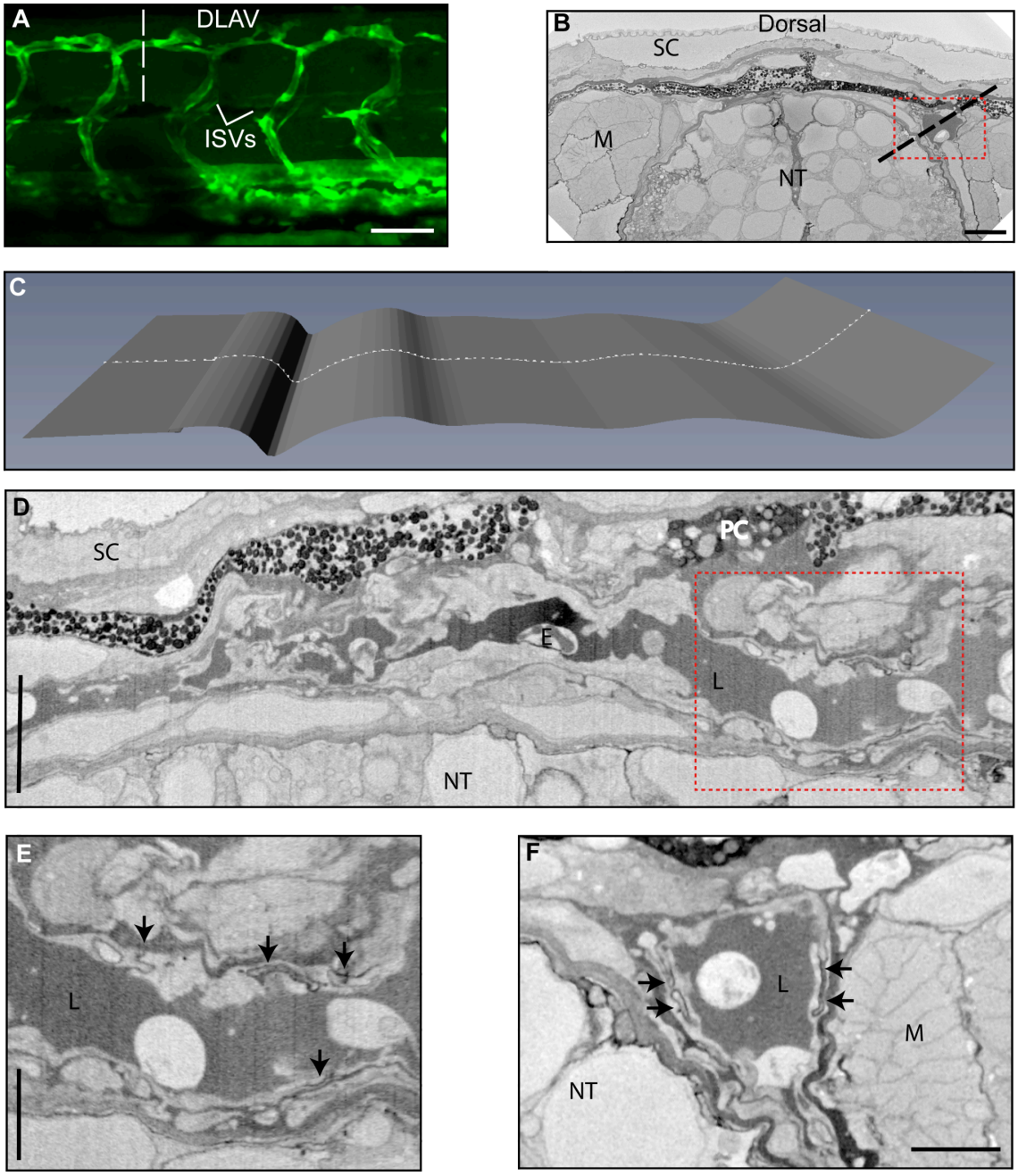

Fig 3.18 Ultrastructure of the formed DLAV.
A. Confocal projection of 72 hpf *Tg(fli1: EGFP)*^{y1} transgenic zebrafish showing the fully formed DLAV. **B.** Transverse section through 3View SBF/SEM dataset showing both DLAVs (dashed line in A). Scales (SC), muscle blocks (M), neural tube (NT). (C) Profile of the CurvedSlice (Amira) through the volume which selects one of the DLAVs (dashed line in (C). **D.** Overview of the CurvedSlice data showing the lumenized DLAV. Lumen (L), erythrocyte (E). **E.** Higher resolution image of the DLAV from the boxed area in D showing electron dense patches between ECs which may represent cell-cell junctions (arrows). **F.** Transverse section through the DLAV. Scale bars represent 50 μm in A, (B) 5 μm in B, 5 μm unidirectional in D, 2.5 μm unidirectional in E, 2.5 μm in F. Adapted from (Armer et al., 2009).

3.2.4 3D EM dataset contain a wealth of information

The adaptation of such 3D EM techniques for use in a whole embryo to study angiogenesis demonstrated that an unprecedented amount of detail for such large datasets is achievable. To prove that data acquired for one particular study can still yield information in further investigations in unrelated fields we analysed the FIB/SEM dataset to identify neuronal projections form the neural tube. 48hpf zebrafish embryos were stained for acetylated tubulin to identify neuronal projections that emanate from the NT into the intraembryonic space between somites and medial structures (Fig 3.19 A). The neurons were identified via their morphology and presence of dense neurofilaments, and reconstructed in the FIB/SEM dataset, comparable to what is observed with antibody staining (Fig 3.19B). This comparative analysis demonstrates the usefulness of such 3D EM techniques and investing the time to collect such large datasets to benefit multiple disciplines.

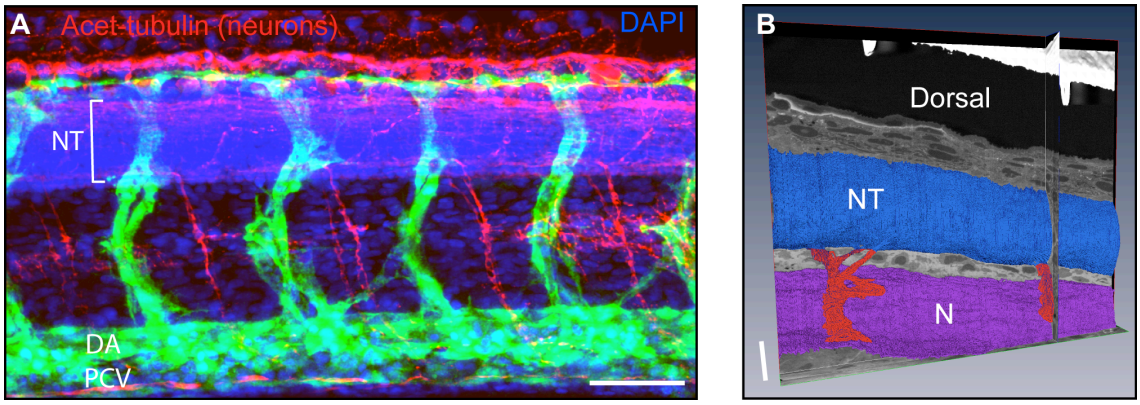

Fig 3.19 3D Reconstruction of neuronal projections in a FIB/SEM dataset originally collect for a vascular study.
A. 48 hpf Tg(fli1: EGFP)y1 transgenic zebrafish displaying formed ISVs and DLAV (green) which grow around and over the NT (blue, DAPI staining). The DLAV lies underneath bundles of neurofilaments (acteylated tubulin, red). Neuronal projections from the NT can also be observed. B. 3D reconstruction and segmentation of a FIB/SEM dataset showing neurons (red) exiting the NT (blue). 3D rendered features are shown overlying x, y and z orthoslices from the original dataset. Notochord (N). Scale bars represent in A 50 μm, in B 10 μm. Adapted from (Armer et al., 2009).

3.3 Discussion

The data described in this chapter gives new insights into the morphogenetic processes that occur during sprouting angiogenesis in the formation of zebrafish DLAVs.

3.3.1 All ECs in Sprouting ISA exhibit some level of activation

Sprouting angiogenesis is characterized by the activation of quiescent ECs, breaking out from the pre-existing vessel in which they reside. EC activation leads to one cell being selected as the tip cell to lead sprout growth and extend filopodia, whilst the trailing cells are referred to as stalk cell (Gerhardt, 2003). Here I have shown that filopodia are present along most of the growing ISV, with stalk cells also extending filopodia suggesting some level of activation.

Tip cell selection is initiated by VEGFA stimulation, inducing migratory behaviour and filopodia to sense the environment (Gerhardt, 2003). Many reports have investigated the mechanism of tip cell selection and the Dll4/Notch pathway has been identified as a major player in this process. VEGFA induces Dll4 expression in the tip cell, which signals to the neighbouring cells through Notch activation. This downregulates VEGFR2 and upregulates VEGFR1 in stalk cells (Suchting et al., 2007), making ECs less responsive to VEGFA (Leslie et al., 2007). The bottom line from such studies was that VEGFA/VEGFRs and Dll4/Notch pathways interact to restrain the sprouting response and allowing a moderate number of tip cells to commence sprouting (Leslie et al., 2007, Siekmann and Lawson, 2007, Hellström et al., 2007, Suchting et al., 2007, Lobov et al., 2007). Indeed if Dll4 is removed, its function blocked or Notch activation inhibited there is excessive sprouting in both developmental settings and pathological situations (Noguera-Troise et al., 2006). This signalling feedback loop results in the selection of one tip cell per sprout as described in the mouse postnatal angiogenesis model, with only cells at the vascular front exhibiting filopodia and migratory behaviour. The data here presented suggests that stalk cells might be exhibiting some activation, as observed by filopodia present along the entirety of the

ISA. As activation I am referring to exploratory filopodia behaviour, as opposed to general VEGFR2 activation, which of course must occur as stalk cells proliferate. The expression of membrane-tagged eGFP confirmed that such filopodia are present not only on the tip cell (Fig 3.2). This raises questions about the current model of tip cell selection and EC activation.

One way to reconcile this observation with current work is to take into consideration other members of the DSL family of Notch ligands. Jag1 is able to bind Notch1 but the signalling output can be the complete opposite when compared to Dll4-induced Notch activation (Benedito et al., 2009). In the mouse retina model, Jag1 and Dll4 are believed to compete for Notch1 binding. The glycosyltransferase *lunatic fringe* can modify Notch1 leading to increased Dll4-signaling and reduced Jag1-dependent signalling. This results in Jag1 having a proangiogenic effect, and its overexpression increases tip and filopodia numbers as well as EC proliferation (Benedito et al., 2009). As Jag1 is not expressed in tip cells, it is believed that it helps increase the robustness of the system, preventing stalk cells from activating Notch in tip cells but also decreasing stalk cell-to-stalk cell Dll4/Notch signalling at the vascular front, helping maintain high levels of VEGFR2 expression. This should allow rapid activation of stalk cells when the formation of a new tip cell is required (Benedito et al., 2009). A similar phenomenon could be happening in the zebrafish ISAs, where stalk cells may be primed and partially activated, ready to switch to the full tip cell phenotype if need be. This also fits with the fact that many cells in the DA do not possess filopodia suggesting these are not activated. To add to this, recent data from our lab using single cell clonal analysis of ECs expressing membrane labelled eGFP in the retina clearly show that cells that are not at the vascular front also posses filopodia, albeit much less than *bona fide* tip cells. These filopodia are polarized towards the periphery and thus towards the gradient of VEGF, again supporting the notion that stalk cells can be partially active and may not simply respond to VEGFA by proliferating as is currently believed (Lapi *et al* unpublished). When looking at the retinal vasculature the term stalk cell might become blurred as ECs further back in the plexus, considered stalk cells, can sprout to fill gaps in the plexus to give the correct density This partial activation hypothesis is further hinted to by work proving that the tip/stalk cell fates are not permanent and ECs compete for the tip position as well as shuffling within the sprout (Jakobsson et al.,

2010). Competitive advantage is dependent on VEGFRs level acting upstream of Dll4/Notch. The ability of EC shuffling is evident in EB sprouting assay but also in the zebrafish vasculature, with tip cell competition observed in the head vasculature (Jakobsson et al., 2010) and more recently also in the sprouting ISAs (Zygmunt et al., 2011), suggesting that stalk cells in the ISA have the angiogenic potential to overtake the tip.

Filopodia activity is only seen to end once the ISAs are lumenized (Movie4). Previous work in understanding how ECs sense oxygen tension has highlighted the role of prolyl hydroxylase 2 (PHD2) as regulator of EC quiescence (Mazzone et al., 2009). In the presence of oxygen PHDs hydroxylate HIF family members inducing their proteolytic degradation. In low oxygen tension as is found during development or in tumours, PHD2 is not able to modify HIF-2α for degradation and thus HIF-2α can activate hypoxia-responsive genes, causing EC activation and angiogenic sprouting (Mazzone et al., 2009). Heterozygosity of PHD2 decreases a cell's ability to destabilize HIFs and its DNA binding activity. This in turn results in the upregulation of sFlt1 and VE-cadherin, leading to amore quiescent vasculature. Upregulation of VE-cadherin stabilizes EC adherens and tight junctions (Carmeliet et al., 1999, Taddei et al., 2008) and sFlt1 acts to restrain excessive sprouting (Krueger et al., 2011, Zygmunt et al., 2011). These pathways can thus provide a link between the observations of lack of filopodia on ECs in the DA, which is perfused, compared to the sprouting ISAs that are not lumenized. The oxygenated aortic ECs will have high oxygen levels and the associated increased PHDs activity. PHDs will hydroxylate HIFs, tagging them for degradation. In the ISAs where blood flow is yet to commence, PHDs have low activity allowing HIFs stability, which can induce expression of pro-angiogenic target genes. This model would allow ECs to retain higher angiogenic potential, projecting filopodia even when in the stalk position.

3.3.2 Adaptive morphological changes

Endothelial cells demonstrate a high level of plasticity, able to change from quiescent, cobblestone-like morphology to an activated and pro-migratory state. ECs

must adapt to their environment at the signalling level as well as at the physical level. The 3D EM data here presented stresses the spatial constraints which the ISAs must face. The space in which the tip cell must migrate and bifurcate to form the DLAV is as small as 500nm in the medial to lateral direction (Fig 3.3, Fig 3.16). The EC undergoes distinct morphological changes as it reaches the neural tube, increasing the size of the lamellopodia at the leading edge. It appears that the cell is adhering and wrapping onto the neural tube and this change in behaviour is very apparent and sudden (Fig 3.3). It would be fascinating to understand how such a change in cellular morphology is brought about. As the sprout migrates from the DA, the space between the notochord and the somites is not as restrictive as what is found just further dorsally between the neural tube and the somites. One can speculate that for a cell to force itself into such an environment, it must experience either some tremendous chemoattraction or repulsion by the rest of the tissues. VEGFA is expressed within the medial portion of somites and in the hypochord but not in the dorsal part of the somites therefore it is unlikely that this could be the attractant (Liang et al., 1998, Lawson, 2002). VEGFC is also expressed in the zebrafish and is required for ISA formation (Ober et al., 2004, Covassin et al., 2006). VEGFC knockdown results in an arrest in the migration at the myoseptum, just ventral to the neural tube but VEGFC expression is only observed in the hypochord and the DA (Covassin et al., 2006). Factors implicated in neuronal development and growth cone guidance are now accepted as playing important functions in vascular development too (Adams and Eichmann, 2010). Thrombospondin type I domain containing 7A (*thsd7a*) is a molecule that has been shown to affect EC migration and tubulogenesis (Wang et al., 2011). In zebrafish *thsd7a* is expressed in the neural tube, most strongly along the ventral side and where it is in proximity of the somites (Wang et al., 2011). Decreased expression of *thsd7a* results in stalled ISA migration and aberrant ISA patterning later in development. In saying this the ISA migratory defect recovers by 50hpf, showing patterning defects close to the DLAV with extra functional branches connecting ISAs along the myoseptum and along the neural tube (Wang et al., 2011). This suggests that a molecule such as *thsd7a* might be involved in driving the tip cells over the neural tube but other mechanisms must also be in place as the migration defects in the morphant are able to recover. A chemoattractive molecule such as *thsd7a* found on the surface of the neural tube could also be an appealing explanation why

ISAs bifurcate upon reaching the dorsal aspect of the embryo. Bifurcation is necessary for DLAV formation to complete primary angiogenic sprouting.

3.3.3 Tip cell Proliferation does not Affect Tip cell Selection and Migration

The expansion of the vasculature is a large-scale feat, starting with differentiation, migration and proliferation. One must marvel at the intricate control of these different morphogenetic processes occurring while the system is expanding as well as functional. The integrity and barrier function are maintained to avoid perturbing tissue homeostasis. One of the major issues in a tubular system is cell division whilst maintaining integrity, particularly in the ISAs where a lumenized vessel cross-section consists of one to two cells. In the zebrafish this problem is circumvented by a collapse of the lumen at the site of division and is later reinstated through the opening of EC junctions (Fig 3.13). An important question is raised by this observation: how does the cell know that the lumen must be collapsed? The ISA in question appears to be unicellular (even though with this transgenic line it is difficult to deduce) and the lumen collapses prior to the commencement of cell division. Hence it cannot be assumed that lumen collapse is coupled to the initiation of cytokinesis and formation of the contractile ring. Is it a process regulated by cell division checkpoints? Could it be that the maintenance of a lumen is an active process that can be blocked, possibly through loss of cell polarization or through a reverse mechanism to lumen formation? MLCII-driven shape changes maybe reversed by dephosphorylation of the motor protein. Some support for this hypothesis rests on the requirement Moesin1 in the maintenance of luminal membrane (Wang et al., 2010a). The quick re-establishment of a luminal surface following division is also astonishing and raises its own set of questions. Are junctions formed across the lumen prior to cell division upon lumen collapse? Or is the cell able to round up, divide almost seamlessly at the same time as creating a new junction with the daughter cell to prevent leakage?

The standard model of Dll4/Notch lateral inhibition regulating tip/stalk cell selection dictates that the absence/reduced Notch signalling experienced by tip cells prevents

them from proliferating and this appears to be the case in the mouse retina model (Gerhardt, 2003). In zebrafish there has been a hint at tip cell proliferation by looking at EC nuclei (Blum et al., 2008) but not the morphology of the dividing cell, which is how tip cells are currently identified due to lack of reliable markers. Here I show that tip cells do indeed divide during zebrafish ISA formation and amazingly cell division does not affect tip cell selection or migration as the cell found at the tip prior division maintains its position and continues to migrate (Fig 3.5). An agent-based computational model involving the VEGFR2-Dll4/Notch feedback loop can simulate tip cell selection, without the need for higher regulation (Bentley et al., 2008). The model has been refined and expanded using data here described to include the effects of anastomosis on tip selection (Bentley et al., 2009). It is fascinating that this biological process can be simplified to these two interacting pathways, of which we have some knowledge but are still far from having elucidated their entire mechanisms and intricacies. One prediction is that cell division will alter the Dll4/Notch battling that occurs between ECs and thus destabilize the current pattern, inducing phenotype switching. The differences between biology and simulation can of course be easily summed up by the oversimplification of the model. But if one is to take a mechanistic view of the discrepancies it could very well be related to the partial activation of ECs within the sprout and the fact that most cells within the sprout experience a medium level of activation. This, along with work relating to Jag1's role (Benedito et al., 2009), might prevent stalk cells from having enough Notch influence on the dividing tip cell. The segregation of Notch receptors and DSL ligands has not been investigated in ECs and could very well provide some explanation for the lack of new battling upon cell division. Even though ECs round up and lose most of their lamellopodia and filopodia during division some level of polarization must be conserved as tip cells instantly restart to extend filopodia and migrate in the correct direction. The ability of EC tip cells to round up for division both while migrating and during anastomosis has to occur in a tight space as discussed above but this stresses the importance of such a cell shape change for cell division. It is believed that such rounding is required for a cell to position the cellular machinery needed for cell division. These shape changes are driven by a balance of osmotic pressure (outward) and actomyosin cortex contractility (inward) (Stewart et al., 2011), and loss of shape change can affect cell division (Fink et al., 2011).

Cell division during anastomosis does not induce further sprouting, again suggesting that more work is required to look at the dynamics of Notch signalling at the single cell level to truly grasp how the level of Notch activation relates to the exploratory behaviour and possible tip cell overtaking/shuffling (Fig 3.6).

3.3.4 Mechanism of Lumen Formation

There appear to be two mechanisms of lumen formation in zebrafish ISAs. Firstly as shown in Fig 3.11 the lumen is established as a result of junctional opening between two ECs within the ISA stem. It is notable early on in the sequence that the junction becomes delineated, as if the junctional architecture has been changed. The cell junction shape reiterates what has been previously described by Blum *et al* on VE-cadherin and ZO-1 distribution within the ISA (Blum et al., 2008), and is again confirmed in this study with the use of the *flk1:mG* construct (Fig 3.2). The time taken for junctional release is extremely short, within 2 minutes, and therefore the modulation of junctional integrity must be rapid. VE-cadherin phosphorylation can induce rapid changes in junctional stability by decreasing the protein's adhesive properties (Dejana et al., 2009). Phosphorylation of the intracellular tail can block the binding of armadillo family proteins p120-catenin and β-catenin preventing VE-cadherin stabilization at the membrane (Gavard and Gutkind, 2006). The absence of these proteins from adherens junctions allows β-arrestin2 to bind and induce VE-cadherin internalization through clathirn-mediated endocytosis, further decreasing junctional stability (Gavard and Gutkind, 2006). The opening of the lumen in the above observations is a quick process occurring in a few minutes, well below the hours required in pinocytic vesicle fusion model derived from Kamei *et al*'s observations (Kamei et al., 2006). The rapid opening is compatible with the hypothesis that initial junction opening is induced by the relocation of negatively charged sialomucins to the luminal membrane, which through repulsion help to overcome the adherens junction force (Strilic et al., 2009, Strilić et al., 2010). The collapse following initial junctional opening further discredits the simple unicellular vesicular fusion model, whereas it supports the need for EC polarization to determine the apical domain. Once this has occurred and the necessary components relocate (VE-cadherin, sialomucins, Moesin and MLC II) then the vessel is primed for lumen opening. This likely occurs through a combination of force-induced cell shape

changes via the action of activated MLC II (Strilic et al., 2009), and through the initiation of blood flow as it has been shown to be required for maintenance of lumen but not for the initial formation (Isogai, 2001, Wang et al., 2010b).

The second mechanism of lumen formation described is reminiscent of unicellular lumen formation in the Drosophila trachea. The lumen pushes through a cell and then connects with pre-existing lumen through the readjustment of a junction (Fig 4.12). Again in this case the advance of the lumen is rapid and does not hint at a presence of vesicles. It is likely that intracellular vesicle are involved in lumen formation through their targeting to specify the apical membrane and expansion of the luminal domain upon EC-EC repulsion.

3.3.5 Anastomosis in Angiogenesis

Anastomosis is a key step in the formation of a tubular network that develops by sprouting. Here the dynamics of anastomosis were investigated by qualitatively and quantitatively describing the process (Fig 3.7-9). Sprout fusion had not been previously investigated and it was assumed that EC tip cells simply come into contact and fuse. It is immediately obvious that anastomosis is not a straightforward process simply based on two tip cells coming into contact. The ability of two tip cells to find one another is in itself quite incredible considering that this is done through thin, long filopodia connections. The fact that the sprouts do not grow over the NT but bifurcate suggests something is signalling to the ECs to change course. It is known that ECs secrete VEGF and this is required in an autocrine signalling loop for survival (Lee et al., 2007) but it has not been demonstrated that this can have chemoattractive effects on other ECs. This could be a plausible explanation for the attraction between tip cells but no VEGFA mRNA has been detected in ISAs to date. Interestingly *flt4* is strongly expressed in nascent ISAs, especially tip cells (Covassin et al., 2006) but its main ligand VEGFC is not expressed ahead of the vasculature (Covassin et al., 2006) and thereforeVEGFR3 maybe acting in heterodimers with VEGFR2 to bind VEGFA (Dixelius, 2003, Nilsson et al., 2010). Another plausible explanation may rest on the ECM found over the NT. Recent evidence has highlighted how certain ECM components can directly or

indirectly alter EC behaviour. Fibronectin and laminin change migration and even Dll4/Notch signalling in ECs (Stenzel et al., 2011, Estrach et al., 2011b). Fibronectin's effects are both at the level of trapping VEGFA and directing the projection of filopodia (Stenzel et al., 2011). Another possible ECM –related mechanism may be to do with EC-induced mechanical changes to the ECM present on the NT, which can be sensed by nearby cells (Reinhart-King et al., 2008) and induce attraction of tip cells towards one another. *Thsd7a,* mentioned above, is required for ISAs to migrate past the myoseptum, at the height of the NT; it could induce ECs to grow along the NT without discriminating on the directionality. The fact that it is not expressed in the dorsal part of the NT (Chu et al., 2011) may explain why ISAs do not crossover prior to anastomosis.

Whatever the mechanism involved, ISA tip cells are always able to find one another but the subsequent filopodia contacts do not always lead to fusion (Fig. 3.9). The filopodia themselves are not directly attracted but tend to grow in the direction of the neighbouring ISA which again hints at polarized projection. The fact that not all contacts are "constructive" (leading to anastomosis) provides a number of possibilities in the mechanism of fusion. Adhesion molecules such as VE-cadherin are important for the stability of newly formed vasculature (Crosby et al., 2005, Montero-Balaguer et al., 2009) as E-cadherin is important in *Drosophila* tracheal fusion (Tanaka-Matakatsu et al., 1996). It is therefore conceivable that different filopodia possess substantially different amounts of such adhesion molecule on their surface, possibly due to stochastic probability or through a more active process requiring myosin-X-dependent transport along actin filaments to the tip of filopodia (Almagro et al., 2010). The active transport of VE-cadherin is important to initiate EC-EC junction formation *in vitro.* Previous work on VE-cadherin in zebrafish was not able to resolve the presence of the adhesion molecule on filopodia and the investigation looked at adhesion molecules distribution at later stages, once the EC cell bodies were in contact (Blum et al., 2008); generating a fluorescent protein-VE-cadherin fusion protein would be instrumental in understanding how VE-cadherin changes in localization during the initial steps of tip cell contact and the subsequent decision for filopodia to remain attached and lead to anastomosis; unfortunately this feat has not proved successful to date. Non-constructive filopodia contacts have limited duration and more than three quarters of the instances recorded last less than eight minutes (Fig 3.9A). Therefore the decision as to whether the pair

will remain connected is quick, most likely as a result of retraction of the filopodia without much resistance from the recently formed contact point. In the *Drosophila* trachea upon the establishment of DE-cadherin contacts, formin3 is recruited to aid the formation of actin structures required for the completion of anastomosis and subsequent lumen opening (Tanaka, 2004). It would be of interest to assess if such mechanisms are conserved in the formation of the vasculature.

There is no statistically significant difference between the mean (~9μm) or the variance of the length of constructive and non-constructive pairs (Fig 3.9B). However the maximum length of filopodia measured shows a profound difference with the fusing pair maximum being almost 50% of the maximum value for non-fusing pairs. I believe there are three possible explanations for this result. Firstly there tend to be very few filopodia that exceed the maximum fusing/constructive length of ~20μm. The 75% percentile is the same for constructive/non-constructive filopodia. It could therefore just be that as there are so few very long (up to 38μm) filopodia the likelihood that they will encounter one from the neighbouring ISA are low. It must also be taken into consideration that such long structures tend to occur when the cell bodies have begun to squeeze over the NT and maybe transitioning into a different environmental setting. This leads to the second possibility that anastomosis, and whether filopodia remain connected, is governed by the local environment. If ECs experience a change in environmental cues when they reach the top of the NT that lead to preparing the tip cell for anastomosis, the filopodia will be shorter as at this stage cell bodies will have moved closer, bringing a spatio-temporal element to the process. I believe that conclusions made from the study of Sema/Plexin in angiogenesis must be included in this discussion. In *obd* mutants (*plxnD1* lesion) and in *plxnD1* morphants ISAs are able to grow in regions of the embryo that are normally avascular and accordingly fuse with their neighbours at the height of the myoseptum (Torresvazquez, 2004). This evidence does not support the environmental cues hypothesis related to the NT, even if the situations being discussed are examples of mispatterned vasculature. The ability of an EC to fuse might be intrinsic and a function that is not restricted to a subset of ECs.

Data on the time delays between contact and fusion brought to light interesting points. The first contact between tip cells is not important with regards to fusion unless

of course anastomosis occurs through this event. It remains unclear whether this is something intrinsic of the individual filopodia or whether it rests upon the failure to generate an intracellular signal. The fact that the delay between final contact and fusion is between one and two and a half hours indicates the possible requirement for outside-in signalling to allow the stabilization of the newly format contact. Further investigation of this phenomenon becomes technically and technologically difficult. The investigation of possible candidates involved in the control of anastomosis would require loss and gain of function studies of pathways such as Dll4/Notch and junctional proteins such as VE-cadherin. These important regulators of angiogenesis are now accepted and implemented in the current models (Potente et al., 2011) and meddling with their function has drastic effects on vessel growth. Therefore to assess the effects of their manipulation on anastomosis would require single cell, rapidly inducible systems for activation/inhibition of these components in specified cells. Even so such manipulations may result in decreased angiogenic potential and allow trailing ECs to replace the original tip cell.

Some of the observations described here were used to instruct a second generation agent-based model of tip/stalk selection in sprouting angiogenesis (explained above)(Bentley et al., 2009) based on a previous version (Bentley et al., 2008). The model output was compared to the quantitative data obtained from live imaging zebrafish embryonic ISAs. The datasets match well, meaning that even with such a simplistic view on the signalling regulating sprouting and tip/stalk selection, the negative feedback loop is sufficient to predict certain aspects of EC behaviour. This highlights the power of using agent-based models where simple local rules can govern and translate to large-scale ‘population’ behaviours.

3.3.6 3 Dimensional EM techniques in Angiogenesis

The 3D EM data acts as proof of concept that such techniques can be used successfully in large datasets, at the whole organism level in this case. Importantly the relocation of AOI within such a large volume with the aid of correlative confocal microscopy supports the notion that such techniques are not limited by one’s ability to

find the AOI without markings and guides. It was indeed fascinating to view the ultrastructure of the zebrafish trunk to such a high spatial resolution. 3D EM techniques have been used for smaller samples, somewhere around two orders of magnitude smaller than the datasets here presented (Knott et al., 2008). The reconstructed images reveal the presence of granular cells at sites of anastomosis, supporting recent work implicating macrophages and angiogenesis (Kubota et al., 2009, Fantin et al., 2010, Rymo et al., 2011) (discussed in Ch.5). The fact that the resolution and magnification were not pushed to the limit in these experiments, for the sake of increasing the chances of relocating the AOI, meaning that there is still a considerable scope to take these 3D EM techniques further and really obtain high quality subcellular resolution to shed light on the intracellular intricacies of anastomosis.

The generation of large datasets presents itself with another set of difficulties regarding data handling. Problems were encountered when attempting to segment the data, even when using top of the range graphic cards and RAM memory. This is a problem that is becoming increasingly apparent and critical, with pressing needs to address it. The volume of data that can be captured with the techniques described in this study, as well as many other imaging techniques, not only increase in size but also in the information density and efforts are required to implement workflows that allow the segmentation and the extraction of useful, quantifiable parameters.

3.3.7 Future Directions

The data here presented help us to understand a little better some of the morphological processes that occur during angiogenic sprouting. These steps are well coordinated in their dynamics to allow the functionality of the system throughout most of its development.

One of the main points that derives from what is probably the simplest piece of data in this study, and an observation that no one has really commented on previously, is the need to revisit the model of tip cell selection (Potente et al., 2011). The fact ECs other than tip cells have filopodia projections and that these cells tend to be only present in the migrating ISA opens up the possibility of differing levels of EC activation.

Mazzone *et al*'s work hints in this direction too with the introduction of a third EC phenotype, the phalanx cell (Mazzone et al., 2009). I personally envisage a less restrictive approach to describing what is happening and would be interested to see whether there is a way to gauge EC activation, something that can be inferred from the cell shuffling and tip cell overtaking experiments (Jakobsson et al., 2010). It may be that ECs have an activation scale and this correlates with their angiogenic potential, prevalence and persistence at the tip etc.

Another important node of understanding the differential cellular responses to angiogenic stimuli is what does this difference boil down to. How are the signals from the same ligand and the same receptor integrated differently? Are the different phosphorylation sites on VEGFR2 phosphorylated at different rates and therefore certain will only react if the receptor is fully activated? In theme with the environmental cues, I am still intrigued by how ISA tip cell are instructed to bifurcate, and what is the mechanism of bifurcation. Bifurcation increases the density of the plexus and understanding the molecular players involved may open up new therapeutic avenues to modulate angiogenesis to reduce/increase vessel density.

It is clear that anastomosis relies on adhesion molecules, whether this is simply form a new junction or is involved in a signalling event. The possibility of following the distribution of certain adhesion molecules (VE-cadherin) live and monitor the dynamics of their accumulation is of great importance if we are to fully understand the multiple steps that transform a nascent sprout to a functional vessel. I have mentioned the technical challenges of generating transgenic lines that would allow this as well as the lack of a technology for single cell inducible LOF an GOF experiments at the specific site of anastomosis. The 3D EM techniques here presented are a neat addition to the toolbox available to scientists to increase the volume and resolution of data acquired. We are currently pursuing this further to obtain higher magnification, higher resolution images of fusing ISAs. Lumen formation is another critical step in angiogenesis and elucidating its mechanism may allow novel anti-angiogenic therapies to be developed. Anti-angiogenics have focused on stopping angiogenic growth but there is now evidence that it is not necessary to thwart the growth of blood vessels but simply to render them dysfunctional. This can be achieved by Dll4 inhibition, leading to

hypersprouting but resulting in a non-perfused plexus, inhibiting tumour growth (Noguera-Troise et al., 2006). Coupling anastomosis and lumen formation, there are many unanswered questions. Firstly the specification of the apical (luminal) membrane through the relocalization of molecules such Par family members is still unclear. This is important for the initiation of lumen formation for the targeting of sialomucins and actomyosin to the correct domain of the EC. We have no idea how a cell senses that it is the right time to lumenize, with VEGFA possibly involved. ECM is likely to be part of this mechanism, especially with regards to determining apical/basal polarity.

Chapter 4. The Role of *heca* in angiogenesis and lumen formation

In this chapter I will be addressing the question of whether anastomosis may be regulated by a genetic programme. As mentioned in Ch.3 the time delay between the final filopodia contact and fusion occurring is within a range that can accommodate for gene transcription, translation and protein activity. For this reason it was decided to investigate possible regulators of anastomosis. Here I describe the role of *heca*, the zebrafish homologue of the Drosophila gene *headcase* that is involved in tracheal anastomosis. *Heca* does not seem to play a direct role in ISA anastomosis but is involved in the later process of DLAVs crossover and fusion. Unexpectedly overexpression of *heca* induces early lumenization of the nascent sprouts, an effect shown to be endothelial cell autonomous. Combined with the earlier observation in Ch.3 where full cessation of filopodia activity only occurs following vessel lumenization, these results suggests that if Heca is playing a role in lumenization (as observed in GOF experiments), loss of Heca could be involved in instructing cells to lumenized and/or dampen filopodia activity a upon lumen formation.

4.1.1 Knockdown of *heca* in zebrafish embryos leads to early cross over of the DLAVs

Many parallels can be drawn between the development of the *Drosophila* tracheal system and sprouting angiogenesis such as the requirement for a morphogen gradient, tip cell selection through Dll/Notch lateral inhibition and the need for anastomosis to form a functional network (Affolter and Caussinus, 2008). Some of the growing tracheal sprouts must connect with their neighbours and this anastomosis involves the expression of a defined set of genes in a restricted number of fusion cells (one per sprout) (Samakovlis et al., 1996b) events. Six genes have been identified as fusion cell markers during tracheal development, with *escargot* (*esg*) controlling the regulation of

the other five; *headcase* (*hdc*) is one such gene (Samakovlis et al., 1996b). *Hdc* was firstly discovered as a marker for cell-cycle re-entry of imaginal discs (Weaver and White, 1995). It was later shown to have a role in tracheal morphogenesis. This is a system that develops with almost no cell division and *hdc*'s role has been pinpointed to the terminal branching/fusion process that occurs during the maturation of the tracheal network (Steneberg et al., 1998).

Retinas from osteopetrotic mice (*op/op*), which lack tissue macrophages, display a decreased branching/fusion vascular phenotype in post-natal retinal vessels (Rymo et al., 2011). Microarray data comparing *op/op* retinas with wildtype highlights increased expression of *heca*, the *hdc* murine homologue (Gerhardt, unpublished). It was therefore decided to investigate *heca*'s potential role in angiogenesis and anastomosis. This study was initiated by assessing whether *heca* really does play a part in angiogenesis and anastomosis. I decided to begin with functional studies using the power of zebrafish for Morpholino-based screening, prior to investing resources and time into understanding the expression and regulation of *heca*.

Two Morpholinos were designed, one targeting the ATG translational start site (MO1) and the other targeting the exon1-intron1 boundary to prevent correct splicing (MO2). The reverse primer used to test *heca* expression is within exon2 so missplicing (which will include intron1) will not result in the amplification of the fragment, as the DNA polymerase lack the processivity to synthetize the large insert within the RNA (Fig 4.1A). Morpholinos were microinjected into 1-4 cells stage embryos. Co-injection of ~3ng of p53 Morpholino was performed to reduce any potential p53-dependent toxicity that has been associated with such oligonucleotides (Robu et al., 2007). Injection with the splice blocking Morpholino (HecaMO2) leads to the loss of the correctly spliced fragment (forward primer at end of exon 1, reverse primer at middle of exon 2, ~480bp; Fig 4.1A-B). The Morpholino effectively leads to the inclusion of intron1 in the mRNA and thus prevents PCR amplification. Knockdown of Heca does not have any major effects on the overall morphology of the embryo at 24, 28 and 32hpf and development of the vasculature is normal (Fig4.2). Sprouting ISAs do not display migratory delays nor do they have defects in anastomosis.

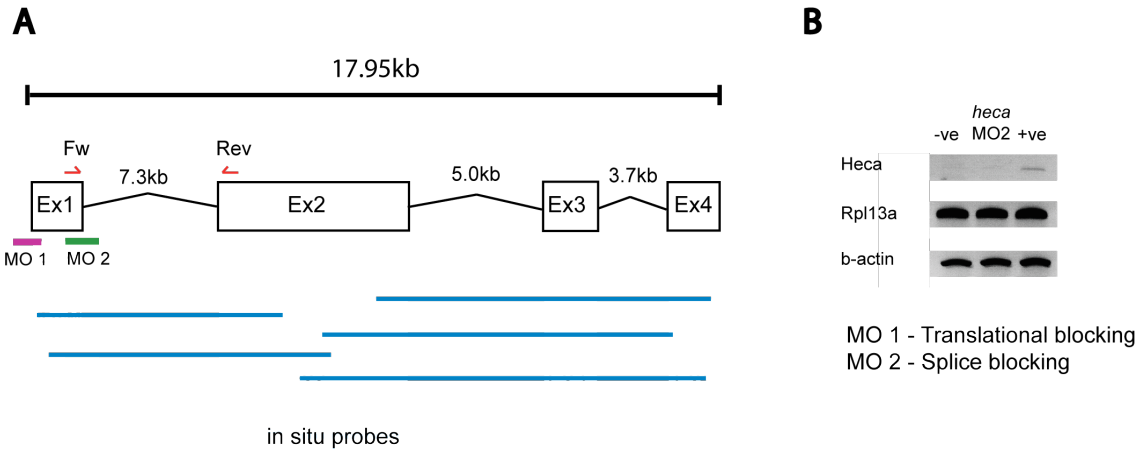

Figure 4.1 Heca gene structure
A. Diagram of exons and introns of the zebrafish *heca* gene. Primers to check for *heca* expression are marked (Fw and Rev, red arrows) as well the site of Morpholino binding (MO1, mauve, and MO2, green). The positions of *in situ* probe complementarity are indicated by the blue bars (Probe1-5). **B.** RT-PCR of cDNA using Heca RT primer pair. Positive control (+ve) is 48hpf wildtype cDNA, negative control (-ve) is mouse pulmonary endothelial cell cDNA, which shouldn't be complementary for primers. Rpl13a and b-actin were used as control primers.

The DLAVs form bilaterally along the trunk of the embryo and by 48hpf there are two parallel DLAVs along the entire length of the embryo (Isogai, 2001). At this stage there are very few cross connections between the DLAVs and these are limited to thin filopodia in the most caudal portion of the trunk (Isogai, 2001). Following 48hpf the DLAVs begin to connect over the neural tube in a caudal to rostral direction but limited to the caudal portion of the trunk, remaining as separate parallel vessels in the cranial part of the trunk. By 3dpf the caudal DLAVs have fused into a reticular plexus whereas the more rostral portion remains as parallel vessels. It is not until 7dpf that the cranial portion of the DLAVs becomes connected (Isogai, 2001). *In heca* morphants the DLAVs crossovers are already evident at 48hpf (Fig 4.3A) and are present along the whole trunk, even in the cranial portion of the DLAVs, a region where this does not normally occur until 7dpf (Fig 4.3B). Quantification of such ectopic DLAV connections demonstrates a significant increase between *heca* morphants compared to control morphants or uninjected embryos (Fig4.3D). The ectopic connections are not simple filopodia crossing over but lumenized vessels (Fig 4.3C). The phenotype resulting from use of the splice-blocking Morpholino is recapitulated with the use of a translation blocking oligonucleotide (HecaMO1, Fig 4.3). It must be noted that penetrance of this phenotype was low, observed only in around 12% of injected embryos. Live imaging of such DLAV connection formation was attempted but the resolution obtained fell short of our expectations. This was due to 1) the difficulty of positioning the embryo vertically so as to have the two parallel DLAVs in the same imaging plane and 2) the optical distortion caused by the tissue architecture along the dorsal aspect of the embryo.

Zebrafish angiogenesis is fascinating as it is based on at least two rounds of angiogenic sprouting that occur sequentially to give a patterned arterial and venous network. Recent work in understanding the mechanisms that discriminate between the different modes of angiogenic sprouting has unearthed some interesting findings. VEGF is important for the sprouting of the vessels from DA and not from the PCV whereas BMP2 is critical for venous sprouting without affecting arterial angiogenesis (Wiley et al., 2011). As *hdc* in Drosophila is regulated by Dpp which is a TGF/BMP family member, and therefore is an indirect downstream Dpp effector, it maybe possible that *heca* is an effector of BMP activity in zebrafish.

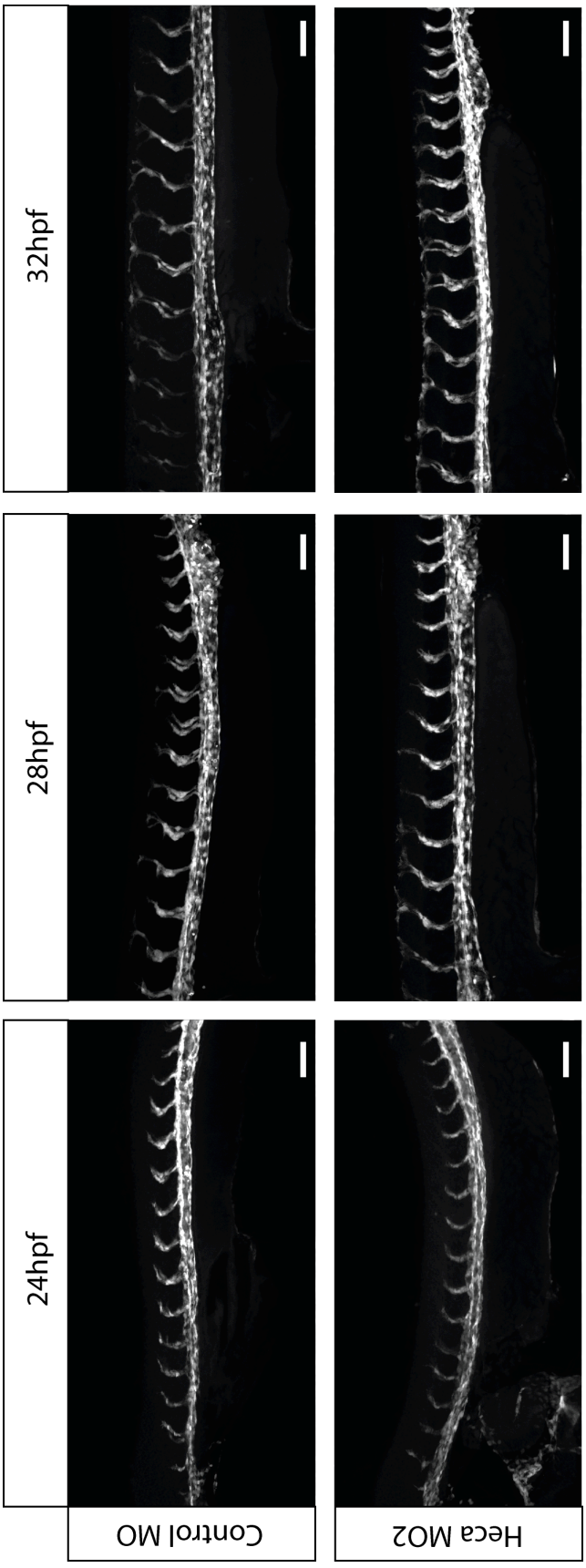

Figure 4.2 Knockdown of *heca* expression does not lead to general vasculogenic or angiogenic abnormalities.
fli:eGFP embryos are able to develop normally following HecaMO2 injection, without exhibiting vasculogenic and angiogenic defects. The axial vessels develop normally and the ISAs can sprout and migrate normally. Scale bars represent 80μm.

Knockdown of *heca* does not induce any defects in sprouting from the PCV that allows normal formation of the caudal plexus (Fig 4.3E) Sprouts emanate form the PCV and a venous networked is formed by 48hpf. Secondary sprouting from the PCV to either connect to the ISVs or to form the parachordal vessel is not impaired by decrease heca expression. *Heca* knockdown does not affect EC proliferation as the number of ECs per ISV was not altered (Fig 4.8B)

Overall, loss of *heca* expression leads to normal embryonic and vascular development with a specific effect on the connections between the DLAVs over the NT. Such an observation can be considered particularly significant as morphant embryos tend to be growth retarded when compared to uninjected ones, and thus possibly even reducing the temporal phenotype observed.

4.2 Heca overexpression leads to early lumenization of migrating sprouts

4.2.1 Migrating sprouts lumenize precociously due to *heca* expression

The effect of *heca* overexpression in zebrafish embryo development was investigated by injection of *in vitro* transcribed mRNA synthetized from cloned *heca* cDNA. The mRNA was titrated to find a dose that would result in minimal toxicity. Injection of ~100pg of *heca* mRNA in zebrafish embryos does not alter the normal overall development (Fig4.4), nor result in early vascular defects as the trunk axial vessels are able to form through vasculogenesis, evidence that angioblasts specification and migration from the lateral plate mesoderm are not affected (Fig 4.5A). The ISAs do not exhibit morphological or migratory abnormalities but lumenize extremely early, already showing extensive lumen opening by the time they reach the horizontal myoseptum. Cross-sections of the ISAs show that the entirety of the nascent vessel is lumenized (Fig4.5B). As this method of overexpression is at the whole embryo level, it was decided to test whether *heca's* effect on ISA lumenization was endothelial cell autonomous or was related to its expression in the surrounding environment. To do so

heca cDNA was cloned downstream of the *flk1* promoter fragment to drive endothelial specific expression, and upstream of a 2A viral peptide followed by dTomato to label overexpressing clones. Viral peptides such as the 2A system employed here can be used to link two open reading frames to give stoichiometric expression of both proteins from a bicistronic sequence. 2A peptides are short amino acid sequences (~20aa) found in picornaviruses and represent a superior alternative to Internal Ribosome Entry Sequences (IRES). The mechanism relies around a Gly-Pro sequence within the 2A peptide that leads to ribosome stalling during translation, the skipping to the following codon and the cleavage of the Gly-Pro bond in the nascent polypeptide. The ribosome can then continue to translate the subsequent portion of the mRNA that contains the second coding sequence, leading to a 1:1 ratio of the two encoded proteins (Szymczak et al., 2004). From my experience with the use of the *flk1* promoter it has become evident that the fluorescent protein marker can be extremely difficult to detect at the early stages of ISV sprouting but it is evident at later stages (Fig 4.6B). Endothelial specific expression of *heca* by transient expression also leads to the aberrant lumenization phenotype (Fig4.6A), illustrating that it is an endothelial cell autonomous phenomenon but is still a multicellular process as lumen formation is not a unicellular event.

To determine whether the lumenization of early ISAs was functional and connected to the trunk circulation, microangiography with fluorescent quantum dots (Qdots) was performed. Qdots are present within the migrating sprouts of *heca* overexpressing embryos while none are observed in control embryos, confirming the presence of open functional lumen within the vessel (Fig 4.7A-B). Concomitant with the early lumen, some ISAs exhibit local cell clustering, with many nuclei close together in the sprout (white asterisks, Fig 4.7B).

4.2.2 Cell cluster phenotype is a result of increased cell numbers

The cell clustering observed in ISAs could be due to an increase in the number of cells in the sprout. *Hdc* is required for imaginal discs to re-enter into the mitotic cell

cycle (Weaver and White, 1995) while in human head & neck cancer cell lines *heca* has the opposite effect (Dowejko et al., 2009).

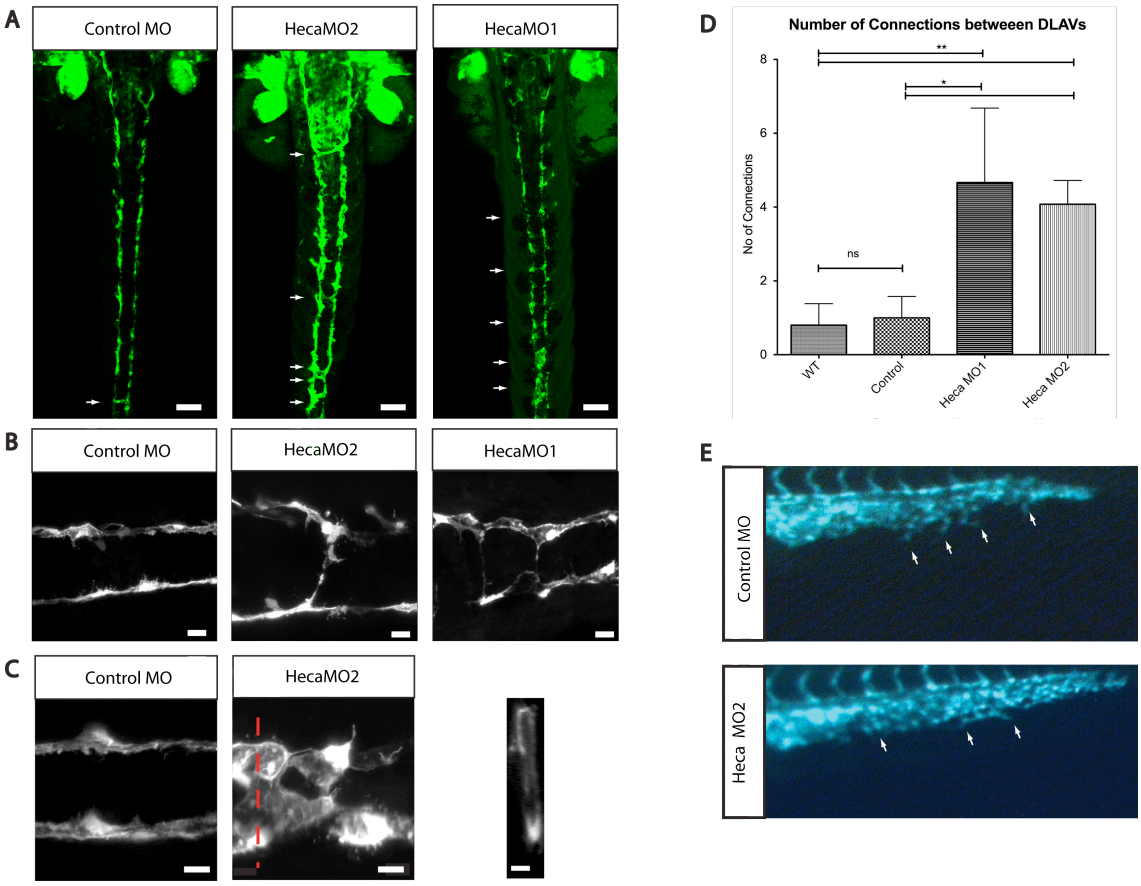

Figure 4.3 Early crossover of DLAVs is observede upon decreased *heca* expression. Knockdown of *heca* expression leads to early and ectopic crossover connection between the DLAVs (A, white arrows). Similar results are observed with splice blocking or translation blocking Morpholinos (Heca M2 and MO1 respectively). B. Close up of ectopic connections in cranial portion of DLAVs. C. Crossover connections are lumenized (cross section in right panel). D. Quantification of crossovers shows significant difference between uninjected and control injected embryos with morphants Heca morphants embryos. (* $p<0.05$, ** $p<0.005$, 4 independent experiments). E. No developmental defects can be observed in the BMP2-dependent vascular plexus formation. Scale bars represent 40um in A, 10μm in B, 10μm in C.

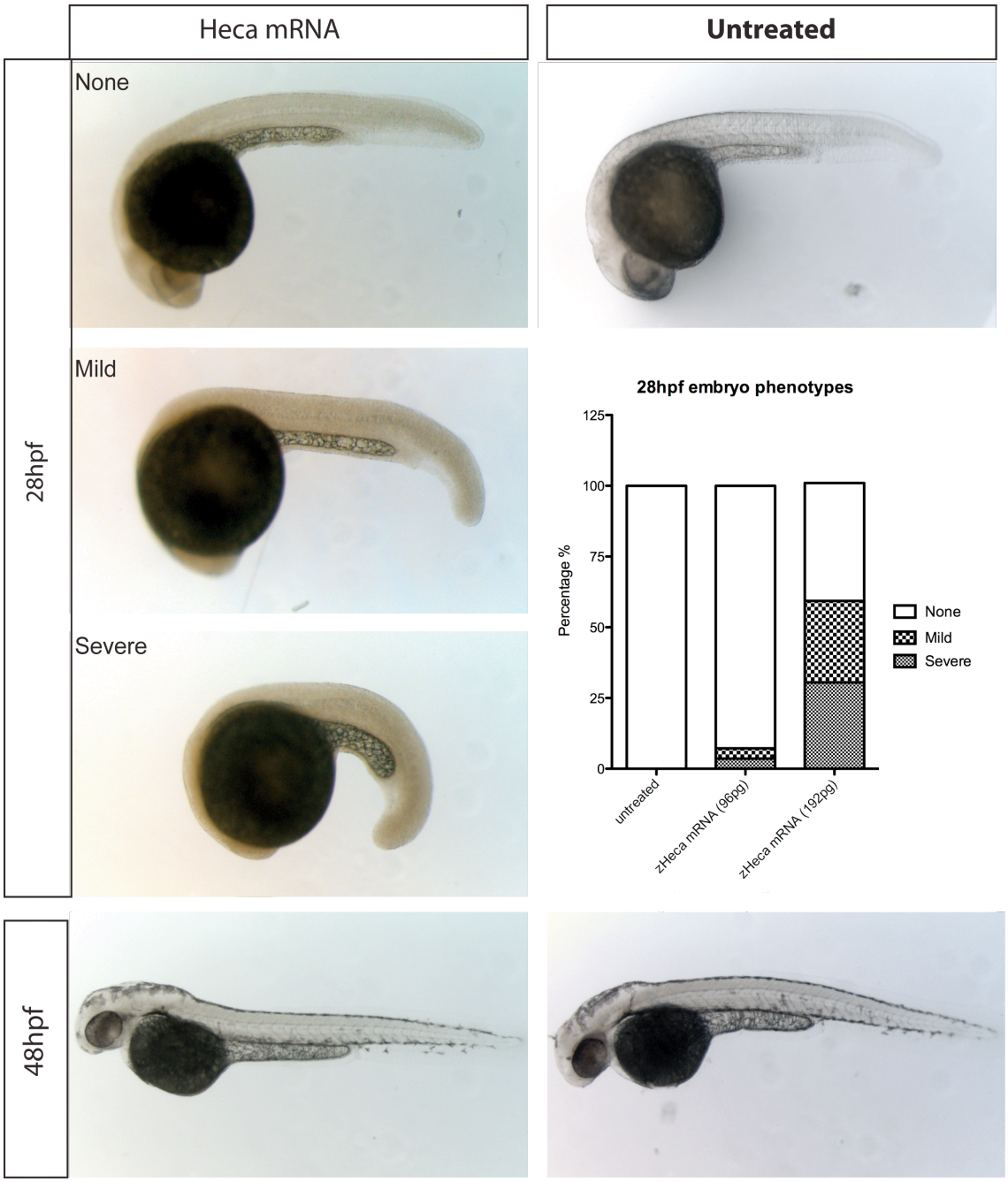

Figure 4.4 No general developmental defects are induced by moderate heca overexpression.
Injection of 100pg of *heca* mRNA does not affect development. A higher dose slows/stops development of embryos (*n*=185, 3 independent experiments). The lower does was used for overexpression experiments.

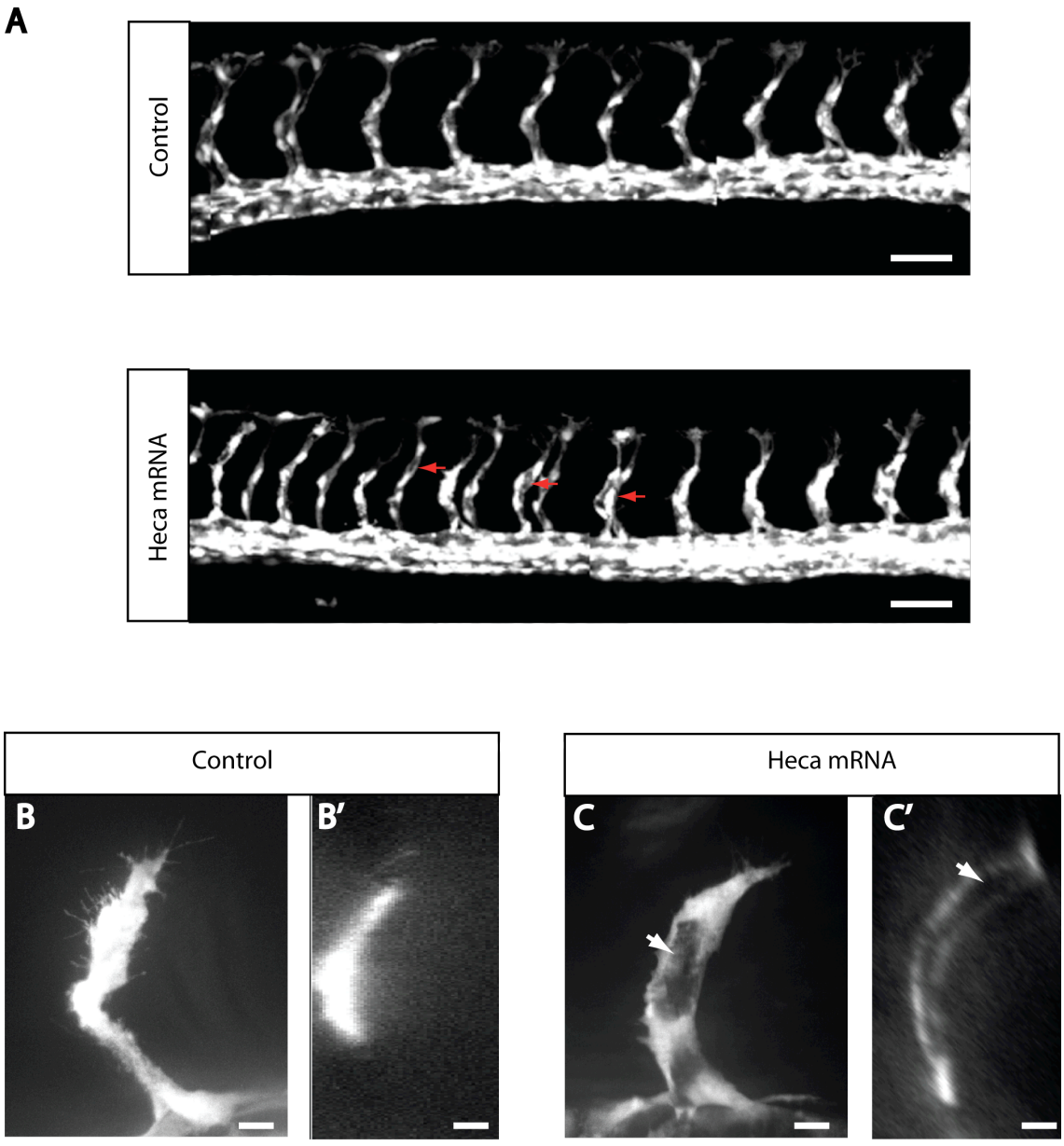

Figure 4.5 Heca overexpression leads to early ISA lumenization.
A. No vascular phenotype is observed at 28hpf therefore Heca isn't affecting axial vessel formation. Precociously lumenized vessels can be seen in the trunk (red arrowheads). B-C. No lumen is observed in the cross section of control ISAs (B-B') whereas the ISA is fully lumenized in Heca mRNA injected embryos (C-C', white arrow). Scale bars represent 50μm in A, 10μm in B-C

Either way *heca* appears to affect cell proliferation in certain systems, though this is not the case in the tracheal network. To asses whether there was an increase in cell numbers in the ISVs, I used the *Tg(flk1:nls-eGFP)* line (Blum et al., 2008) with endothelial specific nuclear-localized eGFP expression to quantify the number of EC nuclei in overexpressing embryos. Overall there was no difference in the number of cells observed per ISA at the whole embryo level (Fig 4.8A-D). If however one compares the average number of EC nuclei in sprouts displaying cell clustering then there is a clear increase in the average (Fig 4.8D). In the most drastic cases three nuclei are seen at the leading edge of the migrating sprout, some lacking the elongated EC appearance, possibly as a result of such crowding at the tip of the ISA (Fig 4.9B-B"). In Fig 4.9 an ISA that has yet to pass the myoseptum contains 5 nuclei, a stage at which usually two to three nuclei are observed (Fig 4.9A-A"). As for the knockdown, the overexpression phenotype was evident in only 10% of injected embryos.

4.2.3 Cell adhesions in ectopic lumen formation

The overexpression phenotypes of early lumenization suggest that *heca* leads to an early determination of the apical surface of ECs whilst cell clustering supports the notion that ECs numbers are greatly increased in sprouting ISAs. The most recent models of vascular lumen formation initially involve the formation of an apical domain of the ECs that allow the segregation of surface molecules such as sialomucins, believed to aid the opening of the lumen. A molecule that is important for the establishment of EC polarity, especially during lumen formation is VE-cadherin (Strilic et al., 2009, Strilić et al., 2010, Wang et al., 2010a). The rearrangement of junctional molecules is also important in lumen formation with regards to cellular movement and intercalation (Blum et al., 2008). VE-cadherin is an important protein in adhesion junctions and plays a major role in vascular stability (Dejana et al., 2009). The migratory behaviour of ECs can also be affected by levels of VE-cadherin and is required for the movement of ECs within a tissue (Perryn et al., 2008). Ve-cadherin localization was assessed in *heca* overexpressing embryos by carrying out immunostaining for ZO-1, a tight junction protein shown to colocalize with VE-cadherin (Blum et al., 2008). This was to ascertain whether the *heca* GOF-induced phenotypes are related to changes in EC junctions.

When observing normal ISAs found in *heca* overexpressing embryos, the junctional architecture is rather similar to what is found in control embryos and with what has been previously described (Fig 4.10A’’’, B’’’)(Blum et al., 2008). This is not the case for ISAs exhibiting clustered ECs, where the junctions clearly reflect the chaotic arrangement of cells (Fig 4.10B’’’, white arrow). Even so the junctions still maintain strong ZO-1 presence at cell boundaries compared to normal ISAs, suggesting that *heca* overexpression is not affecting the formation of EC junctions.

4.3 Heca expression

4.3.1 Zebrafish

The loss and gain of function experiments revealed that *heca* has a role in zebrafish angiogenesis. Therefore I set out to characterize its expression and regulation by using a combination of *in vivo* and *in vitro* approaches. Only one orthologue of *hdc* is found in zebrafish. The expression pattern of *heca* was firstly analysed by *in situ* hybridization using five riboprobes that were designed de novo (Fig 4.1A), to include all exonic sequences in the analysis. At 28hpf *heca* is ubiquitously expressed at low levels throughout the embryo, with slightly stronger staining observed in the head. (Fig 4.11B-F and 4.12B-F). This pattern is consistent for all 5 riboprobes. The weak, sparse expression in the trunk seems to concentrate within the somites as shown in transverse sections (Fig4.12G). The presence of *heca* transcript was confirmed by reverse transcriptase PCR at 8, 24, 32 and 48hpf and by qPCR at 30hpf (Fig4.13). The broad expression in the trunk neither confirmed nor excluded endothelial contribution to *heca* mRNA expression in zebrafish.

The use of commercial anti-Heca antibodies for immunofluorescence did not yield detectable signal in zebrafish embryos therefore custom anti-peptide antibodies were generated using Eurogentec 28-day super speedy polyclonal immunisation protocol (Eurogentec, Seraing, Belgium). Rabbits were immunized with one of two selected peptides.

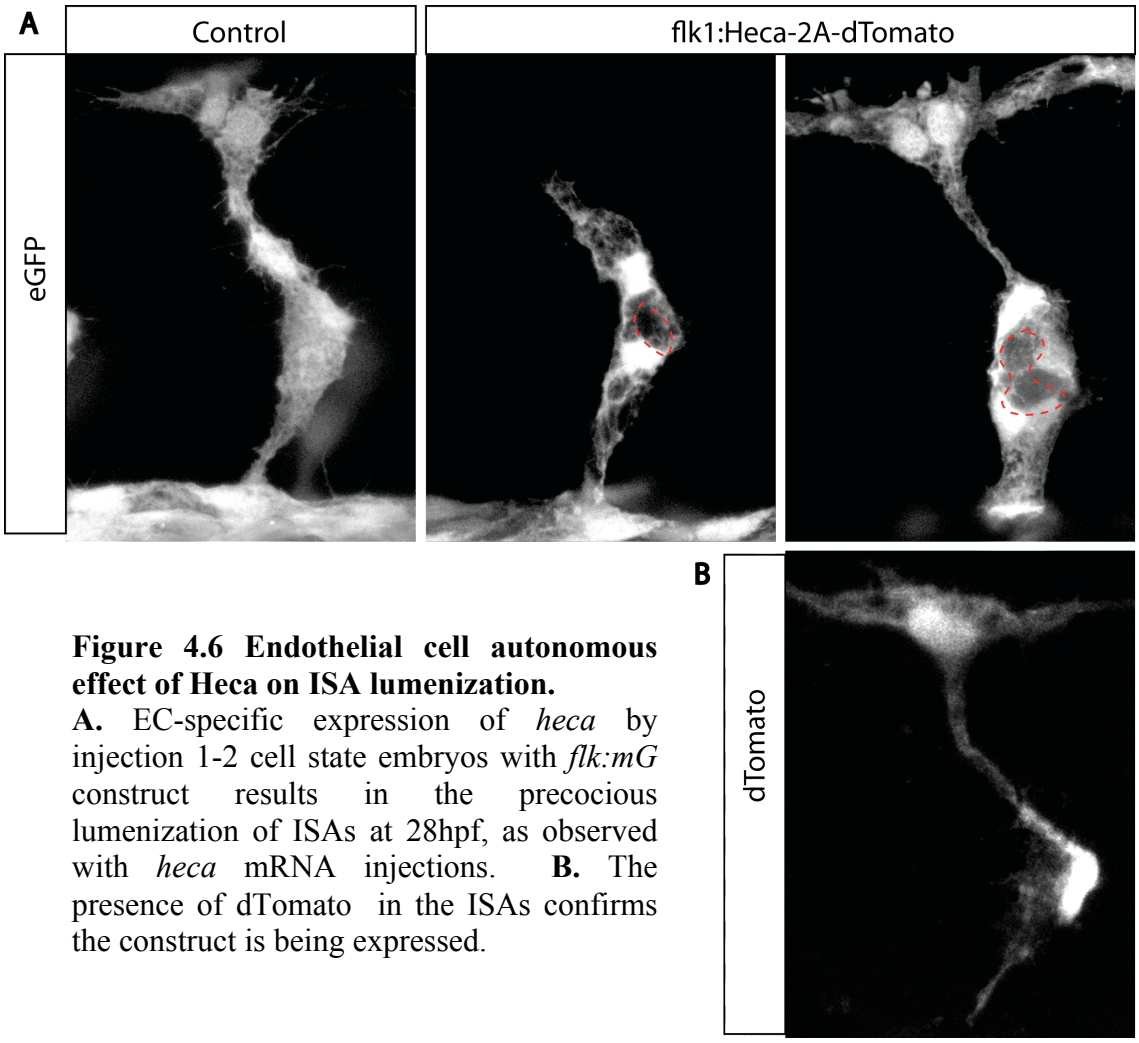

Figure 4.6 Endothelial cell autonomous effect of Heca on ISA lumenization.
A. EC-specific expression of *heca* by injection 1-2 cell state embryos with *flk:mG* construct results in the precocious lumenization of ISAs at 28hpf, as observed with *heca* mRNA injections. **B.** The presence of dTomato in the ISAs confirms the construct is being expressed.

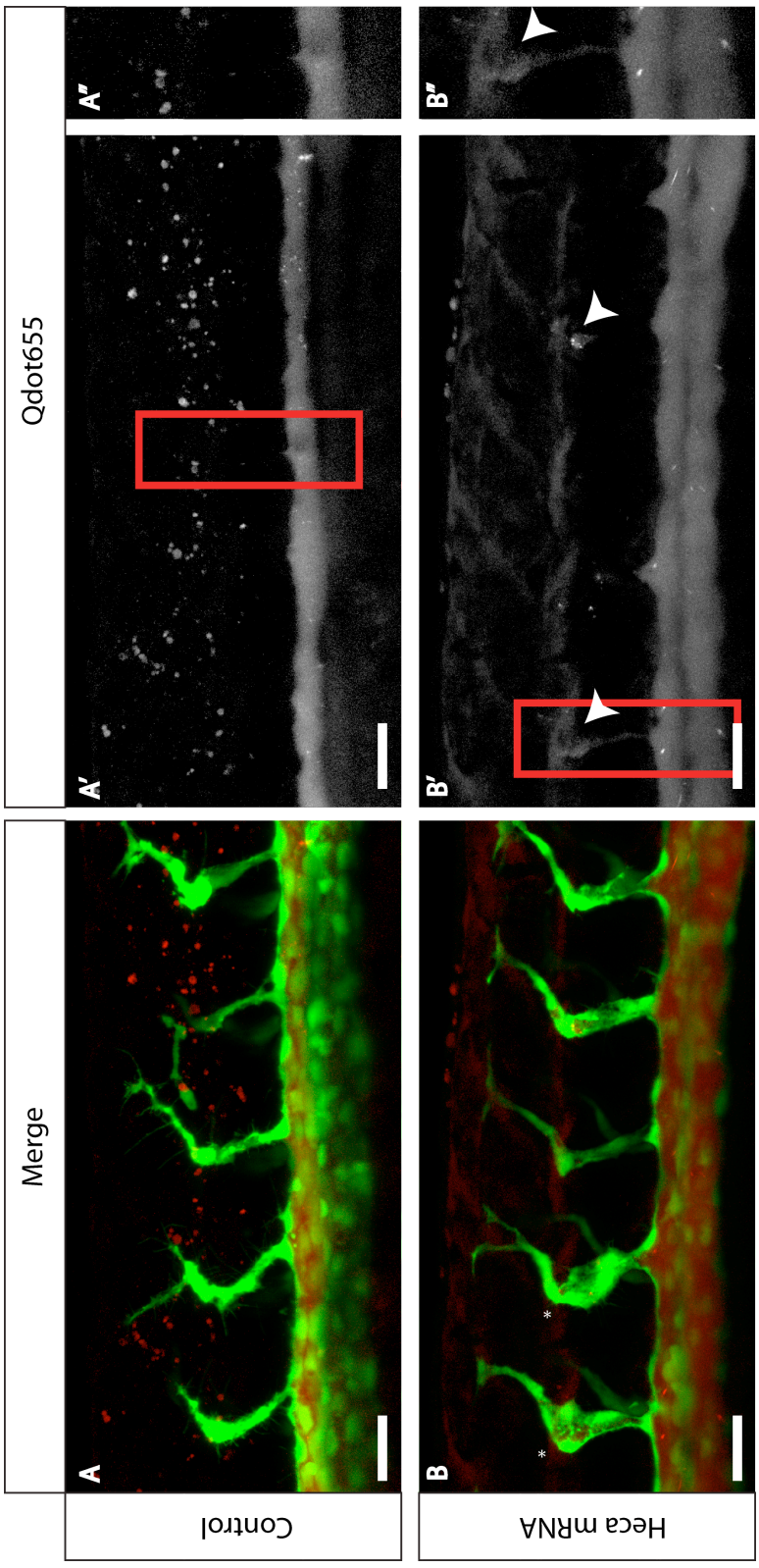

Figure 4.7Lumen phenotype observed in Heca overexpressing embryos is open lumen connected with trunk circulation.
No Qdots can be observed in control ISAs at 28hpf (A-A") whereas they are present in Heca mRNA injected embryo ISAs (B-B", white arrowheads). White * mark cell clumping in ISAs. Scale bars represent 30μm.

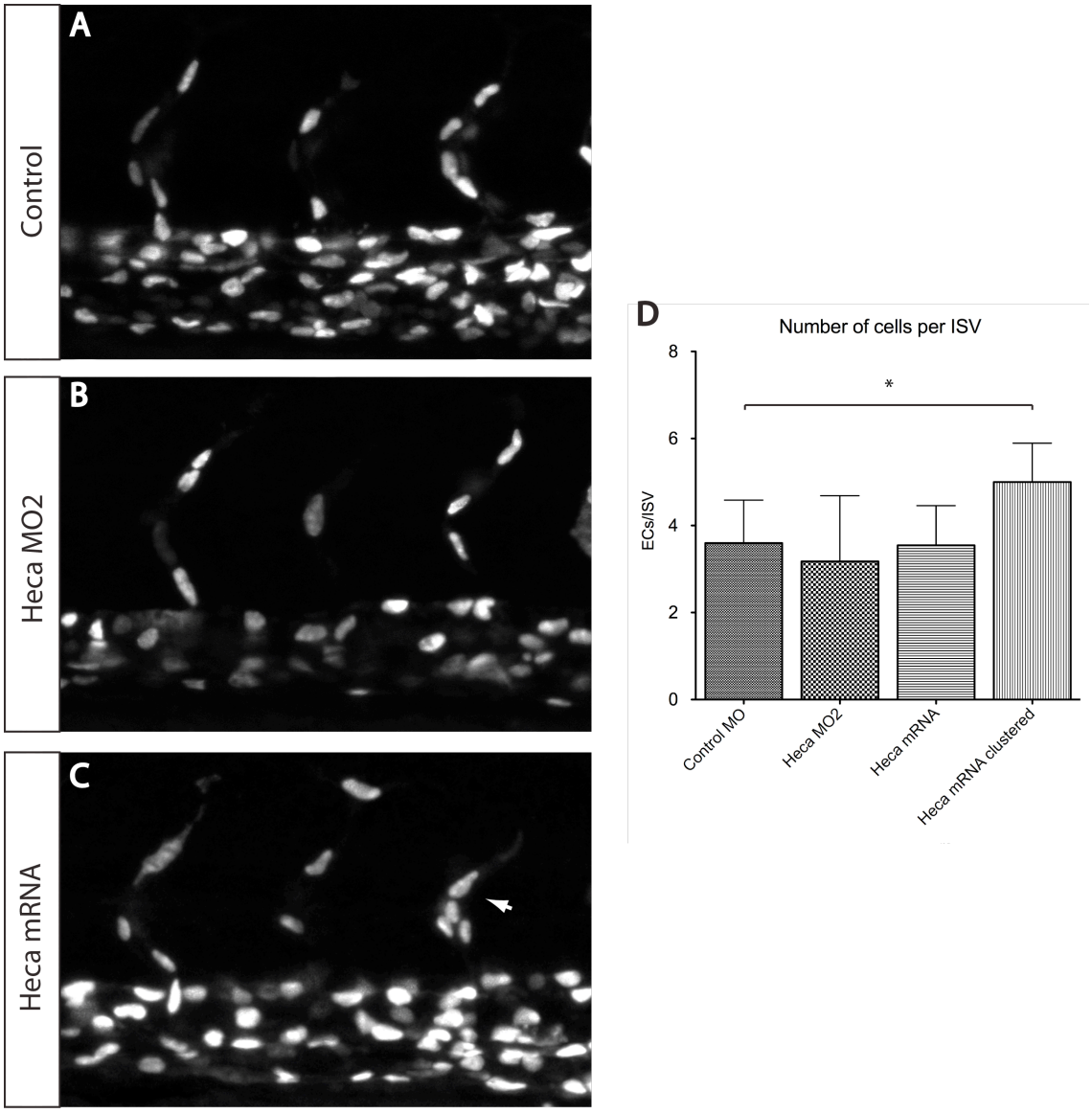

Figure 4.8 Heca overexpression leads to cell clumping due to increase in the number of ECs per ISA.
Injection of Heca mRNA leads to ECs clumping together in certain ISAs (C). Knockdown of Heca expression did not lead to such a phenotype (B). Overall number of cells per ISA is not altered by gain or loss of function Heca but analysis of ISA shows clear increase in *heca* overexpressing ISAs (* = $p < 0.05$) (D). $n = 62$, 2 independent experiments.

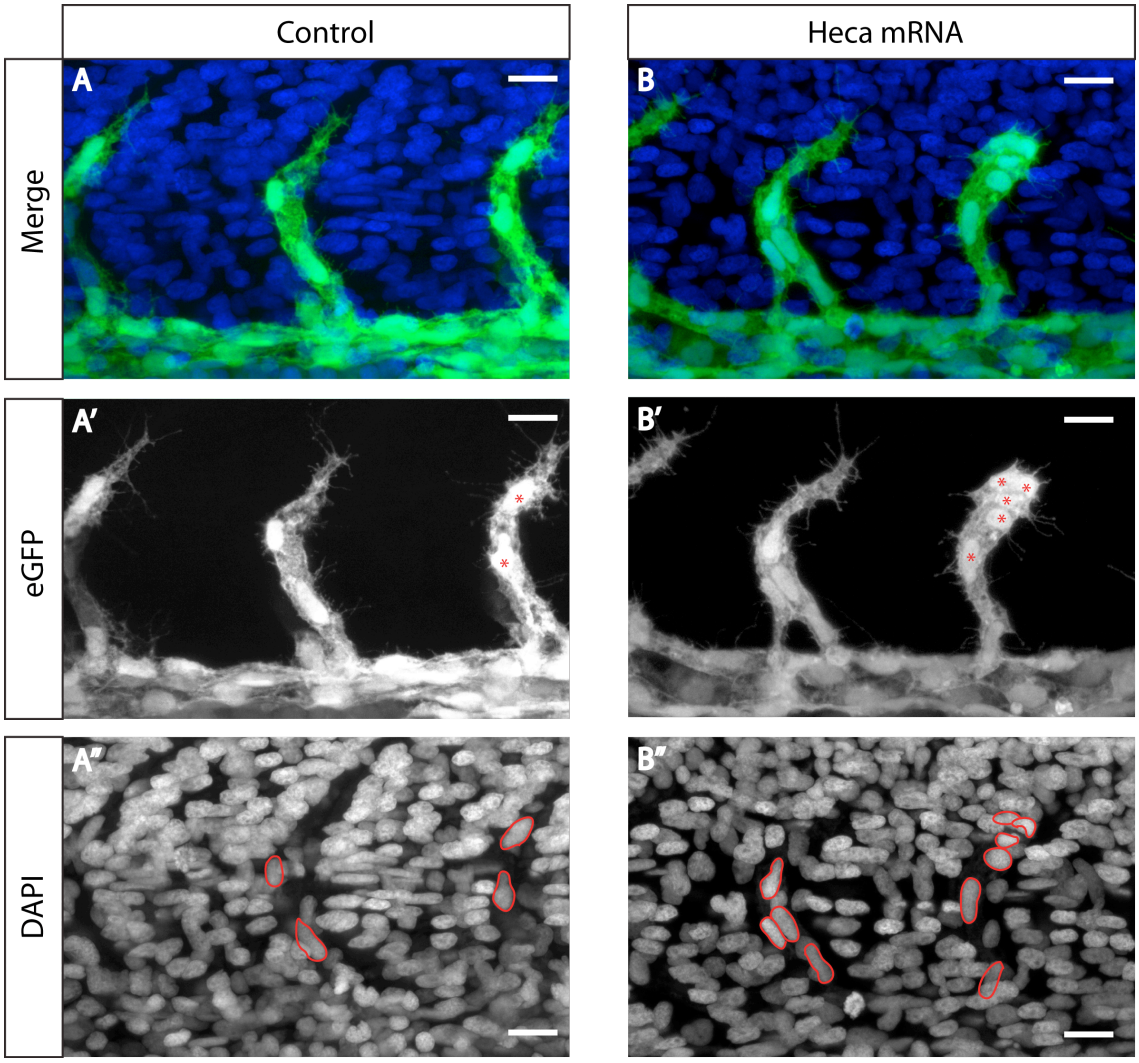

Figure 4.9 Extreme case of nuclei crowding at leading edge of ISA in Heca overexpressing embryo.
Overall vascular appearance is normal in Heca overexpressing embryos (compare A-B) apart from 1 ISA where 4 nuclei are bunched at the growing front (red asterisks in B'). In this extreme case overall nuclei number in ISA are elevated (circled in red in B") with a total of 5 nuclei when compared to control embryos were only 2 nuclei are present at this stage (A"). Scale bars represent 10μm.

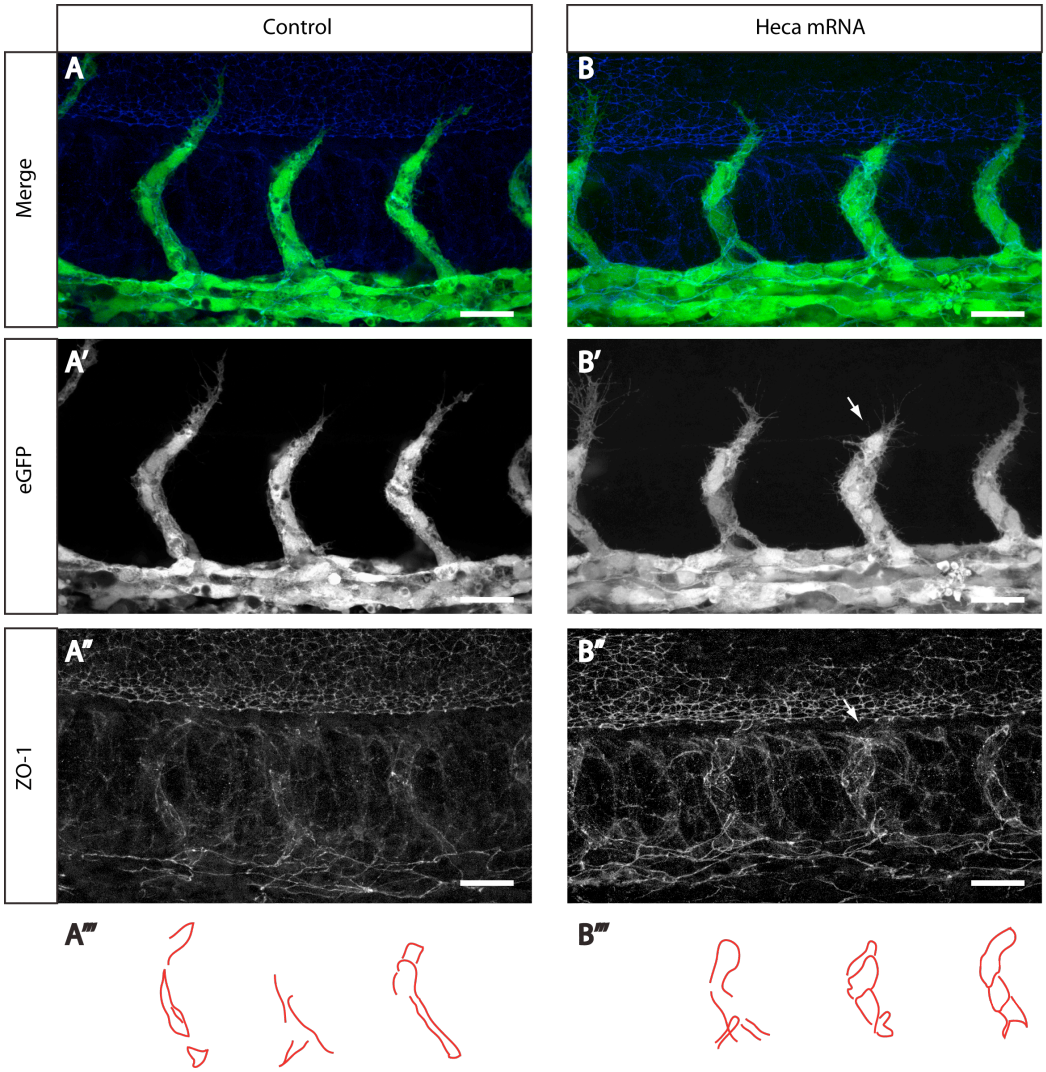

Figure 4.10 Adhesions in heca overexpressing embryos. A-A'''.
Control embryos display normal junctional staining as had been previously described by Blum *et al* (Blum et al., 2008). **B-B'''.** Heca overexpressing embryos possess ISAs with increased number of ECs and the junctions are accordingly affected. Many more junctions are observed in the overcrowded ISA (B''', white arrow) due to the presence of more cells. Scale bars represent 10μm.

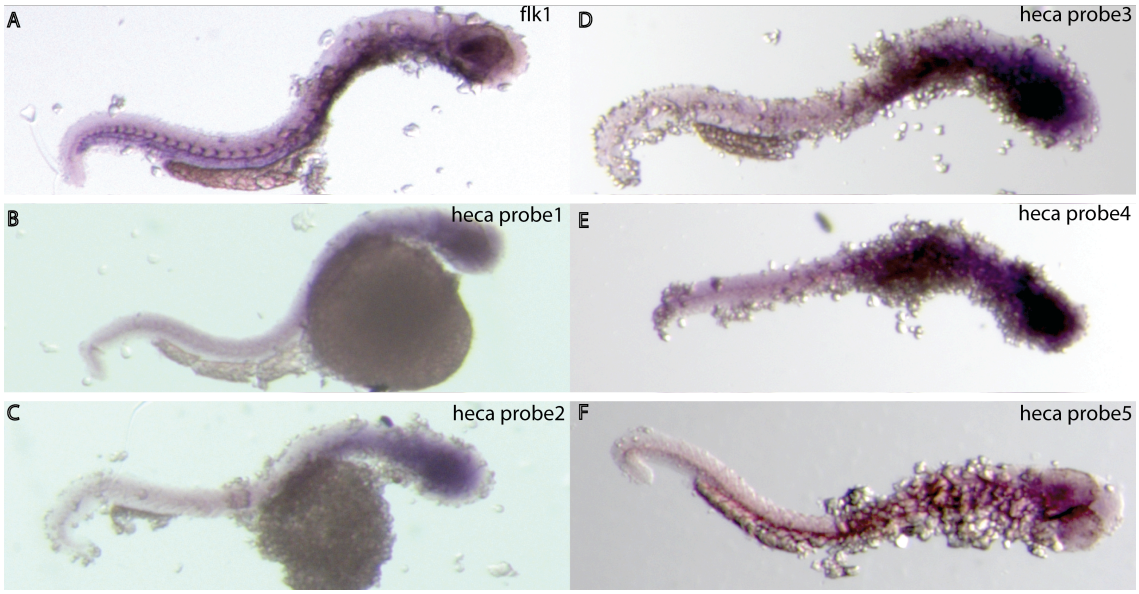

Figure 4.11 *heca in situ* hybridization reveals weak expression.
5 *heca* riboprobes give a weak signal in the trunk while the expression appears stronger in the head (B-F). *flk1 in situ* was performed as control.

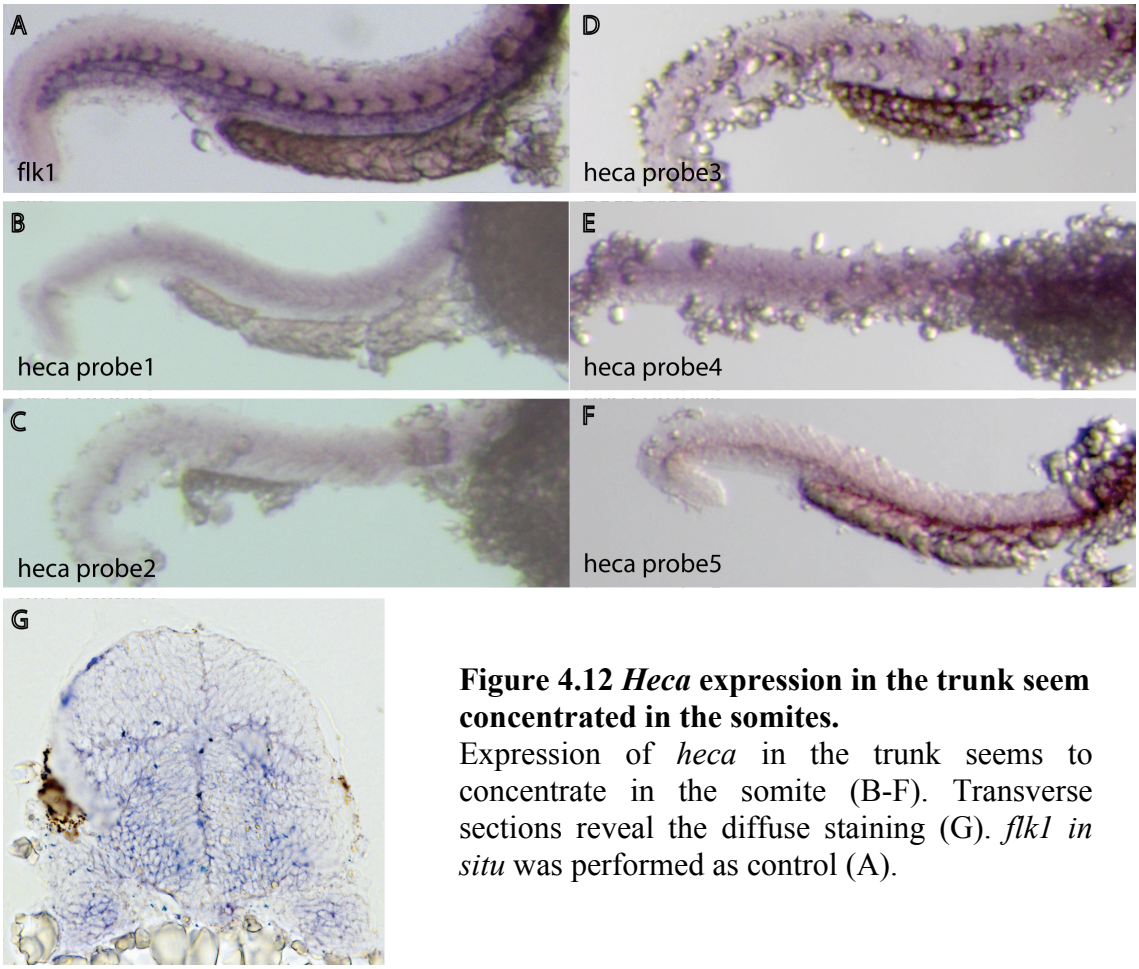

Figure 4.12 *Heca* expression in the trunk seem concentrated in the somites.
Expression of *heca* in the trunk seems to concentrate in the somite (B-F). Transverse sections reveal the diffuse staining (G). *flk1 in situ* was performed as control (A).

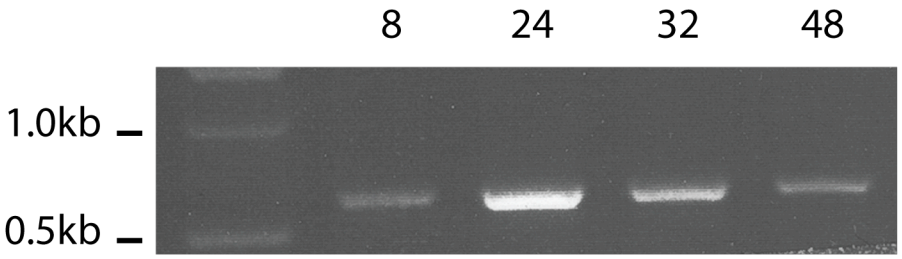

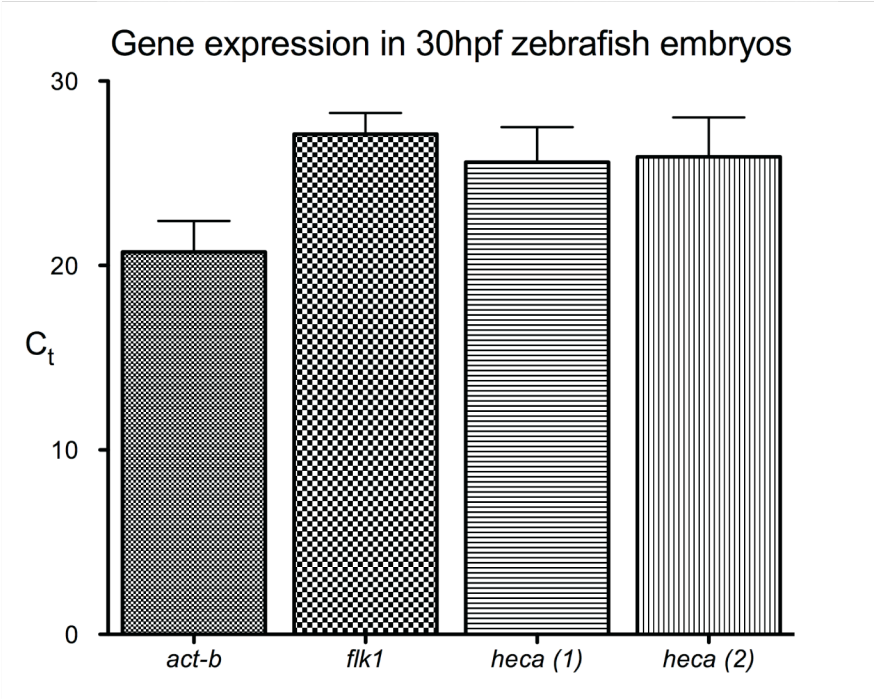

Figure 4.13heca is expressed throughout zebrafish embryonic development.
A. RT-PCR detects expression of *heca* at 8, 24, 32 and 48hpf. B. Expression of *heca* at 30hpf is confirmed by qPCR, comparing its cycle counts with *flk1* and *actb.*

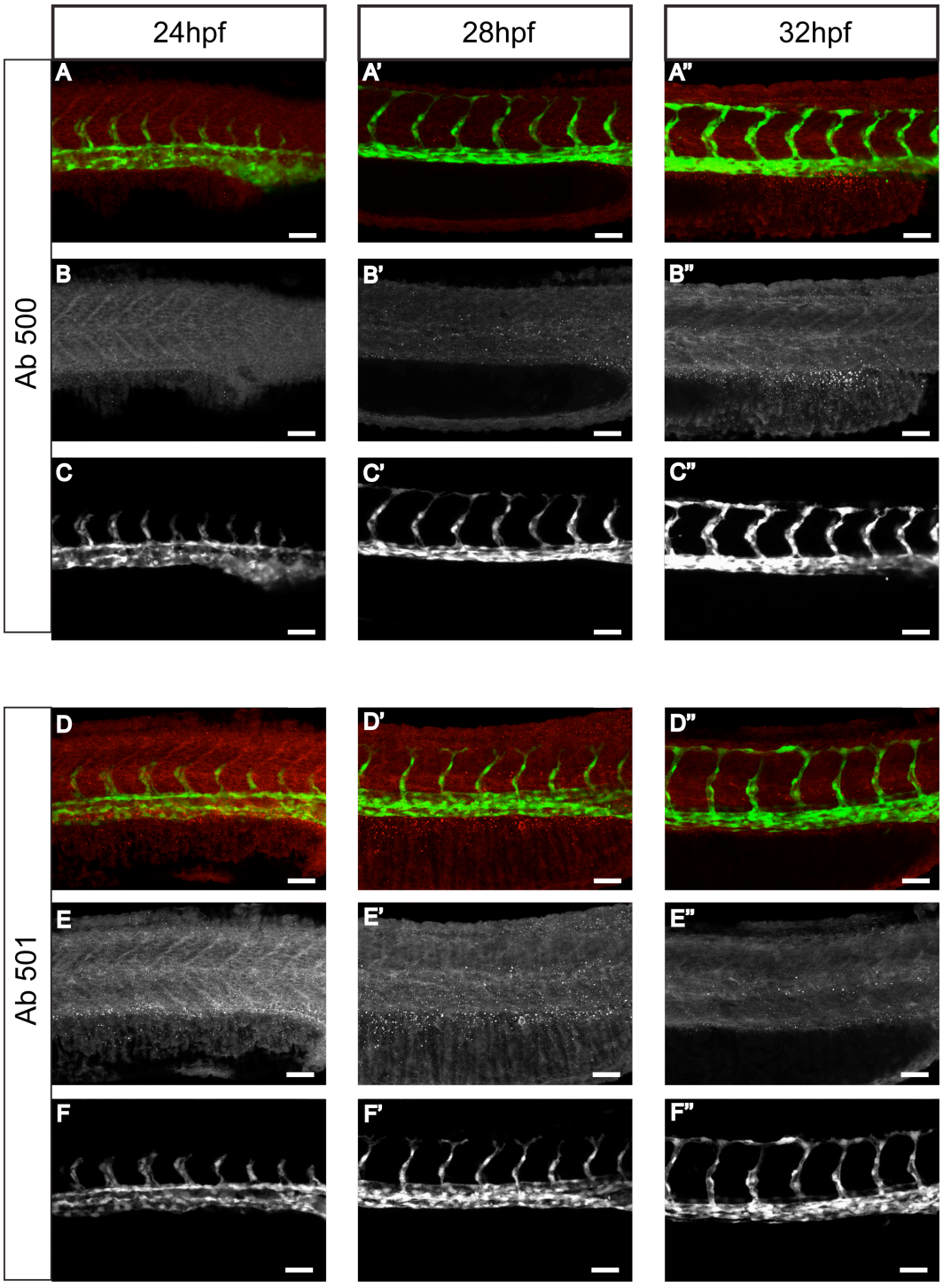

Figure 4.14Custom Heca antibody staining of zebrafish embryos.
A-C. Zebrafish embryos at different developmental stages show presence of Heca protein (with Ab 500) within the somites, with the strongest signal detected at 24hpf. **D-F.** Similar results are obtained when using Ab 501, with a slightly stronger detectable signal compare to Ab500. Scale bars represent 40μm.

Both peptides matched portions of the C-terminus, which is an extremely well conserved region, with 100% homology between species (Fig1.13), hoping to result in antibodies with cross-species reactivity. The antibodies were tested for peptide binding by ELISA and both rabbits developed antibodies that were strongly immunoreactive against one of the two peptides used for immunization. *Heca* expression pattern is similar to the mRNA, ubiquitous and weak, with higher expression in the somites within the trunk (Fig4.14).

4.3.2 Heca expression in mouse retinal vasculature and embryoid bodies

As the *in vivo* zebrafish experiments fell short of confirming endothelial expression of *heca,* its expression was tested in mouse tissue by immunofluorescence to investigate further the localization of its expression. Mouse post-natal retinal vasculature and sprouting embryoid bodies were assayed for the presence of Heca protein.

In mouse post-natal retinas Heca is present in astrocytic nuclei (Fig 4.15A', B'), which can be easily recognized due to their triangular shape and presence of Pax2 (Fig.415C). Astrocytes are glial cells found in the CNS and play an important role in supporting endothelial cells and in the specific case of the retina, they pre-pattern the retina with VEGF to direct angiogenic sprouting to the hypoxic tissue (Gerhardt, 2003). Heca is also present in some ECs and is both nuclear and cytoplasmic, with characteristic elongated EC nuclei (Fig 4.15A'). No difference in presence of expression or levels is evident between the sprouting front, capillary plexus and tip/stalk cells.

Embryoid bodies (EBs) are aggregates of embryonic stem cells that can be induced to differentiate into ECs by plating the spheroids in a collagen matrix and supplementing the growth medium with VEGF. Heca is observed in PECAM-1 positive cells, confirming its presence in ECs, again with no difference between tip and stalk cells, even though some difference in expression is observed between ECs (Fig4.16A'-B'). Surprisingly though, the Heca antibody staining accumulated in the nucleus, even

though previous literature describes it as a cytoplasmic protein (Weaver and White, 1995)

4.3.3 Possible Regulation of Heca

In *Drosophila hdc* is under the transcriptional control of *esg*, which is a member of the Snail family transcriptional repressors/activators (Samakovlis et al., 1996b, Whiteley et al., 1992). *Esg* is induced in tracheal fusion cells once the sprouts have reached the location within the target tissue where the tracheal metameres need to connect. These areas are marked by expression of Dpp, a member of the TGF/BMP superfamily (Vincent et al., 1997). I therefore investigated whether *heca* in zebrafish could be under control of the TGF/BMP-Snail axis.

Dpp is believed to be homologous with BMPs. I investigated the extent of BMP signalling in zebrafish embryos by looking for the presence of phosphorylated R-Smad 1/5/8 (P-Smad 1/5/8). At 30hpf P-Smad 1/5/8 was present in the dermis, in the dorsal portion of the NT and in the pronephric duct (Fig 4.17C). The use of a BMP reporter line (BRE-RFP) (Wu et al., 2011) crossed with *fli1:eGFP* highlights active BMP signalling in the same regions as with immunofluorescence (Fig 4.18). Neither technique indicated that there was any BMP signalling in ECs present in the DA, PCV and ISAs. No signal is observed in the caudal plexus whose formation is BMP-dependent and regulated by phosphorylation of R-Smads (Wiley et al., 2011). Whether this is because of a clear lack of P-Smad 1/5/8-dependent signalling in this vascular bed or because of inadequate sensitivity of the assay is unclear.

Snail family proteins are important in gastrulation as they increase cell motility by decreasing expression of adhesion molecules such as cadherins (Cano et al., 2000). Oddly in *Drosophila esg* leads to the upregulation of DE-Cadherin that is required to form the new junction between the two fusion cells leading to anastomosis (Tanaka-Matakatsu et al., 1996). In human dermal microvascular ECs ectopic expression of Snail family proteins by breast cancer cell-conditioned medium has been shown to downregulate VE-cadherin, an effect achieved by direct binding and repression of the VE-cadherin promoter region (Lopez et al., 2009). It is thus unclear exactly what effect

Snails may have on ECs as VE-cadherin is required for EC movement within a sprout (Perryn 2008) but an increase in Snail family members leads to a shift to mesenchymal characteristics through downregulation of cadherin (Cano et al., 2000). Snail knockout mice are embryonic lethal due to very early gastrulation defects (Carver et al., 2001) but epiblast specific deletion of Snai1 leads to embryonic lethality that has been attributed to vascular network formation and not endothelial differentiation (Lomelí et al., 2009). Snai1a RNA is detectable in the head mesenchyme, brachial arches, in somites and in the tail bud of zebrafish embryos (Herbomel et al., 2001). Snail protein is found in EC nuclei in zebrafish ISAs at what seem to be quite high levels (Fig 4.19). It is possible that Snail is required to allow ECs to move in the vasculature throughout its development. Slug protein could not be detected with the antibodies used. The above data provide evidence of BMP signalling in the area of the embryo where the ectopic and precocious DLAVs crossovers are observed but P-Smad1/5/8 staining indicates that BMPs are not acting on ECs. On the other hand angiogenic events such as the sprouting from the caudal plexus that are dependent on BMP signalling are not affected by loss of expression of *heca* (Fig 4.3E).

In mouse retinas Heca co-localizes with Snail in astrocytic nuclei but this cannot be interpreted as direct evidence of Snail induced Heca expression (Fig 4.15D). BMP4 protein can be observed surrounding the retinal vasculature with the highest level present at the sprouting from. BMP4 is also present ahead of the growing plexus but at lower levels (Fig 4.20A-B). Evaluation of BMP signalling in the retina for P-Smad 1/5/8 resulted inconclusive.

To further investigate the regulation of Heca expression *in vitro* cellular assays were used. The effects of a series of agonists and inhibitors on the expression of Heca and Snail family proteins were tested. EBs can be induced to differentiation into EC by the addition of VEGF to the growth medium. In line with this differentiation, the resulting ECs are able to respond to genetic and pharmacological intervention as in vivo ECs would. Known inhibitors were used on sprouting EBs to assess whether they had an effect on *heca* and *snails* expression.

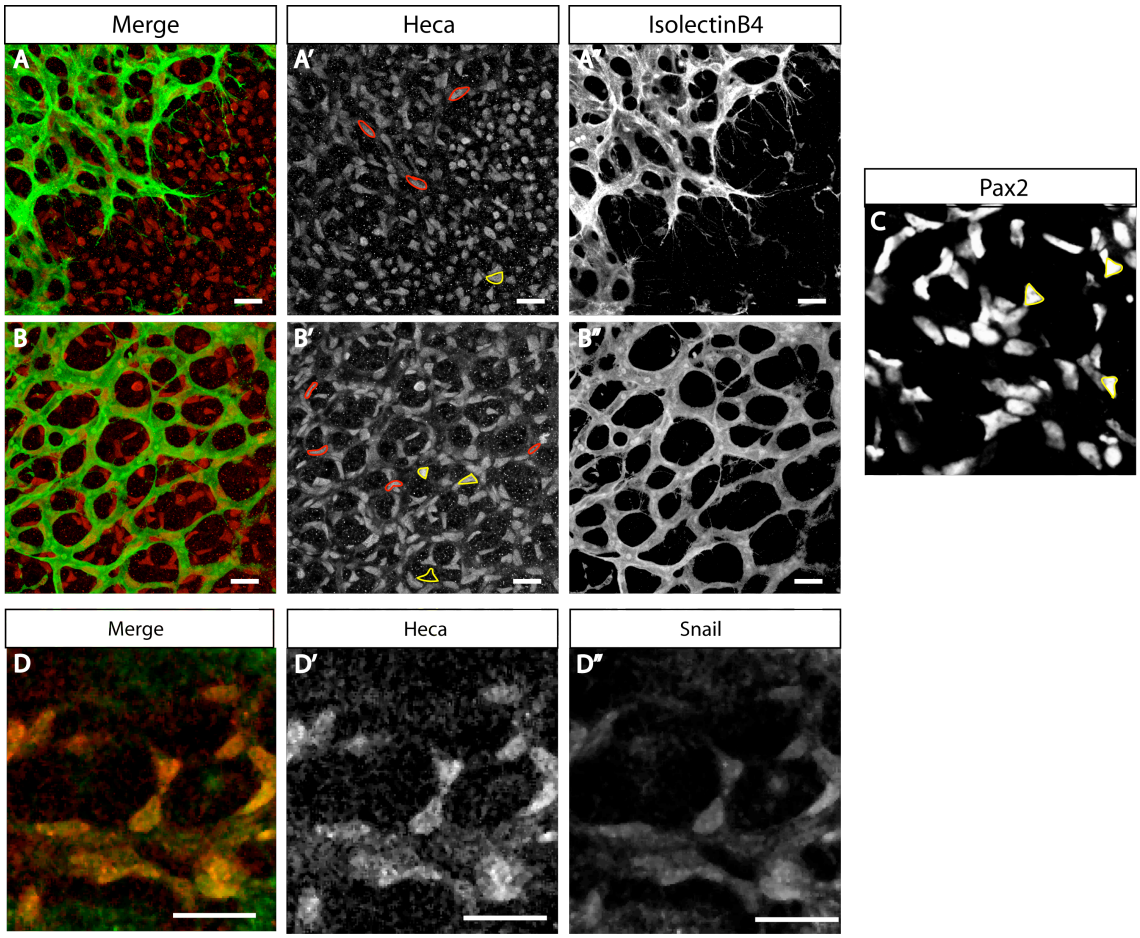

Figure 4.15 Heca is present in ECs and astrocytes within mouse retinal vasculature.
Retinal vasculature at the sprouting front (A) and in the capillary plexus (B). Heca is observed in elongated EC nuclei (A' and B', outlined in red), with some more diffused cytoplasmic staining. Astrocytic nuclei also express Heca (A'-B', outlined in yellow) and can be recognized by their triangular shape (see C, outlined in yellow). D. Snail and Heca co-localize in astrocytic nuclei. Scale bars 10 μm

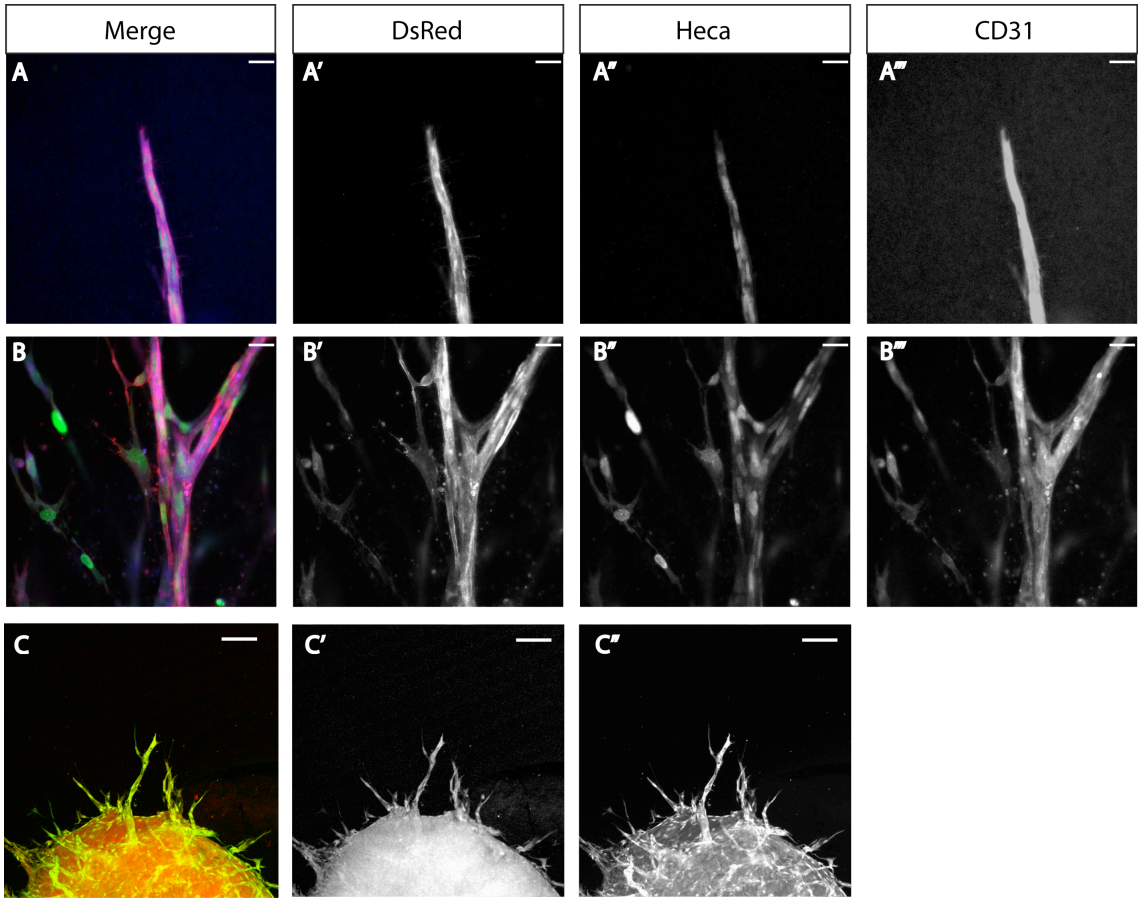

Figure 4.16 Heca is present in EC in EB sprouting assay.
In sprouting embryoid bodies Heca is present in ECs nuclei and at lower levels in the cytoplasm in sprouting vessels in EB assays (A”, B”, C”).

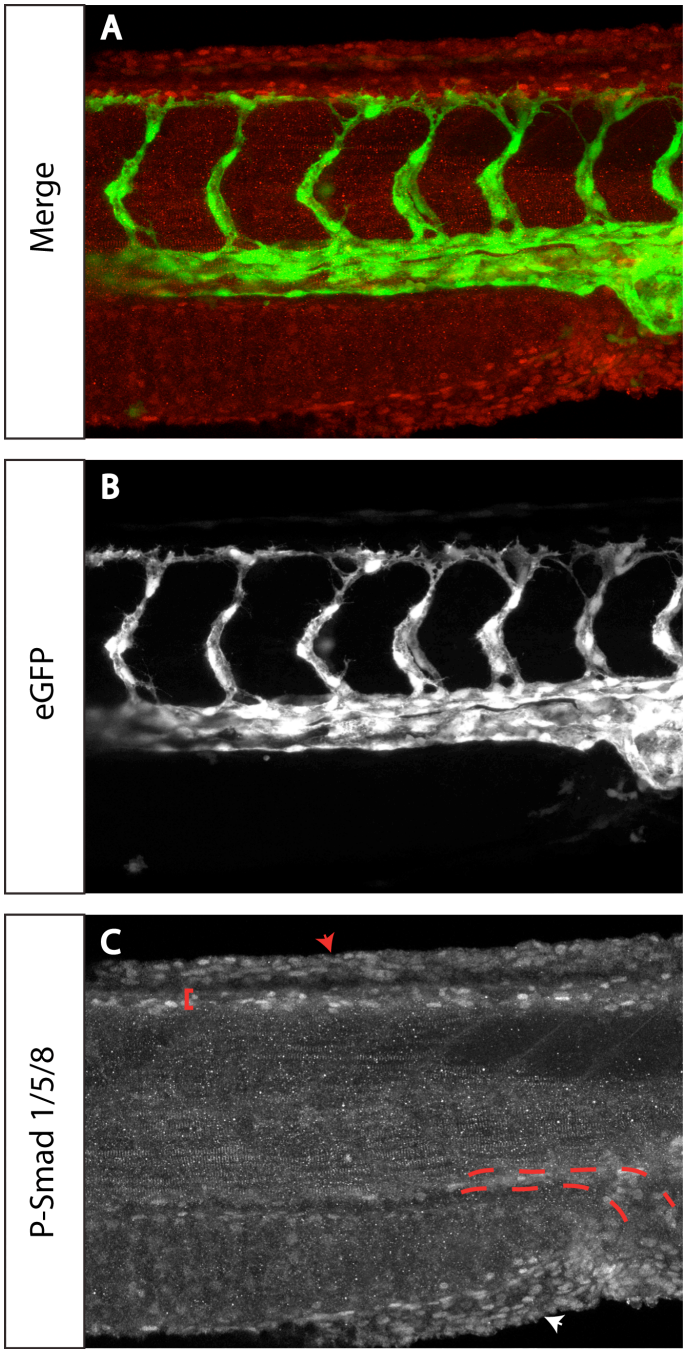

Figure 4.17 Evidence of BMP signalling zebrafish.
P-Smad 1/5/8 is observed in the dermis (red arrowheads), the dorsal portion of the neural tube (red bracket) and pronephric duct (red dotted outline).

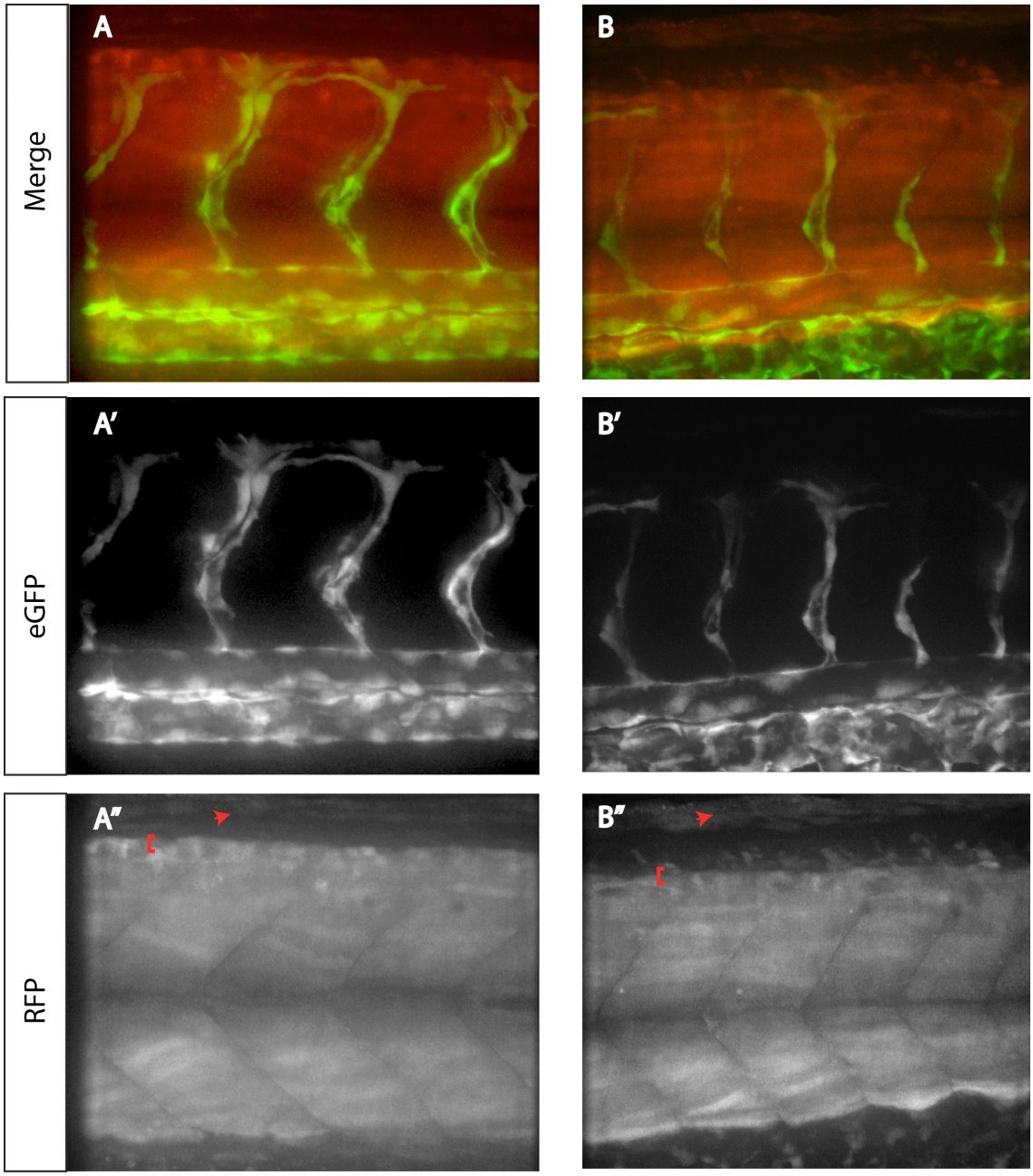

Figure 4.18 BRE-RFP reporter line shows similar BMP signalling activity as P-Smad 1/5/8 immunofluorescence.
The BRE-RFP line was crossed with *fli:eGFP* to investigate whether BMP signalling is detectable in ECs. RFP expression confirms the results observed with P-Smad 1/5/8 immunofluorescence, top of neural tube (A, C, red bracket) and dermis (A, C, red arrowhead). Strong expression is also observed in the somites (A. C).

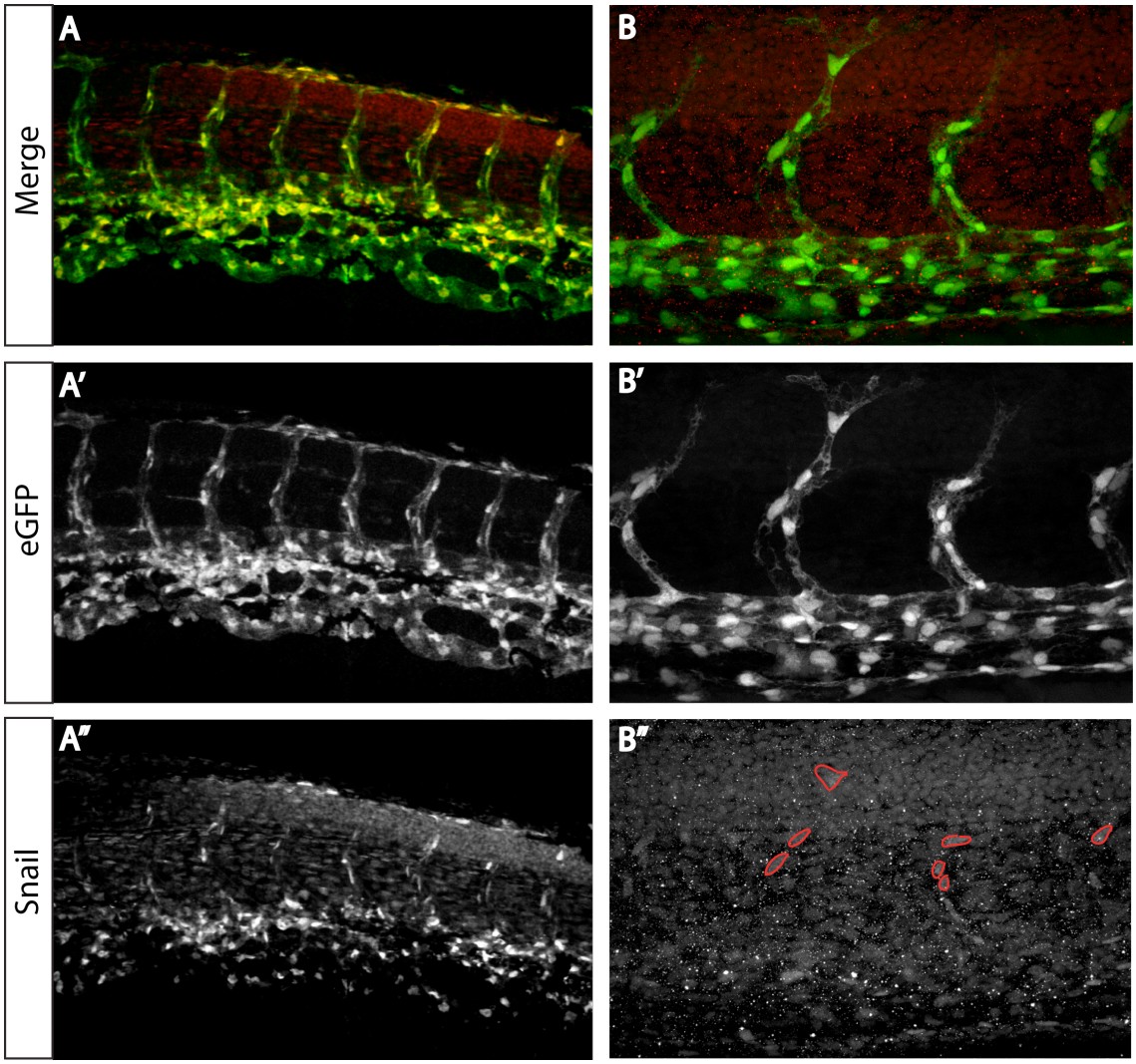

Figure 4.19 Snail in zebrafish.
fli1:eGFP embryos were immunostained for Snail. It is present in the somites as previously reported (Herbomel et al., 2001) and in most ECs in both the tail region (A-A") and the trunk (B", some nuclei circled in red).

The morphological response to such inhibitors was used to test whether the EBs were responding correctly to treatment and thus whether any changes in expression could be directly linked to the inhibitor. EBs increased their sprouting following inhibition of Notch signalling following the addition of DAPT due to increase in tip cell numbers (Fig 4.21B) (Jakobsson et al., 2010). Blocking either endogenous TGF-β or BMP signalling with SBI or Noggin (an endogenous BMP inhibitor) (Kang et al., 2009) also increased the vessel density but the resulting network is more chaotic and less well reorganized (Fig 4.21C-D), which is likely due to defective patterning as vessels were composed of CD31 positive cells, meaning EC differentiation was not affected. Treatment with TGF-β does not affect initial EC differentiation and sprouting but leads to larger calibre and shorter vessels (Fig 4.22F). This treatment also increases the number of pericytes, as assayed by NG2 immunostaining, and results in looser attachment to the vessels (Fig 4.22B",D"), confirming TGF-β is important in the differentiation of mural cell differentiation shown to rely on Snail (Kokudo et al., 2008). Addition of TGF-β four days following plating in collagen, once sprouting has begun, leads to similar large calibre vessels. The bEND5 endothelial cell line was used to test for changes in gene expression through qPCR analysis. Cells treated with TGF-β leading to a massive upregulation of Snai2 (also known as Slug) as would be expected (Fig 4.22E). Unfortunately, the use of antibodies in EBs and qPCR in bEND5 to determine the effect of such treatments on Heca and Snail family protein was not conclusive.

Short hairpin oligonucleotides for expression using the pSilencer3.1 H1 system (Ambion) were designed to knockdown Heca and Snail family proteins to assess their effect on sprouting angiogenesis. The use of shRNA is preferred over siRNA in this setting due to the long set up time of the EB sprouting assay. EBs require 4 days of differentiation in hanging drops and a further 7 days to achieve optimal sprouting. The usual lifetime of siRNA is a few days therefore their activity will most likely be lost prior to the initiation of sprouting. The shRNA system has been shown to give effective gene knockdown, even though efficiency and success rates are low (M. Busse, unpublished data). Unfortunately none of the shRNA designed gave the desired

knockdown of target genes. This was both at the transient transfection level as well as through selection with antibiotic markers.

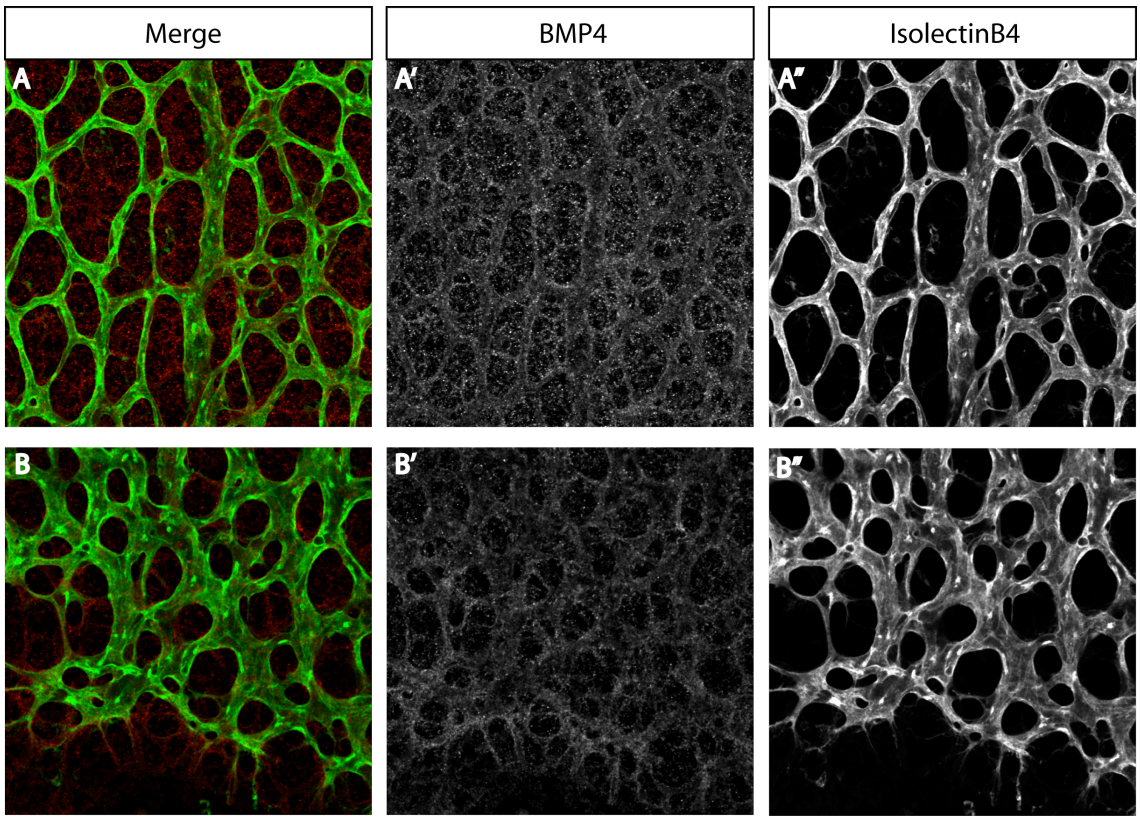

Figure 4.20 BMP4 is present in close association with ECs in retinal vasculature. Immunofluorescence for BMP4 highlights its presence in the vicinity of the retinal vasculature, in a pattern that is reminiscent of astrocytes (A'-B'). BMP4 expression is highest at the vascular front and is present at low levels ahead of the vasculature (B').

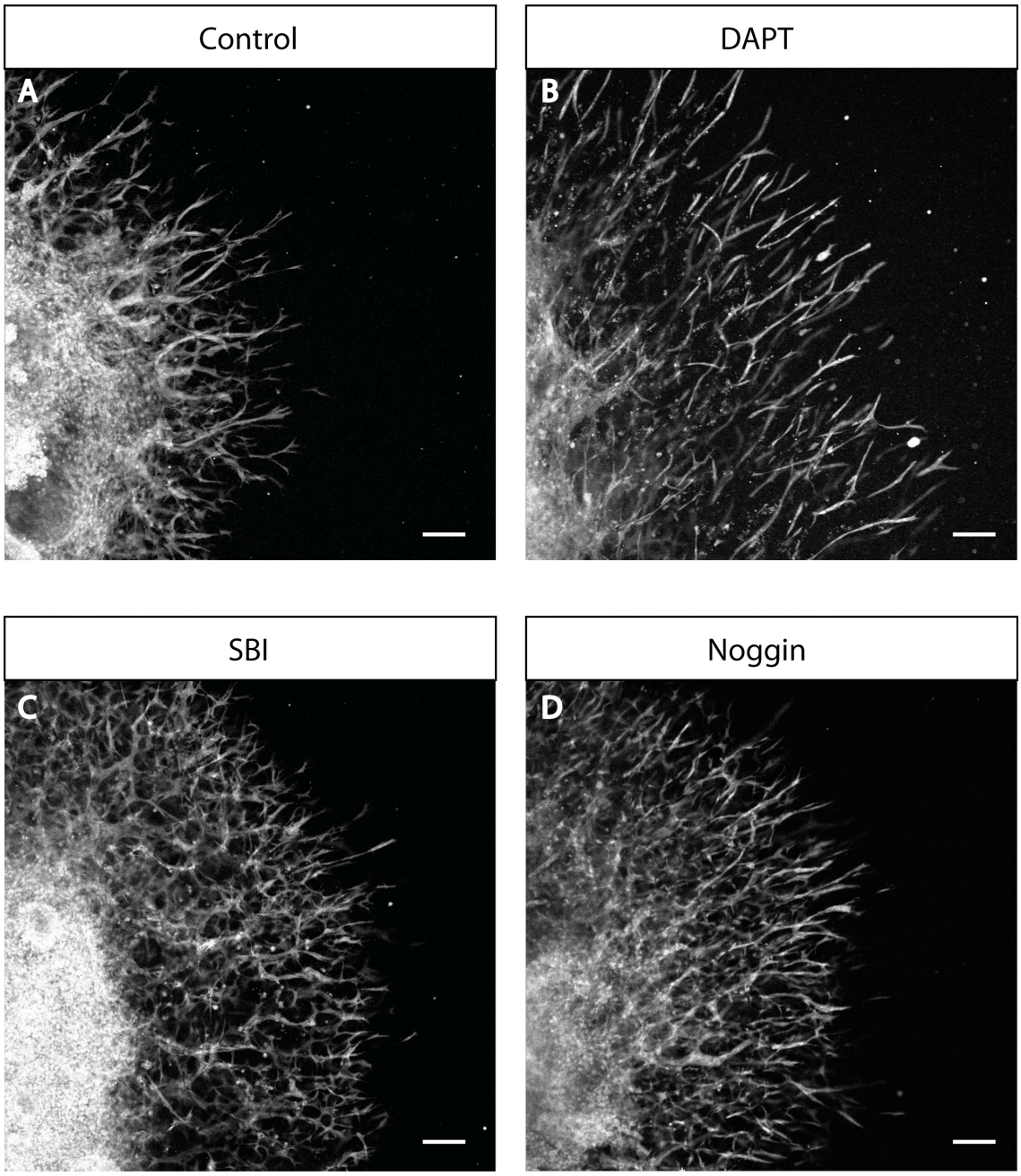

Figure 4.21 EB response to different signalling inhibitors.
EBs were plated in collagen and medium supplemented with signalling inhibitors was added. Sprouting was checked 7 days post plating. B. DAPT treatment resulted in the expected increase in tip cells and migration speed. C-D. TGF- and BMP signalling blockade with SBI and Noggin respectively leads to a chaotic and poorly structured sprouts. The effect is more drastic with SBI as no real sprouts are observed and are replaced by CD31+ migrating cells.

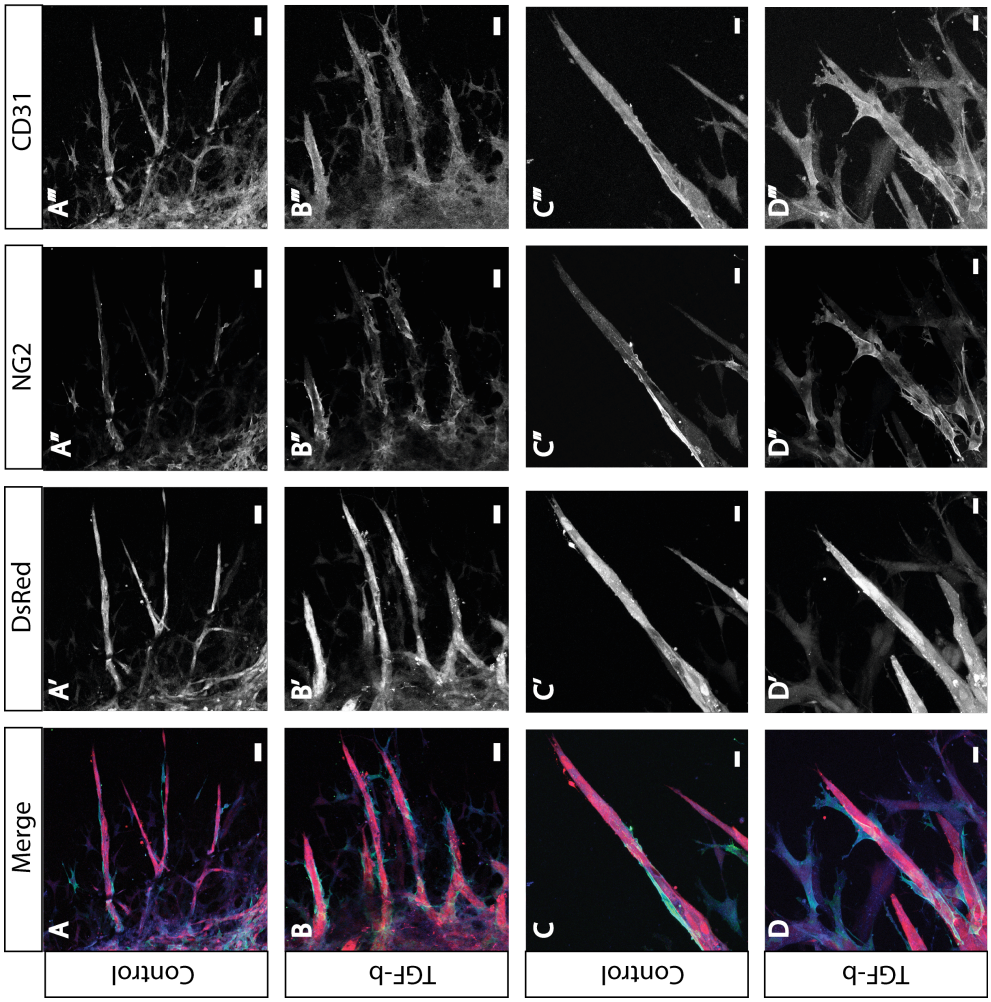

Figure 4.22 EB TGF-β stimulation leads to increased differentiation of pericytes with poor attachment.
Growth medium supplementation with TGF-β leads to larger calibre vessels (B, F) and increased pericyte numbers but with poorer attachment to the vessels (B', D'). E. bEND5 cells were treated with TGF-β in addition to the normal growth medium and RNA was collected 24 hours later. The purified RNA was transcribed to cDNA and qPCR for *heca*, *snail* and *snai2* was performed. Mean of 2 independent experiments plotted with S.D. Scale bars in A and B represent 50µm. C and D and F 15µm.

4.4 Discussion

In this chapter I have described the role of *heca* in angiogenesis. Loss and gain of function experiments lead to quite distinct effects on angiogenesis, by affecting sprouting and lumenization respectively. Contextualizing these observations can help formulate a hypothesis for *heca*'s activity linking it to how lumen formation could be regulating sprouting.

Following sprouting nascent vessels must connect through anastomosis to be able to lumenize and carry blood flow. The only other tubular system where anastomosis during development has been studied is the *Drosophila* trachea. In this system *headcase* is a fusion cell marker, a cellular phenotype required to undergo anastomosis. Because this gene had come to our attention through a microarray comparing retinas from osteopetrotic mice that exhibit decreased branching/fusion, *heca*'s role was investigated in angiogenesis.

I tested the effects of *heca* knockdown on zebrafish ISA sprouting and formation of DLAVs through anastomosis. Decrease in *heca* expression does not lead to defects in EC specification, vasculogenesis, sprouting or anastomosis. The phenotype observed is limited to the crossing over of the DLAVs to join together and form a plexus. The process normally begins at 48hpf at the tail end of the embryo and progresses towards the head, ending at around 7dpf (Fig 4.3) (Isogai, 2001). On its own this result is hard to interpret as attempts made at determining the possible regulation of *heca,* through BMP and Snail as in *Drosophila,* did not yield conclusive results. Evidence for active BMP signalling is present in the dorsal portion of the NT but this is not endothelial. More importantly Snail is found expressed in ECs. ECs have been shown to move within the plexus during vessel morphogenesis (Blum et al., 2008, Jakobsson et al., 2010, Zygmunt et al., 2011). Snail family proteins are involved in increased cellular motility and epiblast-specific deletion of Snail allows EC differentiation but the embryo dies as a result of defective EC migration to form the axial vessel (Lomelí et al., 2009). It is also true that Snail can directly repress VE-cadherin expression, which would be expected to increase cell motility (Lopez et al., 2009).

Expression analysis in zebrafish does not give a clear answer to whether *heca* is expressed in the endothelium but work in the mouse retina model as well a *in vitro* EB sprouting assays confirm that *heca* is present in ECs (Fig 4.15-16). What I find particularly interesting is the phenotype observed in the gain of function experiments. Overexpression of *heca* at the whole organism or EC-autonomous level leads to precocious lumen formation in the nascent sprouts (Fig 4.5-6). The only other published study where migrating ISAs lumenize to this extent is a recent report on the role of *flt1* as a negative regulator of tip cell formation in zebrafish (Krueger et al., 2011). This reinforces what has been proposed by Jakobsson *et al*, with *flt1* acting in a Notch-dependent manner to decrease angiogenic potential (Jakobsson et al., 2010). Surprisingly though the authors of the zebrafish study did not pick up or comment on the ISA lumenization. What I personally find even more reassuring about the published data is that it confirms the predictions that arise from the original tip/stalk selection mechanism that was proposed following the flourish of Dll4/Notch-focused papers in 2007. The reasoning goes as follows: stalk cells are characterized by lower expression of VEGFR2 and higher VEGFR1. This is the basis for the differential response of tip and stalk cells upon VEGF stimulation, with tip cells migrating and stalk cells proliferating (Gerhardt, 2003). Both *in vitro* and *in vivo* work have confirmed that levels of these two receptors affect the angiogenic potential of individual ECs in a chimeric competition setting (Jakobsson et al., 2010). Krueger *et al*'s data shows that ectopically expressing soluble *flt1* places the whole ISA in an environment similar, or even more extreme, than normal stalk cells experience. Accordingly the ECs exhibit robust stalk cell behaviour and engage in lumen formation (Krueger et al., 2011). The data indicates that lumen formation is directly or indirectly dependent on VEGFA signalling. Another study stresses the importance of *sflt1* at limiting vessel branching, again confirming that membrane bound *flt1* has little effect on angiogenesis (Zygmunt et al., 2011).

The situation in *heca* overexpression is similar with regards to lumen formation but the loss of function defects do not match. *Flt1* morphants exhibit ectopic branching in the dorsal part of the ISAs where as for *heca* this does not occur, instead the extra branching is over the neural tube. One may also expect some defects in lumenization in *flt1* morphants but none are observed and even the ectopic branches are functional (Krueger et al., 2011). Notch is a pathway that does not directly affect lumenization but

can affect vessel calibre. Notch controls vessel diameter by preventing ECs from over-responding to angiogenic stimuli, limiting the number of ECs that migrate away from the vessel (Benedito et al., 2008). Oddly enough removing Notch signalling through loss of Dll4 upregulates VEGFR2 as expected but also Robo4, a molecule that has been proven to increase vessel stability *in vivo* (Jones et al., 2008). Even though there clearly are no ECs migrating away from the ISA, if *heca* is an effector of Notch signalling it could be inducing similar effects as s*flt1*, increasing the stalk behaviour of ECs, promoting lumen formation. However, so far the *in vitro* work carried out did not reveal any link between Notch and *heca* expression, nor with regards to VEGFA stimulation.

It is not yet clear whether the cell clumping phenotype precedes or follows lumenization. It is likely to occur prior to lumen formation as sprouts with many nuclei have yet to lumenize (Fig 4.9). There is a significant increase in the number of nuclei found within the sprout and in some cases they are all clustered at the leading edge (Fig 4.9). It might be expected that such a defect is due to increased proliferation or defective migration. An example of increased cell proliferation is found in r*bpsuh* morphant zebrafish embryos that have decreased Notch target genes expression (Siekmann and Lawson, 2007). The ISAs contain increased number of EC nuclei when compared to control morphants, corroborating work done in *dll4* deficient mouse embryos (Hellström et al., 2007, Suchting et al., 2007, Lobov et al., 2007). What is striking though is that ECs do not cluster but are more than able to migrate normally (Siekmann and Lawson, 2007). These morphant cells have increased angiogenic potential as a result of sustained *flt4* expression, which is reflected in the ectopic sprouting seen from the ISAs (Siekmann and Lawson, 2007) but this is not the case in *heca* overexpressing cells.

Very little is currently known with regard to *heca*'s function and activity, and its lack of functional domains, conserved folds and homologues makes it difficult to speculate on its potential role. The protein contains a cysteine rich region that is attributed to protein-protein or protein-RNA interactions. Its localization within the nucleus is puzzling as no Nuclear Localizing Sequence (NLS) is found. A plausible explanation could be that Heca interacts with another protein able to translocate to the nucleus. In the *Drosophila* trachea it is involved in preventing terminal differentiation

(Steneberg et al., 1998) and this could be through interaction with one of the many bHLH transcription factors regulating tracheal development. The fact that it acts non-cell autonomously opens up the possibility that its effect is related to lateral signalling such as through Dll/Notch, maybe potentiating the ligand's signal sending potential. In cancer cells, *heca* controls cell proliferation (Dowejko et al., 2009). As in *Drosophila heca* is believed to interact with cdks (Stanyon et al., 2004), the mitotic effect could be through such a mechanism; this also supports *heca* interacting with other proteins.

To attempt to reconcile the *heca* loss and gain of function results it is important to first conceptualize the phenotypes trying to find a common link. Sprouting and lumen formation can be almost regarded as opposites, with sprouting requiring migration, filopodia extension and the subsequent formation of a new junction, whilst lumen opening stabilizes the vasculature, leads to rearrangements and loss of some junctions. If the *heca* knockdown data is interpreted as ectopic sprouting and the overexpression work is related to precocious lumenization then we can assume the phenotypes are opposites. This can be coupled to the observation in Ch.3 about filopodia activity and lumen formation. It has been assumed that because of the Dll4/Notch lateral inhibition only tip cells will have filopodia activity. This point is supported by the absence of filopodia on the DLAVs in control embryos, as opposed to the large number of filopodia emanating in Dll4 morphants or DAPT treated embryos (Leslie et al., 2007), providing support for the notion that engagement of Dll4/Notch during anastomosis and not blood flow induces a quiescent vasculature. In light of the observations presented in this study, I think it is possible that blood flow is playing a more important role in blocking exploratory filopodia. Current work is highlighting the importance of haemodynamic forces on the vasculature and how this can cause changes at the cellular and molecular level (Nicoli et al., 2010, Bussmann et al., 2011). In Movie4 we observe that even though a patent connections is made, filopodia do not cease until the lumen opens throughout the DLAV. By this stage the Dll4/Notch pathway should have inhibited exploratory behaviour in the ECs that have just anastomosed. On the other hand *cas* knockdown in embryos, which prevents blood flow, does not lead to ectopic sprouting by 60hpf.

4.5 Future Directions

Loss and gain of function of *heca* has lead to some unexpected effects on the zebrafish developing vasculature. Because of singularity in sequence and lack of conserved stretches, it would be important to carry out some biochemical analyses to determine whether *heca* is phosphorylated, can any binding partners be identified through mass spectroscopy? Is *heca* found associated directly or indirectly with chromatin? This will also require the development of new tools as this study was partly limited by the availability of tools and the difficulty in generating our own. Of the two phenotypes I find the gain of function the most intriguing also due to the two phenomenon of EC clustering and precocious lumenization in the ISAs. I believe that the two are linked and as mentioned in Ch.3 it would be invaluable to obtain an adhesion molecule fusion with a fluorescence protein to track changes in EC junctional arrangement. The differences in junctions between control and *heca* morphants can only be attributed to the chaotic arrangement of cells if one bases the conclusion on the static images. The low penetrance of the phenotype raises further questions to what *heca*'s role might really be. Does this suggest that there are proteins that can takeover *heca*'s function? Or is *heca* the molecule that is present as a spare or safety in case the more prominent protein fails? If either is true then why do we not observe any fold or sequence similarity between *heca* and other gene products? One approach that may yield more fruitful results would be to try and gain more information on the function of *heca* in *Drosophila* where more about the regulation and role is understood.

Heca may be involved in either sensing that lumen has formed and therefore alter cell behaviour or be required for the induction of lumenization. The latter hypothesis is the least likely, as lumenization is not affected in morphants. The former hypothesis would fit with the both phenotypes: loss of *heca* means that ECs do no sense lumenization and therefore maintain filopodia activity causing the early DLAV crossovers. This would only have effect in that particular vascular bed. Localized effects on the vasculature have been previously reported, where certain vessel portion can show exquisite sensitivity to partial pathway inhibition (Nicoli et al., 2010).

Chapter 5. Macrophages in Angiogenesis

Live imaging experiments have highlighted the presence of macrophages close to the growing vasculature, with the 3D EM data in Ch.3 showing a granular cell in close contact with two anastomosing tip cells. I therefore decided to investigate such interactions through live imaging and the effect of loss of macrophages on angiogenesis via different approaches. It is clear that macrophages actively interact with ECs during anastomosis and that their loss is not catastrophic for vascular development but leads to a subtle phenotype were the growing sprouts are retarded and display decreased migratory behaviour. Recently three papers were published describing similar observations in mouse (Kubota et al., 2009, Fantin et al., 2010, Rymo et al., 2011).

5.1 Macrophages in retinal vasculature

Endothelial cells are not the only cell type involved in angiogenesis. ECs form the vessel proper but they require accessory cells for the expression of VEGF (such as astrocytes in the retina) to induce their sprouting, migration and proliferation, pericytes for induction of quiescence and stabilising the newly formed vessel and smooth muscle cells for the vessel's contractility. A cell type that has gained attention due to its involvement in angiogenesis especially in cancer and inflammation is the macrophage. Macrophages can influence the various stages of angiogenesis through the secretion of bFGF, VEGF, GM-CSF, angiotropin, TNF-α, TGF-α/β, IFNα/γ and Wnt ligands to name a few (Sunderkötter et al., 1994). Macrophages can control the environment by release of metalloproteases that can alter the extracellular matrix to aid angiogenesis or process immobilized growth factors to alter the morphogen gradient (Squadrito and Palma, 2011).

The mouse retinal vasculature develops post-natally and radiates from the optic nerve (Fig 1.3). In the post-natal retina a special type of macrophage is present, the microglia.

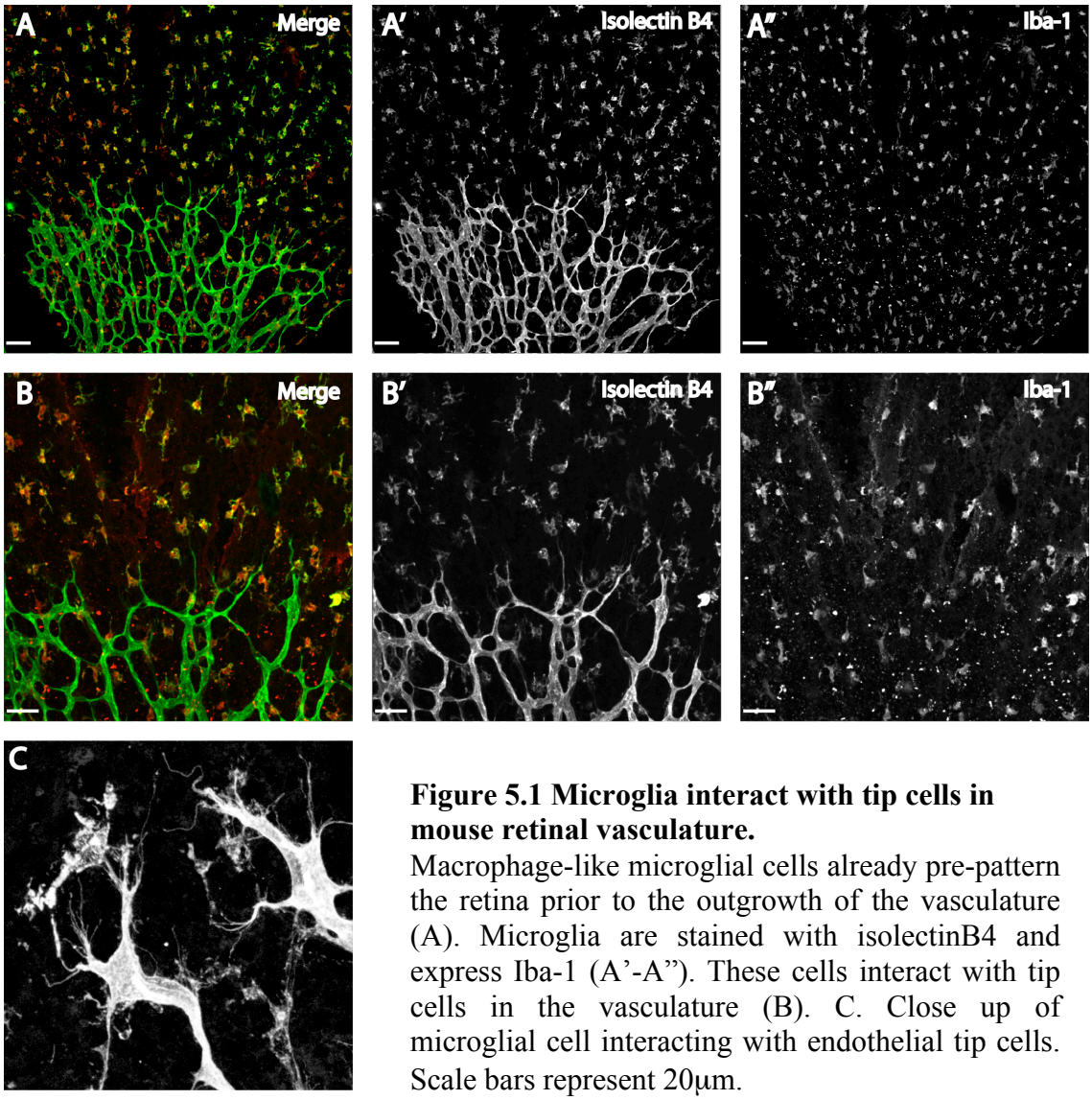

Figure 5.1 Microglia interact with tip cells in mouse retinal vasculature.
Macrophage-like microglial cells already pre-pattern the retina prior to the outgrowth of the vasculature (A). Microglia are stained with isolectinB4 and express Iba-1 (A'-A"). These cells interact with tip cells in the vasculature (B). C. Close up of microglial cell interacting with endothelial tip cells. Scale bars represent 20μm.

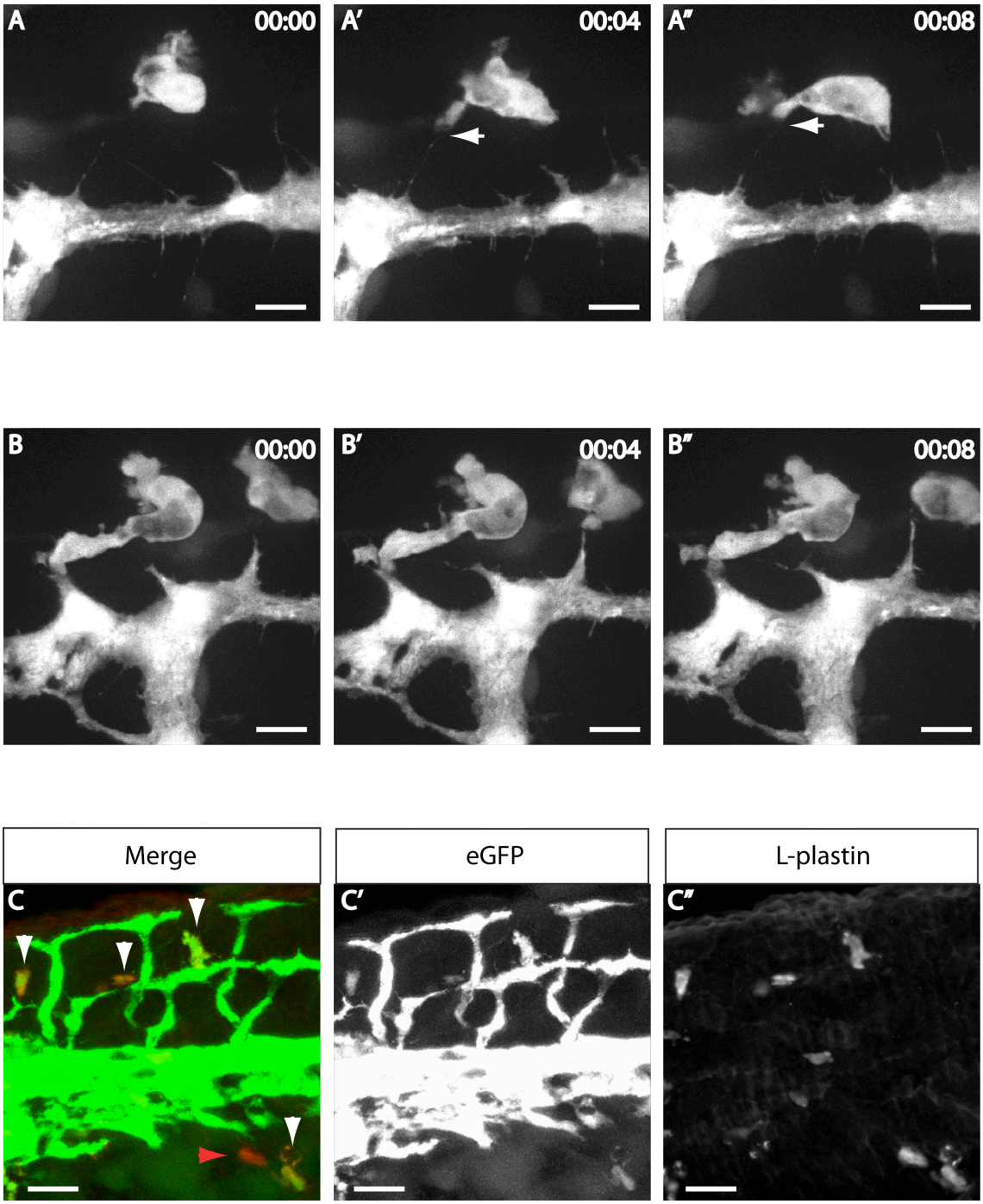

Figure 5.2 Macrophages interact with endothelial cell filopodia in zebrafish developing ISAs.
A-A". A macrophage attracts EC filopodia extension and makes contact (white arrow). B-B". Two macrophages closely interact with ECs while they are in the process of fusing with their neighbouring ISAs. C-C". Macrophages can be identified with anti-L-plastin immunostaining. Some of such macrophages also show eGFP(and this *fli1*) expression (white arrowheads). Other macrophages do not (red arrowhead) meaning that there will be many macrophages not visualized using the *fli:eGFP* line. Scale bars represent 10μm in A and B, 20μm in C.

The retina is pre-patterned with microglial cells that are evenly spaced ahead of the growing vasculature. These cells are identified by their affinity for IsolectinB4 and expression of ionized calcium binding adaptor molecule 1 that is a known macrophage/microglial marker (Iba-1, Fig 5.1A-B) (Imai et al., 1996, Gerhardt, 2003, Rymo et al., 2011), with tip cells closely interacting with microglia. In Fig 3.16 the correlative fluorescence/3D EM data indicates that a granular cell is found at the point of anastomosis between tip cells of ISAs in developing zebrafish embryos and is in physical contact with the fusion point, in some way replicating what is seen in the mouse retina (Fig 5.1A-B). The absence of retinal microglial cells leads to decreased branching/fusion of the vasculature, with tip cells growing radially with a straight trajectory, a decreased exploratory angle of their filopodia and decreased attraction towards other tip cells. (Rymo et al., 2011). One possible explanation for this could be that retinal microglia facilitate tip cells in finding one another`, by attracting the ECs and directing anastomosis and thus the correct patterning of the retina. A recent report investigating the role of microglia in the development of the deeper retinal plexus by Stefater and colleagues discovered that in this context microglia possibly attract the growing sprouts from the superficial layer into the deeper layer of the retina`, but then regulate plexus density by inducing turning of the tip cells. This effect is induced by Wnt-induced expression of soluble Flt1, believed to dampen VEGF signalling by sequestering VEGF-A, translating to a decrease in branching (Stefater et al., 2011). Such evidence as well as the characterisation of pro- and anti-angiogenic macrophages in tumour microenvironment (Squadrito and Palma, 2011) highlights the importance of context in which the role of macrophages is studied. It was briefly mentioned in Ch.3 that macrophages are observed in the vicinity of growing ISAs. Therefore zebrafish embryos were used as a model to investigate the dynamics of possible EC-macrophage interactions and the effect of macrophage ablation through Morpholino knockdown on angiogenesis.

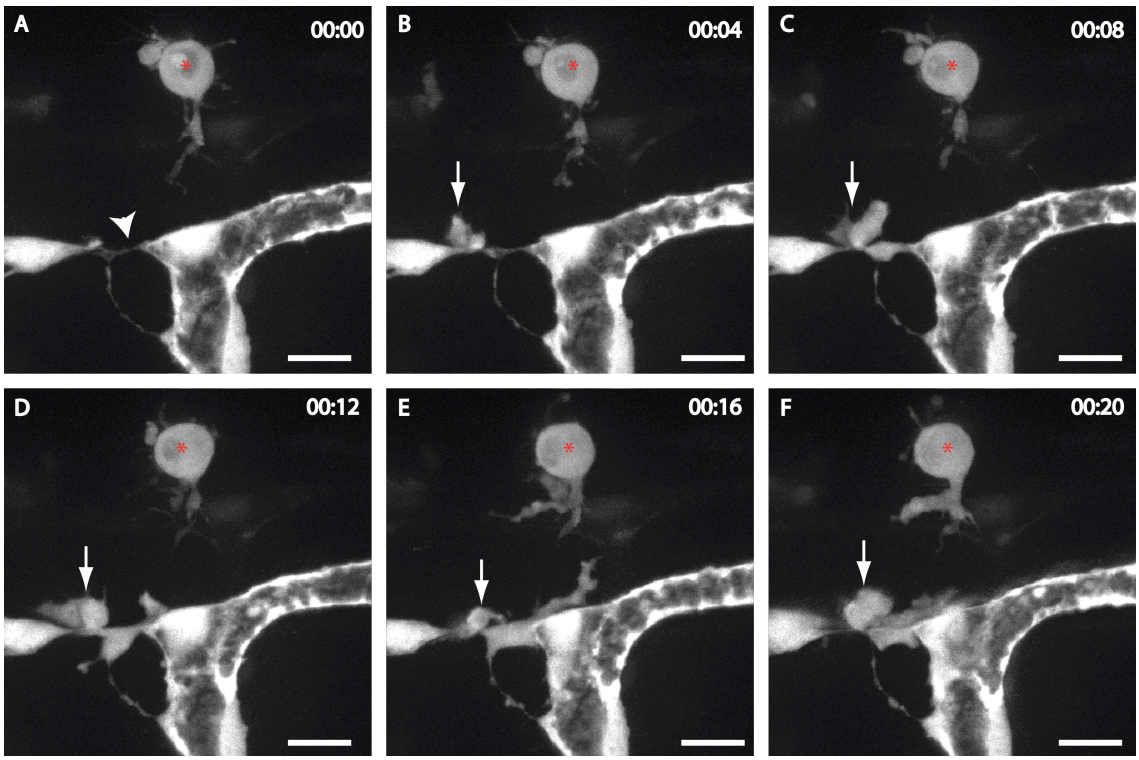

Figure 5.3 Macrophages aid the correct fusion and maturation of failing anastomoses.
28hpf *fli:eGFP* were imaged by confocal microscopy (spinning disc), focusing on the formation of the DLAV. It can occur that two tip cells come into contact, attempt to fuse but the connection weakens and begins to thin out (A, white arrowhead). A macrophage arrives at the site of contact and wraps around it (B, white arrow), remaining till the connection is salvaged (C-E) and lumen begins to form through the connection (F). The red * marks a stationary macrophage that has arborized. Scale bars represent 10μm.

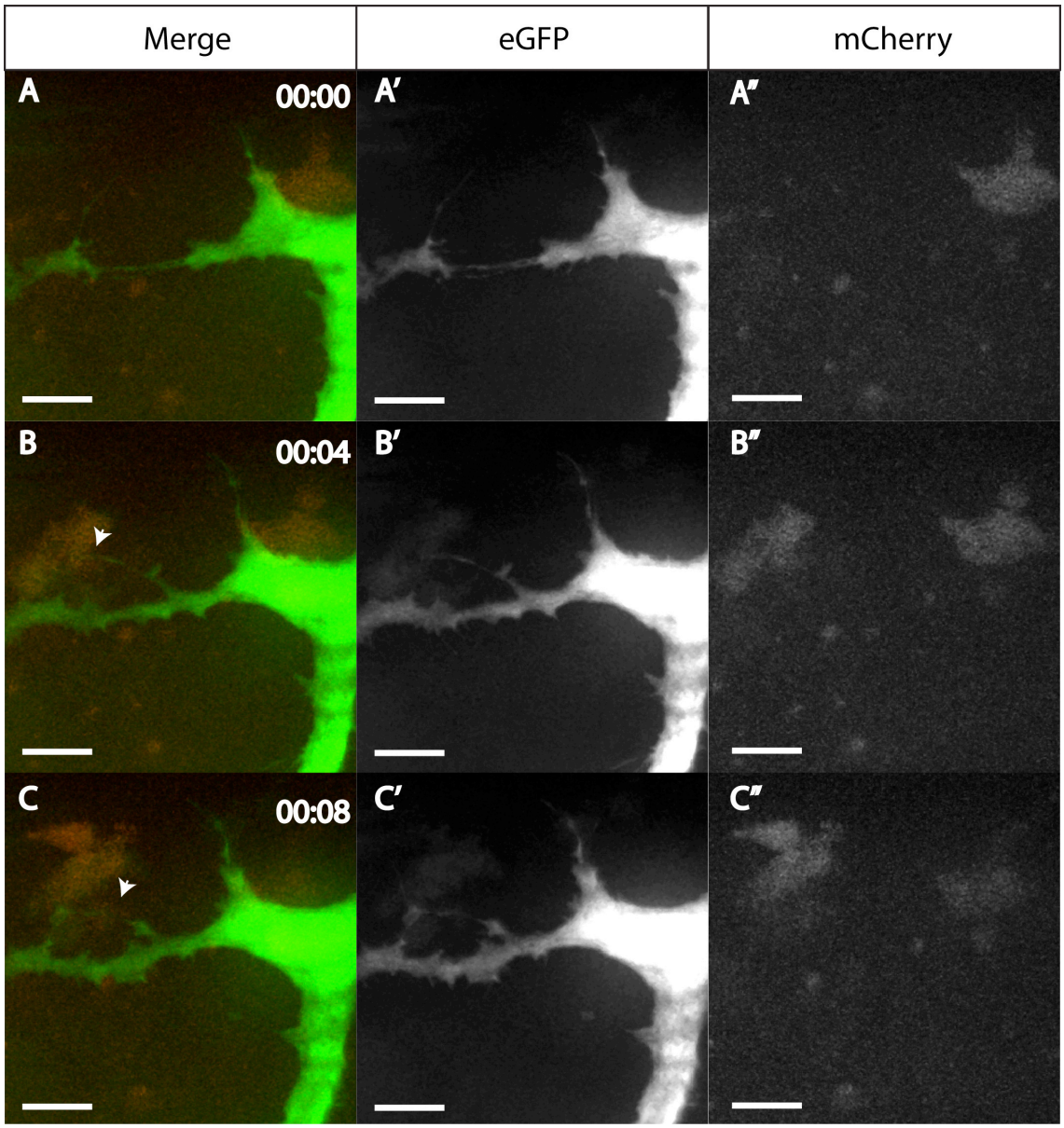

Figure 5.4 Macrophage guides contact of filopodia between two anastomosing tip cells.
28hpf *fms:Gal4* embryos were imaged by confocal microscopy. Two tip cells that are coming into contact (A) extend filopodia towards a macrophage that appears at the site of contact (B, white arrowhead) and the filopodia can then be guided to connect with one another (C, white arrowhead). Scale bars represent 10μm.

5.2 Macrophages interact with ECs during DLAV formation

The *fli1:eGFP* line not only exhibits eGFP expression in ECs, some can also be found in some macrophages (Fig 5.2). The identity of such ameoboid cells is confirmed by the presence of L-plastin, a known macrophage marker in zebrafish (Fig 5.2) (de Arruda et al., 1990). L-plastin is an actin-binding protein that is conserved throughout eukaryote evolution and expressed in the haematopoietic lineage becoming restricted to macrophages following myeloid development (de Arruda et al., 1990). *Fli1* positive macrophages roam throughout the embryonic tissue and migrate along the neural tube where the DLAV will later form (Fig 5.2, Movie1). When the migrating ISAs begin to bifurcate and come into contact with the neighbouring ISAs macrophages can be observed in the vicinity of such events. Macrophages migrate towards the ECs, which in turn extend filopodia and make contact with the macrophages (Fig 5.2). These filopodia behave as though they are actively attracted to the macrophages, even changing direction quite drastically as if in an effort to respond to the macrophage attraction (Fig 5.5).

It can occur that the connection between two tip cells on their way to anastomose begins to fail (Fig. 5.3, Movie3). A macrophage wraps around the junction of interest and remains in contact with ECs until the connection is stabilized and the lumen has begun to push through the anastomosis point (Fig 5.3, Movie3), similar to what has been recently described by Fantin *et al*. With regards to contextualizing the role of macrophages in angiogenesis, such pro-angiogenic macrophages involved in developmental angiogenesis display similar characteristics to pro-angiogenic TEM like the expression of *tie2* and *nrp1* (Fantin et al., 2010).

5.3 Loss of macrophages leads to delay in anastomosis

PU.1 is an ETS-domain transcription factor required for B-lymphoid cell and myeloid differentiation, especially monocytes and macrophages (Klemsz et al., 1990). Loss of *pu.1* in mice results in loss of tissue macrophages, leading to aberrant angiogenesis in the retina and hindbrain (Fantin et al., 2010, Rymo et al., 2011).

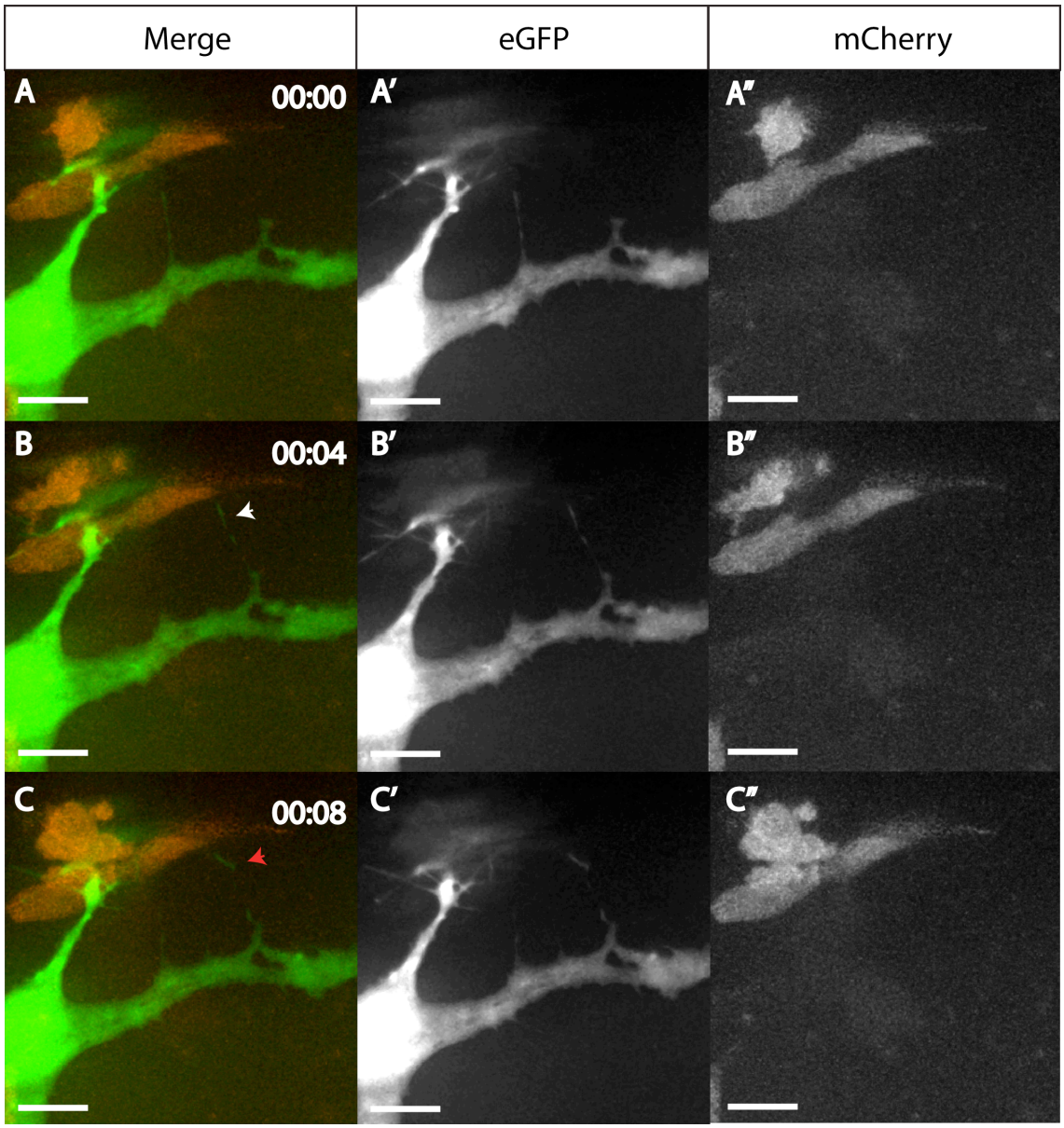

Figure 5.5 Filopodia actively grow towards macrophages by abrupt changes in filopodia direction.
28hpf *fms:Gal4* embryos were imaged by confocal microscopy. A filopodia is observed protruding from the point of anastomosis towards the macrophage (B, red cell). The filopodia kinks, growing more directly towards the macrophage (C, red arrowhead). Scale bars represent 10μm.

Knockdown of *pu.1* expression using a Morpholino effectively disrupts macrophage specification (Rhodes et al., 2005). This Morpholino was used to ablate macrophages in *fli1:eGFP* embryos to assess their effect on angiogenesis with a particular focus on ISA migration and DLAV formation. Loss of macrophages was confirmed by L-plastin immunofluorescence (Fig.5.6). The absence of macrophages leads to a highly significant increase in the contact times between non-fusing filopodia of ISAs prior to forming the DLAV (Fig 5.6E). This increase was not related to any changes in the total number of contacts between tip cells prior to anastomosis (Fig 5.6F). The loss of macrophages results in a 30% increase in the average final contact to fusion delay but this is not statistically significant (Fig 5.6G). The overall vasculature does not exhibit developmental defects and the number of filopodia present per ISA is not altered but the ISAs are retarded and do not bifurcate as freely as in control morphants (Movie8). The *fms:Gal4* line was used to confirm these observations. In this line the presence of an mCherry-nitroreductase (*nfsB*) fusion protein allows the conversion of the prodrug metronidazole into the toxic active compound. Addition of 5mM of metronidazole at 8hpf leads to the effective ablation of most mCherry-nfsB cells in zebrafish embryos (Fig 5.7) (Gray et al., 2011). ISAs of metronidazole treated fms:Gal4 embryos display similar filopodia abnormalities, with shorter filopodia observed at the growing front (Fig 5.7)

Two L-plastin Morpholinos were designed to knockdown its expression (one translation blocking and one splice blocking). Both oligonucleotides resulted in a considerable decrease in expression of *l-plastin* as assayed by qPCR as well as the decrease in macrophage-like cells in the *fms:Gal4* line (Fig 5.7C) but the splice blocking Morpholino exhibited non-specific toxicity. L-plastin morphants display similar migratory phenotype defects as the other two macrophage-ablating techniques, with decreased length of filopodia (Fig 5.7B).

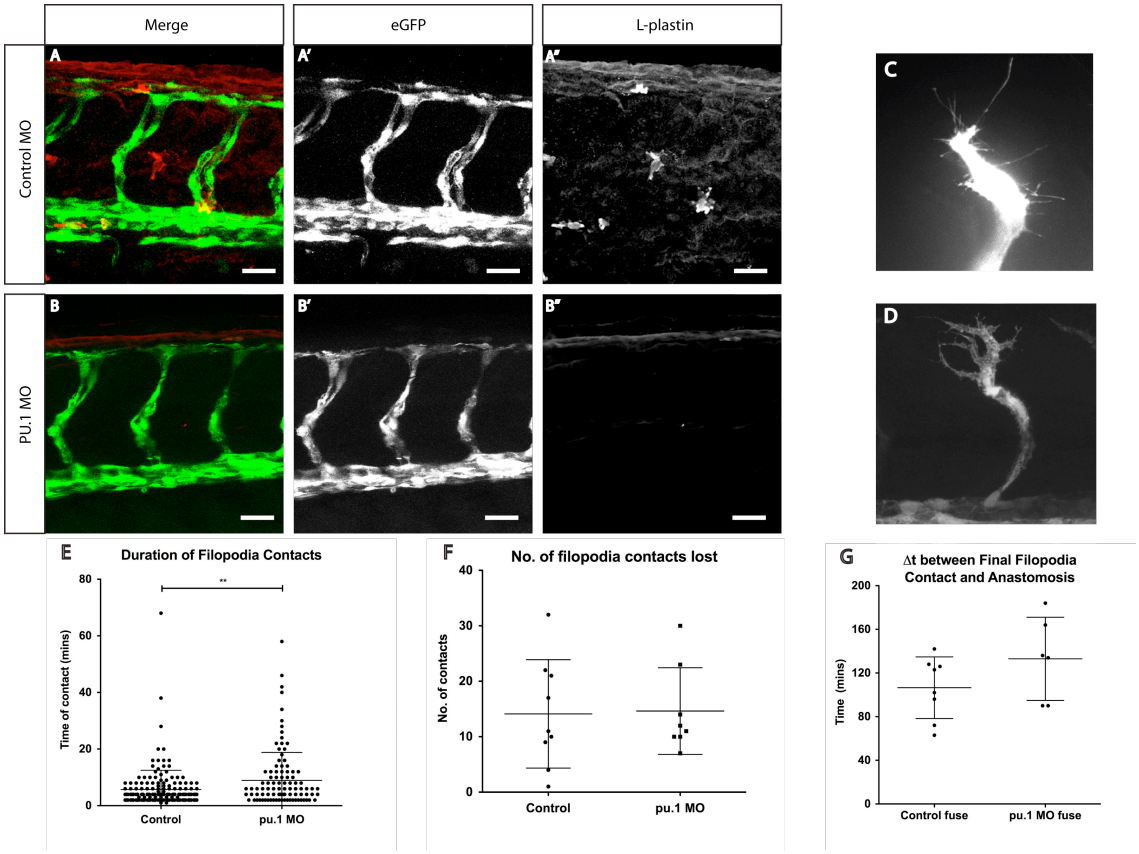

Figure 5.6 Macrophage depletion through loss of pu.1 leads to ISA morphology defects and delay in anastomosis.
PU.1 Morpholino injected embryos exhibit loss of macrophages as assayed by L-plastin immunofluorescence (A-B). Macrophage ablation leads to altered ISA morphology (C-D). This translates into increased contact time between tip cells during anastomosis but does not affect the number of contacts (E-F). There is an increase observed in the time delay between the final contact and fusion but this is not statistically significant (8 independent experiments). Scale bars represent 20μm.

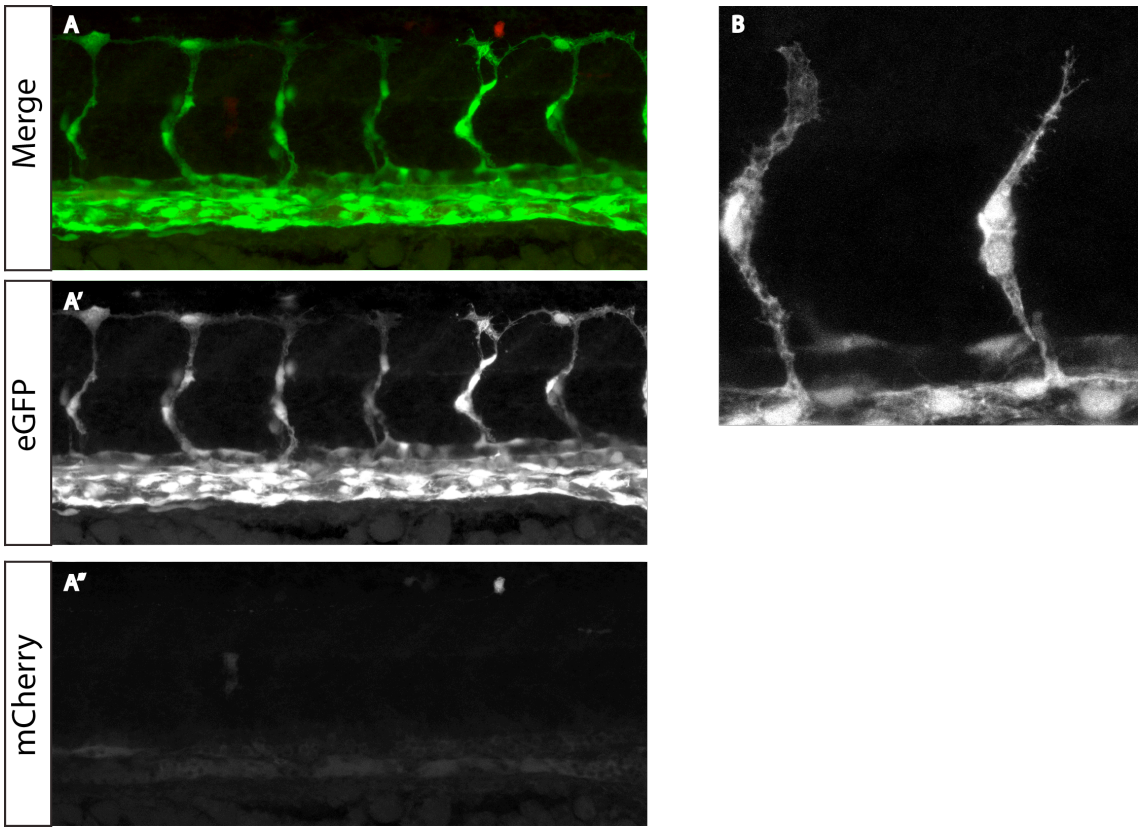

Figure 5.7 Loss of macrophages through two other strategies leads to similar ISV defects. A.
fms:Gal4; UAS:mCherry-NMT embryos were treated with 5mM metronidazole leads to depletion of mCherry expressing cells (A"). This results in aberrant morphology of the ISAs as they migrate. A similar situation is encountered when using *l-plastin* Morpholino to ablate macrophages (B).

5.4 Discussion

Macrophages have been implicated in promoting angiogenesis within the tumour microenvironment but their role in developmental angiogenesis is still not clear. Here I present evidence showing macrophages actively interacting with ECs and involved in anastomosis. Experiments on loss of macrophages reveal that they are not essential for angiogenesis but may act as facilitators.

5.4.1 Macrophages actively interact with ECs during anastomosis

Endothelial cells rely on other cell types to induce the correct development of the vasculature. Many cell types express VEGFA, pericytes help stabilize the vasculature, smooth muscle cells allow contraction and in certain vascular beds astrocytes provide support for EC survival. Here I show that macrophages actively interact with ECs during angiogenesis. A number of studies have been published while this work was being carried out (Kubota et al., 2009, Fantin et al., 2010, Rymo et al., 2011). In all these studies, microglia (specialized macrophage type cells in the CNS) or macrophages are seen in contact with ECs in the developing vasculature but all of the data is on fixed tissue. There is one piece of data in zebrafish indicating there are interaction between ECs and macrophages (Fantin et al., 2010) but the resolution is far from optimal. The images I present here clearly show that filopodia from ECs grow towards macrophages and act as if they are actively attracted to these myeloid cells. Ablation of macrophages affects angiogenesis in the retina and the hindbrain but these defects are not drastic and are not a cause of lethality. The data here suggests similar effects of loss of macrophages on the vasculature, with a mild phenotype that recovers later in development.

The attraction of ECs towards macrophages raises the first question as to what exactly is attracting filopodia extension. Fantin *et al* demonstrated in the mouse that VEGFA is not required in macrophages to allow normal vascular development (Fantin et al., 2010) therefore the obvious candidate can be excluded. A report that was published just prior to the printing of this study gives a hint as to what might be

occurring. Tammela *et al* show macrophages express VEGFC, a member of the VEGF family. VEGFC is able to activate VEGFR3 and VEGFR2, likely through heterodimers of the receptors. Not all macrophages express VEGFC, only the ones that are at the vascular front, especially the ones present at anastomosing tip cells and branch points (Tammela et al., 2011). The authors then go on to show data supporting the fact that VEGFC is able to induce Notch target genes through its action on VEGFR3. Heterozygosity for *vegfc* results in a less dense plexus with more tip cells present at the sprouting front (Tammela et al., 2011). This data though does not really indicate that macrophage derived VEGFC is responsible for tip cell-macrophage attraction. Tip cells are still able to find one another but what seems to be altered is the stability of the new connections. Loss of macrophage VEGFC results in many empty collagenIV sleeves at the front, which are the remnants of ECs that had come into contact but did not anastomose properly and thus released, the reason why more tip cells are seen at the angiogenic front. Movie3 leads to a similar conclusion regarding macrophages helping stabilize connections, where the cell wraps around the failing anastomosis until it is salvaged (Fig 5.3). It seems that VEGFC acts through VEGFR3 to induce Notch target genes and stabilize Notch signalling to allow anastomosis and junction formation to occur. This phenotype is proposed to be similar to what is observed in osteopetrotic mice (Rymo et al., 2011) even though there appear to be more tip cells making more connection in VEGFC heterozygous retinas. Intriguingly another recent report suggests that Dll4 found on tip cells activates macrophages through Notch1 and this is required for the correct interaction between the two cell types (Outtz et al., 2011). Another interesting point is that VEGFC expressing macrophages are also Tie2-postive. This is a molecular signature of pro-angiogenic macrophages and is the receptor required for macrophages to respond to tumour-secreted Ang2. The Ang2-Tie2 interaction is required for macrophage EC interaction in tumours and subsequent induction of angiogenesis (Mazzieri et al., 2011). Ang2 blockade is currently being tested as an antiangiogenic therapy with a number of investigational agents and this could be an unexpected but positive addition to the mechanism of action of such agents. It also offers a cleaner toxicology profile by eliminating a lot of the serious side effects VEGFA/VEGFR2 inhibition can cause. The mild effects on developmental angiogenesis are also encouraging in the sense that macrophage ablation (especially

pro-angiogenic TAMs) could be a potential therapeutic strategy against tumours. One would of course increase the risk of infections.

5.4.2 Future Directions

I think that understanding what exactly is the factor that attracts ECs to macrophages is an important questions that remains to be answered. Also no vegfc has been detected in zebrafish macrophages, possibly through a lack of adequate sensitivity. A point that has not yet been addressed is what attracts macrophages to sprouting ECs. A two way communication system has been hinted at by others (Rymo et al., 2011). In the case of the retina this might not be as critical as the microglia pre-pattern the retina prior to vascularization but in the zebrafish they clearly purposefully migrate to the sites of anastomosis. The factor involved might be the same (if there is one) that draws tip cells towards one another. Or it could be solely attracting macrophages that in turn attract tip cells. One must also remember that in the lines used in this study we are not able to visualize all macrophages therefore understanding more about macrophage cell biology may aid in the generation of better macrophage specific reporter lines.

The fms:Gla4;UAS:mCherry-NMT line used in this study is a great tool to address some of these question. It is now possible to design miRNAs that target specific sequences to obtain the desired gene knockdown. Such miRNAs can be cloned and used to generate transgenic lines expressing them. Combine this with a cell specific driver (such as the fms:Gal4) and one can investigate the knockdown of specific genes in system organisms like the zebrafish where tissue specific knockouts are still no an easy feat.

Chapter 6. Conclusion

Angiogenesis is a complex developmental process that involves many coordinated morphological events. The work I have described in this study furthers our understanding of angiogenesis, and in particular a qualitative and quantitative description of the events leading to angiogenesis. The data also provides evidence for the involvement on *heca* in lumenization and the downregulation of filopodia activity, hinting at a flow specific control of sprouting. Macrophages have been shown to play part in angiogenesis and here I show dynamic interactions between macrophages and ECs as well as a mild angiogenic defect upon macrophage ablation.

A lot of work has gone into understanding how sprouting angiogenesis is initiated, what factors induce it, how vessels are guided and patterned but little attention has been given to how new sprouts go on to form a functional loop through anastomosis and subsequent lumen formation. In Ch.3 I present various observations with regards to filopodia activity, anastomosis, cell division and lumen formation. The fact that all ECs in the growing sprout exhibit some degree of filopodia activity questions the current model of tip cell selection where only the tip cell posses filopodia/migratory phenotype (Phng and Gerhardt, 2009). Recent evidence begins to support a notion where ECs can possess a spectrum of activation levels and this can result in tip cell change and EC shuffling within the sprout (Jakobsson et al., 2010). This links up with the report on the presence of more than two EC phenotypes in the growing vasculature, with the addition of the quiescent phalanx cell along tip and stalk cells (Mazzone et al., 2009). All these data taken together leads to a model where ECs in the sprout might be able to rapidly respond in case the present tip cell shows decreased VEGFR2 signalling and thus suboptimal migration as suggested by Benedito *et al* with regards to the role of Jag1 in the retinal plexus (Benedito et al., 2009).

The data clearly shows that anastomosis is not a rapid process and tip cells in adjacent ISAs usually get into contact multiple times prior to remaining connected and fusing. Filopodia play an important role in tip cells find one another and bringing the

cell bodies closer for anastomosis. The quantitative analysis indicates that the time frame between contact and fusion may involve genetic regulation.

Lumen formation is shown to occur through a mechanism compatible with junctional opening, which indicates a prior determination of apical luminal surface. Such a mechanism has been described in the mouse aorta but not in the zebrafish (Strilic et al., 2009). A second mechanism that involves the lumen pushing through what appears to be a single cell is described. This may also be related to an EC junction opening very much like a zipper. Both these mechanisms and their time scale do not agree with previous work on intracellular pinocytic vesicle fusion, leading to a solely unicellular and intracellular lumen (Kamei et al., 2006).

In Ch.4 I investigated the role of *heca* in zebrafish angiogenesis and in anastomosis. *Heca* is shown to have quite unique effects in gain and loss of function experiments, with the former resulting in precocious sprout lumenization whereas knockdown leads to ectopic fusion between the DLAVs over the NT. The phenotypes may seem unrelated but if this is contexualised with the observations that lumen formation appears to be the driver for termination of filopodia activity, then some link can be made. It is quite possible that lumen formation can control EC activity, if one considers that increasing the supply of oxygen is what drives angiogenesis. *Heca* does not affect filopodia protrusion and lumen but also at the level of the number of ECs present in the sprout, suggesting that EC organisation and possibly junctional arrangement are affected (even though I do not report any).

Finally, while this study was on-going a few reports have emerged linking macrophages to developmental angiogenesis. Here I demonstrate dynamic and direct interaction between macrophages and ECs. The phenotype observed upon macrophage ablation is not drastic, meaning that macrophage paly a non-essential role in angiogenesis but can be seen as fine tuning the system and facilitating the process.

Overall this work indicates how the various morphological processes in angiogenesis are important for the correct development of the vasculatures. It also highlights how all these events may be interlinked, with the initial step of filopodia activity being controlled by the final step of lumen formation.

Chapter 7. Reference List

ABRAHAM, S., YEO, M., MONTERO-BALAGUER, M., PATERSON, H., DEJANA, E., MARSHALL, C. J. & MAVRIA, G. 2009. VE-Cadherin-Mediated Cell-Cell Interaction Suppresses Sprouting via Signaling to MLC2 Phosphorylation. *Current Biology,* 19**,** 668-674.

ADAMS, R. H. & ALITALO, K. 2007. Molecular regulation of angiogenesis and lymphangiogenesis. *Nat Rev Mol Cell Biol,* 8**,** 464-478.

ADAMS, R. H. & EICHMANN, A. 2010. Axon guidance molecules in vascular patterning. *Cold Spring Harb Perspect Biol,* 2**,** a001875.

AFFOLTER, M. & CAUSSINUS, E. 2008. Tracheal branching morphogenesis in Drosophila: new insights into cell behaviour and organ architecture. *Development,* 135**,** 2055-2064.

ALBUQUERQUE, R. J. C., HAYASHI, T., CHO, W. G., KLEINMAN, M. E., DRIDI, S., TAKEDA, A., BAFFI, J. Z., YAMADA, K., KANEKO, H., GREEN, M. G., CHAPPELL, J., WILTING, J., WEICH, H. A., YAMAGAMI, S., AMANO, S., MIZUKI, N., ALEXANDER, J. S., PETERSON, M. L., BREKKEN, R. A., HIRASHIMA, M., CAPOOR, S., USUI, T., AMBATI, B. K. & AMBATI, J. 2009. Alternatively spliced vascular endothelial growth factor receptor-2 is an essential endogenous inhibitor of lymphatic vessel growth. *Nature Medicine***,** 1-10.

ALLINGHAM, M. J., VAN BUUL, J. D. & BURRIDGE, K. 2007. ICAM-1-mediated, Src- and Pyk2-dependent vascular endothelial cadherin tyrosine phosphorylation is required for leukocyte transendothelial migration. *J Immunol,* 179**,** 4053-64.

ALMAGRO, S., DURMORT, C., CHERVIN-PETINOT, A., HEYRAUD, S., DUBOIS, M., LAMBERT, O., MAILLEFAUD, C., HEWAT, E., SCHAAL, J. P., HUBER, P. & GULINO-DEBRAC, D. 2010. The Motor Protein Myosin-X Transports VE-Cadherin along Filopodia To Allow the Formation of Early Endothelial Cell-Cell Contacts. *Mol Cell Biol,* 30**,** 1703-1717.

AMBATI, B. K., NOZAKI, M., SINGH, N., TAKEDA, A., JANI, P. D., SUTHAR, T., ALBUQUERQUE, R. J. C., RICHTER, E., SAKURAI, E., NEWCOMB, M. T., KLEINMAN, M. E., CALDWELL, R. B., LIN, Q., OGURA, Y., ORECCHIA, A., SAMUELSON, D. A., AGNEW, D. W., ST. LEGER, J., GREEN, W. R., MAHASRESHTI, P. J., CURIEL, D. T., KWAN, D., MARSH, H., IKEDA, S., LEIPER, L. J., COLLINSON, J. M., BOGDANOVICH, S., KHURANA, T. S., SHIBUYA, M., BALDWIN, M. E., FERRARA, N., GERBER, H.-P., DE

FALCO, S., WITTA, J., BAFFI, J. Z., RAISLER, B. J. & AMBATI, J. 2006. Corneal avascularity is due to soluble VEGF receptor-1. *Nature,* 443**,** 993-997.

ANDERSON, M. G., PERKINS, G. L., CHITTICK, P., SHRIGLEY, R. J. & JOHNSON, W. A. 1995. drifter, a Drosophila POU-domain transcription factor, is required for correct differentiation and migration of tracheal cells and midline glia. *Genes & Development,* 9**,** 123-37.

ARMER, H. E. J., MARIGGI, G., PNG, K. M. Y., GENOUD, C., MONTEITH, A. G., BUSHBY, A. J., GERHARDT, H. & COLLINSON, L. M. 2009. Imaging transient blood vessel fusion events in zebrafish by correlative volume electron microscopy. *PLoS ONE,* 4**,** e7716.

ASHIKARI-HADA, S. 2005. Heparin Regulates Vascular Endothelial Growth Factor165-dependent Mitogenic Activity, Tube Formation, and Its Receptor Phosphorylation of Human Endothelial Cells: COMPARISON OF THE EFFECTS OF HEPARIN AND MODIFIED HEPARINS. *Journal of Biological Chemistry,* 280**,** 31508-31515.

BACON, N. C., WAPPNER, P., O'ROURKE, J. F., BARTLETT, S. M., SHILO, B., PUGH, C. W. & RATCLIFFE, P. J. 1998. Regulation of the Drosophila bHLH-PAS protein Sima by hypoxia: functional evidence for homology with mammalian HIF-1 alpha. *Biochem Biophys Res Commun,* 249**,** 811-6.

BALLMER-HOFER, K., ANDERSSON, A. E., RATCLIFFE, L. E. & BERGER, P. 2011. Neuropilin-1 promotes VEGFR-2 trafficking through Rab11 vesicles thereby specifying signal output. *Blood,* 118**,** 816-826.

BAYLESS, K. J. & DAVIS, G. E. 2003. Sphingosine-1-phosphate markedly induces matrix metalloproteinase and integrin-dependent human endothelial cell invasion and lumen formation in three-dimensional collagen and fibrin matrices. *Biochem Biophys Res Commun,* 312**,** 903-13.

BAYLESS, K. J., SALAZAR, R. & DAVIS, G. E. 2010. RGD-Dependent Vacuolation and Lumen Formation Observed during Endothelial Cell Morphogenesis in Three-Dimensional Fibrin Matrices Involves the αvβ3 and α5β1 Integrins. *Am J Pathol,* 156**,** 1673-1683.

BAZZONI, G. & DEJANA, E. 2004. Endothelial cell-to-cell junctions: molecular organization and role in vascular homeostasis. *Physiological Reviews,* 84**,** 869-901.

BEDELL, V. M., YEO, S.-Y., PARK, K. W., CHUNG, J., SETH, P., SHIVALINGAPPA, V., ZHAO, J., OBARA, T., SUKHATME, V. P., DRUMMOND, I. A., LI, D. Y. & RAMCHANDRAN, R. 2005. roundabout4 is essential for angiogenesis in vivo. *Proc Natl Acad Sci USA,* 102**,** 6373-8.

BENEDITO, R., ROCA, C., SORENSEN, I., ADAMS, S., GOSSLER, A., FRUTTIGER, M. & ADAMS, R. H. 2009. The Notch Ligands Dll4 and Jagged1 Have Opposing Effects on Angiogenesis. *Cell,* 137**,** 1124-1135.

BENEDITO, R., TRINDADE, A., HIRASHIMA, M., HENRIQUE, D., DA COSTA, L., ROSSANT, J., GILL, P. S. & DUARTE, A. 2008. Loss of Notch signalling induced by Dll4 causes arterial calibre reduction by increasing endothelial cell response to angiogenic stimuli. *BMC Dev Biol,* 8**,** 117.

BENEST, A. V., HARPER, S. J., HERTTUALA, S. Y., ALITALO, K. & BATES, D. O. 2008. VEGF-C induced angiogenesis preferentially occurs at a distance from lymphangiogenesis. *Cardiovasc Res,* 78**,** 315-323.

BENTLEY, K., GERHARDT, H. & BATES, P. A. 2008. Agent-based simulation of notch-mediated tip cell selection in angiogenic sprout initialisation. *J Theor Biol,* 250**,** 25-36.

BENTLEY, K., MARIGGI, G., GERHARDT, H. & BATES, P. A. 2009. Tipping the balance: robustness of tip cell selection, migration and fusion in angiogenesis. *PLoS Comput Biol,* 5**,** e1000549.

BERTHOD, F., GERMAIN, L., TREMBLAY, N. & AUGER, F. A. 2006. Extracellular matrix deposition by fibroblasts is necessary to promote capillary-like tube formation in vitro. *J. Cell. Physiol.,* 207**,** 491-498.

BLUM, Y., BELTING, H., ELLERTSDOTTIR, E., HERWIG, L., LUDERS, F. & AFFOLTER, M. 2008. Complex cell rearrangements during intersegmental vessel sprouting and vessel fusion in the zebrafish embryo. *Developmental Biology,* 316**,** 312-322.

BREIER, G., BREVIARIO, F., CAVEDA, L., BERTHIER, R., SCHNÜRCH, H., GOTSCH, U., VESTWEBER, D., RISAU, W. & DEJANA, E. 1996. Molecular cloning and expression of murine vascular endothelial-cadherin in early stage development of cardiovascular system. *Blood,* 87**,** 630-41.

BRUICK, R. K. 2001. A Conserved Family of Prolyl-4-Hydroxylases That Modify HIF. *Science,* 294**,** 1337-1340.

BURRI, P. H. & DJONOV, V. 2002. Intussusceptive angiogenesis--the alternative to capillary sprouting. *Molecular Aspects of Medicine,* 23**,** S1-27.

BUSSMANN, J., BOS, F. L., URASAKI, A., KAWAKAMI, K., DUCKERS, H. J. & SCHULTE-MERKER, S. 2010. Arteries provide essential guidance cues for lymphatic endothelial cells in the zebrafish trunk. *Development,* 137**,** 2653-2657.

BUSSMANN, J., LAWSON, N., ZON, L., SCHULTE-MERKER, S. & COMMITTEE, Z. N. 2008. Zebrafish VEGF receptors: a guideline to nomenclature. *PLoS Genetics,* 4**,** e1000064.

BUSSMANN, J., WOLFE, S. A. & SIEKMANN, A. F. 2011. Arterial-venous network formation during brain vascularization involves hemodynamic regulation of chemokine signaling. *Development***,** 1-10.

CABERNARD, C. & AFFOLTER, M. 2005. Distinct roles for two receptor tyrosine kinases in epithelial branching morphogenesis in Drosophila. *Developmental Cell,* 9**,** 831-42.

CANO, A., PÉREZ-MORENO, M. A., RODRIGO, I., LOCASCIO, A., BLANCO, M. J., DEL BARRIO, M. G., PORTILLO, F. & NIETO, M. A. 2000. The transcription factor snail controls epithelial-mesenchymal transitions by repressing E-cadherin expression. *Nat Cell Biol,* 2**,** 76-83.

CARMELIET, P., FERREIRA, V., BREIER, G., POLLEFEYT, S., KIECKENS, L., GERTSENSTEIN, M., FAHRIG, M., VANDENHOECK, A., HARPAL, K., EBERHARDT, C., DECLERCQ, C., PAWLING, J., MOONS, L., COLLEN, D., RISAU, W. & NAGY, A. 1996. Abnormal blood vessel development and lethality in embryos lacking a single VEGF allele. *Nature,* 380**,** 435-9.

CARMELIET, P., LAMPUGNANI, M. G., MOONS, L., BREVIARIO, F., COMPERNOLLE, V., BONO, F., BALCONI, G., SPAGNUOLO, R., OOSTHUYSE, B., DEWERCHIN, M., ZANETTI, A., ANGELLILO, A., MATTOT, V., NUYENS, D., LUTGENS, E., CLOTMAN, F., DE RUITER, M. C., GITTENBERGER-DE GROOT, A., POELMANN, R., LUPU, F., HERBERT, J. M., COLLEN, D. & DEJANA, E. 1999. Targeted deficiency or cytosolic truncation of the VE-cadherin gene in mice impairs VEGF-mediated endothelial survival and angiogenesis. *Cell,* 98**,** 147-57.

CARVER, E. A., JIANG, R., LAN, Y., ORAM, K. F. & GRIDLEY, T. 2001. The mouse snail gene encodes a key regulator of the epithelial-mesenchymal transition. *Mol Cell Biol,* 21**,** 8184-8.

CASTETS, M., COISSIEUX, M.-M., DELLOYE-BOURGEOIS, C., BERNARD, L., DELCROS, J.-G., BERNET, A., LAUDET, V. & MEHLEN, P. 2009. Inhibition of Endothelial Cell Apoptosis by Netrin-1 during Angiogenesis. *Developmental Cell,* 16**,** 614-620.

CATTELINO, A. 2003. The conditional inactivation of the -catenin gene in endothelial cells causes a defective vascular pattern and increased vascular fragility. *J Cell Biol,* 162**,** 1111-1122.

CENTANIN, L., DEKANTY, A., ROMERO, N., IRISARRI, M., GORR, T. A. & WAPPNER, P. 2008. Cell autonomy of HIF effects in Drosophila: tracheal cells

sense hypoxia and induce terminal branch sprouting. *Developmental Cell,* 14**,** 547-58.

CHEN, L., YAO, J.-H., ZHANG, S.-H., WANG, L., SONG, H.-D. & XUE, J.-L. 2005. Slit-like 2, a novel zebrafish slit homologue that might involve in zebrafish central neural and vascular morphogenesis. *Biochemical and Biophysical Research Communications,* 336**,** 364-71.

CHEN, T. T., LUQUE, A., LEE, S., ANDERSON, S. M., SEGURA, T. & IRUELA-ARISPE, M. L. 2010. Anchorage of VEGF to the extracellular matrix conveys differential signaling responses to endothelial cells. *J Cell Biol,* 188**,** 595-609.

CHIEN, C.-C., CHANG, C.-C., YANG, S.-H., CHEN, S.-H. & HUANG, C.-J. 2006. A homologue of the Drosophila headcase protein is a novel tumor marker for early-stage colorectal cancer. *Oncol Rep,* 15**,** 919-26.

CHILDS, S., CHEN, J.-N., GARRITY, D. M. & FISHMAN, M. C. 2002. Patterning of angiogenesis in the zebrafish embryo. *Development,* 129**,** 973-82.

CHU, H., GAO, J., CHEN, C.-W., HUARD, J. & WANG, Y. 2011. Injectable fibroblast growth factor-2 coacervate for persistent angiogenesis. *Proceedings of the National Academy of Sciences***,** 1-6.

CLAXTON, S. & FRUTTIGER, M. 2004. Periodic Delta-like 4 expression in developing retinal arteries. *Gene Expr Patterns,* 5**,** 123-7.

COLAMARINO, S. A. & TESSIER-LAVIGNE, M. 1995. The axonal chemoattractant netrin-1 is also a chemorepellent for trochlear motor axons. *Cell,* 81**,** 621-9.

CORADA, M. 2001. Monoclonal antibodies directed to different regions of vascular endothelial cadherin extracellular domain affect adhesion and clustering of the protein and modulate endothelial permeability. *Blood,* 97**,** 1679-1684.

CORADA, M. 2002. A monoclonal antibody to vascular endothelial-cadherin inhibits tumor angiogenesis without side effects on endothelial permeability. *Blood,* 100**,** 905-911.

COVASSIN, L. D., VILLEFRANC, J. A., KACERGIS, M. C., WEINSTEIN, B. M. & LAWSON, N. D. 2006. Distinct genetic interactions between multiple Vegf receptors are required for development of different blood vessel types in zebrafish. *Proc Natl Acad Sci USA,* 103**,** 6554-9.

CROSBY, C. V., FLEMING, P. A., ARGRAVES, W. S., CORADA, M., ZANETTA, L., DEJANA, E. & DRAKE, C. J. 2005. VE-cadherin is not required for the formation of nascent blood vessels but acts to prevent their disassembly. *Blood,* 105**,** 2771-6.

DAVIS, G. E. & BAYLESS, K. J. 2003. An integrin and Rho GTPase-dependent pinocytic vacuole mechanism controls capillary lumen formation in collagen and fibrin matrices. *Microcirculation,* 10**,** 27-44.

DAVIS, G. E. & CAMARILLO, C. W. 1996. An alpha 2 beta 1 integrin-dependent pinocytic mechanism involving intracellular vacuole formation and coalescence regulates capillary lumen and tube formation in three-dimensional collagen matrix. *Experimental Cell Research,* 224**,** 39-51.

DE ARRUDA, M. V., WATSON, S., LIN, C. S., LEAVITT, J. & MATSUDAIRA, P. 1990. Fimbrin is a homologue of the cytoplasmic phosphoprotein plastin and has domains homologous with calmodulin and actin gelation proteins. *J Cell Biol,* 111**,** 1069-79.

DE MAZIÈRE, A., PARKER, L., VAN DIJK, S., YE, W. & KLUMPERMAN, J. 2008. Egfl7 knockdown causes defects in the extension and junctional arrangements of endothelial cells during zebrafish vasculogenesis. *Dev. Dyn.,* 237**,** 580-591.

DE PALMA, M., VENNERI, M. A., GALLI, R., SERGI SERGI, L., POLITI, L. S., SAMPAOLESI, M. & NALDINI, L. 2005. Tie2 identifies a hematopoietic lineage of proangiogenic monocytes required for tumor vessel formation and a mesenchymal population of pericyte progenitors. *Cancer Cell,* 8**,** 211-26.

DEJANA, E., TADDEI, A. & RANDI, A. M. 2007. Foxs and Ets in the transcriptional regulation of endothelial cell differentiation and angiogenesis. *Biochim Biophys Acta,* 1775**,** 298-312.

DEJANA, E., TOURNIER-LASSERVE, E. & WEINSTEIN, B. M. 2009. The Control of Vascular Integrity by Endothelial Cell Junctions: Molecular Basis and Pathological Implications. *Developmental Cell,* 16**,** 209-221.

DEL TORO, R., PRAHST, C., MATHIVET, T., SIEGFRIED, G., KAMINKER, J. S., LARRIVEE, B., BREANT, C., DUARTE, A., TAKAKURA, N., FUKAMIZU, A., PENNINGER, J. & EICHMANN, A. 2010. Identification and functional analysis of endothelial tip cell-enriched genes. *Blood,* 116**,** 4025-4033.

DIXELIUS, J. 2003. Ligand-induced Vascular Endothelial Growth Factor Receptor-3 (VEGFR-3) Heterodimerization with VEGFR-2 in Primary Lymphatic Endothelial Cells Regulates Tyrosine Phosphorylation Sites. *Journal of Biological Chemistry,* 278**,** 40973-40979.

DOMENGA, V. 2004. Notch3 is required for arterial identity and maturation of vascular smooth muscle cells. *Genes & Development,* 18**,** 2730-2735.

DOMINGUEZ, M. G., HUGHES, V. C., PAN, L., SIMMONS, M., DALY, C., ANDERSON, K., NOGUERA-TROISE, I., MURPHY, A. J., VALENZUELA, D. M., DAVIS, S., THURSTON, G., YANCOPOULOS, G. D. & GALE, N. W. 2007. Vascular endothelial tyrosine phosphatase (VE-PTP)-null mice undergo

vasculogenesis but die embryonically because of defects in angiogenesis. *Proc Natl Acad Sci USA,* 104**,** 3243-8.

DOWEJKO, A., BAUER, R. J., MULLER-RICHTER, U. D. A. & REICHERT, T. E. 2009. The human homolog of the Drosophila headcase protein slows down cell division of head and neck cancer cells. *Carcinogenesis,* 30**,** 1678-1685.

DUARTE, A. 2004. Dosage-sensitive requirement for mouse Dll4 in artery development. *Genes & Development,* 18**,** 2474-2478.

DUMONT, D. J. 1998. Cardiovascular Failure in Mouse Embryos Deficient in VEGF Receptor-3. *Science,* 282**,** 946-949.

DURRANS, A. & STUHLMANN, H. 2010. A role for Egfl7 during endothelial organization in the embryoid body model system. 1-12.

ELICEIRI, B. P., PAUL, R., SCHWARTZBERG, P. L., HOOD, J. D., LENG, J. & CHERESH, D. A. 1999. Selective requirement for Src kinases during VEGF-induced angiogenesis and vascular permeability. *Mol Cell,* 4**,** 915-24.

ENGLUND, C., STENEBERG, P., FALILEEVA, L., XYLOURGIDIS, N. & SAMAKOVLIS, C. 2002. Attractive and repulsive functions of Slit are mediated by different receptors in the Drosophila trachea. *Development,* 129**,** 4941-51.

ERRINGTON, J., DANIEL, R. A. & SCHEFFERS, D.-J. 2003. Cytokinesis in bacteria. *Microbiol Mol Biol Rev,* 67**,** 52-65, table of contents.

ESTRACH, S., CAILLETEAU, L., FRANCO, C. A., GERHARDT, H., STEFANI, C., LEMICHEZ, E., GAGNOUX-PALACIOS, L., MENEGUZZI, G. & METTOUCHI, A. 2011a. Laminin-binding integrins induce Dll4 expression and Notch signaling in endothelial cells. *Circ Res,* 109**,** 172-82.

ESTRACH, S., CAILLETEAU, L., FRANCO, C. A., GERHARDT, H., STEFANI, C., LEMICHEZ, E., GAGNOUX-PALACIOS, L., MENEGUZZI, G. & METTOUCHI, A. 2011b. Laminin-Binding Integrins Induce Dll4 Expression and Notch Signaling in Endothelial Cells. *Circulation Research,* 109**,** 172-182.

FANTIN, A., VIEIRA, J. M., GESTRI, G., DENTI, L., SCHWARZ, Q., PRYKHOZHIJ, S., PERI, F., WILSON, S. W. & RUHRBERG, C. 2010. Tissue macrophages act as cellular chaperones for vascular anastomosis downstream of VEGF-mediated endothelial tip cell induction. *Blood,* 116**,** 829-40.

FERRARA, N., CARVER-MOORE, K., CHEN, H., DOWD, M., LU, L., O'SHEA, K. S., POWELL-BRAXTON, L., HILLAN, K. J. & MOORE, M. W. 1996. Heterozygous embryonic lethality induced by targeted inactivation of the VEGF gene. *Nature,* 380**,** 439-42.

FINK, J., CARPI, N., BETZ, T., BÉTARD, A., CHEBAH, M., AZIOUNE, A., BORNENS, M., SYKES, C., FETLER, L., CUVELIER, D. & PIEL, M. 2011. External forces control mitotic spindle positioning. *Nature Publishing Group,* 13**,** 1-10.

FISCHER, A. 2004. The Notch target genes Hey1 and Hey2 are required for embryonic vascular development. *Genes & Development,* 18**,** 901-911.

FONG, G. H., ROSSANT, J., GERTSENSTEIN, M. & BREITMAN, M. L. 1995. Role of the Flt-1 receptor tyrosine kinase in regulating the assembly of vascular endothelium. *Nature,* 376**,** 66-70.

FOO, S. S., TURNER, C. J., ADAMS, S., COMPAGNI, A., AUBYN, D., KOGATA, N., LINDBLOM, P., SHANI, M., ZICHA, D. & ADAMS, R. H. 2006. Ephrin-B2 controls cell motility and adhesion during blood-vessel-wall assembly. *Cell,* 124**,** 161-73.

FRUTTIGER, M. 2007. Development of the retinal vasculature. *Angiogenesis,* 10**,** 77-88.

FUKUSHIMA, Y., OKADA, M., KATAOKA, H., HIRASHIMA, M., YOSHIDA, Y., MANN, F., GOMI, F., NISHIDA, K., NISHIKAWA, S.-I. & UEMURA, A. 2011. Sema3E-PlexinD1 signaling selectively suppresses disoriented angiogenesis in ischemic retinopathy in mice. *Journal of Clinical Investigation,* 121**,** 1974-1985.

GALE, N. W., DOMINGUEZ, M. G., NOGUERA, I., PAN, L., HUGHES, V., VALENZUELA, D. M., MURPHY, A. J., ADAMS, N. C., LIN, H. C., HOLASH, J., THURSTON, G. & YANCOPOULOS, G. D. 2004. Haploinsufficiency of delta-like 4 ligand results in embryonic lethality due to major defects in arterial and vascular development. *Proc Natl Acad Sci USA,* 101**,** 15949-54.

GAVARD, J. & GUTKIND, J. S. 2006. VEGF controls endothelial-cell permeability by promoting the β-arrestin-dependent endocytosis of VE-cadherin. *Nat Cell Biol,* 8**,** 1223-1234.

GAVARD, J., PATEL, V. & GUTKIND, J. S. 2008. Angiopoietin-1 prevents VEGF-induced endothelial permeability by sequestering Src through mDia. *Developmental Cell,* 14**,** 25-36.

GERBER, H. P., HILLAN, K. J., RYAN, A. M., KOWALSKI, J., KELLER, G. A., RANGELL, L., WRIGHT, B. D., RADTKE, F., AGUET, M. & FERRARA, N. 1999. VEGF is required for growth and survival in neonatal mice. *Development,* 126**,** 1149-59.

GERHARDT, H. 2003. VEGF guides angiogenic sprouting utilizing endothelial tip cell filopodia. *The Journal of Cell Biology,* 161**,** 1163-1177.

GERHARDT, H., RUHRBERG, C., ABRAMSSON, A., FUJISAWA, H., SHIMA, D. & BETSHOLTZ, C. 2004. Neuropilin-1 is required for endothelial tip cell guidance in the developing central nervous system. *Dev. Dyn.,* 231**,** 503-509.

GERHARDT, H., WOLBURG, H. & REDIES, C. 2000. N-cadherin mediates pericytic-endothelial interaction during brain angiogenesis in the chicken. *Dev Dyn,* 218**,** 472-9.

GITLER, A. D., LU, M. M. & EPSTEIN, J. A. 2004. PlexinD1 and semaphorin signaling are required in endothelial cells for cardiovascular development. *Developmental Cell,* 7**,** 107-16.

GLAZER, L. & SHILO, B. Z. 1991. The Drosophila FGF-R homolog is expressed in the embryonic tracheal system and appears to be required for directed tracheal cell extension. *Genes & Development,* 5**,** 697-705.

GRAY, C., LOYNES, C. A., WHYTE, M. K. B., CROSSMAN, D. C., RENSHAW, S. A. & CHICO, T. J. A. 2011. Simultaneous intravital imaging of macrophage and neutrophil behaviour during inflammation using a novel transgenic zebrafish. *Thromb Haemost***,** 1-9.

GU, C. 2005. Semaphorin 3E and Plexin-D1 Control Vascular Pattern Independently of Neuropilins. *Science,* 307**,** 265-268.

GUARANI, V., DEFLORIAN, G., FRANCO, C. A., KRÜGER, M., PHNG, L.-K., BENTLEY, K., TOUSSAINT, L., DEQUIEDT, F., MOSTOSLAVSKY, R., SCHMIDT, M. H. H., ZIMMERMANN, B., BRANDES, R. P., MIONE, M., WESTPHAL, C. H., BRAUN, T., ZEIHER, A. M., GERHARDT, H., DIMMELER, S. & POTENTE, M. 2011. Acetylation-dependent regulation of endothelial Notch signalling by the SIRT1 deacetylase. *Nature,* 473**,** 234-238.

GUILLEMIN, K., GROPPE, J., DUCKER, K., TREISMAN, R., HAFEN, E., AFFOLTER, M. & KRASNOW, M. A. 1996. The pruned gene encodes the Drosophila serum response factor and regulates cytoplasmic outgrowth during terminal branching of the tracheal system. *Development,* 122**,** 1353-62.

HARPER, S. J. & BATES, D. O. 2008. VEGF-A splicing: the key to anti-angiogenic therapeutics? *Nat Rev Cancer,* 8**,** 880-7.

HASHIMOTO, T. 2003. Expression of the Flk1 receptor and its ligand VEGF in the developing chick central nervous system. *Gene Expression Patterns,* 3**,** 109-113.

HELLSTRÖM, M., PHNG, L.-K., HOFMANN, J. J., WALLGARD, E., COULTAS, L., LINDBLOM, P., ALVA, J., NILSSON, A.-K., KARLSSON, L., GAIANO, N., YOON, K., ROSSANT, J., IRUELA-ARISPE, M. L., KALÉN, M., GERHARDT, H. & BETSHOLTZ, C. 2007. Dll4 signalling through Notch1 regulates formation of tip cells during angiogenesis. *Nature,* 445**,** 776-780.

HERBERT, S. P., HUISKEN, J., KIM, T. N., FELDMAN, M. E., HOUSEMAN, B. T., WANG, R. A., SHOKAT, K. M. & STAINIER, D. Y. R. 2009. Arterial-Venous Segregation by Selective Cell Sprouting: An Alternative Mode of Blood Vessel Formation. *Science,* 326**,** 294-298.

HERBOMEL, P., THISSE, B. & THISSE, C. 2001. Zebrafish early macrophages colonize cephalic mesenchyme and developing brain, retina, and epidermis through a M-CSF receptor-dependent invasive process. *Developmental Biology,* 238**,** 274-88.

HÉROULT, M., SCHAFFNER, F. & AUGUSTIN, H. G. 2006. Eph receptor and ephrin ligand-mediated interactions during angiogenesis and tumor progression. *Experimental Cell Research,* 312**,** 642-50.

HODKINSON, P. S., ELLIOTT, P. A., LAD, Y., MCHUGH, B. J., MACKINNON, A. C., HASLETT, C. & SETHI, T. 2007. Mammalian NOTCH-1 activates beta1 integrins via the small GTPase R-Ras. *J Biol Chem,* 282**,** 28991-9001.

HOGAN, B. M., HERPERS, R., WITTE, M., HELOTERA, H., ALITALO, K., DUCKERS, H. J. & SCHULTE-MERKER, S. 2009. Vegfc/Flt4 signalling is suppressed by Dll4 in developing zebrafish intersegmental arteries. *Development,* 136**,** 4001-4009.

HOLDERFIELD, M. T., HENDERSON ANDERSON, A. M., KOKUBO, H., CHIN, M. T., JOHNSON, R. L. & HUGHES, C. C. W. 2006. HESR1/CHF2 suppresses VEGFR2 transcription independent of binding to E-boxes. *Biochemical and Biophysical Research Communications,* 346**,** 637-48.

HUANG, L., YU, W., LI, X., NIU, L., LI, K. & LI, J. 2009. Robo1/Robo4: Different expression patterns in retinal development. *Experimental Eye Research,* 88**,** 583-588.

HUMINIECKI, L. 2002. Magic Roundabout Is a New Member of the Roundabout Receptor Family That Is Endothelial Specific and Expressed at Sites of Active Angiogenesis. *Genomics,* 79**,** 547-552.

IBRAHIMI, O. A., ZHANG, F., HRSTKA, S. C. L., MOHAMMADI, M. & LINHARDT, R. J. 2004. Kinetic model for FGF, FGFR, and proteoglycan signal transduction complex assembly. *Biochemistry,* 43**,** 4724-30.

IKEYA, T. & HAYASHI, S. 1999. Interplay of Notch and FGF signaling restricts cell fate and MAPK activation in the Drosophila trachea. *Development,* 126**,** 4455-63.

IMAI, Y., IBATA, I., ITO, D., OHSAWA, K. & KOHSAKA, S. 1996. A novel gene iba1 in the major histocompatibility complex class III region encoding an EF hand protein expressed in a monocytic lineage. *Biochem Biophys Res Commun,* 224**,** 855-62.

ISOGAI, S. 2001. The Vascular Anatomy of the Developing Zebrafish: An Atlas of Embryonic and Early Larval Development. *Developmental Biology,* 230**,** 278-301.

ISOGAI, S. 2003. Angiogenic network formation in the developing vertebrate trunk. *Development,* 130**,** 5281-5290.

JAKOBSSON, L., DOMOGATSKAYA, A., TRYGGVASON, K., EDGAR, D. & CLAESSON-WELSH, L. 2007a. Laminin deposition is dispensable for vasculogenesis but regulates blood vessel diameter independent of flow. *FASEB J,* 22**,** 1530-1539.

JAKOBSSON, L., FRANCO, C. A., BENTLEY, K., COLLINS, R. T., PONSIOEN, B., ASPALTER, I. M., ROSEWELL, I., BUSSE, M., THURSTON, G., MEDVINSKY, A., SCHULTE-MERKER, S. & GERHARDT, H. 2010. Endothelial cells dynamically compete for the tip cell position during angiogenic sprouting. *Nature Publishing Group,* 12**,** 943-953.

JAKOBSSON, L., KREUGER, J. & CLAESSON-WELSH, L. 2007b. Building blood vessels--stem cell models in vascular biology. *The Journal of Cell Biology,* 177**,** 751-755.

JAKOBSSON, L., KREUGER, J., HOLMBORN, K., LUNDIN, L., ERIKSSON, I., KJELLÉN, L. & CLAESSON-WELSH, L. 2006. Heparan sulfate in trans potentiates VEGFR-mediated angiogenesis. *Developmental Cell,* 10**,** 625-34.

JAŹWIŃSKA, A. & AFFOLTER, M. 2004. A family of genes encoding zona pellucida (ZP) domain proteins is expressed in various epithelial tissues during Drosophila embryogenesis. *Gene Expr Patterns,* 4**,** 413-21.

JIANG, L. 2006. dysfusion Transcriptional Control of Drosophila Tracheal Migration, Adhesion, and Fusion. *Mol Cell Biol,* 26**,** 6547-6556.

JIANG, L. & CREWS, S. T. 2007. Transcriptional Specificity of Drosophila Dysfusion and the Control of Tracheal Fusion Cell Gene Expression. *Journal of Biological Chemistry,* 282**,** 28659-28668.

JIN, S., HANSSON, E. M., TIKKA, S., LANNER, F., SAHLGREN, C., FARNEBO, F., BAUMANN, M., KALIMO, H. & LENDAHL, U. 2008. Notch Signaling Regulates Platelet-Derived Growth Factor Receptor- Expression in Vascular Smooth Muscle Cells. *Circulation Research,* 102**,** 1483-1491.

JOHNSON, K., KNUST, E. & SKAER, H. 1999. bloated tubules (blot) encodes a Drosophila member of the neurotransmitter transporter family required for organisation of the apical cytocortex. *Developmental Biology,* 212**,** 440-54.

JOHNSTON, S. H., RAUSKOLB, C., WILSON, R., PRABHAKARAN, B., IRVINE, K. D. & VOGT, T. F. 1997. A family of mammalian Fringe genes implicated in boundary determination and the Notch pathway. *Development,* 124**,** 2245-54.

JONES, C. A., LONDON, N. R., CHEN, H., PARK, K. W., SAUVAGET, D., STOCKTON, R. A., WYTHE, J. D., SUH, W., LARRIEU-LAHARGUE, F., MUKOUYAMA, Y.-S., LINDBLOM, P., SETH, P., FRIAS, A., NISHIYA, N., GINSBERG, M. H., GERHARDT, H., ZHANG, K. & LI, D. Y. 2008. Robo4 stabilizes the vascular network by inhibiting pathologic angiogenesis and endothelial hyperpermeability. *Nat Med,* 14**,** 448-453.

JONES, C. A., NISHIYA, N., LONDON, N. R., ZHU, W., SORENSEN, L. K., CHAN, A. C., LIM, C. J., CHEN, H., ZHANG, Q., SCHULTZ, P. G., HAYALLAH, A. M., THOMAS, K. R., FAMULOK, M., ZHANG, K., GINSBERG, M. H. & LI, D. Y. 2009. Slit2–Robo4 signalling promotes vascular stability by blocking Arf6 activity. *Nature,* 11**,** 1325-1331.

KAMEI, M., BRIAN SAUNDERS, W., BAYLESS, K. J., DYE, L., DAVIS, G. E. & WEINSTEIN, B. M. 2006. Endothelial tubes assemble from intracellular vacuoles in vivo. *Nature,* 442**,** 453-456.

KANG, H.-W., WALVICK, R. & BOGDANOV, A. 2009. In vitro and In vivo imaging of antivasculogenesis induced by Noggin protein expression in human venous endothelial cells. *FASEB J,* 23**,** 4126-4134.

KAO, H. Y., ORDENTLICH, P., KOYANO-NAKAGAWA, N., TANG, Z., DOWNES, M., KINTNER, C. R., EVANS, R. M. & KADESCH, T. 1998. A histone deacetylase corepressor complex regulates the Notch signal transduction pathway. *Genes & Development,* 12**,** 2269-77.

KAUR, S. 2006. Robo4 Signaling in Endothelial Cells Implies Attraction Guidance Mechanisms. *Journal of Biological Chemistry,* 281**,** 11347-11356.

KAWAMURA, H., LI, X., GOISHI, K., VAN MEETEREN, L. A., JAKOBSSON, L., CEBE-SUAREZ, S., SHIMIZU, A., EDHOLM, D., BALLMER-HOFER, K., KJELLEN, L., KLAGSBRUN, M. & CLAESSON-WELSH, L. 2008. Neuropilin-1 in regulation of VEGF-induced activation of p38MAPK and endothelial cell organization. *Blood,* 112**,** 3638-3649.

KAWASAKI, T., KITSUKAWA, T., BEKKU, Y., MATSUDA, Y., SANBO, M., YAGI, T. & FUJISAWA, H. 1999. A requirement for neuropilin-1 in embryonic vessel formation. *Development,* 126**,** 4895-902.

KHAIBULLINA, A. A., ROSENSTEIN, J. M. & KRUM, J. M. 2004. Vascular endothelial growth factor promotes neurite maturation in primary CNS neuronal cultures. *Brain Res Dev Brain Res,* 148**,** 59-68.

KIDD, T., BROSE, K., MITCHELL, K. J., FETTER, R. D., TESSIER-LAVIGNE, M., GOODMAN, C. S. & TEAR, G. 1998. Roundabout controls axon crossing of the CNS midline and defines a novel subfamily of evolutionarily conserved guidance receptors. *Cell,* 92**,** 205-15.

KIM, J., OH, W.-J., GAIANO, N., YOSHIDA, Y. & GU, C. 2011. Semaphorin 3E-Plexin-D1 signaling regulates VEGF function in developmental angiogenesis via a feedback mechanism. *Genes & Development,* 25**,** 1399-1411.

KLAMBT, C., GLAZER, L. & SHILO, B. Z. 1992. breathless, a Drosophila FGF receptor homolog, is essential for migration of tracheal and specific midline glial cells. *Genes & Development,* 6**,** 1668-1678.

KLEMSZ, M. J., MCKERCHER, S. R., CELADA, A., VAN BEVEREN, C. & MAKI, R. A. 1990. The macrophage and B cell-specific transcription factor PU.1 is related to the ets oncogene. *Cell,* 61**,** 113-24.

KNOTT, G., MARCHMAN, H., WALL, D. & LICH, B. 2008. Serial Section Scanning Electron Microscopy of Adult Brain Tissue Using Focused Ion Beam Milling. *Journal of Neuroscience,* 28**,** 2959-2964.

KOCH, A. W., MATHIVET, T., LARRIVÉE, B., TONG, R. K., KOWALSKI, J., PIBOUIN-FRAGNER, L., BOUVRÉE, K., STAWICKI, S., NICHOLES, K., RATHORE, N., SCALES, S. J., LUIS, E., TORO, R. D., FREITAS, C., BRÉANT, C., MICHAUD, A., CORVOL, P., THOMAS, J.-L., WU, Y., PEALE, F., WATTS, R. J., TESSIER-LAVIGNE, M., BAGRI, A. & EICHMANN, A. 2011. Robo4 Maintains Vessel Integrity and Inhibits Angiogenesis by Interacting with UNC5B. *Developmental Cell,* 20**,** 33-46.

KOH, W., MAHAN, R. D. & DAVIS, G. E. 2008. Cdc42- and Rac1-mediated endothelial lumen formation requires Pak2, Pak4 and Par3, and PKC-dependent signaling. *Journal of Cell Science,* 121**,** 989-1001.

KOKUDO, T., SUZUKI, Y., YOSHIMATSU, Y., YAMAZAKI, T., WATABE, T. & MIYAZONO, K. 2008. Snail is required for TGF -induced endothelial-mesenchymal transition of embryonic stem cell-derived endothelial cells. *Journal of Cell Science,* 121**,** 3317-3324.

KREBS, L. T. 2004. Haploinsufficient lethality and formation of arteriovenous malformations in Notch pathway mutants. *Genes & Development,* 18**,** 2469-2473.

KRUEGER, J., LIU, D., SCHOLZ, K., ZIMMER, A., SHI, Y., KLEIN, C., SIEKMANN, A., SCHULTE-MERKER, S., CUDMORE, M., AHMED, A. & LE NOBLE, F. 2011. Flt1 acts as a negative regulator of tip cell formation and branching morphogenesis in the zebrafish embryo. *Development,* 138**,** 2111-2120.

KRUGER, R. P., AURANDT, J. & GUAN, K.-L. 2005. Semaphorins command cells to move. *Nat Rev Mol Cell Biol,* 6**,** 789-800.

KUBOTA, Y., TAKUBO, K., SHIMIZU, T., OHNO, H., KISHI, K., SHIBUYA, M., SAYA, H. & SUDA, T. 2009. M-CSF inhibition selectively targets pathological angiogenesis and lymphangiogenesis. *Journal of Experimental Medicine,* 206**,** 1089-1102.

KUIJPER, S., TURNER, C. J. & ADAMS, R. H. 2007. Regulation of angiogenesis by Eph-ephrin interactions. *Trends Cardiovasc Med,* 17**,** 145-51.

LAMPUGNANI, M. G. 2003. Contact inhibition of VEGF-induced proliferation requires vascular endothelial cadherin, beta-catenin, and the phosphatase DEP-1/CD148. *J Cell Biol,* 161**,** 793-804.

LANCRIN, C., SROCZYNSKA, P., STEPHENSON, C., ALLEN, T., KOUSKOFF, V. & LACAUD, G. 2009. The haemangioblast generates haematopoietic cells through a haemogenic endothelium stage. *Nature,* 457**,** 892-895.

LARRIVEE, B., FREITAS, C., SUCHTING, S., BRUNET, I. & EICHMANN, A. 2009. Guidance of Vascular Development: Lessons From the Nervous System. *Circulation Research,* 104**,** 428-441.

LARRIVEE, B., FREITAS, C., TROMBE, M., LV, X., DELAFARGE, B., YUAN, L., BOUVREE, K., BREANT, C., DEL TORO, R., BRECHOT, N., GERMAIN, S., BONO, F., DOL, F., CLAES, F., FISCHER, C., AUTIERO, M., THOMAS, J.-L., CARMELIET, P., TESSIER-LAVIGNE, M. & EICHMANN, A. 2007. Activation of the UNC5B receptor by Netrin-1 inhibits sprouting angiogenesis. *Genes & Development,* 21**,** 2433-2447.

LARSON, J. D., WADMAN, S. A., CHEN, E., KERLEY, L., CLARK, K. J., EIDE, M., LIPPERT, S., NASEVICIUS, A., EKKER, S. C., HACKETT, P. B. & ESSNER, J. J. 2004. Expression ofVE-cadherin in zebrafish embryos: A new tool to evaluate vascular development. *Dev. Dyn.,* 231**,** 204-213.

LAWSON, N. 2002. In Vivo Imaging of Embryonic Vascular Development Using Transgenic Zebrafish. *Developmental Biology,* 248**,** 307-318.

LAWSON, N. D., SCHEER, N., PHAM, V. N., KIM, C. H., CHITNIS, A. B., CAMPOS-ORTEGA, J. A. & WEINSTEIN, B. M. 2001. Notch signaling is required for arterial-venous differentiation during embryonic vascular development. *Development,* 128**,** 3675-83.

LE BORGNE, R. & SCHWEISGUTH, F. 2003. Unequal segregation of Neuralized biases Notch activation during asymmetric cell division. *Developmental Cell,* 5**,** 139-48.

LEE, P., GOISHI, K., DAVIDSON, A. J., MANNIX, R., ZON, L. & KLAGSBRUN, M. 2002. Neuropilin-1 is required for vascular development and is a mediator of VEGF-dependent angiogenesis in zebrafish. *Proc Natl Acad Sci USA,* 99**,** 10470-5.

LEE, S., CHEN, T. T., BARBER, C. L., JORDAN, M. C., MURDOCK, J., DESAI, S., FERRARA, N., NAGY, A., ROOS, K. P. & IRUELA-ARISPE, M. L. 2007. Autocrine VEGF Signaling Is Required for Vascular Homeostasis. *Cell,* 130**,** 691-703.

LESLIE, J. D., ARIZA-MCNAUGHTON, L., BERMANGE, A. L., MCADOW, R., JOHNSON, S. L. & LEWIS, J. 2007. Endothelial signalling by the Notch ligand Delta-like 4 restricts angiogenesis. *Development,* 134**,** 839-844.

LEWIS, J. 1998. Notch signalling and the control of cell fate choices in vertebrates. *Semin Cell Dev Biol,* 9**,** 583-9.

LIANG, D., XU, X., CHIN, A. J., BALASUBRAMANIYAN, N. V., TEO, M. A., LAM, T. J., WEINBERG, E. S. & GE, R. 1998. Cloning and characterization of vascular endothelial growth factor (VEGF) from zebrafish, Danio rerio. *Biochim Biophys Acta,* 1397**,** 14-20.

LIEBNER, S., CORADA, M., BANGSOW, T., BABBAGE, J., TADDEI, A., CZUPALLA, C. J., REIS, M., FELICI, A., WOLBURG, H., FRUTTIGER, M., TAKETO, M. M., VON MELCHNER, H., PLATE, K. H., GERHARDT, H. & DEJANA, E. 2008. Wnt/ -catenin signaling controls development of the blood-brain barrier. *J Cell Biol,* 183**,** 409-417.

LIN, E. Y., LI, J.-F., GNATOVSKIY, L., DENG, Y., ZHU, L., GRZESIK, D. A., QIAN, H., XUE, X.-N. & POLLARD, J. W. 2006. Macrophages Regulate the Angiogenic Switch in a Mouse Model of Breast Cancer. *Cancer Research,* 66**,** 11238-11246.

LLIMARGAS, M. 1999. The Notch pathway helps to pattern the tips of the Drosophila tracheal branches by selecting cell fates. *Development,* 126**,** 2355-64.

LOBOV, I. B., RAO, S., CARROLL, T. J., VALLANCE, J. E., ITO, M., ONDR, J. K., KURUP, S., GLASS, D. A., PATEL, M. S., SHU, W., MORRISEY, E. E., MCMAHON, A. P., KARSENTY, G. & LANG, R. A. 2005. WNT7b mediates macrophage-induced programmed cell death in patterning of the vasculature. *Nature,* 437**,** 417-421.

LOBOV, I. B., RENARD, R. A., PAPADOPOULOS, N., GALE, N. W., THURSTON, G., YANCOPOULOS, G. D. & WIEGAND, S. J. 2007. Delta-like ligand 4 (Dll4) is induced by VEGF as a negative regulator of angiogenic sprouting. *Proc Natl Acad Sci USA,* 104**,** 3219-24.

LOGEAT, F., BESSIA, C., BROU, C., LEBAIL, O., JARRIAULT, S., SEIDAH, N. G. & ISRAËL, A. 1998. The Notch1 receptor is cleaved constitutively by a furin-like convertase. *Proc Natl Acad Sci USA,* 95**,** 8108-12.

LOMELÍ, H., STARLING, C. & GRIDLEY, T. 2009. Epiblast-specific Snai1 deletion results in embryonic lethality due to multiple vascular defects. *BMC Res Notes,* 2**,** 22.

LONDON, N. R., ZHU, W., BOZZA, F. A., SMITH, M. C. P., GREIF, D. M., SORENSEN, L. K., CHEN, L., KAMINOH, Y., CHAN, A. C., PASSI, S. F., DAY, C. W., BARNARD, D. L., ZIMMERMAN, G. A., KRASNOW, M. A. & LI, D. Y. 2010. Targeting Robo4-Dependent Slit Signaling to Survive the Cytokine Storm in Sepsis and Influenza. *Science Translational Medicine,* 2**,** 23ra19-23ra19.

LOPEZ, D., NIU, G., HUBER, P. & CARTER, W. 2009. Tumor-induced upregulation of Twist, Snail, and Slug represses the activity of the human VE-cadherin promoter. *Archives of Biochemistry and Biophysics,* 482**,** 77-82.

LU, X., LE NOBLE, F., YUAN, L., JIANG, Q., DE LAFARGE, B., SUGIYAMA, D., BRÉANT, C., CLAES, F., DE SMET, F., THOMAS, J.-L., AUTIERO, M., CARMELIET, P., TESSIER-LAVIGNE, M. & EICHMANN, A. 2004. The netrin receptor UNC5B mediates guidance events controlling morphogenesis of the vascular system. *Nature,* 432**,** 179-86.

MAKINEN, T. 2005. PDZ interaction site in ephrinB2 is required for the remodeling of lymphatic vasculature. *Genes & Development,* 19**,** 397-410.

MAZZIERI, R., PUCCI, F., MOI, D., ZONARI, E., RANGHETTI, A., BERTI, A., POLITI, LETTERIO S., GENTNER, B., BROWN, JEFFREY L., NALDINI, L. & DE PALMA, M. 2011. Targeting the ANG2/TIE2 Axis Inhibits Tumor Growth and Metastasis by Impairing Angiogenesis and Disabling Rebounds of Proangiogenic Myeloid Cells. *Cancer Cell,* 19**,** 512-526.

MAZZONE, M., DETTORI, D., LEITE DE OLIVEIRA, R., LOGES, S., SCHMIDT, T., JONCKX, B., TIAN, Y.-M., LANAHAN, A. A., POLLARD, P. & RUIZ DE ALMODOVAR, C. 2009. Heterozygous Deficiency of PHD2 Restores Tumor Oxygenation and Inhibits Metastasis via Endothelial Normalization. *Cell***,** 13.

MEHLEN, P. 2005. The dependence receptor notion: another way to see death. *Cell Death Differ,* 12**,** 1003-1003.

MIZUGUCHI, H. 2000. IRES-Dependent Second Gene Expression Is Significantly Lower Than Cap-Dependent First Gene Expression in a Bicistronic Vector. *Molecular Therapy,* 1**,** 376-382.

MOESSLER, H., MERICSKAY, M., LI, Z., NAGL, S., PAULIN, D. & SMALL, J. V. 1996. The SM 22 promoter directs tissue-specific expression in arterial but not

in venous or visceral smooth muscle cells in transgenic mice. *Development,* 122**,** 2415-25.

MONTERO-BALAGUER, M., SWIRSDING, K., ORSENIGO, F., COTELLI, F., MIONE, M., DEJANA, E. & CALLAERTS, P. 2009. Stable Vascular Connections and Remodeling Require Full Expression of VE-Cadherin in Zebrafish Embryos. *PLoS ONE,* 4**,** e5772.

MORITA, K., SASAKI, H., FURUSE, M. & TSUKITA, S. 1999. Endothelial claudin: claudin-5/TMVCF constitutes tight junction strands in endothelial cells. *J Cell Biol,* 147**,** 185-94.

MORTIMER, N. T. & MOBERG, K. H. 2009. Regulation of Drosophila embryonic tracheogenesis by dVHL and hypoxia. *Developmental Biology,* 329**,** 294-305.

NASEVICIUS, A. & EKKER, S. C. 2000. Effective targeted gene 'knockdown' in zebrafish. *Nat Genet,* 26**,** 216-20.

NAVANKASATTUSAS, S., WHITEHEAD, K. J., SULI, A., SORENSEN, L. K., LIM, A. H., ZHAO, J., PARK, K. W., WYTHE, J. D., THOMAS, K. R., CHIEN, C.-B. & LI, D. Y. 2008. The netrin receptor UNC5B promotes angiogenesis in specific vascular beds. *Development,* 135**,** 659-667.

NAVARRO, P., RUCO, L. & DEJANA, E. 1998. Differential localization of VE- and N-cadherins in human endothelial cells: VE-cadherin competes with N-cadherin for junctional localization. *J Cell Biol,* 140**,** 1475-84.

NG, Y.-S., RAMSAUER, M., LOUREIRO, R. M. B. & D'AMORE, P. A. 2004. Identification of genes involved in VEGF-mediated vascular morphogenesis using embryonic stem cell-derived cystic embryoid bodies. *Lab Invest,* 84**,** 1209-1218.

NICOLI, S., STANDLEY, C., WALKER, P., HURLSTONE, A., FOGARTY, K. E. & LAWSON, N. D. 2010. MicroRNA-mediated integration of haemodynamics and Vegf signalling during angiogenesis. *Nature,* 464**,** 1196-1200.

NIESSEN, C. M. 2007. Tight Junctions/Adherens Junctions: Basic Structure and Function. *J Investig Dermatol,* 127**,** 2525-2532.

NIKOLIC, I., PLATE, K.-H. & SCHMIDT, M. H. 2010. EGFL7 meets miRNA-126: an angiogenesis alliance. *J Angiogenes Res,* 2**,** 9.

NILSSON, I., BAHRAM, F., LI, X., GUALANDI, L., KOCH, S., JARVIUS, M., S&OUML;DERBERG, O., ANISIMOV, A., KHOLOV&AACUTE, I., PYTOWSKI, B., BALDWIN, M., YL&AUML;-HERTTUALA, S., ALITALO, K., KREUGER, J. & CLAESSON-WELSH, L. 2010. VEGF receptor 2/-3 heterodimers detected in situ by proximity ligation on angiogenic sprouts. *The EMBO Journal***,** 1-12.

NITTA, T., HATA, M., GOTOH, S., SEO, Y., SASAKI, H., HASHIMOTO, N., FURUSE, M. & TSUKITA, S. 2003. Size-selective loosening of the blood-brain barrier in claudin-5-deficient mice. *J Cell Biol,* 161**,** 653-60.

NOGUERA-TROISE, I., DALY, C., PAPADOPOULOS, N. J., COETZEE, S., BOLAND, P., GALE, N. W., CHIEH LIN, H., YANCOPOULOS, G. D. & THURSTON, G. 2006. Blockade of Dll4 inhibits tumour growth by promoting non-productive angiogenesis. *Nature,* 444**,** 1032-1037.

NOTTEBAUM, A. F., CAGNA, G., WINDERLICH, M., GAMP, A. C., LINNEPE, R., POLASCHEGG, C., FILIPPOVA, K., LYCK, R., ENGELHARDT, B., KAMENYEVA, O., BIXEL, M. G., BUTZ, S. & VESTWEBER, D. 2008. VE-PTP maintains the endothelial barrier via plakoglobin and becomes dissociated from VE-cadherin by leukocytes and by VEGF. *Journal of Experimental Medicine,* 205**,** 2929-2945.

OBER, E. A., OLOFSSON, B., MÄKINEN, T., JIN, S.-W., SHOJI, W., KOH, G. Y., ALITALO, K. & STAINIER, D. Y. R. 2004. Vegfc is required for vascular development and endoderm morphogenesis in zebrafish. *EMBO Rep,* 5**,** 78-84.

OLSSON, A.-K., DIMBERG, A., KREUGER, J. & CLAESSON-WELSH, L. 2006. VEGF receptor signalling — in control of vascular function. *Nat Rev Mol Cell Biol,* 7**,** 359-371.

OUTTZ, H. H., TATTERSALL, I. W., KOFLER, N. M., STEINBACH, N. & KITAJEWSKI, J. 2011. Notch1 controls macrophage recruitment and Notch signaling is activated at sites of endothelial cell anastomosis during retinal angiogenesis in mice. *Blood***,** 1-15.

PAN, Q., CHATHERY, Y., WU, Y., RATHORE, N., TONG, R. K., PEALE, F., BAGRI, A., TESSIER-LAVIGNE, M., KOCH, A. W. & WATTS, R. J. 2007. Neuropilin-1 Binds to VEGF121 and Regulates Endothelial Cell Migration and Sprouting. *Journal of Biological Chemistry,* 282**,** 24049-24056.

PARK, K. 2003. Robo4 is a vascular-specific receptor that inhibits endothelial migration. *Developmental Biology,* 261**,** 251-267.

PARK, K. W., CROUSE, D., LEE, M., KARNIK, S. K., SORENSEN, L. K., MURPHY, K. J., KUO, C. J. & LI, D. Y. 2004. The axonal attractant Netrin-1 is an angiogenic factor. *Proc Natl Acad Sci USA,* 101**,** 16210-5.

PARKER, L. H., SCHMIDT, M., JIN, S.-W., GRAY, A. M., BEIS, D., PHAM, T., FRANTZ, G., PALMIERI, S., HILLAN, K., STAINIER, D. Y. R., DE SAUVAGE, F. J. & YE, W. 2004. The endothelial-cell-derived secreted factor Egfl7 regulates vascular tube formation. *Nature,* 428**,** 754-8.

PERRYN, E. D., CZIRÓK, A. & LITTLE, C. D. 2008. Vascular sprout formation entails tissue deformations and VE-cadherin-dependent cell-autonomous motility. *Developmental Biology,* 313**,** 545-55.

PHNG, L., POTENTE, M., LESLIE, J., BABBAGE, J., NYQVIST, D., LOBOV, I., ONDR, J., RAO, S., LANG, R. & THURSTON, G. 2009. Nrarp Coordinates Endothelial Notch and Wnt Signaling to Control Vessel Density in Angiogenesis. *Developmental Cell,* 16**,** 70-82.

PHNG, L.-K. & GERHARDT, H. 2009. Angiogenesis: A Team Effort Coordinated by Notch. *Developmental Cell,* 16**,** 196-208.

PITULESCU, M. E., SCHMIDT, I., BENEDITO, R. & ADAMS, R. H. 2010. Inducible gene targeting in the neonatal vasculature and analysis of retinal angiogenesis in mice. *Nature Protocols,* 5**,** 1518-1534.

POLVERINI, P. J., COTRAN, P. S., GIMBRONE, M. A. & UNANUE, E. R. 1977. Activated macrophages induce vascular proliferation. *Nature,* 269**,** 804-6.

POTENTE, M., GERHARDT, H. & CARMELIET, P. 2011. Basic and Therapeutic Aspects of Angiogenesis. *Cell,* 146**,** 873-887.

PRINCE, V. E., HOLLEY, S. A., BALLY-CUIF, L., PRABHAKARAN, B., OATES, A. C., HO, R. K. & VOGT, T. F. 2001. Zebrafish lunatic fringe demarcates segmental boundaries. *Mech Dev,* 105**,** 175-80.

REINHART-KING, C. A., DEMBO, M. & HAMMER, D. A. 2008. Cell-Cell Mechanical Communication through Compliant Substrates. *Biophysical Journal,* 95**,** 6044-6051.

RHODES, J., HAGEN, A., HSU, K., DENG, M., LIU, T., LOOK, A. & KANKI, J. 2005. Interplay of Pu.1 and Gata1 Determines Myelo-Erythroid Progenitor Cell Fate in Zebrafish. *Developmental Cell,* 8**,** 97-108.

RIBEIRO, C., EBNER, A. & AFFOLTER, M. 2002. In vivo imaging reveals different cellular functions for FGF and Dpp signaling in tracheal branching morphogenesis. *Developmental Cell,* 2**,** 677-83.

RIBEIRO, C., NEUMANN, M. & AFFOLTER, M. 2004. Genetic control of cell intercalation during tracheal morphogenesis in Drosophila. *Curr Biol,* 14**,** 2197-207.

RISAU, W. 1997. Mechanisms of angiogenesis. *Nature,* 386**,** 671-4.

ROBU, M. E., LARSON, J. D., NASEVICIUS, A., BEIRAGHI, S., BRENNER, C., FARBER, S. A. & EKKER, S. C. 2007. p53 activation by knockdown technologies. *PLoS Genetics,* 3**,** e78.

ROTH, P. 2003. The Drosophila nucleoporin DNup88 localizes DNup214 and CRM1 on the nuclear envelope and attenuates NES-mediated nuclear export. *J Cell Biol,* 163**,** 701-706.

RUHRBERG, C. 2002. Spatially restricted patterning cues provided by heparin-binding VEGF-A control blood vessel branching morphogenesis. *Genes & Development,* 16**,** 2684-2698.

RYMO, S. F., GERHARDT, H., WOLFHAGEN SAND, F., LANG, R., UV, A. & BETSHOLTZ, C. 2011. A Two-Way Communication between Microglial Cells and Angiogenic Sprouts Regulates Angiogenesis in Aortic Ring Cultures. *PLoS ONE,* 6**,** e15846.

SAMAKOVLIS, C., HACOHEN, N., MANNING, G., SUTHERLAND, D. C., GUILLEMIN, K. & KRASNOW, M. A. 1996a. Development of the Drosophila tracheal system occurs by a series of morphologically distinct but genetically coupled branching events. *Development,* 122**,** 1395-407.

SAMAKOVLIS, C., MANNING, G., STENEBERG, P., HACOHEN, N., CANTERA, R. & KRASNOW, M. A. 1996b. Genetic control of epithelial tube fusion during Drosophila tracheal development. *Development,* 122**,** 3531-6.

SAMANT, G. V., SCHUPP, M., FRANCOIS, M., MOLERI, S., KOTHINTI, R. K., CHUN, C. Z., SINHA, I., SELLARS, S., LEIGH, N., PRAMANIK, K., HORSWILL, M. A., REMADEVI, I., LI, K., WILKINSON, G. A., TABATABAI, N. M., BELTRAME, M., KOOPMAN, P. & RAMCHANDRAN, R. 2011. Sox factors transcriptionally regulate ROBO4 expression in developing vasculature in Zebrafish. *Journal of Biological Chemistry***,** 1-13.

SATO, M. & KORNBERG, T. B. 2002. FGF is an essential mitogen and chemoattractant for the air sacs of the drosophila tracheal system. *Developmental Cell,* 3**,** 195-207.

SAWAMIPHAK, S., SEIDEL, S., ESSMANN, C. L., WILKINSON, G. A., PITULESCU, M. E., ACKER, T. & ACKER-PALMER, A. 2010. Ephrin-B2 regulates VEGFR2 function in developmental and tumour angiogenesis. *Nature,* 465**,** 487-491.

SAWANO, A. 2001. Flt-1, vascular endothelial growth factor receptor 1, is a novel cell surface marker for the lineage of monocyte-macrophages in humans. *Blood,* 97**,** 785-791.

SCHMIDT, M., PAES, K., DE MAZIERE, A., SMYCZEK, T., YANG, S., GRAY, A., FRENCH, D., KASMAN, I., KLUMPERMAN, J., RICE, D. S. & YE, W. 2007. EGFL7 regulates the collective migration of endothelial cells by restricting their spatial distribution. *Development,* 134**,** 2913-2923.

SCHMIDT, M. H. H., BICKER, F., NIKOLIC, I., MEISTER, J., BABUKE, T., PICURIC, S., MÜLLER-ESTERL, W., PLATE, K. H. & DIKIC, I. 2009. Epidermal growth factor-like domain 7 (EGFL7) modulates Notch signalling and affects neural stem cell renewal. *Nat Cell Biol,* 11**,** 873-880.

SCHUH, A. C., FALOON, P., HU, Q. L., BHIMANI, M. & CHOI, K. 1999. In vitro hematopoietic and endothelial potential of flk-1(-/-) embryonic stem cells and embryos. *Proc Natl Acad Sci USA,* 96**,** 2159-64.

SEEGER, M., TEAR, G., FERRES-MARCO, D. & GOODMAN, C. S. 1993. Mutations affecting growth cone guidance in Drosophila: genes necessary for guidance toward or away from the midline. *Neuron,* 10**,** 409-26.

SHALABY, F., ROSSANT, J., YAMAGUCHI, T. P., GERTSENSTEIN, M., WU, X. F., BREITMAN, M. L. & SCHUH, A. C. 1995. Failure of blood-island formation and vasculogenesis in Flk-1-deficient mice. *Nature,* 376**,** 62-6.

SHELDON, H., ANDRE, M., LEGG, J. A., HEAL, P., HERBERT, J. M., SAINSON, R., SHARMA, A. S., KITAJEWSKI, J. K., HEATH, V. L. & BICKNELL, R. 2008. Active involvement of Robo1 and Robo4 in filopodia formation and endothelial cell motility mediated via WASP and other actin nucleation-promoting factors. *FASEB J***,** 10.

SHIBUYA, M. 2006. Vascular endothelial growth factor receptor-1 (VEGFR-1/Flt-1): a dual regulator for angiogenesis. *Angiogenesis,* 9**,** 225-230.

SIEKMANN, A. F. & LAWSON, N. D. 2007. Notch signalling limits angiogenic cell behaviour in developing zebrafish arteries. *Nature,* 445**,** 781-784.

SORENSEN, L. K., BROOKE, B. S., LI, D. Y. & URNESS, L. D. 2003. Loss of distinct arterial and venous boundaries in mice lacking endoglin, a vascular-specific TGFbeta coreceptor. *Developmental Biology,* 261**,** 235-50.

SQUADRITO, M. L. & PALMA, M. D. 2011. Macrophage regulation of tumor angiogenesis: Implications for cancer therapy. *Molecular Aspects of Medicine,* 32**,** 123-145.

STALMANS, I. 2002. Arteriolar and venular patterning in retinas of mice selectively expressing VEGF isoforms. *Journal of Clinical Investigation,* 109**,** 327-336.

STANLEY, P. 2007. Regulation of Notch signaling by glycosylation. *Curr Opin Struct Biol,* 17**,** 530-5.

STANYON, C. A., LIU, G., MANGIOLA, B. A., PATEL, N., GIOT, L., KUANG, B., ZHANG, H., ZHONG, J. & FINLEY, R. L., JR. 2004. A Drosophila protein-interaction map centered on cell-cycle regulators. *Genome Biol,* 5**,** R96.

STEFATER, J. A., LEWKOWICH, I., RAO, S., MARIGGI, G., CARPENTER, A. C., BURR, A. R., FAN, J., AJIMA, R., MOLKENTIN, J. D., WILLIAMS, B. O., WILLS-KARP, M., POLLARD, J. W., YAMAGUCHI, T., FERRARA, N., GERHARDT, H. & LANG, R. A. 2011. Regulation of angiogenesis by a non-canonical Wnt-Flt1 pathway in myeloid cells. *Nature,* 474**,** 511-5.

STENEBERG, P., ENGLUND, C., KRONHAMN, J., WEAVER, T. A. & SAMAKOVLIS, C. 1998. Translational readthrough in the hdc mRNA generates a novel branching inhibitor in the Drosophila trachea. *Genes & Development,* 12**,** 956-967.

STENEBERG, P., HEMPHÄLÄ, J. & SAMAKOVLIS, C. 1999. Dpp and Notch specify the fusion cell fate in the dorsal branches of the Drosophila trachea. *Mech Dev,* 87**,** 153-63.

STENZEL, D., LUNDKVIST, A., SAUVAGET, D., BUSSE, M., GRAUPERA, M., VAN DER FLIER, A., WIJELATH, E. S., MURRAY, J., SOBEL, M., COSTELL, M., TAKAHASHI, S., FASSLER, R., YAMAGUCHI, Y., GUTMANN, D. H., HYNES, R. O. & GERHARDT, H. 2011. Integrin-dependent and -independent functions of astrocytic fibronectin in retinal angiogenesis. *Development***,** 1-13.

STEWART, K. S., ZHOU, Z., ZWEIDLER-MCKAY, P. & KLEINERMAN, E. S. 2011. Delta-like ligand 4-Notch signaling regulates bone marrow-derived pericyte/vascular smooth muscle cell formation. *Blood,* 117**,** 719-726.

STONE, J., ITIN, A., ALON, T., PE'ER, J., GNESSIN, H., CHAN-LING, T. & KESHET, E. 1995. Development of retinal vasculature is mediated by hypoxia-induced vascular endothelial growth factor (VEGF) expression by neuroglia. *J Neurosci,* 15**,** 4738-47.

STRASSER, G. A., KAMINKER, J. S. & TESSIER-LAVIGNE, M. 2010. Microarray analysis of retinal endothelial tip cells identifies CXCR4 as a mediator of tip cell morphology and branching. *Blood,* 115**,** 5102-5110.

STRILIĆ, B., EGLINGER, J., KRIEG, M., ZEEB, M., AXNICK, J., BABÁL, P., MÜLLER, D. J. & LAMMERT, E. 2010. Electrostatic Cell-Surface Repulsion Initiates Lumen Formation in Developing Blood Vessels. *Current Biology,* 20**,** 2003-2009.

STRILIC, B., KUCERA, T., EGLINGER, J., HUGHES, M. R., MCNAGNY, K. M., TSUKITA, S., DEJANA, E., FERRARA, N. & LAMMERT, E. 2009. The Molecular Basis of Vascular Lumen Formation in the Developing Mouse Aorta. *Developmental Cell,* 17**,** 505-515.

SU, F., JUAREZ, M. A., COOKE, C. L., LAPOINTE, L., SHAVIT, J. A., YAMAOKA, J. S. & LYONS, S. E. 2007. Differential regulation of primitive myelopoiesis in the zebrafish by Spi-1/Pu.1 and C/ebp1. *Zebrafish,* 4**,** 187-99.

SUCHTING, S., FREITAS, C., LE NOBLE, F., BENEDITO, R., BRÉANT, C., DUARTE, A. & EICHMANN, A. 2007. The Notch ligand Delta-like 4 negatively regulates endothelial tip cell formation and vessel branching. *Proc Natl Acad Sci USA,* 104**,** 3225-30.

SUMMERTON, J. & WELLER, D. 1997. Morpholino antisense oligomers: design, preparation, and properties. *Antisense Nucleic Acid Drug Dev,* 7**,** 187-95.

SUNDERKÖTTER, C., STEINBRINK, K., GOEBELER, M., BHARDWAJ, R. & SORG, C. 1994. Macrophages and angiogenesis. *Journal of Leukocyte Biology,* 55**,** 410-22.

SUTHERLAND, D., SAMAKOVLIS, C. & KRASNOW, M. A. 1996. branchless encodes a Drosophila FGF homolog that controls tracheal cell migration and the pattern of branching. *Cell,* 87**,** 1091-101.

SZYMCZAK, A. L., WORKMAN, C. J., WANG, Y., VIGNALI, K. M., DILIOGLOU, S., VANIN, E. F. & VIGNALI, D. A. A. 2004. Correction of multi-gene deficiency in vivo using a single 'self-cleaving' 2A peptide-based retroviral vector. *Nat Biotechnol,* 22**,** 589-94.

TADDEI, A., GIAMPIETRO, C., CONTI, A., ORSENIGO, F., BREVIARIO, F., PIRAZZOLI, V., POTENTE, M., DALY, C., DIMMELER, S. & DEJANA, E. 2008. Endothelial adherens junctions control tight junctions by VE-cadherin-mediated upregulation of claudin-5. *Nat Cell Biol,* 10**,** 923-934.

TAKAHASHI, T., FOURNIER, A., NAKAMURA, F., WANG, L. H., MURAKAMI, Y., KALB, R. G., FUJISAWA, H. & STRITTMATTER, S. M. 1999. Plexin-neuropilin-1 complexes form functional semaphorin-3A receptors. *Cell,* 99**,** 59-69.

TAMMELA, T., ZARKADA, G., NURMI, H., JAKOBSSON, L., HEINOLAINEN, K., TVOROGOV, D., ZHENG, W., FRANCO, C. A., MURTOMÄKI, A., ARANDA, E., MIURA, N., YLÄ-HERTTUALA, S., FRUTTIGER, M., MÄKINEN, T., EICHMANN, A., POLLARD, J. W., GERHARDT, H. & ALITALO, K. 2011. VEGFR-3 controls tip to stalk conversion at vessel fusion sites by reinforcing Notch signalling. *Nature Cell Biology,* 13**,** 1-14.

TAMMELA, T., ZARKADA, G., WALLGARD, E., MURTOMÄKI, A., SUCHTING, S., WIRZENIUS, M., WALTARI, M., HELLSTRÖM, M., SCHOMBER, T., PELTONEN, R., FREITAS, C., DUARTE, A., ISONIEMI, H., LAAKKONEN, P., CHRISTOFORI, G., YLÄ-HERTTUALA, S., SHIBUYA, M., PYTOWSKI, B., EICHMANN, A., BETSHOLTZ, C. & ALITALO, K. 2008. Blocking VEGFR-3 suppresses angiogenic sprouting and vascular network formation. *Nature,* 454**,** 656-660.

TANAKA, H. 2004. Formin3 is required for assembly of the F-actin structure that mediates tracheal fusion in Drosophila. *Developmental Biology,* 274**,** 413-425.

TANAKA-MATAKATSU, M., UEMURA, T., ODA, H., TAKEICHI, M. & HAYASHI, S. 1996. Cadherin-mediated cell adhesion and cell motility in Drosophila trachea regulated by the transcription factor Escargot. *Development,* 122**,** 3697-705.

THOMSON, J. A. 1998. Embryonic Stem Cell Lines Derived from Human Blastocysts. *Science,* 282**,** 1145-1147.

TORRESVAZQUEZ, J. 2004. Semaphorin-Plexin Signaling Guides Patterning of the Developing Vasculature. *Developmental Cell,* 7**,** 117-123.

TRINDADE, A., RAM KUMAR, S., SCEHNET, J. S., LOPES-DA-COSTA, L., BECKER, J., JIANG, W., LIU, R., GILL, P. S. & DUARTE, A. 2008. Overexpression of delta-like 4 induces arterialization and attenuates vessel formation in developing mouse embryos. *Blood,* 112**,** 1720-1729.

TZIMA, E., IRANI-TEHRANI, M., KIOSSES, W. B., DEJANA, E., SCHULTZ, D. A., ENGELHARDT, B., CAO, G., DELISSER, H. & SCHWARTZ, M. A. 2005. A mechanosensory complex that mediates the endothelial cell response to fluid shear stress. *Nature,* 437**,** 426-431.

UV, A. 2003. Drosophila tracheal morphogenesis: intricate cellular solutions to basic plumbing problems. *Trends Cell Biol,* 13**,** 301-309.

VAN DER LOOP, F. T., SCHAART, G., TIMMER, E. D., RAMAEKERS, F. C. & VAN EYS, G. J. 1996. Smoothelin, a novel cytoskeletal protein specific for smooth muscle cells. *J Cell Biol,* 134**,** 401-11.

VILLA, N., WALKER, L., LINDSELL, C. E., GASSON, J., IRUELA-ARISPE, M. L. & WEINMASTER, G. 2001. Vascular expression of Notch pathway receptors and ligands is restricted to arterial vessels. *Mech Dev,* 108**,** 161-4.

VINCENT, S., RUBERTE, E., GRIEDER, N. C., CHEN, C. K., HAERRY, T., SCHUH, R. & AFFOLTER, M. 1997. DPP controls tracheal cell migration along the dorsoventral body axis of the Drosophila embryo. *Development,* 124**,** 2741-50.

VITTET, D., PRANDINI, M. H., BERTHIER, R., SCHWEITZER, A., MARTIN-SISTERON, H., UZAN, G. & DEJANA, E. 1996. Embryonic stem cells differentiate in vitro to endothelial cells through successive maturation steps. *Blood,* 88**,** 3424-31.

WALLEZ, Y., CAND, F., CRUZALEGUI, F., WERNSTEDT, C., SOUCHELNYTSKYI, S., VILGRAIN, I. & HUBER, P. 2007. Src kinase phosphorylates vascular endothelial-cadherin in response to vascular endothelial growth factor: identification of tyrosine 685 as the unique target site. *Oncogene,* 26**,** 1067-1077.

WALLEZ, Y. & HUBER, P. 2008. Endothelial adherens and tight junctions in vascular homeostasis, inflammation and angiogenesis. *Biochim Biophys Acta,* 1778**,** 794-809.

WANG, C.-H., CHEN, I.-H., KUO, M.-W., SU, P.-T., LAI, Z.-Y., WANG, C.-H., HUANG, W.-C., HOFFMAN, J., KUO, C. J., YOU, M.-S. & CHUANG, Y.-J. 2011. Zebrafish Thsd7a is a neural protein required for angiogenic patterning during development. *Dev. Dyn.,* 240**,** 1412-1421.

WANG, Y., KAISER, M. S., LARSON, J. D., NASEVICIUS, A., CLARK, K. J., WADMAN, S. A., ROBERG-PEREZ, S. E., EKKER, S. C., HACKETT, P. B., MCGRAIL, M. & ESSNER, J. J. 2010a. Moesin1 and Ve-cadherin are required in endothelial cells during in vivo tubulogenesis. *Development,* 137**,** 3119-3128.

WANG, Y., NAKAYAMA, M., PITULESCU, M. E., SCHMIDT, T. S., BOCHENEK, M. L., SAKAKIBARA, A., ADAMS, S., DAVY, A., DEUTSCH, U., LÜTHI, U., BARBERIS, A., BENJAMIN, L. E., MÄKINEN, T., NOBES, C. D. & ADAMS, R. H. 2010b. Ephrin-B2 controls VEGF-induced angiogenesis and lymphangiogenesis. *Nature,* 465**,** 483-486.

WEAVER, T. A. & WHITE, R. A. 1995. headcase, an imaginal specific gene required for adult morphogenesis in Drosophila melanogaster. *Development,* 121**,** 4149-60.

WEINSTEIN, B. M., STEMPLE, D. L., DRIEVER, W. & FISHMAN, M. C. 1995. Gridlock, a localized heritable vascular patterning defect in the zebrafish. *Nat Med,* 1**,** 1143-7.

WHITELEY, M., NOGUCHI, P. D., SENSABAUGH, S. M., ODENWALD, W. F. & KASSIS, J. A. 1992. The Drosophila gene escargot encodes a zinc finger motif found in snail-related genes. *Mech Dev,* 36**,** 117-27.

WILEY, D. M., KIM, J.-D., HAO, J., HONG, C. C., BAUTCH, V. L. & JIN, S.-W. 2011. Distinct signalling pathways regulate sprouting angiogenesis from the dorsal aorta and the axial vein. *Nature Publishing Group,* 13**,** 687-693.

WILK, R., WEIZMAN, I. & SHILO, B. Z. 1996. trachealess encodes a bHLH-PAS protein that is an inducer of tracheal cell fates in Drosophila. *Genes & Development,* 10**,** 93-102.

WU, M. Y., RAMEL, M. C., HOWELL, M. & HILL, C. S. 2011. SNW1 is a critical regulator of spatial BMP activity, neural plate border formation, and neural crest specification in vertebrate embryos. *PLoS Biol,* 9**,** e1000593.

XIAO, K., GARNER, J., BUCKLEY, K. M., VINCENT, P. A., CHIASSON, C. M., DEJANA, E., FAUNDEZ, V. & KOWALCZYK, A. P. 2005. p120-Catenin regulates clathrin-dependent endocytosis of VE-cadherin. *Mol Biol Cell,* 16**,** 5141-51.

XU, K., SACHARIDOU, A., FU, S., CHONG, DIANA C., SKAUG, B., CHEN, ZHIJIAN J., DAVIS, GEORGE E. & CLEAVER, O. 2011. Blood Vessel Tubulogenesis Requires Rasip1 Regulation of GTPase Signaling. *Developmental Cell,* 20**,** 526-539.

YOU, L.-R., LIN, F.-J., LEE, C. T., DEMAYO, F. J., TSAI, M.-J. & TSAI, S. Y. 2005. Suppression of Notch signalling by the COUP-TFII transcription factor regulates vein identity. *Nature,* 435**,** 98-104.

YUAN, L., MOYON, D., PARDANAUD, L., BRÉANT, C., KARKKAINEN, M. J., ALITALO, K. & EICHMANN, A. 2002. Abnormal lymphatic vessel development in neuropilin 2 mutant mice. *Development,* 129**,** 4797-806.

YUAN, L., SACHARIDOU, A., STRATMAN, A. N., LE BRAS, A., ZWIERS, P. J., SPOKES, K., BHASIN, M., SHIH, S.-C., NAGY, J. A., MOLEMA, G., AIRD, W. C., DAVIS, G. E. & OETTGEN, P. 2011. RhoJ is an endothelial cell-restricted Rho GTPase that mediates vascular morphogenesis and is regulated by the transcription factor ERG. *Blood***,** 1-35.

ZEISBERGER, S. M., ODERMATT, B., MARTY, C., ZEHNDER-FJÄLLMAN, A. H. M., BALLMER-HOFER, K. & SCHWENDENER, R. A. 2006. Clodronate-liposome-mediated depletion of tumour-associated macrophages: a new and highly effective antiangiogenic therapy approach. *Br J Cancer,* 95**,** 272-281.

ZHAN, Y., MAUNG, S. W., SHAO, B. & MYAT, M. M. 2010. The bHLH Transcription Factor, Hairy, Refines the Terminal Cell Fate in the Drosophila Embryonic Trachea. *PLoS ONE,* 5**,** e14134.

ZHANG, Y., SINGH, M. K., DEGENHARDT, K. R., LU, M. M., BENNETT, J., YOSHIDA, Y. & EPSTEIN, J. A. 2009. Tie2Cre-mediated inactivation of plexinD1 results in congenital heart, vascular and skeletal defects. *Developmental Biology,* 325**,** 82-93.

ZYGMUNT, T., GAY, CARL M., BLONDELLE, J., SINGH, MANVENDRA K., FLAHERTY, KATHLEEN M., MEANS, PAULA C., HERWIG, L., KRUDEWIG, A., BELTING, H.-G., AFFOLTER, M., EPSTEIN, JONATHAN A. & TORRES-VÁZQUEZ, J. 2011. Semaphorin-PlexinD1 Signaling Limits Angiogenic Potential via the VEGF Decoy Receptor sFlt1. *Developmental Cell***,** 1-14.